INSTITUTO DE SISTEMAS OPTOELECTRÓNICOS Y MICROTECNOLOGÍA

(INSTITUTE FOR SYSTEMS BASED ON OPTOELECTRONICS AND MICROTECHNOLOGY)

Activity Report (2007-2009)

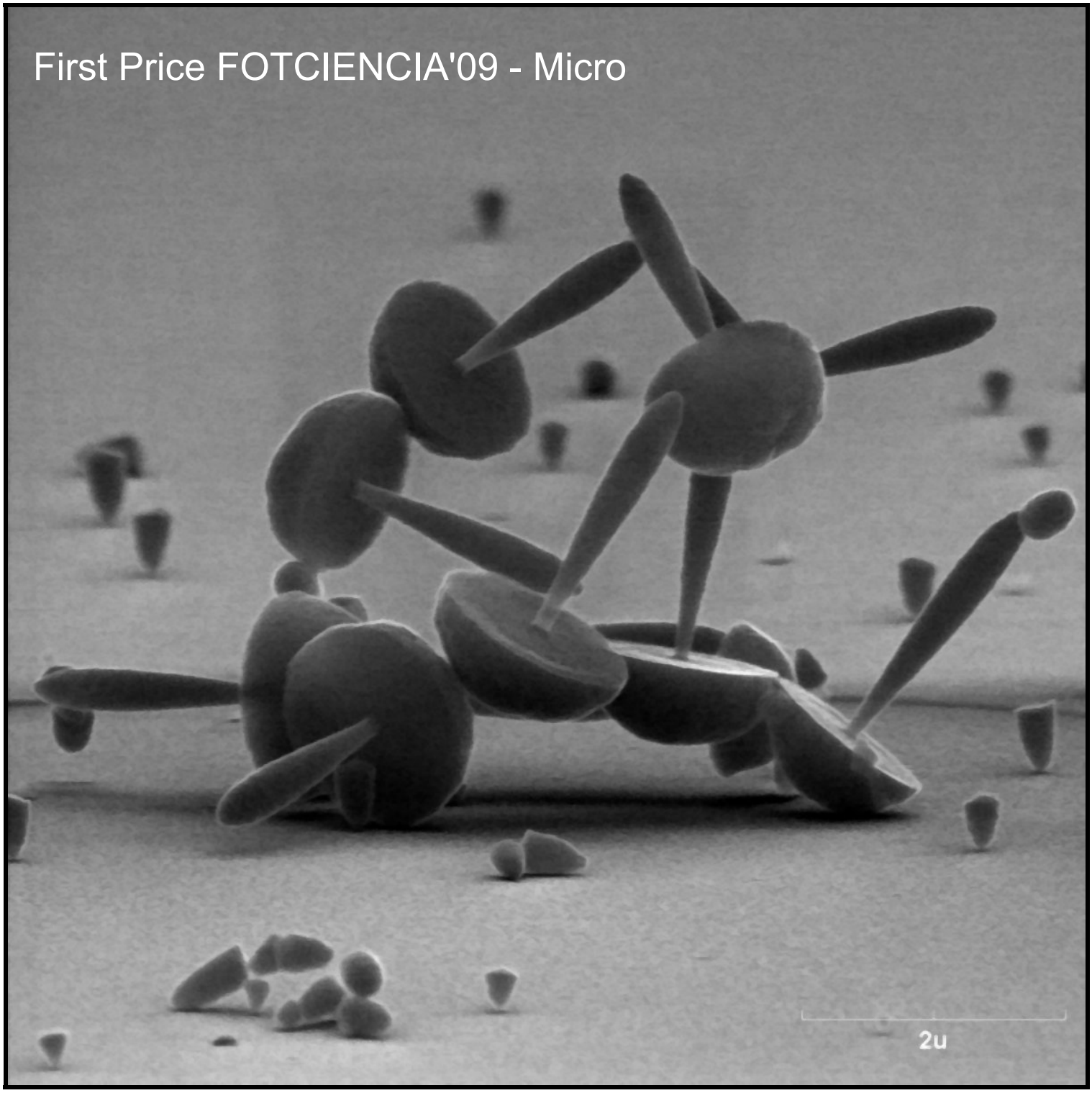

Universidad Politécnica de Madrid

INSTITUTO DE SISTEMAS OPTOELECTRÓNICOS Y MICROTECNOLOGÍA

(INSTITUTE FOR SYSTEMS BASED ON OPTOELECTRONICS AND MICROTECHNOLOGY)

Activity Report (2007-2009)

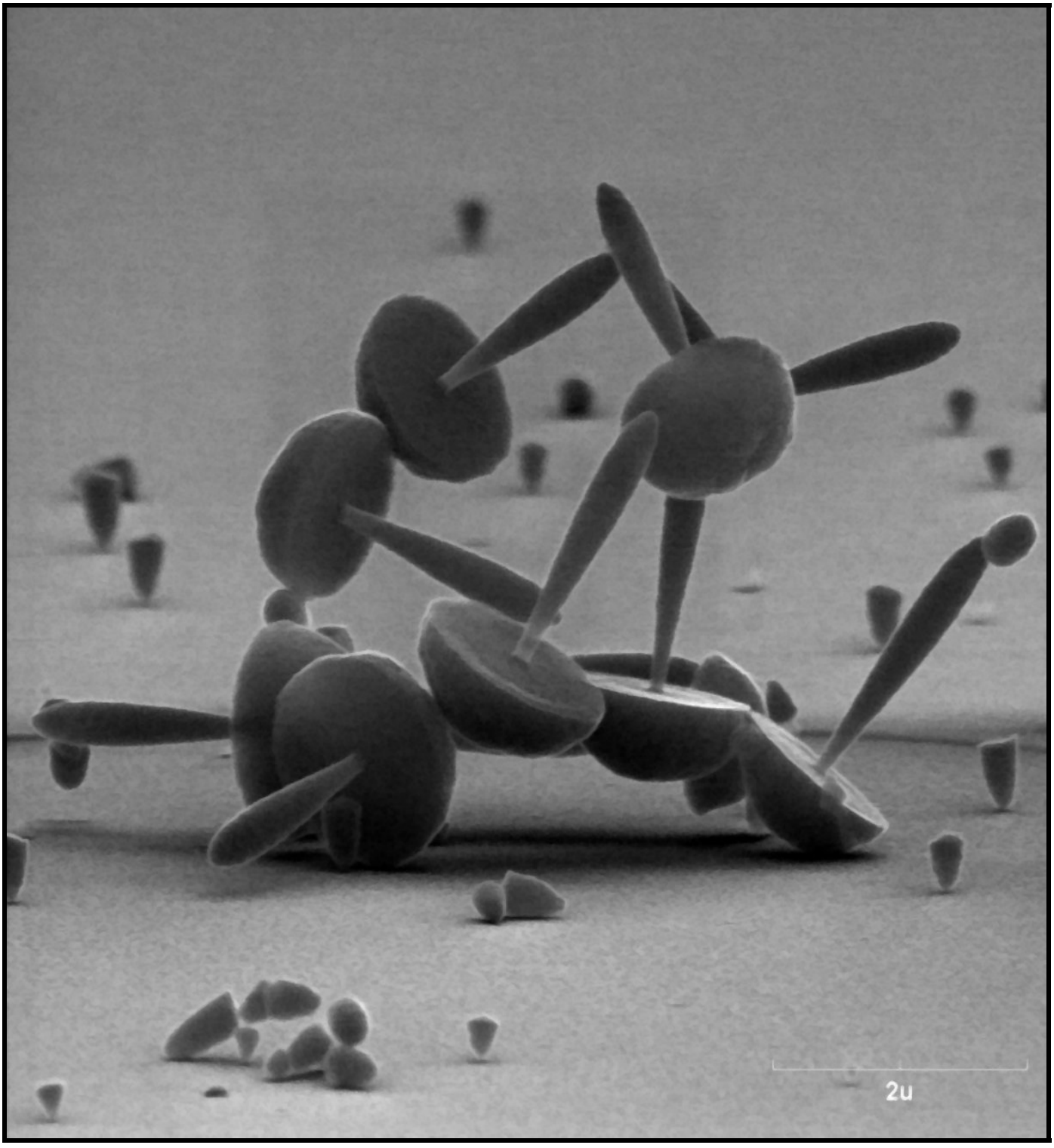

The microscopic beings weigh only nanograms (a millionth of a millionth of a kilogram). With that mass, gravity has a negligible influence and the interatomic forces rule the microscopic world. Here, where weight has no meaning, the surface forces can hold a structure that would be impossible in real size. In the figure we see some micro-mushrooms deposited electrolitically with cobalt on a resin mould. When the resin is removed, the "mushrooms" can stick together in any random possition. Now it is easier to understand why geckoes, that are very light, can walk on the ceiling on their toes and why Spiderman cannot exist (I hope we do not dissapoint you).

Instituto de Sistemas Optotelectrónicos y Microtecnología

(INSTITUTE FOR SYSTEMS BASED ON OPTOELECTRONICS AND MICROTECHNOLOGY)

Universidad Politécnica de Madrid

Activity Report

2007-2009

E.T.S. Ingenieros de Telecomunicación
Ciudad Universitaria s/n
28040, Madrid
Teléfono: (34) 91 336 6832 Fax: (34) 91 453 3567
http://www.isom.upm.es

PREFACE


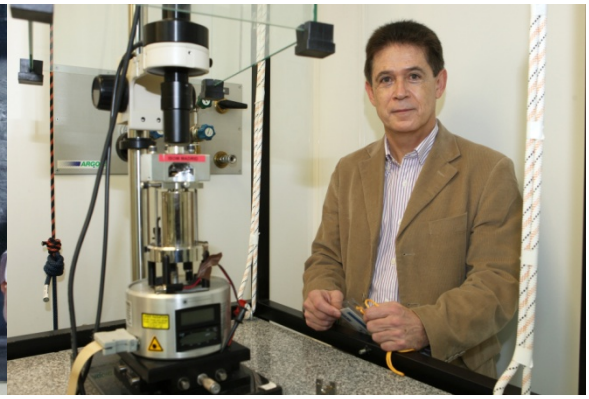

The Institute for Systems based on Optoelectronics and Microtechnology (ISOM) is devoted to research and development activities in information and communication technologies based on III-V semiconductors, magnetic and non-metallic materials. This report summarizes the technical and scientific activities carried out at ISOM in the period 2007-2009. This period relates to a very fruitful scientific activity in several areas, where knowledge, experience, and technology have been consolidated. ISOM has now three main groups devoted to Semiconductor Devices, Magnetic Devices, and Non-metallic Simulation. New staff members joined ISOM during this period, establishing new research lines and reinforcing the already existing ones. During this period, research on nanoscience and nanotechnology has boosted in the areas of semiconductor and magnetic materials and devices. Nanorods, Quantum Dots, Nanocavities, NanoLEDs, and magnetic Nanoparticles are some examples of the activities in this field at ISOM.

ISOM still profits from the program launched by UPM in 2005 aiming to provide tenure research positions to young researchers with outstanding scientific curricula, as well as from the national Ministry of Education (MEC) programs for postdoctoral fellows (Ramón y Cajal) that allowed ISOM to gain four more experienced research members during this period.

In 2009 UPM launched a very ambitious initiative, called Nanotech, aiming to promote activities in the nano area. A relevant part of this initiative is the “ISAAC PERAL” program, an Industry-Academia BBVA Foundation-UPM international Chair, within the Marie Curie Action co-fund (FP7), on Nano-photovoltaics and Nanosensors. An important action in this new program is to incorporate in 2010 a Senior Researcher that will allow setting up a research group in this specific area. This position is accompanied by a full package of research funding and human resources, and it is expected that this new position and activities on Nanotechnology will link with ISOM using its available facilities and infrastructures.

During this period new equipments have been incorporated to ISOM: a XRD system, a Current-Voltage stage for the existing AFM (capability to address individual nanostructures), and a perfilometer with 10 nm resolution. In few months a new Inductively Coupled Plasma (ICP) dry etcher system will be purchased. These new tools will reinforce the ISOM capabilities in the nano area.

Research on semiconductor materials and devices at ISOM has been largely based on binary and alloy compounds containing nitrogen (group-III nitrides), leading to either wide or narrow band-gap heterostructures. Progress

in optical detectors based on nitride Quantum Dots (QDs) and Quantum Wells (QWs), nanocavity structures for quantum computing, nanoemitters (LED), IR lasers based on dilute nitrides, surface acoustic wave devices, MEMS and NEMS (nanoresonators, RF-switches), high temperature electronics, and in understanding the surface physico-chemical properties of AlGaN/GaN transistors, have continued in this period.

Four new research lines were launched during this period related to semiconductor materials. A first one based on ZnO (films and nanorods) for UV solar radiation monitoring and imaging systems. A second one on Integrated Optical Micro and Nanosystems (optical biosensors integrated in a chip, Lab-on-a-chip). A third one on devices for energy conversion and photovoltaics, dealing with High efficiency InGaN heterojunction (nano) Solar Cells grown by MBE, High Performance Organic-Nanorod Hybrid Photovoltaic Devices, Nitride-based HEMTs and switches for efficient energy power converters, and MEMS and NEMS for energy harvesting based in nitrides and oxides. The last research line refers to the development of efficient, phosphor-free arrays of nano-LEDs for white light generation, based on III-nitrides grown by MBE on nanopatterned substrates (Silicon) and Ti nanohole masks. In the area of magnetic materials, research focused on magnetic sensors and devices, Spintronics and magnetic nanoparticles for biomedical applications. Activities on simulation focused on non-metallic materials and complex fluids, molecular dynamics methodology and advanced Monte Carlo techniques, adsorption and nanostructured materials, "single-molecule" sensors for biomolecules (proteins, toxins), and jammed structures and glassy materials.

The research period covered by this report shows a significant participation of ISOM in European Union research programs, in both the VII Framework Program and through the European Defence Agency. A new line of research on smart and efficient white lighting was initiated in 2009 as a participation in an EU FP7 project coordinated by OSRAM (Germany).

As summarized in this report, ISOM significantly participated in national and regional research programs. Rapid developments in information, communication and nanotechnologies moved us to seek and to develop participation in frontier research areas, as nanotechnology, biosensors and MEMS. ISOM cooperation with Spanish industries and Institutions has been reinforced in this period.

Along this period the activities of ISOM, as a dedicated Scientific and Technological Singular Facility (ICTS), acknowledged by the Spanish MEC in 2001 and redefined in 2005 to provide technological services to external academic laboratories, have been increased, as testified by a higher number of services provided, not only for Spanish Institutions, but also within the EU.

Finally, I wish to thank all ISOM scientific staff members, PhD students and support personnel for their commitment and continuous efforts through these years. We acknowledge the support of the various funding Institutions for their confidence in our activities. Thanks also are given to the Electronic Engineering, Applied Physics and Chemistry Departments, to the ETSIT and ETSII Directors and to the UPM Rector for their continuous support and understanding.

Madrid, January 2010

Enrique Calleja Pardo

Director

Activity Report 2007-2009

CONTENTS

1 PRESENTATION AND OBJECTIVES

ISOM-UPM Image Gallery with some selected pictures of our Laboratories and Equipment.

The *Instituto de Sistemas Optoelectrónicos y Microtecnología* (ISOM) is an interdepartmental research Institution of *Universidad Politécnica de Madrid* (UPM). ISOM was created on March 16th 2000. ISOM technological facilities are located at the basement of the *López Araujo* building at the *Escuela Técnica Superior de Ingenieros de Telecomunicación* (ETSIT) of UPM (*Ciudad Universitaria* campus). These facilities include a 400 m^2 clean room and 300 m^2 of characterization and system development laboratories. Simulation activities of non-metallic materials are carried out at the *Escuela Técnica Superior de Ingenieros Industriales* (ETSII) of UPM (*Nuevos Ministerios* location). The Institute has presently 42 researchers, 1 computer manager, 1 clean room engineer, 4 technicians and 2 administrative assistants. Researchers from Electronics, Physics and Chemistry Departments are combining their research efforts in a truly multidepartmental and pluridisciplinar R&D Institute.

The mission of ISOM is to perform research in the fields of detection, processing, transmission and recording of information by means of micro and nanotechnologies based on the optical, electronic, magnetic and chemical properties of materials and structures. As a University Institute, education and training of innovative professionals and scientists is a first priority, to be accomplished through their participation in research and development activities seeking new knowledge, and through graduate education programs.

The Technology Centre of ISOM was awarded the recognition as a "*Scientific and Technological Singular Facility*" (ICTS) by the Spanish Ministry of Education in 2001. Through periodic public calls, ICTS-ISOM offers its services on technology, processing and characterization to the Spanish and EU scientific and technical community.

The transfer of R&D results to the industry and the cooperation with external Laboratories and Institutions, are very important objectives pursued by the Institute. ISOM seeks to be a R&D laboratory able to participate and to lead research projects at the European Union and international level. ISOM aims to be a centre of excellence, a reference research laboratory, and a singular scientific and technological facility that openly provides assessment and services to other academic and non-academic entities. The Institute intends to contribute to the generation of spin-off companies by means of temporary agreements on use of clean room space and processing equipment as well as by providing its R&D expertise.

Since 2002 ISOM is an Associate Unit of the *Consejo Superior de Investigaciones Científicas* (CSIC) linked to the IMB-CNM (*Instituto de Microelectrónica de Barcelona, Centro Nacional de Microelectrónica*).

2 ORGANIZATION CHART

ISOM uses a number of sample holders for the connection of the devices depending on the nature of the measurement that will be performed: optical, magnetic, electrical at high or low frequency, etc. The picture shows a chip with 45 devices connected with wirebonding to a non-magnetic high frequency chip-holder.

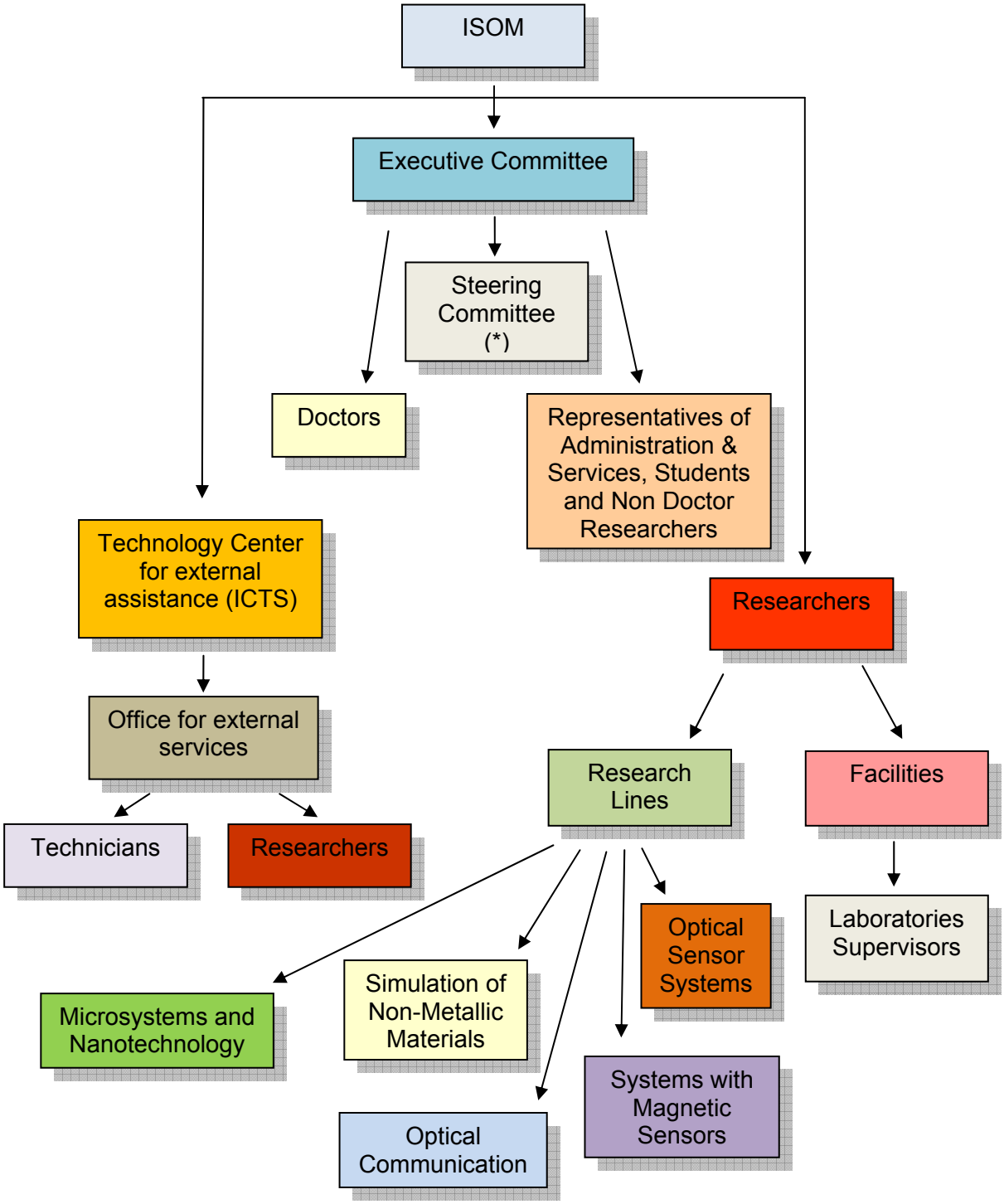

(*) STEERING COMMITTEE:

Director:	Enrique Calleja Pardo
Vice-director:	Fernando Calle Gómez
Secretary:	José Luis Prieto Martín
Technical coordinator:	Claudio Aroca Hernández-Ros
ICTS coordinator:	María del Mar Sanz Lluch

3 ICTS (SCIENTIFIC AND TECNOLOGICAL SINGULAR INFRASTRUCTURE)

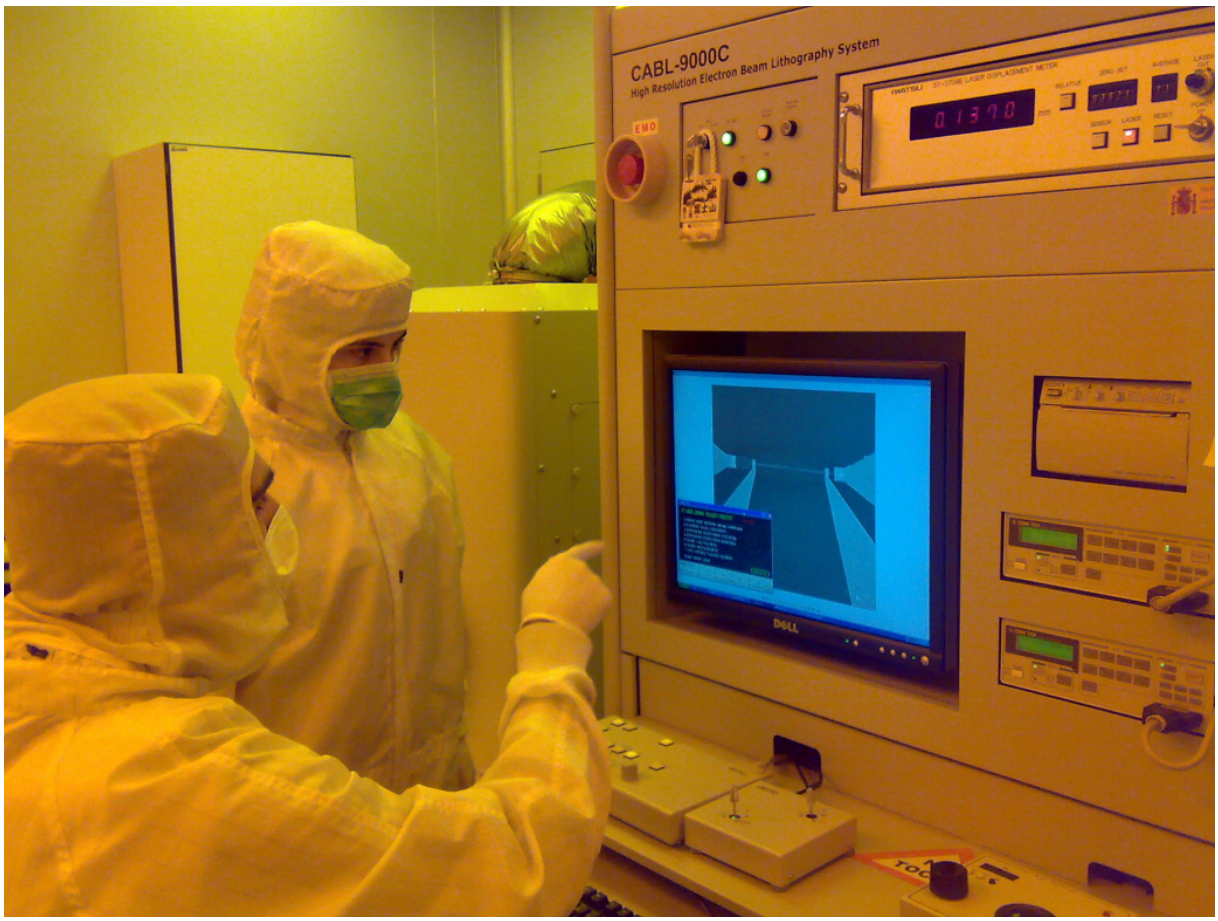

Electron Beam Lithography System. This is a Crestec 9500 system characterized by its great stability in beam current and position. The minimum line width is 10 nm. Its stability allows the patterning of large areas with high reproducibility of the features. It also has a very good stitching and overlay accuracy, allowing the processing of multilayered devices on up to 4" wafers.

3.1 Description of the ICTS: "CT-ISOM"

At the end of 2001, the "Technology Center of ISOM" (CT-ISOM) was acknowledged as a Large Scientific Infrastructure (GIC) by the Spanish Ministry of Science and Technology. Later on (BOE June 16th 2006) the GICs were renamed as "Singular Scientific and Technological Infrastructure" (ICTS). This title acknowledges the important material and human resources of the Centre that are open to offer scientific and technological services and assistance. Thanks to these resources, we are able to develop state of the art technology and to establish scientific links with other top research Centres, both inside Spain and overseas, in the fields of Micro and Nanotechnology. We should highlight that so far our Institute is currently the only ICTS in Spain belonging to a University.

The CT-ISOM has a Clean Room and different Laboratories for devices and materials characterization. In these facilities researchers, technicians and administrative personnel work together to sustain our research lines and to provide external services.

The facilities at the CT-ISOM allow the fabrication of different materials, technological processing and the implementation of different devices and integrated electric, optic, optoelectronic and magnetic structures. Indeed CT-ISOM has the capacity to develop and fabricate LED and laser diodes for instrumentation, environment and optic communications; high power and high temperature microwave transistors; infrared detectors for military and non-military applications; ultraviolet detectors to monitor the UV radiation from the sun and for military applications; visible light detectors for biophotonic applications, magnetic sensors for all sort of applications and also SAW RF filters for sensors and mobile phones. The range of possibilities of the CT-ISOM covers not only the micrometric scale, but also the nanometric frontier (< 300 nm) thanks to the newly acquired e-beam lithography system. This tool is performing up to its best standards, reaching a line resolution of about 10 nm.

The CT-ISOM has developed processing and fabrication protocols that provide a control of incidences and the final quality of the structure. Each processing order is filed by a "processing form" where all the individual processes and their incidences are recorded. This gives a feedback for future processing so it can be improved or reproduced. The information from these forms is later incorporated to the Specific Protocols of the CT-ISOM.

3.2 Services offered by the CT-ISOM

The CT-ISOM offers external services within the research lines (Chapter VI) and capabilities of the Institute (Chapter V), from a simple characterization to the complete device fabrication (sensors, actuators, transistors, integrated structures, filters, emitters, etc). CT-ISOM has the capability to fabricate and optimize a designed structure thanks to its technology line, design and fabrication of masks, deposition of many types of materials and characterization of the final product/device. These external services are offered to the industry and to the scientific community, national and international.

The academic researches interested on using the facilities of the CT-ISOM have now the possibility of doing it free of charge under the call *"**Ayudas financieras para la mejora de las Infraestructuras Científicas y Tecnológicas Singulares (ICTS) y para el acceso a las mismas**"* **(BOE 11/06/09).** Find details in our website:

http://www.isom.upm.es

- **CT- ISOM: Singular Scientific and Technological Infrastructure.**

- **Services offered by the CT-ISOM.**

This initiative from the *Ministerio de Ciencia e Innovación* (MICINN) has the following objective: ***"to promote the access of new research groups or individual investigators to ICTS, for the acquisition of new knowledge, their formation on the technology available at the Installation or for the completion of their research work"***

The selection of works that could benefit from the terms of this service is first done by an internal committee from the CT-ISOM. In this evaluation, the Institute determines the viability of the research requested and selects a number of proposals. Further, an External Committee, formed by prestigious national researchers, chooses and ranks among the proposals selected.

Today, the equipment needed for micro and nanotechnology is very expensive and requires a (also expensive) constant maintenance. Therefore a national policy from MICINN has been launched to improve and maintain the equipments and to allow **all** researchers to access the equipments available at the different ICTS, so they can complete their research.

3.3 Some examples of works done at CT-ISOM

Since its beginning (in year 2000), CT-ISOM has given support and provided services to external users, but from year 2005 the Spanish MICINN (former *Ministerio de Educación y Ciencia*) started a new program to promote and support the use of the ICTS by external users from the academic community. Hence, since 2006 most of the work developed for external users has been funded by the Spanish MICINN. Since the year 2006, CT-ISOM has performed more than 90 services to external users from the academic community. Some of them represent one week work, but this period of time can be extended up to two weeks for PhD students. There has been a wide plethora of services with different degree of difficulty: from basic standard processing such as microsoldering or reactive ion etching with well known parameters, to more complex and challenging works, mainly related to nanotechnology.

Here, we mention a couple of examples of work developed at CT-ISOM:

1.- Development of Hall-bars to measure transport properties in graphene.

The goal of this service was to design and build specific Hall-bars to investigate the quantum Hall effect in graphene. Up to this request, ISOM did not have any previous experience on this material; therefore, the difficulty of such work has been twofold: on one hand to determine the proper parameters to be used in all the processing steps; on the other hand, the variety of different processing steps themselves to obtain a final device ready to be used to characterize transport properties in graphene.

The steps to be followed in order to carry out such Hall-bars consist of a preliminary study of dimensions and position of the graphene flakes to be able to contact them. Afterwards the Hall-bar had to be defined on graphene by means of oxygen plasma. Finally, the Hall-bar was contacted to an appropriate holder (non-magnetic)

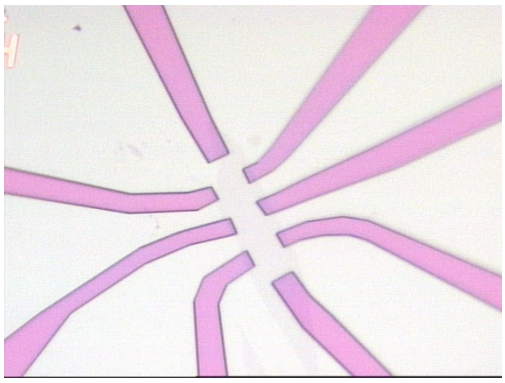

***Figure 1**: Optical image of a lithography on PMMA of contact pads aligned with graphene flake. Ready to evaporate Ti/Au metals.*

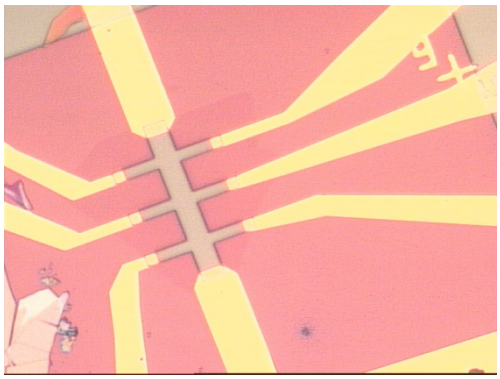

***Figure 2**: Optical image of a lithography on PMMA of MESA, ready for oxygen plasma etching.*

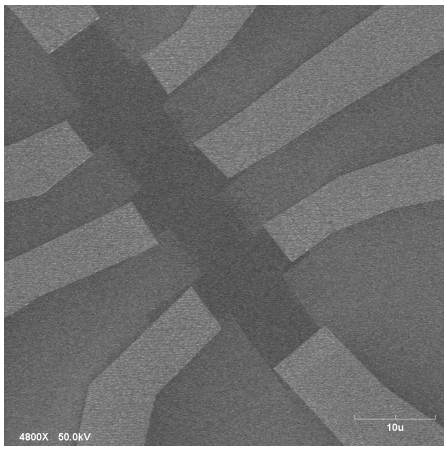

***Figure 3**: SEM image of a Hall bar on graphene, ready to be soldered.*

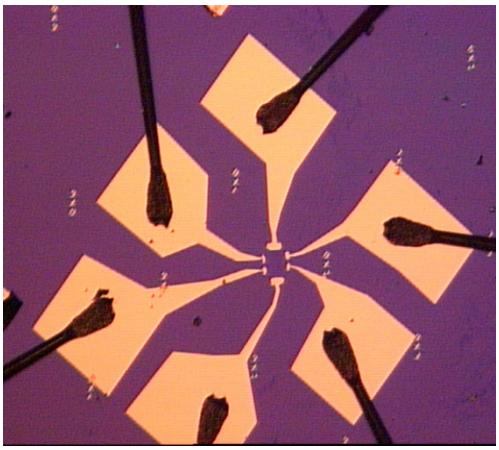

***Figure 4**: Optical image of a complete Hall bar after once soldered to the holder.*

References

[1]E. Diez, V. Bellani, M. Hilke, D. López-Romero, D.K. Maude, D. Shahar, D.L. Sivco, A.Y. Cho, "Saturation Regime in the Quantum Hall Effect". *17th International Conference on Electronic Properties of Two-Dimensional Systems (EP2DS-17) and of the 13th International Conference on Modulated Semiconductor structures (MSS-13)*. Genova, Italy (2007).

[2]M. Amado, E. Diez, V. Bellani, D. López-Romero, P. Orellana, F. Domínguez-Adame, L. Sorba y G. Biasiol, "Control of electron transport in quantum wires and quantum rings with side-coupled nano-gates", *22nd General Conference of the Condensed Matter Division of the European Physical Society*. Roma, Italy (2008).

[3]M. Amado, E. Díez, D. López-Romero, F. Rossella, J.M. Caridad, F. Dionigi, V. Bellani, and D.K. Maude, "Plateau-insulator transition in graphene", *submitted to New Journal of Physics*, 2010.

2.- Gold nanoantennas:

The work proposal was based on the fabrication of periodical gold structures. Such structures were proposed as dimer and trimer-type, all of them with critical dimensions close to 10 nm. Therefore the challenge here was to reach the desirable dimensions in the very limit of our nanolithography system.

The final objective of these processes is the characterization of the electromagnetic field near the nanostructures by means of SNOM (Scanning Near-field Optical Microscopy), and study the resonance near the wavelength of the surface plasmons on nanostructures. The results will be compared with former theoretical calculations developed by the user.

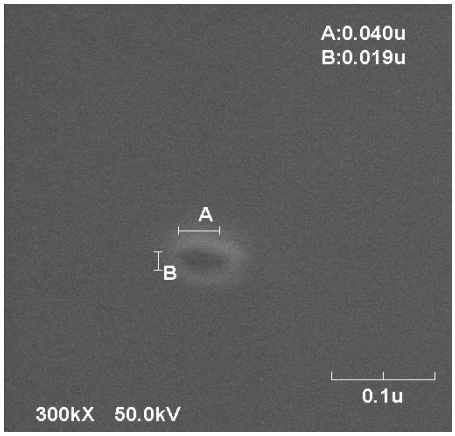

***Figure 1**: SEM image showing typical dimensions of the monomer structure for the nanoantennas pattern.*

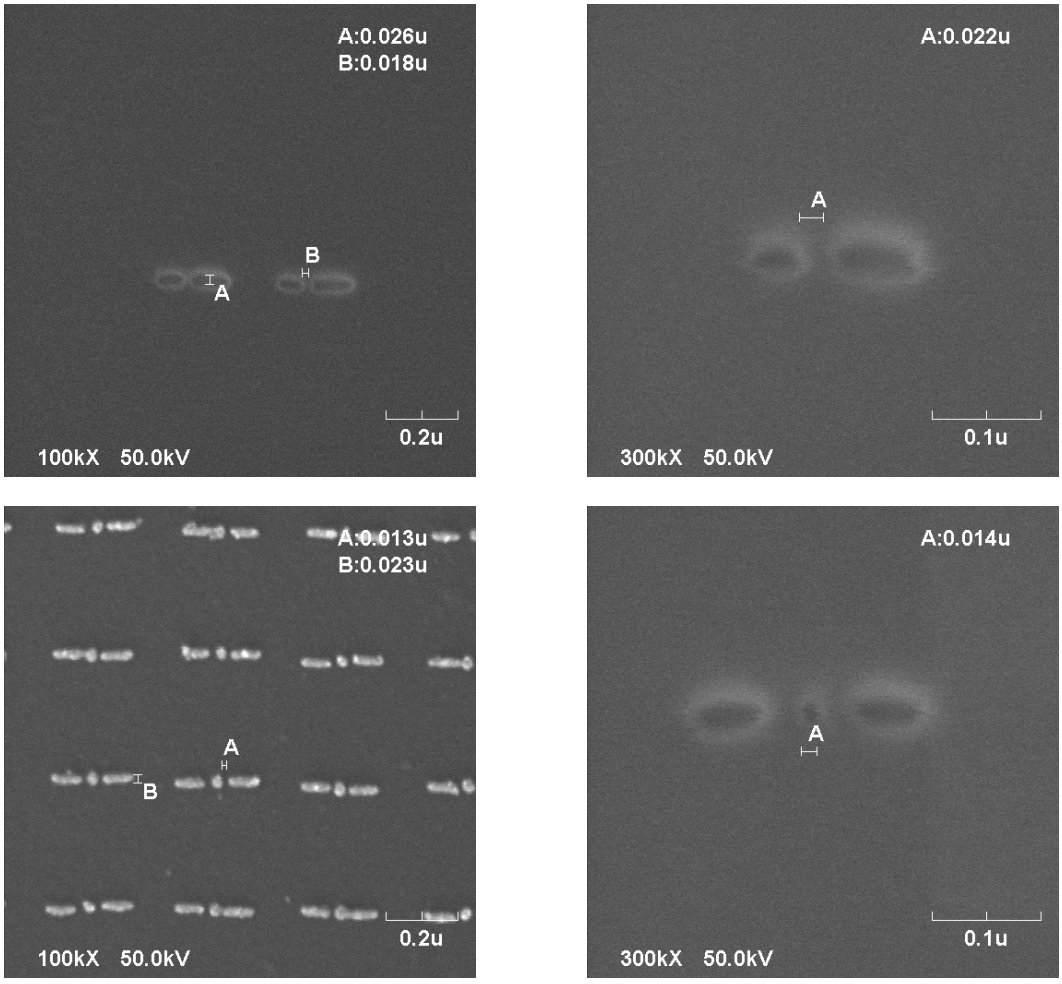

***Figure 2**: SEM images showing a dimer structure (upper) and a trimer structure (lower)*

After having successfully obtained the nanostructures, some surface characterization was performed by AFM (Atomic Force Microscopy) as shown in figure 3.

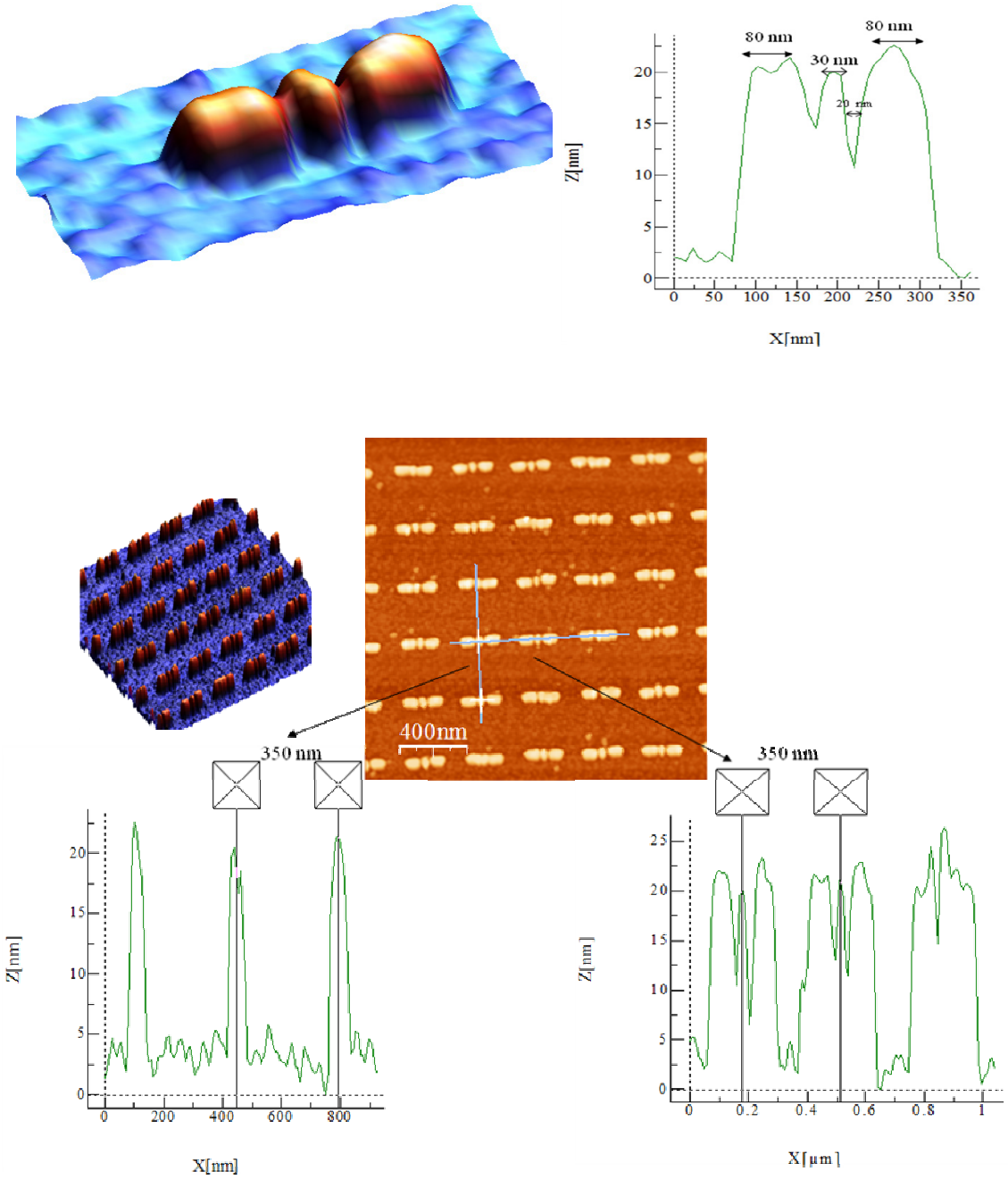

***Figure 3**: AFM characterization of the gold trimer structure*

References

[1]R. Rodríguez-Oliveros, J.A. Sánchez-Gil, , M.U. González, A. Vitrey, D. López-Romero, M.M. Sanz and C. Domingo, *to be submitted to Optics Express.*

4 TECHNOLOGICAL AND CHARACTERIZATION FACILITIES

Compact 21S RIBER MBE system dedicated to the growth of III-Nitrides materials (GaN, AlN, InN and their alloys). The MBE system has 7 source ports, including a central flange for the installation of the radio-frequency plasma source to activate the nitrogen. Introduction of samples is implemented by the use of a loadlock chamber. The system is also provided with standard in-situ real-time characterization techniques such as RHEED (reflection high energy electron diffraction) and RGA (residual gas analyzer).

4.1 Materials Growth and Processing Systems

- Molecular Beam Epitaxy (MBE) (3 systems)
- Magnetron Sputtering (3 systems)
- UV Photolithography MJB3 aligner (resolution >1 μm)
- UV Photolithography MJB4 aligner (resolution 500 nm)
- Electron-Beam Lithography (Raith) system (resolution >0.2 μm)
- High resolution nanolithography system (line resolution 10 nm)
- Chemical Vapour Deposition systems (CVD and PECVD)
- Metal Deposition (Joule, e-beam) (5 systems)
- Ar- Ion Milling system
- Standard and Rapid Thermal Annealing (RTA) (5 systems)
- Reactive Ion Etching (RIE)
- High precision Blade (3 systems) and Diamond Scribers
- Ultrasound and Thermocompression Microsoldering (2 systems)

4.2 Characterization Systems

A) Surface and Structural properties

- High Resolution X-Ray Diffractometers (HR-XRD) (2 systems)
- Scanning Electron Microscope (SEM) with EDAX and EBIC
- Atomic Force Microscope (AFM) with I-V stage
- Thickness Profiler (DekTak)
- Optical profiler by interferometry

B) Electric and Magnetic properties

- Electronic Systems for Characterization and Measurement (curve tracer, curve analyser, sampling oscilloscopes, nanovolt generators, lock-in amplifiers, etc.)
- Cryogenic Hall Effect system
- Cryogenic Giant Magnetoresistance system
- Microprobe station and systems for RF (up to 20 GHz) network analysis
- Carrier Traps and Defect Analysis Techniques (DLTS, PCFRS, AS, etc.)
- Electrical and Optical Characterization systems under Hydrostatic Pressure.
- Electrochemical C-V Profiler
- Magnetic Characterization (Vibrating Sample Magnetometer: VSM)
- Magnetic transport measurements, including spin transfer and velocity of domain walls with a 2,5 GHz oscilloscope

C) Optical properties

- UV, VIS and IR photoluminescence (PL) (4 systems)
- VIS and IR Fourier Transform Absorption Spectrometer (FTIRS) (Nicolet 760)
- Ellipsometry system
- High Resolution Nomarski Optical Microscopy
- Cryogenic systems (5 systems)

D) Devices characterization

- Probe Stations (low Capacitance) for VLSI and discrete devices (2 systems)
- Electrical and Optical Characterization at high T (up to 400ºC)
- Electrical Characterization systems for Transistors and Devices up to 1 GHz (C-V, I-V, C-f, 1/f noise, T, etc.)
- Photonic Devices Characterization system
- Image Capture and Analysis system
- Optical Characterization of Lasers
- Optical Characterization of Detectors

5 RESEARCH LINES

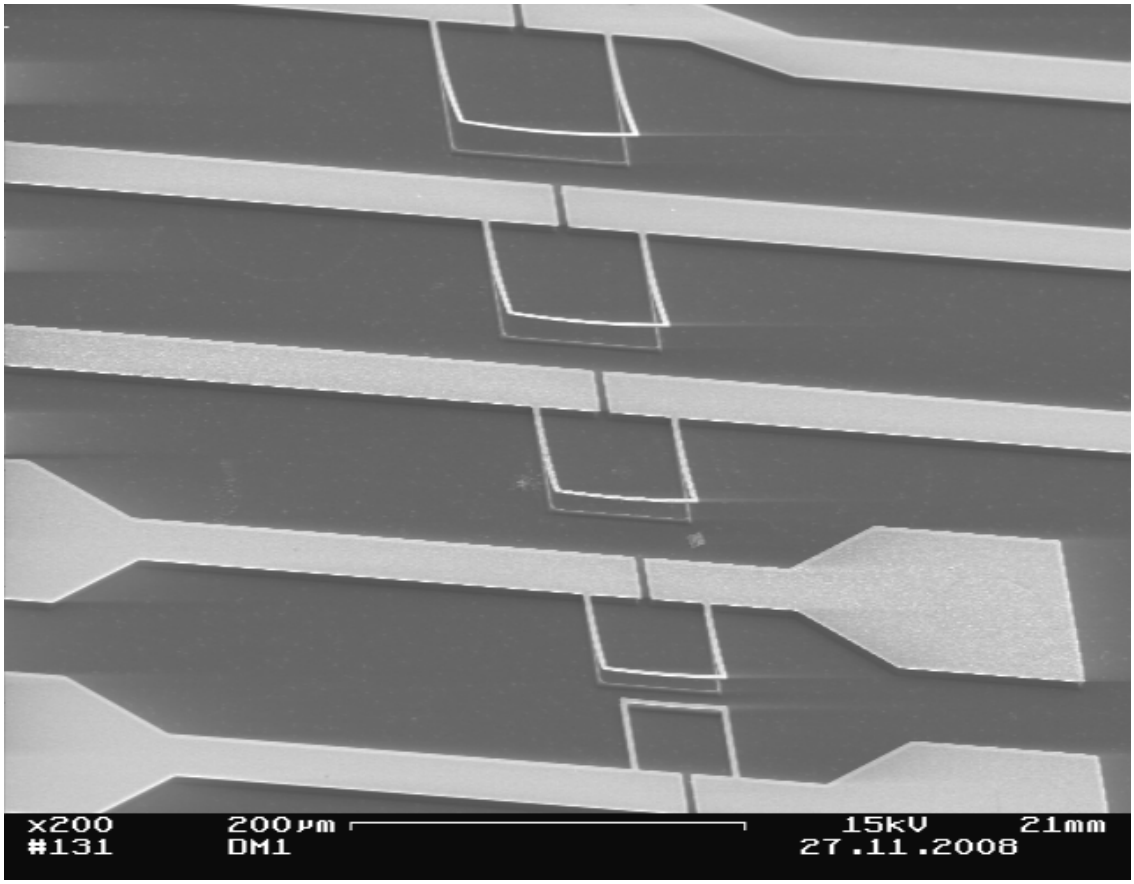

SEM micrograph of an array of U-frame resonators, used to determine the dynamic acoustic velocity, with W = L. The observed out-of-plane deflection is due to the large tensile residual stress in the metal layer covering the structure.

5.1 Optical Devices and Systems

A) UV photo-detection systems (Prof. E. Muñoz, Dr. A. Hierro, Dr. F. Calle)

- UV solar radiation monitoring and imaging systems based on wide bandgap semiconductors (GaN and ZnO).
- Applications of UV detectors in astrophysics, fire detection systems, combustion control, and enviroment and water contaminant detection.
- VIS and UV photodetectors for integrated biosensors and fluorescence systems.

B) Infrared photo-detection systems (Dr. A. de Guzmán, Dr. A. Hierro, Prof. E. Calleja, Dr. M.A. Sánchez)

- High sensitivity and multispectral response detectors. AlGaAs/InGaAs quantum well and dot (QWIP's, QDIP's) technology.
- Multispectral integration. Associated electronics.
- Environmental related IR detection.
- InN QWs for photodetection at 1.5 μm.
- Nanocolumnar intersub-band IR photodetectors.

C) Components for optical communications, quantum computing, and lighting (Dr. A. Hierro, Dr. A. de Guzmán, Prof. E. Calleja, Dr. M.A. Sánchez)

- LEDs/LDs/Photodetectors for optical communications at 1.3 and 1.55 um with arsenide/dilute nitride QWs and QDs.
- Devices grown on substrates with non-conventional orientations (GaAs (111)).
- UV LED emitters incorporating QWs and QDs based on III-Nitrides.
- Phosphor-free white light nanoLED arrays based on III-Nitrides.
- Micro and Nanocavities based on III-Nitrides for quantum computing.

D) Electronic devices and microsystems for communications (Prof. E. Muñoz, Dr. F. Calle)

- AlGaN/GaN HEMTs for μwave applications (X- and L-Band). Manufacturing technology. Transport properties, piezoelectric effects, reliability.
- Surface Acoustic Wave (SAW) RF devices.
- MEMS y NEMS: nanoresonators, RF-switches.
- High temperature device performance and applications.

E) Integrated optical micro and nanosystems (Dr. C.A. Barrios)

- Optical biosensors integrated in a chip (Lab-on-a-chip).
- Integrated optical sensors based on novel materials.
- Ultra-high sensitivity nanomechanical optical sensors.

F) Devices for energy conversion and photovoltaics (Prof. E. Calleja, Dr. M.A. Sánchez, Dr. F. Calle)

- High efficiency InGaN heterojunction (nano) Solar Cells grown by MBE.
- High Performance Organic-Nanorod Hybrid Photovoltaic Devices.
- Nitride-based HEMTs and switches for efficient energy power converters.
- MEMS and NEMS for energy harvesting based in nitrides and oxides.

5.2 Magnetic Materials and Systems

A) Magnetic sensors and Devices (Prof. C. Aroca, Prof. P. Sánchez)

- Magnetometric sensors for low magnetic field measurements: fluxgates, piezoelectric magnetostrictive, magnetoresistive and magnetooptic sensors.
- Multisensors:
  - Vehicle detection applications
  - Ground airplane control and guiding
  - Applications to monitoring large battery complexes
- Planar devices. Applications to planar inductors for commuting sources and antennas.
- Low frequency intelligent cards with magnetic sensors.

B) Spintronics (Dr. J.L. Prieto, Dr. M. Muñoz)

- Metalic magnetic multilayers. Spin valves. CPP measurements.
- Dynamics of magnetic domain walls around defects in magnetic nanowires.
- Spin transfer torque on magnetic domain walls and magnetic nanostructures.

C) Magnetic Nanoparticles (Dr. M. Maicas, Dr. M. Sanz)

- Magnetic nanoparticles synthesized by sputtering.
- Magnetic nanodots.
- Nanoparticles for biomedical applications.

5.3 Non-metallic materials simulation

(Prof. M. Laso, Dr. Nikolaos Karayiannis)

- Non-metallic materials and complex fluid simulation.
- Molecular dynamics methodology and advanced Monte Carlo techniques.
- Adsorption and nanostructured materials.
- "Single-molecule" sensors for biomolecules (proteins, toxins).
- Jammed structures and glassy materials.

6 RESEARCH REPORTS

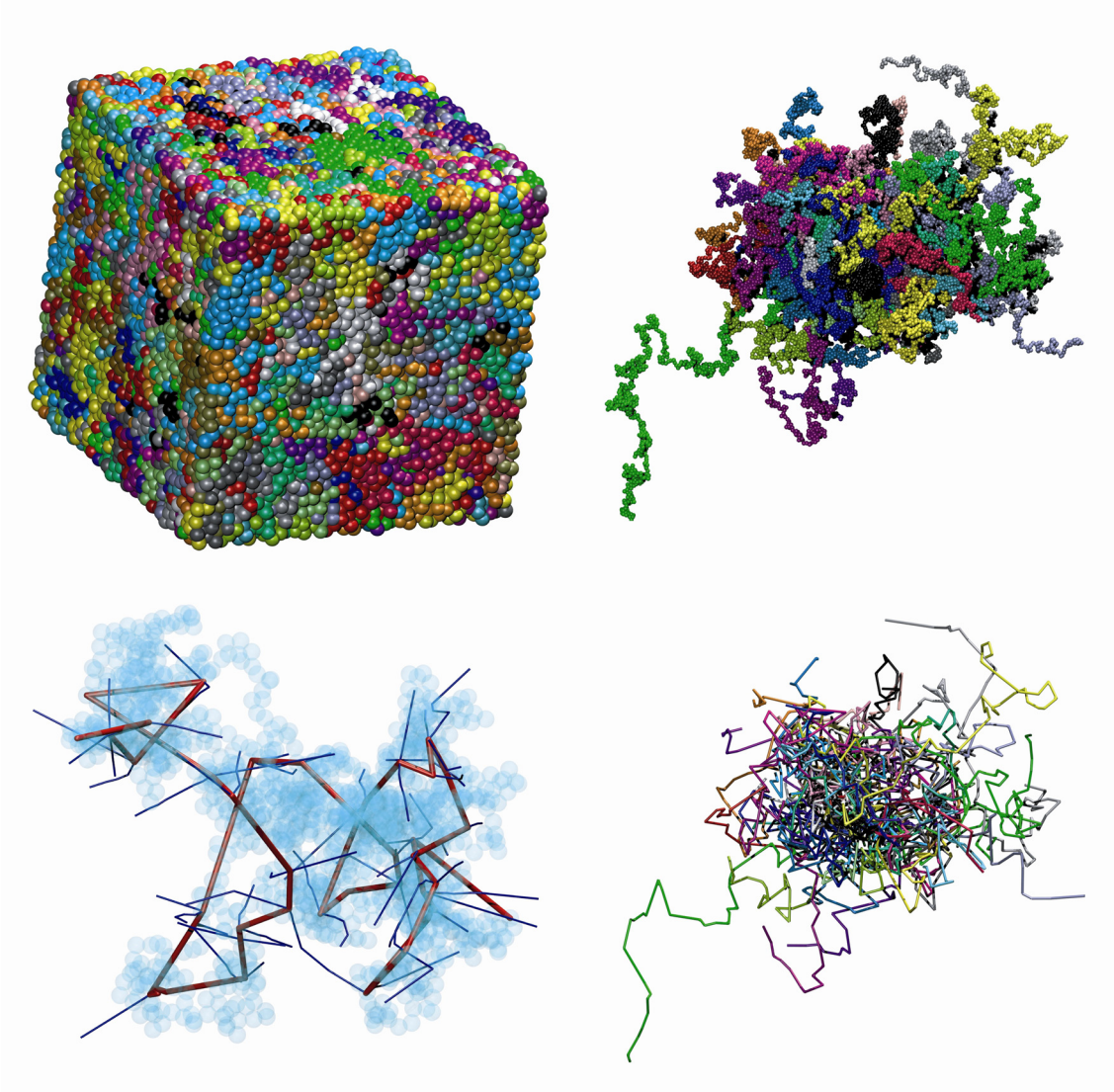

Clockwise from top left: Representative configuration of 54-chain, hard-sphere system of molecular length 1000 in the vicinity of the MRJ state, with coordinates of sphere centers (a) wrapped, subject to three-dimensional periodic boundary conditions and (b) fully unwrapped in space. (d) The underlying primitive path network, after the application of the Z1 topological algorithm, with entanglement coordinates unwrapped in space. (c) An arbitrary selected single chain of high knotting complexity (10.153) with constituent sites shown as transparent spheres. Also shown is the corresponding primitive path, and segments of other primitive paths with which it is entangled.

6.1 Nanoscience and Nanodevices based on III-Nitrides grown by MBE[1]

In the last three years the Group of Semiconductor Devices (GDS) of the ISOM focused on the research of semiconductor materials and heterostructures suitable to develop new devices at nanoscale size. Both fundamental physical properties and device designs have been considered, relying on III-nitrides as the best choice materials for many optoelectronic applications. In the following, the activities related to nanoscience and nanodevices research lines will be summarized.

A) Evidence of electron accumulation at nonpolar surfaces of InN nanocolumns.

A basic issue in InN refers to the predicted electron accumulation at the surface, leading to a strong surface conductivity. The Fermi level pinning at surface states generated by dangling bonds that for most semiconductors occurs within the band gap, takes place above the CB in InN at about 0.9 eV, thus, causing an electron accumulation in a few nanometer thick surface layer. Segev and Van de Walle [1] reported recently on the Fermi level pinning at the surface of GaN and InN in polar (*c*-plane) and nonpolar (*m*-plane, *a*-plane) orientations based on band structure and total energy methods. These calculations predict the Fermi level pinning in polar GaN and InN at E_v+1.8 eV and E_c+0.7 eV, respectively, when the surface reconstructs under metal-rich conditions. In the case of nonpolar GaN and InN, a similar pinning occurs under metal-rich surface reconstruction at E_v+1.8 eV and E_c+0.6 eV, respectively. This last result is most relevant because electron accumulation is predicted in nonpolar InN provided that In adlayers are present at the surface. Experimental evidence of surface electron accumulation was obtained from capacitance-voltage [2] Hall [3] and inelastic electron scattering data [4] and most recently by angle-resolved photoemission spectroscopy [5] that also showed electron quantization in a thin surface layer.

However, all these studies have been accomplished on polar InN surfaces. The growth of nonpolar InN was only rarely reported and resulted usually in films with high densities of defects such as threading dislocations that are a major contribution to the high electron concentration in InN [6]. Thus, to study of the electron accumulation in nonpolar surfaces, a high-quality InN material has to be employed. This can be achieved in InN nanocolumns (NCs) which are grown defect-free single crystalline [7] and exhibit nonpolar sidewalls.

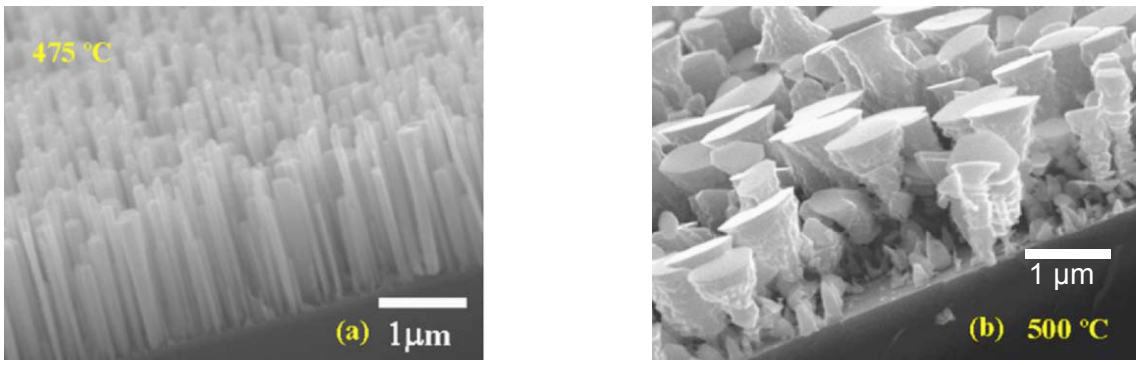

Figure 1. *Typical SEM images of InN NCs grown by PAMBE on a Si(111) substrate: (a) at optimal temperature (475 °C) and (b) at too high temperature (500 °C).*

Various samples of nanocolumnar InN were grown on bare *n*-type Si(111) substrates by PAMBE with average diameters ranging from 40 to 120 nm. Since temperature is the most critical factor to grow InN,

[1] *Contact person: Enrique Calleja* calleja@die.upm.es

either layers or NCs, due to its low dissociation temperature, a reproducibly growth temperature for all InN NCs was achieved by monitoring the reflection high energy electron diffraction (RHEED) pattern. Figure 1 shows scanning electron microscopy (SEM) images of InN NCs grown at 475 °C (Fig. 1.a) and 500 °C (Fig. 1.b), evidencing how critical the growth temperature can be to achieve an optimal nanocolumnar morphology. Figure 1.b shows how the excess temperature promotes a very strong diffusion of In adatoms upwards the NC sidewalls that increases its diameter (*d*) resulting in a mushroom-like morphology. This effect is also moderately present at lower temperatures yielding an undulation of the NC sidewall. According to this effect, In-rich sidewalls are expected on the as-grown NCs, which will be most relevant to interpret the following results on the *I-V* characterization.

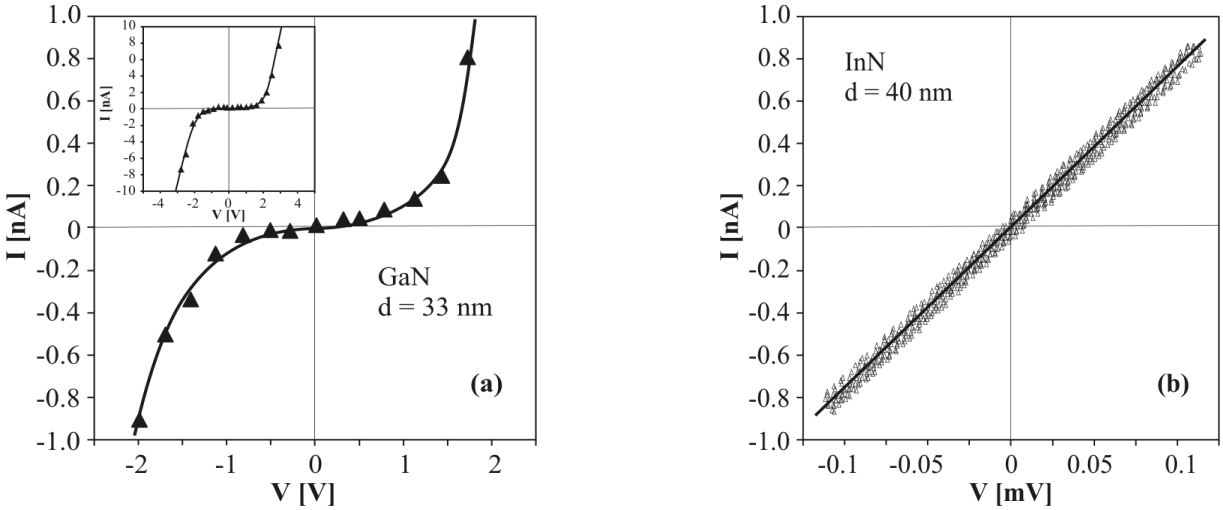

***Figure 2**. I-V characteristics of (a) GaN NCs showing a nonlinear Schottky behavior and (b) InN NCs with a linear ohmic behavior. The inset in (a) shows the I-V characteristic of the GaN NC for higher currents.*

I-V characteristics were measured by AFM with a Si tip covered with a metal (CoPt, TiN, Pt). The geometry of the nanocolumnar samples was determined by high-resolution SEM and AFM. The conductivity of the GaN NCs was determined from the slope of the linear part of the *I-V* characteristic above the threshold voltage (Fig. 2.a). In this case, for small enough diameters, the conduction channel along the NC may drastically shrink due to the space charge regions arising from the lateral surface potential [8] thus increasing the resistivity (pinch-off like). In contrast, InN NCs of similar heights and diameters exhibit a completely linear *I-V* characteristic and a much higher conductivity (Fig. 2.b). However, this *I-V* plot does not give details about the conduction path in InN NCs, namely, whether electrical conduction proceeds through the NC volume or its lateral surface. Then, InN NCs with different diameters ranging from 40 to 120 nm were measured. Basically, the conductivity of a *bulk* material is independent of its size, i.e., the conductivity of a NC will be independent of its diameter, as it is shown in figure 3.a. However, if electron accumulation occurs at the NCs sidewalls, conductivity has two contributions, one through the “volume” independent on NC diameter, and another one through the sidewalls “skin” that would be dependent on the diameter reciprocal.

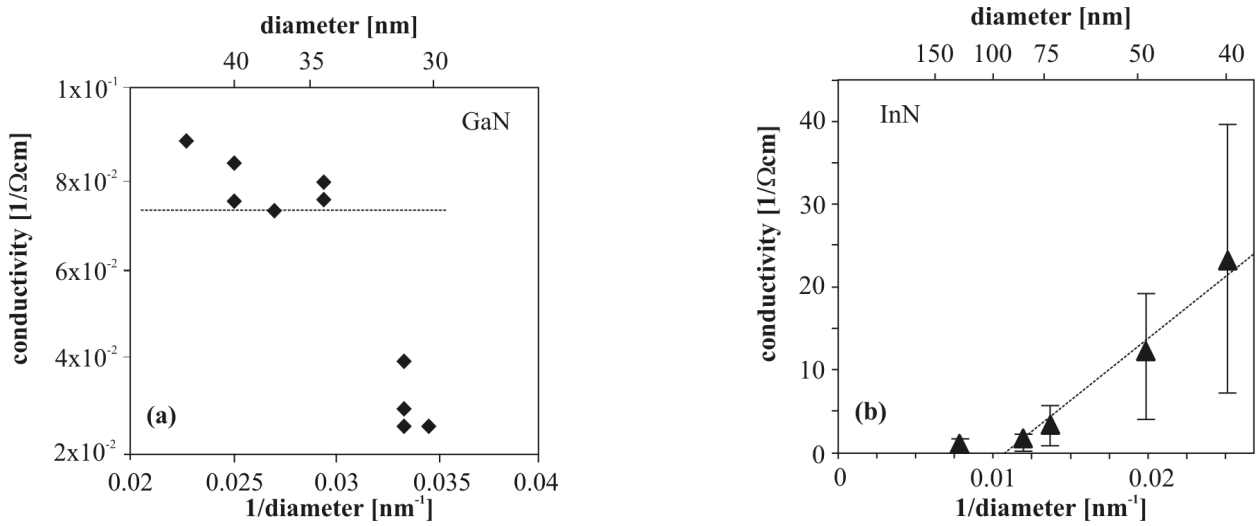

Figure 3. *Conductivity dependence with the reciprocal diameter of (a) GaN and (b) InN NCs.*

This is shown in figure 3.b for InN NCs, where the conductivity trend is roughly linear with 1/*d*. It must be noticed that increasing *d* may eventually lead to a non-negligible current contribution through the NC volume that should make conductivity depart from a linear trend.

In summary we have shown that electrical conduction in InN NCs proceeds in a very different way as in GaN ones. While in GaN NCs conduction proceeds through the volume, being severely limited by the surface depletion due to space charge regions for diameters below a critical value, in InN NCs there is no evidence of surface depletion and the conduction path is located mainly at their lateral surface. These facts prove that there is electron accumulation in as-grown nonpolar InN surfaces, according to calculations of the Fermi level pinning in InN [9].

References

[1] D. Segev and C.G. Van de Walle, Surf. Sci. Lett., **601**, L15 (2007).
[2] S.X. Li, K.M. Yu, J. Wu, R.E. Jones, W. Walukiewicz, J.W. Ager III, W. Shan, E.E. Haller, H. Lu, and W.J. Schaff, Phys. Rev. B**71**, 161201 (2005).
[3] H. Lu, W. J. Schaff, L.F. Eastman, and C.E. Stutz, Appl. Phys. Lett., **82**, 1736 (2003).
[4] I. Mahboob, T.D. Veal, C.F. McConville, H. Lu, and W.J. Schaff, Phys. Rev. Lett., **92**, 036804 (2004).
[5] L. Colakerol, T.D. Veal, H.K. Jeong, L. Plucinski, A. DeMasi, T.Learmonth, P.A. Glans, S. Wang, Y. Zhang, L.F.J. Piper, P.H. Jefferson, A. Fedorov, T.C. Chen, T.D. Moustakas, C.F. McConville, and K.E. Smith, Phys. Rev. Lett., **97**, 237601 (2006).
[6] V. Cimalla, V. Lebedev, F.M. Morales, R. Goldhahn, and O. Ambacher, Appl. Phys. Lett., **89**, 172109 (2006).
[7] M.A. Sánchez-García, J. Grandal, E. Calleja, S. Lazic, J.M. Calleja, and A. Trampert, Phys. Stat. Sol. (b) 243, 1490 (2006).
[8] M. Niebelschütz, V. Cimalla, O. Ambacher, T. Machleidt, J. Ristic, and E. Calleja, Physica E**37**, 200 (2007).
[9] E. Calleja, J. Grandal, M.A. Sánchez-García, M. Niebelschütz, V. Cimalla, and O. Ambacher, Appl. Phys. Lett., **90**, 262110 (2007).

B) InN nanocolumns grown by plasma-assisted MBE on A-plane GaN templates.

Due to the interest to obtain nonpolar III-nitrides, avoiding polarization field effects which are detrimental to the efficiency of LEDs, there has been an increasing number of works on the growth of nonpolar InN layers, though most of them reported on films with high densities of defects [10].

This work focuses on the growth and characterization of InN NCs on *a*-plane GaN templates, grown on *r*-plane sapphire substrates. An MBE system with a rf-plasma source for nitrogen and standard Knudsen cells for metals was used. Substrate temperature is the most critical parameter for *c*-plane InN layers. In fact, no growth is observed for temperatures above 500°C [11,12] for In-polar films, and 600°C [13] for N-polar InN. Samples grown above 550°C presented In droplets on top of the GaN template, typical from InN decomposition [11] and no InN was grown. Only samples grown in the range of 500–525°C showed good crystal quality NCs with no compact InN epilayer between them and the GaN template so the optimal growth temperature was set to 525 °C.

SEM images in figure 4 show the morphology of the InN NCs grown on *a*-plane templates. The NCs with high aspect ratio show clear side facets and even inclined facets on top, in contrast to *c*-plane oriented NCs with flat end. This shape of the NCs arises from the specific growth orientation and the anisotropy in the surface energies. Assuming the *a*-plane base with rectangular geometry (see inset in Fig. 4), the perpendicular side facets are given by *m*- and *c*-planes (1−100) and (0001) respectively, whereas the top facets point to low-index planes of (10−11) and (1−100) types.

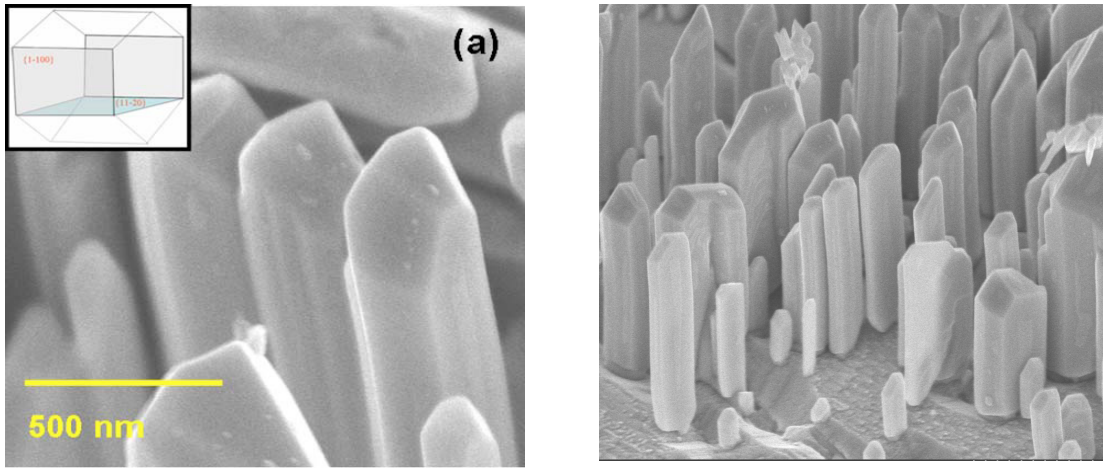

Figure 4. *HR-SEM images of InN NCs grown on a-plane GaN, showing faceted a- and m-plane topsides. The inset shows the a-plane base rectangular geometry.*

Raman Scattering (RS) measurements confirmed the wurtzite structure of the NCs and their crystallographic orientation. For a 632.8 nm laser excitation, the nanocolumnar sample shows the allowed E_2 mode at 488.5 ± 0.5 cm^{-1}. Wang *et al.*[14] determined experimentally that the strain-free Raman frequency of the E_2 high mode of hexagonal InN is 490.1±0.2 cm^{-1}.

According to their experiments, we can conclude that the InN NCs grown on *a*-plane GaN templates are fully relaxed ($\varepsilon_a < 0.08\%$, with the measurement accuracy being 0.05%). Measurements were performed in back-scattering configuration with light propagating along the growth axis and a polarizer placed perpendicular to this direction, modifying the polarization angle of the incident light.

Selection rules [15] imply that the intensity of the E_2 mode should be maximum for polarization perpendicular to the *c*-axis and zero for polarization parallel to it. For the case of InN NCs grown along the *c*-axis, the polarization of the incident light is always perpendicular to the growth direction; therefore, the E_2 mode intensity is independent of the angle of the polarizer (dots in Fig. 5). In the case of InN NCs grown on *a*-plane GaN templates, the intensity of the E_2 mode reaches maxima and minima as the polarization angle varies from perpendicular to parallel to the *c*-axis, respectively (squares in Fig. 5). The same behavior is observed for the *a*-plane GaN template (stars in Fig. 5), as expected. The minimum at 135° of the InN NCs does not go to zero due to some elastic light scattering at the NCs which is absent in the flat GaN template. This result unambiguously shows that the NCs grow perpendicular to the *c*-axis, which corresponds to the measurements taken at 135° angle in figure 5.

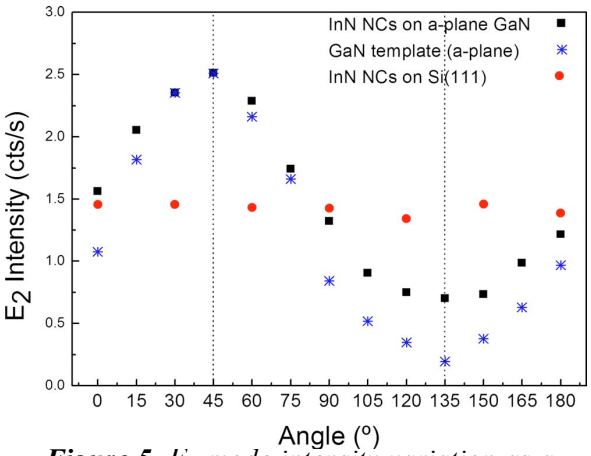

Figure 5. *E_2 mode intensity variation as a function of the polarization angle. Dots are c-axis InN NCs, squares stand for InN NCs along a-plane GaN templates and stars for the a-plane GaN template.*

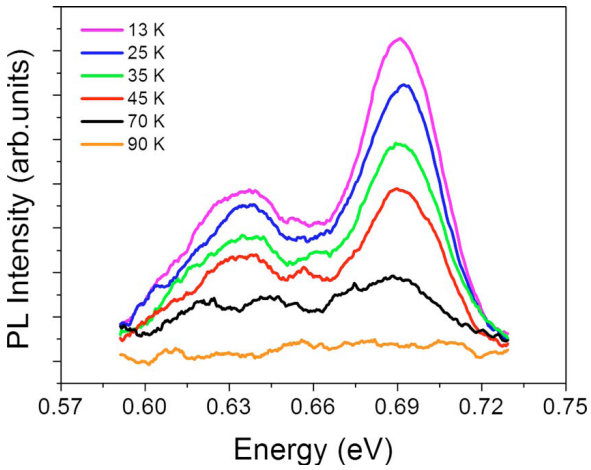

Figure 6. *PL spectra vs. temperature of InN NCs grown on a-plane GaN templates.*

Low temperature (13K) PL measurements of InN NCs grown on *a*-plane GaN templates reveal a main emission at 0.69 eV, typical of good quality wurtzite InN, with a second one at 0.63 eV (Fig. 6). The emission intensity decreases as temperature increases and the position of both peaks experiment a small redshift before total quenching at 77 K. No variation was observed on the peak position energy when changing the excitation power over two orders of magnitude while a linear increase of the main emission (0.69 eV) integrated intensity was obtained. In summary, good crystal quality wurtzite InN NCs were grown directly on *a*-plane GaN templates. RS measurements indicate that the InN NCs grow fully relaxed and their crystallographic orientation is along the *a*-axis [16].

References

[10] H. Lu, W.J. Schaff, L.F. Eastman, J. Wu, W. Walukiewicz, V. Cimalla, and O. Ambacher, Appl. Phys. Lett. **83**, 1136 (2003).

[11] J. Grandal and M.A. Sánchez-García, J. Cryst. Growth **278**, 373 (2005).

[12] C.S. Gallinat, G.Koeblmüller, J.S. Brown, and J.S. Speck, J. Appl. Phys. **102**, 064907 (2007).

[13] K. Xu and A. Yoshikawa, Appl. Phys. Lett. **83**, 251 (2003).

[14] X. Wang, S. B. Che, S. Ishitani, and A. Yoshikawa, Appl. Phys. Lett., **89**, 171907 (2006).

[15] M. Cardona, G. Güntherodt, R. Chang, M. Long, and H. Vogt, in ***Light scattering in Solids II***, edited by M. Cardona and G. Güntherodt (Springer, Berlin, 1982).

[16] J. Grandal, M.A. Sánchez-García, E. Calleja, E. Gallardo, J.M. Calleja, E. Luna, A. Trampert, and U. Jahn, Appl. Phys. Lett., **94**, 221908 (2009).

C) Cathodoluminescence spectroscopy and imaging of GaN/(Al,Ga)N nanocolumns containing quantum disks.

The self-organized formation of GaN NCs during plasma-assisted molecular-beam epitaxy (PAMBE) is a promising mechanism which even allows for the fabrication of heterostructures such as GaN/ (Al,Ga)N quantum disks (QDisk) [17,18], GaN/AlN Bragg reflectors [19], or (In,Ga)N/GaN multiple QDisk light-emitting diodes (LEDs) [20] embedded within nanometer-scale columnar crystals. The electronic properties of such heterostructures are significantly influenced by a laterally inhomogeneous distribution of strain and carrier concentration as well as by band bending near the surfaces [21] which in turn depend strongly on the geometrical parameters of the NC. A macroscopic physical characterization of the electronic properties of NCs containing heterostructures, as has been done so far by PL or RS, generally averages over variations among the NCs within a sample. In order to determine the true intrinsic electronic properties of nanostructures, an optical analysis of a single NC consisting of a heterolayer system is highly desirable. We report on cathodoluminescence (CL) spectroscopy and imaging of nanocolumnar heterostructures with high spatial resolution, which allows for the characterization of a few or even a single NC. Samples with GaN/ (Al,Ga)N NCs containing five QDisks were fabricated by PAMBE.

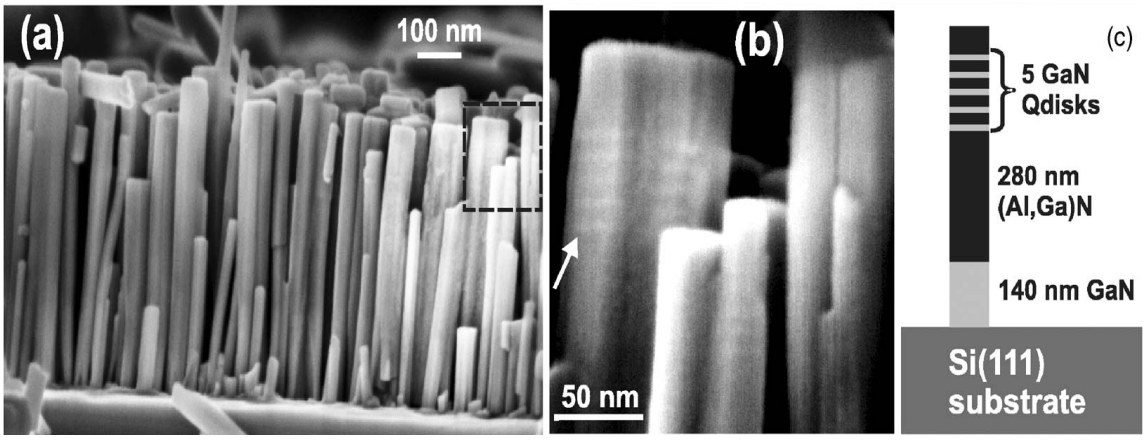

Figure 7. *(a) SEM image of GaN/(Al,Ga)N NCs with 3-nm-thick GaN QDisks. (b) Magnified SEM image of the sample region marked by the dashed rectangle in (a). The arrow points to the 3-nm-thick QDisks.(c) Schematic diagram of the columnar heterostructure.*

Figure 7.a shows a scanning electron microscope (SEM) image of the NC structure of a sample containing 3nm-thick GaN QDisks. The height of the NCs amounts to about 0.55 μm. Their diameter varies between 30 and 80 nm. A magnified image of the region marked by the dashed rectangle in figure 7.a is depicted in figure 7.b. Five bright stripes are clearly visible representing the 3-nm-thick GaN QDisks. A schematic diagram of the whole columnar heterostructure of the investigated samples is depicted in figure 7.c. The NCs consist of a 140-nm-thick GaN base, 280 nm (Al,Ga)N, five QDisks separated by about 8-nm-thick (Al,Ga)N layers, and a 40-nm-thick (Al,Ga)N cap layer. The nominal AlN mole fraction of the NCs (Al,Ga)N regions amounts to 28%.

In the following, we discuss the optical properties of a sample, which contains 4.2-nm-thick QDisks. Figure 8.a represents a CL spectrum obtained for a large number of NCs of this sample. The spectrum consists of two broad bands centered at about 3.48 and 3.91 eV. In figure 8.b the CL image obtained for a detection energy (*Ed)* of 3.482 eV (dark) is superimposed on the one obtained for *Ed* =3.915 eV (bright). The high *Ed* CL image has been acquired simultaneously with the SEM image of figure 8.c. The comparison of the CL images with the SEM image clearly confirms that the low-energy CL band originates from the NCs top and can therefore be assigned to the emission from the QDisks. The high energy CL band represents undoubtedly the thick (Al,Ga)N layer situated between the QDisks and GaN base of the NCs. In figure 8.a both the spectrum of the QDisks and the one of the (Al,Ga)N are rather broad. Their full widths at half maximum (FWHM) values amount to 155 and 205 meV respectively. In order to separate contributions

of the spectral broadening caused by averaging over a large number of NCs from intrinsic broadening mechanisms, we have performed CL experiments on a single NC.

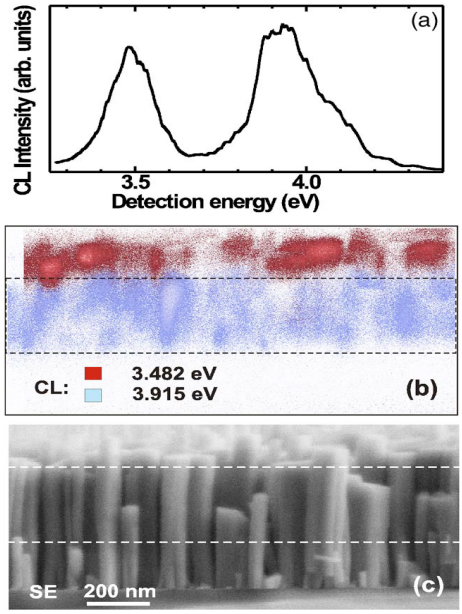

Figure 8. *(a) CL spectrum @ 6K of a large number of GaN/(Al,Ga)N NCs with 4.2 nm-thick QDisks.(b)Superimposed CL images with detection energies of 3.482 and 3.915 eV. (dark and bright colored images),(c)SEM image of GaN/(Al,Ga)N NCs measured by CL in (a) and (b).*

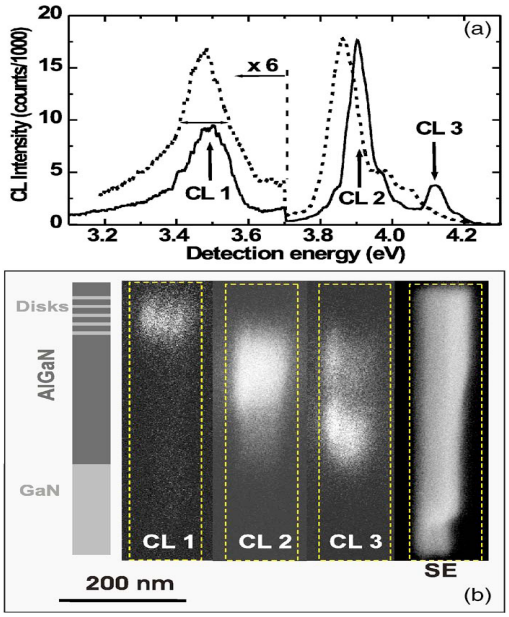

Figure 9*. (a) CL spectra of two single GaN/(Al,Ga)N NCs at 6K.(b) CL images and SEM image of the single NC represented by the solid line in (a) at 6K. The detection energies used for CL imaging are marked by arrows in (a).*

CL spectra of figure 9.a originate from two single NCs of the same sample, as shown in figure 8. The FWHM of the QDisk-related CL bands is smaller (about 130 meV) compared with that in figure 8.a, but is still much larger than the one corresponding to quantum well (QW) spectra (~ 20 meV). The pictures CL 2 and CL 3 reveal that the thick (Al,Ga)N layer of the NC has various regions with different optical emission energy, indicating an inhomogeneous distribution of the AlN mole fraction along the NC maybe caused by strain arising from the lattice mismatch between the GaN base and the thick (Al,Ga)N layer of the NC.

Therefore an averaging over many NCs results in a broad (Al,Ga)N-related CL spectrum, as shown in figure 8.a. Concerning the spectral broadening of the QDisk CL, rough interfaces can be ruled out, since high-resolution transmission-electron-microscope (TEM) investigations (not shown) revealed smooth (Al,Ga)N/GaN/(Al,Ga)N interfaces.

According to theoretical studies a considerable contribution to the broadening of the QDisk luminescence is expected to be an inherent property of mesoscopic structures such as the investigated QDisks [21], due to an inhomogeneous lateral strain distribution induced by the large surface-to-volume ratio. Besides the lateral strain distribution, other factors can additionally contribute to the CL spectra broadening such as band filling, inhomogeneous electric-field screening of the QDisks stack due to the surface depletion layer as well as variations among them.

In conclusion, while the luminescence lines of single homoepitaxial GaN NCs and GaN/ (Al,Ga)N QWs are as narrow as 2–5 and 20 meV, respectively, the FWHM of GaN/(Al,Ga)N QDisks spectra is as large as 80 meV, which can partly be caused by inherent optical properties of mesoscopic structures due to a laterally inhomogeneous distribution of strain. This interpretation is consistent with recently published theoretical results predicting unexpectedly low quantum efficiencies for thin GaN/(Al,Ga)N QDisks and

generally broad optical spectra caused by a laterally separated confinement of electrons and holes, a lateral inhomogeneous carrier distribution, and a laterally as well as vertically inhomogeneous screening of the electric field within the QDisks [22]

References

[17] J. Ristić, E. Calleja, M.A. Sánchez-García, J.M. Ulloa, J. Sáchez-Páramo, J.M. Calleja, U. Jahn, A. Trampert, and K.H. Ploog, Phys. Rev. B **68**, 125305 (2003).
[18] M. Yoshizawa, A. Kikuchi, N. Fujita, K. Kushi, H. Sasamoto, and K. Kishino, J. Cryst., Growth **189/190**, 138 (1998).
[19] J. Ristić, E. Calleja, A. Trampert, S. Fernández-Garrido, C. Rivera, U. Jahn, and K.H. Ploog, Phys. Rev. Lett., **94**, 146102 (2005).
[20] A. Kikuchi, M. Kawai, M. Tada, and K. Kishino, Jpn. J. Appl. Phys., Part 2 **43**, L1524 (2004).
[21] J. Ristić, C. Rivera, E. Calleja, S. Fernández-Garrido, M. Povoloskyi, and A. di Carlo, Phys. Rev. B**72**, 085330 (2005).
[22] U. Jahn, J. Ristić and E. Calleja, Appl. Phys. Lett., **90**, 161117 (2007).

D) Time-resolved spectroscopy on GaN nanocolumns grown by MBE on Si substrates

Even though the activity in the field of nanocolumnar heterostructures has been quite significant in the past decade, rather little attention has been devoted to the detailed study of optical properties of pure GaN NCs, in relation to their particular geometry. Indeed, most optical studies were aimed at characterizing the crystalline and chemical quality of the NCs since quantum confinement effects, in single NCs, were neither expected nor convincingly observed, due to the large diameter of the NCs, compared to the excitonic Bohr radius. This work presents the results of time-integrated and time-resolved photoluminescence (TI- and TR-PL) studies performed on GaN NCs grown on Si substrates, discussing some original features of excitonic emission spectra that differ from those of GaN compact epilayers.

The studied GaN NCs were grown by PAMBE on bare Si (111) and Si (001) substrates far below stoichiometric conditions (III/V ratio <<1). The exceptional crystalline quality of the NCs was verified previously by TEM and RS studies, proving that they are strain-free. Concerning their morphology, figure 10 shows SEM micrographs for two samples, together with the corresponding continuous-wave PL spectra. In general, SEM reveals arrays of well separated NCs, aligned along the *c* direction, whatever crystallographic plane of the substrate used. Such measurements provided a proper estimation of the average NC radii. Figure 10 also suggests a possible correlation between the PL spectra and the sample morphology.

Figure 11 shows the TI-PL spectra taken from 8 to 200 K for a NC sample with average diameter of 25 nm. What really changes among samples is the intensity ratio between the dominant lines, at 3470.0±0.1 and 3448.5±0.2 meV. In addition, weaker lines are observed at 3476.9±0.4 and 3485±1 meV. The relative intensity increase of these higher energy lines with temperature with respect to the line at 3470.0 meV suggest that they correspond to the free excitons *A* (FXA) and *B* (FXB), respectively.

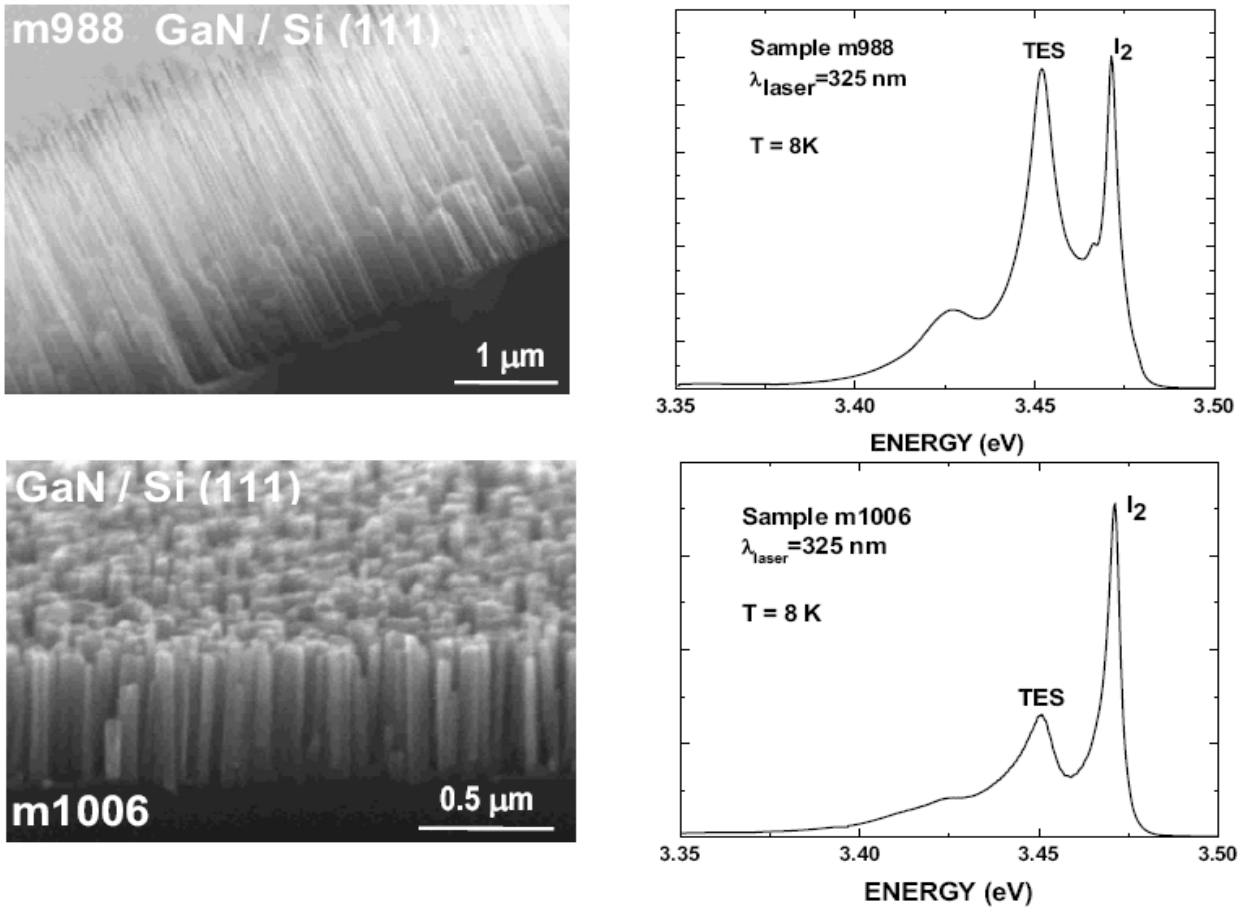

Figure 10. *SEM images of GaN NCs grown on Si(111) substrates with respective continuous-wave PL spectra excited by laser radiation at 325 nm. The NC diameters are much smaller in sample m988 (15 nm), and the PL line at 3.45 eV is also much more intense than in sample m1006 (24 nm).*

The peak at 3470.0 meV is then readily assigned to the so-called I_2 recombination of *A*-exciton bound to a neutral donor (D°X). As already noticed,6 these energies for bound and free exciton transitions correspond to fully unstrained GaN [17] which seems contradictory with the somewhat large linewidths (FWHM of ~5 meV, typically) observed. We will comment later in this work that these linewidths may have an intrinsic origin, not related to strain. Due to these linewidth values, it is difficult to assign the I_2 line to a specific donor (Si or O).

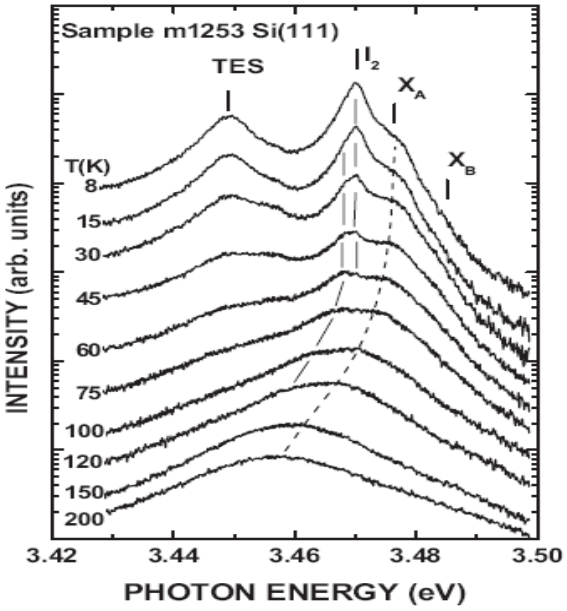

Figure 11. *Evolution with temperature of the TI PL spectrum (sample m1253) in the excitonic region. The log scale allows to see free exciton transitions at 3.477 and 3.485 eV.*

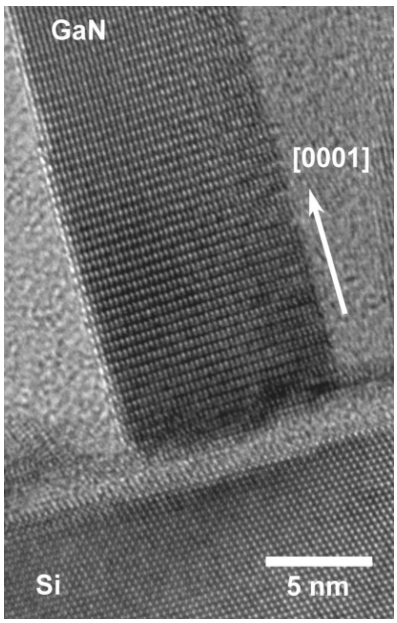

Figure 12. *Cross-sectional TEM image of a GaN NC epitaxially aligned to the Si(111) substrate.*

Nevertheless, we assume that the dominant donor be silicon [24] given the nature of the substrate. In fact, between lattice temperatures of 15 and 45 K, due to less efficient thermal detrapping of the exciton, a second line appears on the low-energy side of the main I2 line that certainly relates to a deeper donor.

Concerning the 3448.5 meV line, the evolution of its intensity with temperature follows that of I_2, confirming its excitonic nature. Moreover, since the LO-phonon energy in GaN is 91 meV, this line cannot be assigned to a LO-phonon replica of excitonic lines. Weak E_2-phonon- assisted replicas are sometimes observed 17.6 meV below the I_2 line [25] which is far from the energy separation of 21.5±0.3 meV between the I_2 and 3448.5 meV lines. The origin of the 3448.5 meV transition is yet to be ascertained, in spite of several PL studies carried out on similar types of structures [26,27]. The position of this line relative to the I_2 one coincides with the so-called two-electron satellites (TES) of the donor-bound exciton line, in agreement with several reports [24,25,28]. Contrary to Ref. 27 we discard the possibility that this line corresponds to the so-called *Y*1 transition assigned to inversion domains in N-face GaN, because our NCs have no extended defects (figure 12) and recent studies by convergent beam electron diffraction have established that they grow with Ga polarity [29]. Finally, the energy position of the line we observe here does not show any energy shift with the excitation density (see Fig. 9.b in Ref. 26), unlike what is reported for the *Y*1 line. Therefore, we assign the 3448.5 meV luminescence to the TES.

In spite of this assignment, two points remain to be explained: (i) the above-mentioned large linewidths, unusual for such a high-quality unstrained GaN and (ii) the unusually high relative intensity of the TES line, in comparison to the I_2. First, we observe for both I_2 and TES a typical FWHM of 5 meV. Yet, the studied samples exhibit a very high crystalline quality and are unstrained. Since these structures present a large surface-to-volume ratio, we believe that surface effects have to be taken into account.

To support this suggestion, we remark that the energy and the wave function of the n=1 level of a donor are perturbed if the last lies from the surface less than its Bohr radius, a_D (3 nm for GaN). Without calculation, we understand that n=2 states, having a radial envelope function decreasing like $\exp(-r/2a_D)$, will be affected when the nucleus approaches the surface by typically less than $\sim 2a_D$, i.e., ~6 nm in GaN. The same reasoning stands for the D°X complex: the influence of the surface will be significant for a donor-to-surface distance smaller than the typical values for electron-nucleus and hole-nucleus distances.

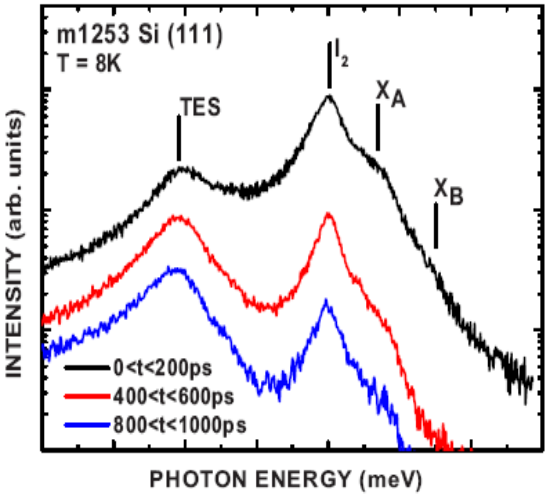

Figure 13. *Time dependence of PL intensities of the X_A, I_2, and TES lines at 8K .*

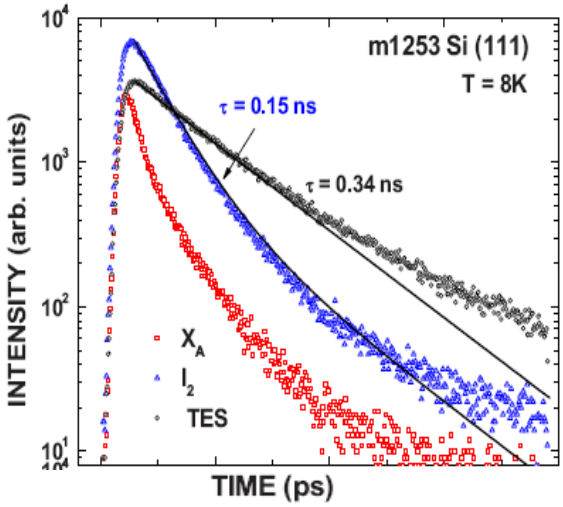

Figure 14. *Evolution with time of PL spectra at 8K. The domination at short delays of the I2 line is shown.*

When the donor nucleus lies within a surface layer some ~7 nm thick, the energies of the ground and excited states of the D°X and of the D° are modified. Therefore, since the donor positions are statistically distributed in this surface layer, the transition energies related to these donors are distributed too. For NCs with a radius of 15 nm (30 nm) the volume of this surface layer constitutes 71% (41%) of the total volume, and the random distribution of donor sites may be an *intrinsic* origin of the broadening of all PL lines involving donors. Notice that in a typical PL experiment on GaN compact layers, the penetration depth of the excitation laser is about 100–200 nm, thus reducing the surface-layer volume to 3%–7% of the overall probed volume.

Concerning the unusually intense TES lines, we suggest that the proximity of a donor to the surface may deform the D°X and D° envelope functions to perturb the relative probabilities of the different allowed transitions. In other words, it is believed that the favored recombination channels of donor-bound excitons depend on the position of the donors within the NCs. A donor situated in the NC core is equivalent to those in regular epilayers, i.e., the D°X recombines preferentially into the $D°_{n=1}$ (1*s*) state and seldom into the $D°_{(n=2)}$ state. On the other hand, when the donor lies close to the surface layer defined above, the deformation of envelope functions of *all* states for the initial D°X and for the final D° would increase the relative probability of involving donor excited states.

Paskov *et al.* [25] observed that the TES (D°X:2*s*) shows a slower decay than the I_2 ($D°X_A$:1*s*) line. They attributed this unexpected behavior to the possibility of different sites for the donor nucleus, where the respective dynamics of TES and I_2 lines could be different. In our NC structures we also observe that the apparent decay of the TES luminescence is always slower than that of I_2 (Figs. 13 and 14). This is why the PL signal of the TES dominates the spectrum after a few hundreds of picoseconds.

To explain this result, we have developed a core-shell model that relies on donor position dependent dynamics of the two principal donor-related excitonic transitions. The good agreement between the model and experiments confirms that the smaller the NC radius, the larger the average influence of the surface on excitonic transitions. We believe that this influence manifests itself through the alteration of the wave functions of the D°X and D° states involved. This simultaneously explains slight fluctuations in energies (thus large linewidths) and modified relative probabilities for the I_2 and TES recombinations. Thorough calculations of all quantum states of D°X and D° as a function of the distance to the NC surface are needed to quantitatively support our conclusions [30].

References

[23] K. Kornitzer, T. Ebner, K. Thonke, R. Sauer, C. Kirchner, V. Schwegler, M. Kamp, M. Leszczynski, I. Grzegory, and S. Porowski, Phys. Rev. B**60**, 1471 (1999).

[24] J.A. Freitas, W.J. Moore, B.V. Shanabrook, G.C.B. Braga, D.D. Koleske, S.K. Lee, S.S. Park, and J.Y. Han, Phys. Status Solidi (b) **240**, 330 (2003).

[25] .P. Paskov, B. Monemar, A. Toropov, J.P. Bergman, and A. Usui, Phys. Status Solidi (c) **4**, 2601 (2007).

[26] E. Calleja, M.A. Sánchez-García, F.J. Sánchez, F. Calle, F.B. Naranjo, E. Muñoz, U. Jahn, and K. Ploog, Phys. Rev. B**62**, 16826 (2000).

[27] L.H. Robins, K.A. Bertness, J.M. Barker, N.A. Sanford, and J.B. Schlager, J. Appl. Phys. **101**, 113506 (2007).

[28] M.A. Reshchikov and H. Morkoç, J. Appl. Phys., **97**, 061301 (2005).

[29] D. Cherns, L. Meshi, I. Griffiths, S. Khongphetsak, S.V. Novikov, N. Farley, R.P. Campion, and C.T. Foxon, Appl. Phys. Lett., **92**, 121902 (2008).

[30] P. Corfdir, P. Lefebvre, J. Ristić, P. Valvin, E. Calleja, A. Trampert, J.D. Ganière, and B. Deveaud-Plédran, J. Appl. Phys., **105**, 013113 (2009).

6.2 Materials, Processing, Strain Issues and Performance at High Temperature of AlGaN/GaN HEMTs[2]

Progress in AlGaN/GaN high-electron-mobility transistors (HEMTs) has been really remarkable in the last decade. Power efficiency, breakdown voltage and frequency performance have been steadily improving. Device power densities larger than 40 W/mm at 4 GHz, power gain at frequencies beyond 200 GHz and single devices delivering more than 200 W have been achieved [1]. Commercialization of HEMTs has brought the need for device failure studies, and for a better understanding of the physical mechanisms involved. The electrical reliability of GaN-based HEMTs is critical issues for the wide-spread use of this technology, but neither materials growth nor processing details are mature yet.

In this context, we have been studying a number of issues related to materials, processing and strain in relation to GaN HEMT stability and degradation. One of the objectives has been to span the relation between expected device performance, estimated from as-grown heterostructures (HS) properties, and the obtained final HEMT characteristics. A second objective has been to contribute to delineate *those failure mechanisms more intrinsic in the nitrides,* from those ones derived from general device processing. In non-intentionally doped GaN HEMTs, surface properties, layer strain and polarization fields and are key factors in determining the final channel electron concentration.

Nitride HEMTs are expected to drive high currents at high voltages, thus producing self-heating which may degrade device performance. Some channel temperature simulations of HEMTs on SiC have been carried out which confirm the important role of the substrate and the operation conditions. On the other hand, devices based in these wide band materials are promising for *high temperature electronics*. Furthermore, temperature is an important variable to study a number of phenomena, such as the presence of defects, and becomes an important tool for reliability tests. Therefore, *a significant research effort has been made at ISOM for the thermal characterization of HEMT devices.* We have performed DC, small signal and power analysis, from ambient temperatures (RT) up to 600 K.

Our studies at ISOM have been carried out under the KORRIGAN initiative (*K*ey *Or*ganization for *R*esearch in *I*ntegrated circuits in *GaN* technology), a large European Programme (29 partners from 7 countries) dedicated to the development of GaN technology for defense applications launched in 2005. Our laboratory has been involved in several research areas such as materials, processing and reliability. At the Spanish level, the strong collaboration with the UAM (Prof. C. Palacios and Prof. A. Climent) for ion-beam analyses has been very valuable for present studies. Heterostructures and devices used in this study were provided by different suppliers, mainly 3-5 Labs, Picogiga, Qnetiq and Selex.

Experimental studies have been conducted using a full set of AlGaN/GaN HS wafers and HEMT devices with the same approximate nominal layer structure, a 20-30 nm-thick undoped AlGaN barriers (28-36%Al), on a high-resistivity GaN buffer layer, and grown by MOCVD on 4H SiC or sapphire substrates, or by MBE on Si or SiC substrates. Ni/Au Schottky gates were mainly used. Besides, some material characterization has been made in structures using lattice-matched AlInN barriers grown by MOCVD and in HS with AlN spacer.

Heterostructure Wafer Assessment

Standard characterization and mapping procedures has been usually made in as-grown AlGaN/GaN HS wafers (HRXRD, AFM, PL, Hg-probe C-V, non-contact resisitivity, etc.). Complementary, ion beam analysis (IBA) techniques have been used to address: a) absolute methods for Al composition determination in the AlGaN barriers, and comparison with HRXRD characterization; b) the presence of H in such wafers,

[2] *Contact persons: Elías Muñoz elias@die.upm.es and Fernando Calle calle@die.upm.es*

for the various growth techniques; c) detection of phase separation in AlInN/GaN HS; d) comparative role of GaN and AlN nucleation layers in wafers containing AlN spacer.

X-ray diffraction (XRD) analysis is frequently used as a routine technique for the determination of the Al incorporation, x, in $Al_xGa_{1-x}N$ layers. This method provides indirect information about the Al content, and another disadvantage is that an Al profile analysis is not straightforward and may require tedious techniques. Our motivation was to conduct a comparative study about the determination of the Al content by XRD and by other methods providing more absolute values of composition. IBA techniques are one of the most powerful techniques to assess compositional depth profiles in thin films and coatings. Among IBA methods, Rutherford backscattering spectrometry (RBS) can provide additional structural information by performing RBS in channelling mode (RBS/C). Heavy-ion elastic recoil detection analysis (HI-ERD) can be used to increase the Al sensitivity due to the lack of signal overlap. Samples with different Al contents, $0.1 < x < 0.3$, have been studied. Our results indicate *that XRD is quite reliable in the determination of the average Al content within the layer*. This study shows that the values extracted from XRD data *are averaged over the sampling depth*. Also, a slight overestimation of the average content is found when strain is present in the films [2].

The incorporation of H in AlGaN/GaN HJ grown by H-free (N-plasma MBE) and by H-containing precursors (MOCVD and ammonia based MBE) was determined by nuclear reaction analysis (NRA). It was shown that *the presence of H is independent of the growth technique,* and its profile decreases monotonously from the surface with *no accumulation* detected at interfaces, to become negligible at the GaN layer. Its origin seems to be related to post-growth incorporation. It was also found that *H surface concentration depends on sample topography and quality* [3].

AlGaN/GaN HEMT heterostructures grown on sapphire using AlN nucleation layers have a *narrower GaN FWMH than those with GaN*. Rutherford backscattering spectrometry experiments in channeling configuration (RBS/C) were performed along <0001> and <-2113> axes of the wurtzite structure, to determine the strain with depth resolution (profile). Complementary reciprocal space maps (RSM) were obtained for (0004) and (10-15) planes. Results demonstrate that *dislocations and defects near the sapphire-nucleation layer interface were highly reduced when using the AlN NL*, although a very high quality monocrystal was found for the remaining upper part of the layer [4].

Surface-Related Studies

Two sets of problems have been studied: a) AlGaN/GaN HEMT heterostructure electrical characteristics vs. AlGaN surface cleaning and treatments during processing; and b) surface treatments before HEMT surface passivation. For the first case, we selected three representative cleaning procedures and surface treatments that are analogous to the ones HEMT wafers suffer during the various device fabrication steps: organics cleaning, exposure to N_2-plasma atmosphere and annealing treatment (RTA). After environmental exposure, AlGaN surfaces are studied by X-ray photoelectron spectroscopy (XPS). Carbon and oxygen contamination are found, [C] = 10-30% and [O] = 5-15%. The presence of carbon contamination is established as a key factor on the AlGaN surface. The AlGaN surface contamination amount has no correlation with the substrate used for HEMT heterostructure growth. After N_2-plasma surface treatment, a strong contamination reduction is achieved, down to [C] = 5%. Capacitance-voltage Hg-profiles, after exposure to N_2-plasma, show a reduction of the 2DEG carrier concentration, $\Delta n_s = (-2.4 \pm 0.3)\ 10^{12}\ cm^{-2}$, and the pinch off voltage, $\Delta V_{th} = (1.3 \pm 0.4)$ V. On the other side, the RTA process increases the 2DEG charge density, $\Delta n_s = (1.4 \pm 0.3)\ 10^{12}\ cm^{-2}$. From XPS results, the stronger power of the N_2-plasma, aside from the RTA, *reveals itself as a great carbon surface cleaner*, reducing carbon concentration up to a (70 ± 6) % [5].

Surface passivation of HEMT devices has been recognized as a critical processing step to enhance channel 2DEG concentration and to alleviate the current collapse problem. The problem has many variables, and we have focused on using SiN as passivation layer (the most widely used solution) and to study *surface pre-treatments just prior to the SiN deposition* step, mainly using nitrogen plasma. The impact of in situ low power plasma pre-treatment prior to silicon nitride (SiN) deposition was investigated in AlGaN/GaN HEMT and in GaN metal-insulator-semiconductor (MIS) test structures. In the standard passivation processing, SiN was deposited at 300 ºC in a conventional RF (13.56 MHz) Plasma-Enhanced Chemical Vapour Deposition (PE-CVD) system. SiH_4 and NH_3 were used as precursors, obtaining a slightly N-rich SiN layer with n=1.83 and εr= 7.0, as determined by ellipsometry [6].

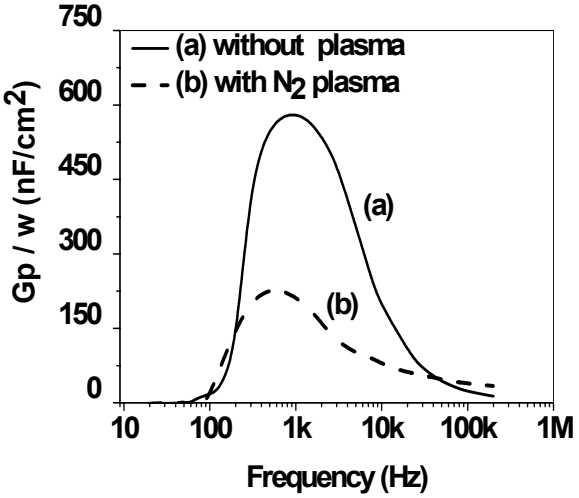

Figure 1. *n-GaN/SiN MIS parallel conductance G_p/w versus frequency (0 V bias) without (a), and with (b) nitrogen plasma treatment.*

Prior to SiN deposition, the treatment investigated was an in situ nitrogen plasma, at 200 ºC for 1 min at low power (60 W), after a wet cleaning with NH_4OH at 50 ºC for 15 min. Metal-insulator-semiconductor structures were also fabricated on n-type GaN with and without the N_2 plasma pre-treatment before the SiN deposition. Pulsed measurements on HEMT devices reveal *a strong reduction of interface traps after the plasma treatment*, with trapping-detrapping time constant in the wide range from 1μs to hundred of ms. This nitrogen plasma treatment on transistors enhances the mitigation of current collapse and gate lag effects by SiN passivation. A *60% lower interface charge density was obtained on MIS structures with N_2 plasma pre-treatment* with respect to those without such pre-treatment (see figure 1) [7].

Strain-Related Device Degradation

The original strain present in the layers of as-grown HS may be modified during device processing, or during device operation due to the presence of high electric fields. Thus, two sets of problems have been studied. The case of electric field-induced strain degradation via the converse piezoelectric effect has been addressed, from a *theoretical point of view for the first time*. Besides, some specific electrical stress experiments in fully-off HEMT were conducted. The idea of strain relaxation caused by the high electric fields present in GaN HEMT, blaming to the piezoelectric effect, was originally proposed by *del Alamo's* group based on experimental findings in off-state reliability studies [8]. This failure mechanism would be *intrinsic* to strained GaN devices and it received a priority attention at ISOM. As a second source of strain changes, we have tried to contribute to elucidate if certain processing steps or thermal storage tests may induce strain relaxation in the HS. Along this line, most of our experimental studies have been conducted in relation to the effects on layer strain of the rapid thermal annealing (RTA) step needed for ohmic contact formation.

To determine self-consistently the strain of each layer in the HEMT, the approach used is the minimization of the electric enthalpy functional, including the converse piezoelectric effect (CPE effect). The internal stored elastic energy is then determined in each layer, as a function of the vertical and horizontal electric field. A critical electric field is obtained related to the critical thickness of each layer, or to its electrical breakdown voltage. Such *critical field* would mark the onset of layer relaxation and defect formation. We observe that the electric field increases the strain in the GaN buffer, whereas the opposite behaviour is found in the $Al_{0.25}Ga_{0.75}N$ barrier. This result reflects the fact that the piezoelectric effect is *sensitive to the direction of the electric field*. Therefore, degradation by strain relaxation will be possible in this case for the GaN layer in off-state operation (applied electric field in the [0001] direction) at high

reverse voltages, since GaN is under compressive strain. In contrast, the same *applied electric field will reduce the out-of-plane dilation in the AlGaN layers under tensile strain*. Namely, we found that *the overall strain decreases as gate-source voltage (V_{GS}) becomes more negative*, i.e. for V_{GS} decreasing in the off state, whereas the opposite behaviour takes place for positive values. *The piezoelectrically-induced degradation is only expected under on-state operation*. Conclusions presented here were estimated for a nominal transistor structure as that used in project KORRIGAN (i.e., 28% Al content in the barrier and 30 nm barrier thickness). Note that the maximum variation of strain for the source and drain sides is different when $V_{DS} \neq 0$ [9].

The degradation of AlGaN/GaN passivated HEMTs, with different gate lengths and distances to drain and source, was experimentally studied by stressing independently V_{GS} from -10 to -35 V (hereafter test V_z) and V_{DS} from 0 to 45 V (hereafter test V_x), under off-state conditions in steps of 5 V. Gate (I_G) and drain (I_D) currents were monitored during all experiments in order to detect abrupt changes. Following each test, *I-V* characteristics were recorded both in AC and DC to assess the impact of the electric field stress on the on-state HEMT operation. $I_G > I_D$ was found throughout all tests, indicating that no signs of drain-source/gate-source breakdown were detected.

In relation to *the effects of HEMT processing steps* on the electrical and mechanical properties of AlGaN/GaN structures, two AlGaN/GaN wafers (hereafter wafers A and B) were grown on SiC with the same structure. As an *ad-hoc* experiment in our lab, similar HRXRD and C-V characterizations were performed in: 1) as-grown HS; 2) after ohmic contact deposition and RTA; 3) after surface cleaning and Schottky gate deposition; 4) after surface treatment and SiN passivation. The extended ohmic contact consists of Ti/Al/Ti/Au (20/80/50/55 nm), deposited and annealed during 45 s at 850 ºC in a nitrogen atmosphere. Schottky contacts with a circular geometry were made of a Ni/Au bilayer (30/170 nm), with three different diameters around 1020, 420 and 220 µm, respectively. Prior to both metal depositions, the surface was cleaned using an oxygen plasma treatment followed by an HF bath (1:10) during 10 s. Finally, the insulator used in the passivation was a 120-nm-thick SiN layer deposited by plasma-enhanced chemical-vapor deposition, with a previous N-plasma treatment at 60 W for 60 s (step 4). The electrical characterization was performed by *C-V* measurements using either an Hg probe with a 735-µm-diameter circular Schottky contact on the as-grown wafer, or with the fabricated Schottky diodes. The XRD characterization was carried out using a Bede Scientific Instruments D3 diffractometer with a minimum spot size of 2 mm diameter. XRD θ/2θ scans for the 00.6 reflection were recorded in three points for each sample in order to account for any spatial inhomogeneity [10].

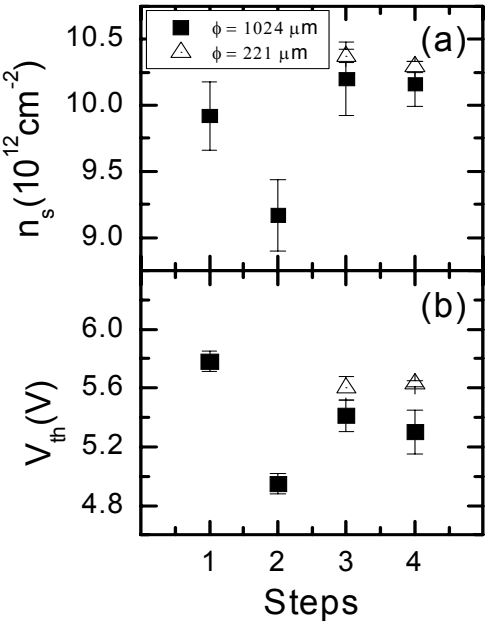

***Figure 2**. (a) C-V characteristics for wafer A, (b) 2DEG density (n_s), and carrier concentration profile versus depth (x_d).*

Figure 2 summarizes the main electrical parameters of the heterostructure, n_s and threshold voltage (V_{th}), along the different processing steps for wafer A. The results of *X-ray characterization show that the strain state of the AlGaN and GaN layers is* modified by the ohmic contact deposition and subsequent annealing, as well as by the SiN passivation.

From XRD results for the wafer A in Steps 1 (as-grown wafer) and 4 (after passivation), the AlGaN peak position largely shifts from ~1.619º to ~1.670º for Steps 1 and 4, respectively. Similarly, smaller shifts in the GaN peak position are detected from ~3.433º to ~3.456º for Steps 1 and 4, respectively. These results can be related to structural changes according to Bragg's law for the 00.6 reflection as $c = 6\lambda/2\sin\theta$, where c denotes the lattice constant of the c axis, λ is the x-ray wavelength (1.54056 Å for Cu $K_{\alpha 1}$ radiation), and θ is the diffraction angle. In both cases, the tensile strain for the AlGaN layer decreases whereas the residual compressive strain in the GaN layer is consistently increased in the free-contact area. This change has impact on the carrier concentration in the 2DEG formed in the

channel due to piezoelectric coupling. However, we show that the difference in the chemical composition (residual contamination) on the surface is the main factor explaining the reduction of channel carrier concentration observed in capacitance-voltage measurements, with a variation as large as ~2×10^{12} cm^{-2} [10].

HEMT Performance at High Temperatures

DC behaviour. The thermal evolution of the main HEMT parameters, such as drain and gate currents (I_D, I_G), transconductance (g_m), and source and drain parasitic resistances (R_S and R_D), has been evaluated for several substrates. As T_{amb} increases, I_D and g_m decrease due to the rise of the optical phonon scattering, which produces a reduction in the electron mobility. This effect has been proved either by means of electron mobility simulations, which take into account the main scattering mechanisms, and also through TLM measurements, from which the electron mobility has been extracted [11]. On the other hand, the evolution of I_G with temperature is more related to the stability of the gate contact. I_G usually increases slightly as the device is heated for stable Schottky contacts, but it can also decrease when the contact is not well annealed, or increase significantly when the contact degrades.

The substrate thermal conductivity (θ) also affects the high temperature device performance [12]. The typical substrates used for AlGaN/GaN HEMTs are sapphire (θ = 0.35 W/cm·ºC), Si (θ = 1.57 W/cm·ºC), and SiC (θ = 3.3 W/cm·ºC). At RT, HEMTs on SiC show better performance than the HEMTs on Si or sapphire, thanks to their higher thermal conductivity which mitigates the self-heating effect. Nevertheless, as T_{amb} rises, the substrate effect is reduced since its thermal conductivity becomes lower and mainly because the dissipated power by the transistor is smaller. Therefore, DC measurements in HEMTs on Si and sapphire with similar layout and processing show almost the same performance at 600 K.

Other parameters which influence the high temperature behaviour are the gate length (L_G) and the distance between contacts [12]. The decrease of DC parameters with temperature, similar to the reduction in the drift mobility, is more important for HEMTs with higher L_G and/or drain-source distances. This observation can be explained by the different intensity of the electric fields under the gate as a function of L_G. Higher L_G means lower electric fields under the gate, so that the devices work in a linear regime in terms of drift velocity vs electric field curves. Nevertheless, as distances are shorter, the fields increase and the transistors work in the saturation region, where the thermal dependencies are less important.

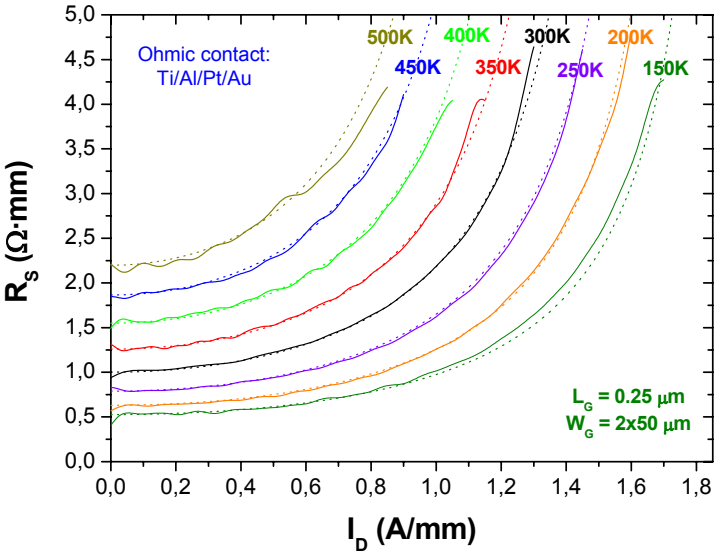

***Figure 3**. Evolution of RS with ID for Tamb from 150 K to 500 K, in a HEMT device with LGS = 1.3 µm and LDG = 2.2 µm. Measurements are plotted in solid lines and simulations in dot lines*

The behaviour of R_S and R_D as a function of T_{amb} and I_D has also been studied. For low I_D, both resistances increase with T_{amb}, following the trend of the contact and sheet resistances. In this way, increments in R_S and R_D up to 60% between RT and 500 K have been measured in HEMTs on SiC. As I_D increases, at a fixed T_{amb}, parasitic resistances also rise in a non-linear way. A model which predicts R_S and R_D behaviour with both T_{amb} and I_D dependences has been proposed, showing a good agreement between simulations and data (Fig. 3).

Small signal assessment. F_T and f_{max}, as well as the small signal equivalent circuit, have been calculated by means of S-parameter measurements from 0.25 GHz to 20 GHz [13, 14]. Typically, in a HEMT on SiC with a L_G = 0.25 µm, the maximum of f_T diminishes ~35-40% from RT to 600 K (see Fig. 4). A similar trend is observed for f_{max}. The reduction in both frequencies is related to the DC behaviour explained above. The main elements of the small signal circuit have been analyzed. The intrinsic transconductance ($g_{m,int}$) decreases ~30% between RT and 600 K, due to the reduction in the effective velocity of the electrons in the channel. On the other hand, C_{gs} follows a slight increase with T_{amb}, probably linked to the changes induced in the permittivity of both the passivation layer and the AlGaN barrier. C_{gd} shows a clear decrease for low currents as the devices are heated, likely related to the presence of traps. The other parameters of the equivalent circuit can be considered thermal independent, except for R_{ds} which increases with T_{amb}.

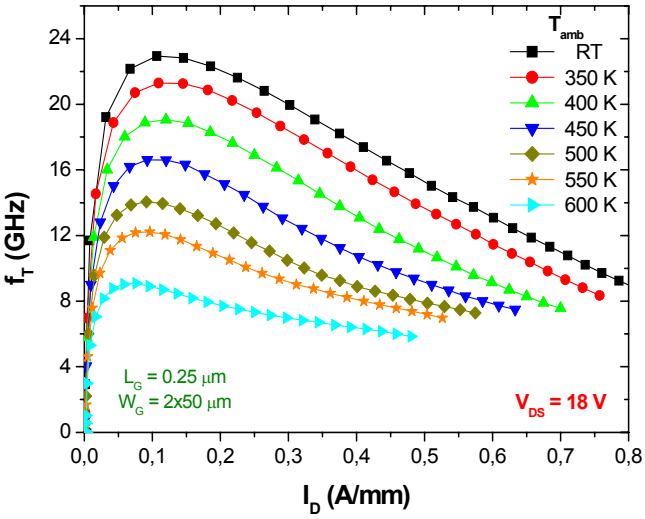

***Figure. 4**. Thermal evolution of f_T for different I_D at V_{DS} = 18 V. T_{amb} goes from RT (296 K) to 600 K, each 50 K*

Power measurements. Once the transistor is studied under DC and small signal regimes, it is necessary to complete its analysis showing its response under a continuous wave with a variable input power. In this way, P_{out}, G_p and PAE parameters have been extracted as a function of T_{amb}. For example, P_{out} decreases around 60% from RT to 600 K for an input power of -8 dBm. Besides, measurements with two and several tones are in process in order to evaluate the intermodulation parameters.

Instabilities and Traps. Two problems linked with trapping effects and trap generation have been addressed. First, the presence of *kinks in the output characteristics* of a significant number of HEMT has been studied. It was considered if such kink effects may be related to HEMT reliability [15]. The *kink* is the step-like behaviour of the I_D at the end of the linear region that appears in some transistors, linked to the trapping and releasing of traps. This effect can be observed in several transistors at RT, increasing its amplitude between RT and 375 K. For higher temperatures, the *kink* decreases and disappears beyond 500 K. This thermal behaviour of the *kink effect* depends on the specific transistor and the V_{GS} applied. In this way, the maximum *kink effect* is found for V_{GS} between -2 and -4 V in the transistors under study. This kink has been related with the deep levels responsible for the yellow band observed by cathodoluminescence.

A second study refers to investigate *thermal storage stress tests* in AlGaN/GaN high electron mobility transistors (HEMT) in order to evaluate Ni/Au gate stability, trap generation and device reliability. $Al_{0.3}GaN_{0.7}N$/GaN heterostructures grown on SiC by metal-organic chemical vapour deposition (MOCVD) were used in this work. Ni/Au (30/300 nm) bilayer was used for the gate Schottky contacts. DC and pulsed I-V measurements (gate pulse width 500 µs, 10 ms period) from -7 V (1 V lower than pinch-off) to 0 V (open channel) were used to characterize AlGaN/GaN HEMT before and after the tests. Complementary gate-drain I-V and C-V-T-f, from -263ºC to 277ºC measurements were carried out in FAT-FET devices.

Devices submitted to a short thermal storage up to 300 ºC (steps of 50 ºC and holding 30 min at each temperature) showed a slight reduction of the gate reverse current, and barrier height shows a small increase after the test. Similar results were observed in circular equivalent Schottky diodes on AlGaN/GaN HS after a short test at 300 ºC for 600 h in a conventional oven under air atmosphere. Above results seem to point that a *short baking is beneficial and enhances the Ni/Au Schottky gate contact quality.* Other pieces were submitted to different long thermal storage tests for 2000 h at 250ºC, 300ºC and 350ºC, respectively. After the long thermal storage test at 350ºC, gate barrier height decreased by 10%, and a detrimental degradation in HEMT characteristics was found in pulsed I-V characteristics. A dramatic degradation of the output characteristics

was present after the test, in particular near the knee voltage. The generated traps were characterized by high and low temperature capacitance measurements in FAT-FET devices.

Acknowledgements

This work has been carried out inside the KORRIGAN project (EU-FP6-MOU 04/102.052/032). The financial support of the Ministry of Defense of Spain-DGAM/SDG TECEN /CIDA is acknowledged.

References

[1] U.K. Mishra, L. Shen, T.E. Kazior, and Y.F. Wu, Proc. IEEE **96**, 287 (2008).
[2] A. Redondo-Cubero, R.Gago, F.González-Posada, U. Kreissig, M.A. di Forte Poisson, A.F. Braña, and E. Muñoz, Thin Solid Films **516**, 8147 (2008).
[3] F. González-Posada Flores, A. Redondo-Cubero, R. Gago, A. Bengoechea, A. Jiménez, D. Grambole, A.F. Braña, and E. Muñoz, J. Phys. D: Appl. Phys. **42**, 055406 (2009).
[4] V. Tasco, A. Campa, I. Tarantini, A. Passaseo, F. González-Posada, A. Redondo-Cubero, K. Lorenz, N. Franco, and E. Muñoz, J. Appl. Phys. **105**, 063510 (2009).
[5] F. González-Posada, J.A. Bardwell, S. Moisa, S. Haffouz, H. Tang, A.F. Braña, and E. Muñoz, Appl. Surf. Sci. **253**, 6185 (2007).
[6] A. Redondo-Cubero, R.Gago, M.F. Romero, A. Jiménez, F. González-Posada, A.F. Braña, E. Muñoz, phys stat. sol. (c) **5**, 518 (2008).
[7] M.F. Romero, A. Jiménez, J. Miguel-Sánchez, A.F. Braña, F. González-Posada, R. Cuerdo, F. Calle, and E. Muñoz, IEEE Electr. Dev. Lett. **29**, 209 (2008).
[8] J. Joh and J.A. del Alamo, IEEE Electron Device Lett. **29**, 287 (2008).
[9] C. Rivera and E. Muñoz, Appl. Phys. Lett. **94**, 053501 (2009).
[10] F. González-Posada, C. Rivera and E. Muñoz, Appl. Phys. Lett. **95**, 203504 (2009).
[11] R. Cuerdo, J. Pedrós, A. Navarro, A.F. Braña, J.L. Pau, E. Muñoz, and F. Calle, J. Mat. Sci.: Mat. Electron. **19**, 189 (2008).
[12] R. Cuerdo, F. Calle, A.F. Braña, Y. Cordier, M. Azize, N. Baron, S. Chenot, and E. Muñoz, phys. stat. sol. (c) **5**, 1971 (2008).
[13] R. Cuerdo, E. Sillero, M.F. Romero, M.J. Uren, M.-A. di Forte Poisson, E. Muñoz, and F. Calle, IEEE Electron Device Letters **30**, 808 (2009).
[14] R. Cuerdo, Y. Pei, F. Recht, N. Fichtenbaum, S. Keller, S.P. Denbaars, F. Calle, U.K. Mishra, phys. stat. sol. (c) **5**, 2994 (2008).
[15] R. Cuerdo, Y. Pei, Z. Chen, S. Keller, S.P. DenBaars, F. Calle, and U.K. Mishra, IEEE Electron Device Letters **30**, 209 (2009).

6.3 Microsystems and electroacoustic devices[3]

The technology processes available at ISOM allow the manufacture of materials, their technological processing, and the manufacture of electroacoustic devices. At present, ISOM has the capability to develop and manufacture surface and bulk acoustic wave devices (SAW and BAW) for microwave, RF and mobile communication systems used in a wide range of applications from consumer electronics to military applications. Besides, the simulation of the filtering characteristics of these devices is investigated. Most of the outstanding characteristics of SAW devices rely on the correct choice of the piezoelectric substrate material used for their fabrication. AlN layers combine a high sound velocity, a considerable electromechanical coupling and an outstanding thermal and chemical stability. However, the required heteroepitaxial growth of nitrides imposes the study of the acoustic propagation properties and the dispersion of the particular layered system. In addition, wave confinement may arise on these systems depending on the layer(s)-substrate combination. On the other hand, the semiconductor character and direct bandgap of nitrides enables the combination of SAW devices with electronics and optoelectronics. The ISOM has maintained during the last years an intense research activity on group III-nitride-based electroacoustic devices. In contrast to previous research, current efforts have been focused on the development of devices based on advanced new structures such as diamond based electroacoustic devices. In addition to this device development activity, attention has been paid to some basic aspects in such novel devices, with the double objective of understanding the physics involved and to propose new device concepts.

Surface and Bulk Wave electroacoustic devices

- **Surface Acoustic Waves devices (SAW)**

A SAW device structure consists on a film of piezoelectric material on top of which interdigital transducers (IDT) are fabricated. These transducers convert high frequency (GHz) electric fields into surface acoustic waves and viceversa. The input IDT converts the applied voltage into elastic perturbations that are propagated through the surface of the material until they reach the output IDT, which converts it into alternate voltage to the load. The figure shows how the elastic wave is excited efficiently when the frequency of the input signal verifies $f = v_{ph}/\lambda$, where v_{ph} is the propagation speed of the wave in the piezoelectric material and λ is the periodicity of the IDT. Almost all the materials employed are insulating, and they do not allow monolithic integration with other electrical components. On this issue, Nitrides, especially AlN, [1] present ideal characteristics for its operation in SAW structures; the use of thin films allows the integration of compact modules with other devices and the exploitation of new functions by combining them with detectors or HEMT structures. [2]

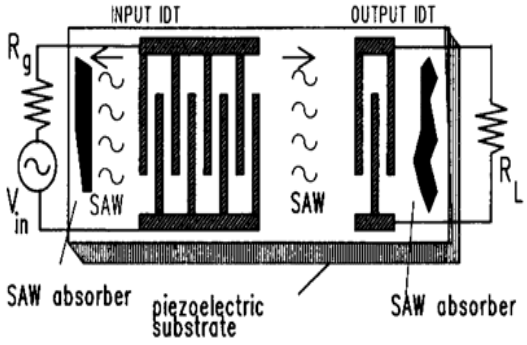

***Figure.1**. Principal of a SAW-Filter*

[3] *Contact person: Fernando Calle calle@die.upm.es and Gonzalo Fuentes gonzalo.fuenteso@upm.es*

• Film Bulk Acoustic Resonator, FBAR

FBARs resonators are made of a layer of piezoelectric material sandwiched between two metal layers. The request of mobile and LAN technologies require to develop FBAR between 3 and 6 GHz (C-band); Fujitsu has already manufactured at 5 GHz [3], and there are preliminary results of operation in the X and Ku bands (up to 18 GHz). Traditionally, electroacoustic devices, such as resonators, filters and delay lines have been fabricated on single crystalline piezoelectric substrates such as quartz, LiNbO3, LiTaO3, etc. For bulk acoustic wave (BAW) devices, the direct relationship between the frequency of operation and the thickness of the crystal i.e. f=d/2v where d= λ/2 is the device thickness, λ is the wavelength and v is the acoustic velocity, makes the use of single crystals impractical for mass produced devices operating in the microwave region. Thus, new materials with high acoustic velocities are desirable.

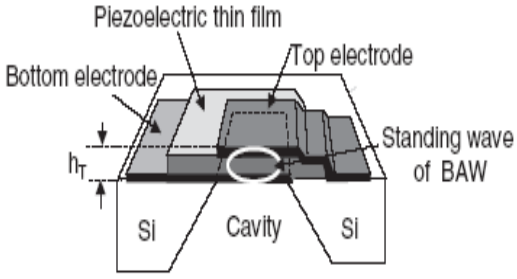

***Figure.2**. Bulk micromachined membrane type resonator*

Home built AlN reactive sputter deposition system

C-axis oriented AlN has a high acoustic velocity (12.350 m/s and 6.000 m/s for bulk and surface acoustic waves respectively), moderate coupling coefficient (6.5% for BAW and 0.8% for SAW), low leakage currents, as well as relatively high material Q of around 3.000 and in a wide process window. This makes AlN a very suitable material for the fabrication thin film acoustic devices. One of the primary quantities of interest for such devices is the quality factor, which to a large extent is determined by the acoustic losses. In polycrystalline films, these losses are larger than those in the single crystalline material due to the presence of grain boundaries and large concentrations of defects as well as due to the different in-plane orientation of the grains. When synthesized by reactive sputtering, thin film properties such as grain boundaries, defects or crystallographic orientation are strongly dependent on the texture and smoothness of the substrate material on which they are deposited. Thus, study and optimization of AlN growth on conducting thin films suitable for bottom electrodes is needed [4]. The results of the optimisation processes shown here can be used for the fabrication of Thin Film Bulk Resonators (FBAR) resonators of membrane type.

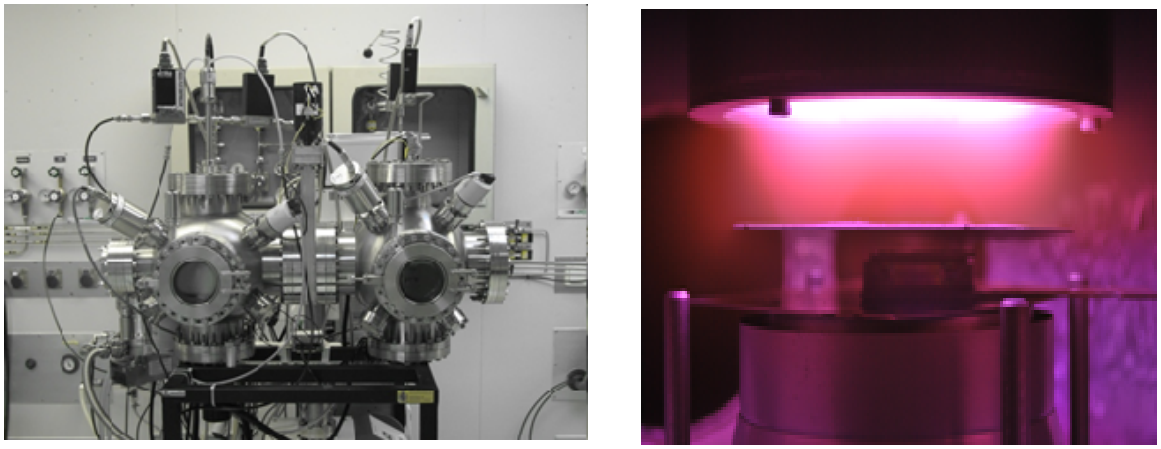

***Figure 3**. Home built AlN reactive sputter deposition system (left) and plasma discharge inside the AlN deposition chamber (right)*

The main parameters normally considered to have a direct impact on the degree of c-axis orientation of AlN thin films deposited by reactive sputtering are: a) Substrate temperature, b) Substrate lattice mismatch, c) Substrate bias, d) Film thickness, e) Base pressure, f) Target-substrate distance, g) Deposition rate, h) Gas flow ratio (Ar/N_2), i) Target power, j) Process pressure.

In order to study all this parameters in detail, a reactive sputter deposition system exclusively dedicated to AlN has been built at ISOM.

Cristallographic and structural characterization of AlN thin films

As an example, the properties of layered film structures consisting of a piezoelectric material layer (AlN) and a crystalline magnesium oxide (MgO) substrate have been examined. Highly textured AlN thin films have been deposited at ambient temperature by reactive sputtering onto MgO.The thickness of the AlN layer was of 1.5µm whereas the MgO substrate was 1mm thick. Standard one-port SAW resonators with Al metallisation have been subsequently fabricated and evaluated. Experimental results indicate that the fundamental as well as higher Rayleigh SAW modes are excited. X-ray diffraction analysis of the multilayer structure (AlN/MgO) indicates that the deposited AlN films were c-axis oriented with a Full Width Half Maximum (FWHM) of the rocking curve of the AlN-002-peak of 2.85°. Figure 4 shows the FWHM of the (0002) AlN peak of films deposited using several target powers under excess of Ar and N2, respectively. According to these results, it looks like the Ar/N2 gas flow ratio should be kept below 1.The film orientation was determined by rocking curve measu-rements using a Phillips X-PertPro MRD diffractometer.

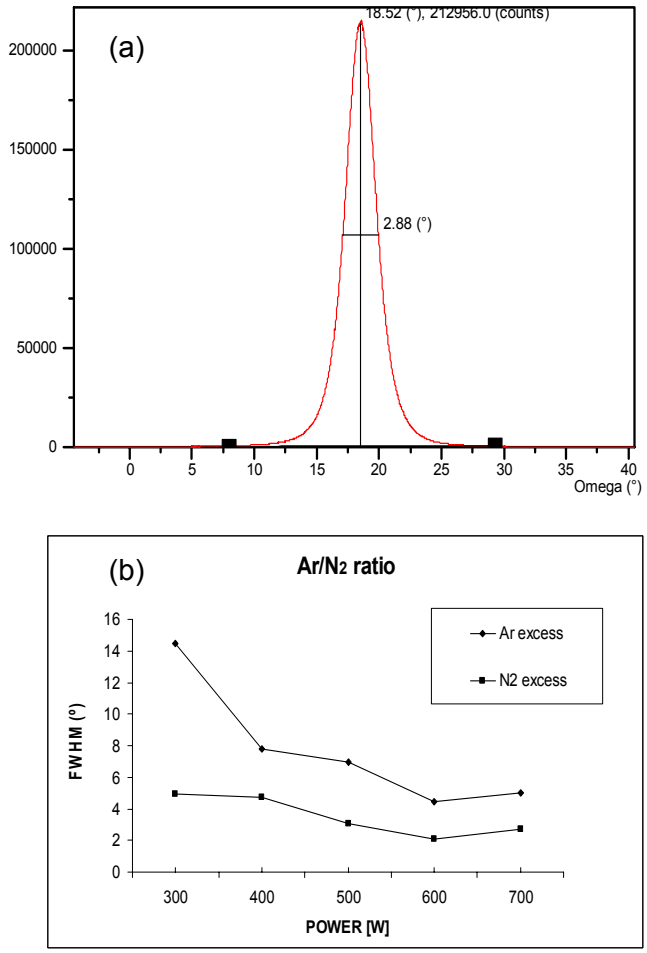

Figure 4. *(a) shows the FWHM of the (0002) AlN peak of films deposited on MgO substrates (b) shows the FWHM of the (0002) AlN peak of films deposited using several target powers*

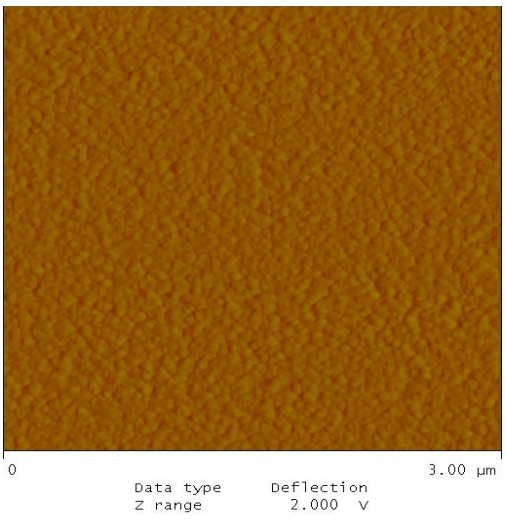

Figure 5. *2D AFM picture of highly oriented AlN deposited on on Silicon (111) at room temperature. Scan area is 3.0µm x 3.0µm, from left to right.*

We also took a look at the surface roughness of AlN films (grown on standard Si-(111) wafers coated with a 200nm Ti layer prior to the AlN deposition) as measured by Atomic Force Microscopy (AFM) [6]. The roughness of the Si wafer was not measured: while that of the Ti films was 2.591 nm for a scan area of 5x5 µm. Figure 3 visualizes AFM micrographs of the AlN surfaces. The AlN films deposited on both a thin Ti layer and the Si-(111) wafers were all 1 micron thick. As seen when comparing the RMS (root mean square) and Ra (variation from the surface average roughness) values in both tables for the different scan areas, surface roughness is slightly higher when the AlN is deposited on top of sputter deposited titanium. This observation agrees with another general observation confirmed by many researchers, namely that the quality of the AlN films is strongly dependent on the smoothness of the substrate and to a lesser extent to the crystallographic structure of the later [4].

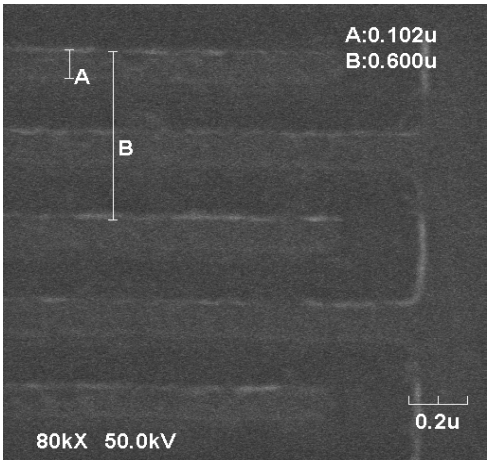

***Figure 6**. IDT with 100 nm wide elect rodes after lift-off.*

For optimized AlN layers synthesized at room temperature [7,8], a clear and continuously linear wave-like stripe pattern without terrace edges is found by AFM (see figure 5). For comparison, surface roughness measurements of AlN films grown on Si-(111) were also analized.

Nanolithography

Part of our work deals with the micro-fabrication process developed to manufacture nano-IDTs (interdigital transducers) to be used in surface acoustic wave (SAW) applications [5]. The combination of electron-beam (e-beam) lithography and lift-off process is shown to be effective in fabricating well-defined IDT finger patterns with a line width below 100 nm and good yield. A very thin organic anti-static layer works well to avoid charge accumulation during e-beam lithography on the resist layer, which is easy to occur on insulating piezoelectric substrates and results in the e-beam deflection. It is remarkable how although AlN is an insulating material, when it is resting on a semiconducting substrate such as Si, a successful e-beam lithography step for line widths below 100nm can be obtained without using any antistatic layer.

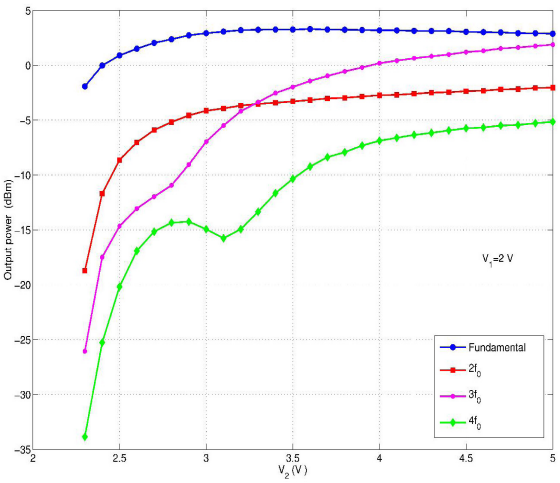

***Figure 7**. Measured output power level at fundamental frequency and different harmonics for an oscillator developed using a SAW filter on an AlGaN/GaN hetero-structure. Oscillation frequency is 475 MHz.*

Voltage controlled SAW filters

Voltage controlled SAW filters have been fabricated on AlGaN/GaN heterostuctures [9,10]. Surface acoustic wave (SAW) devices on AlGaN/GaN heterostructures have recently attracted much attention. Their integration with the high electron mobility transistor (HEMT) technology is of particular interest for the development of monolithic microwave integrated circuits for signal processing and frequency control applications. The role and efficiency of a thin insulating film, deposited below the control gate, as an acoustic spacer, is demonstrated. The device is formed by a metal-insulator-semiconductor (MIS) diode with the insulated gate placed within the acoustic path of a SAW delay line. The heterostructure, grown by metal-organic vapour phase epitaxy on a *c*-sapphire substrate, consists of a 5.3 µm-thick GaN buffer layer, followed by a 1.6 nm-thick AlN and a 25 nm-thick $Al_{0.25}Ga_{0.75}N$ barrier layers, and capped bywith a 1.6 nm-thick GaN layer to prevent oxidation. The sample has a sheet carrier density of 6.4 10^{12} cm^{-2} and a mobility of 1930 cm^2/Vs. The ohmic contacts of the diode were formed by a Ti/Al/Ti/Au multilayer annealed at 850ºC during 45 s in a N_2 atmosphere. A 300 nm-thick Si_3N_4 layer was then deposited by chemical vapour deposition at 300ºC and patterned by reactive ion etching (RIE), using SiH_4:NH_3 and Ar:SF_6 mixtures, respectively. The RIE was controlled by an interferometric end-point detector. Finally, the gate contact of the diode and the IDTs were formed by a Pt/Ti/Au multilayer. The interaction between the 2DEG in the heterostructure and the SAWs is responsible for the insertion loss control in these filters. A temperature coefficient of delay of 17.5 ppm/ºC has been obtained. An AlGaN/GaN based SAW delay-line oscillator with analog control of the loop gain and the output spectrum has been demonstrated.

MEMS RF switches and diamond micromachined structures

MEMS RF switches are promising devices for microwave monolithic integrated circuits. Their good performance, low dimensionality and good integration capabilities make these devices attractive for microwave switching. The technology has rapidly evolved and MEMS switches may overcome other monolithic switching technology in the near future [11]. The integration of these devices with III-N technology may allow the fabrication of high performance MMICs for high temperature, high frequency and high power applications.

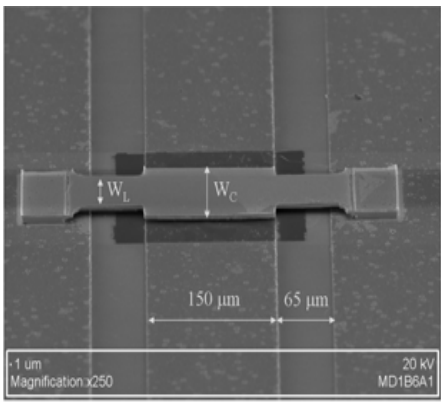

***Figure 8**. SEM micrograph of a fabricated device. The CPW dimensions are shown and the two main design variables, the widths of the membrane and of the supporting beam.*

A set of electrostatic switches was designed for operation on coplanar waveguides on GaN substrates. The fabrication technology is presented and discussed in [12,13]. On the other hand, sputtered AlN was employed as an insulator for the contact area due to its high dielectric permittivity and breakdown voltage.Capacitive contact RF MEMS switches devices were designed, simulated and fabricated on GaN substrates for MMIC applications. Electrostatic actuation was employed using sputtered AlN layers as insulator. The switch characteristics were designed to operate in narrow bands between 8 and 30 GHz with a maximum bandwidth of 15 GHz for an isolation of -30 dB. Piezoelectric actuation is under development.

The devices were designed and simulated using finite element models. HFSS was employed for the design of the electromagnetic characteristics while ANSYS Multiphysics was used to predict the electro-mechanical properties, such as actuation voltages or switching times. The devices had a variable contact area and supporting beams, defining two design parameters, WL being the width of the supporting beam and WC the width of the contacting membrane. The influence of these parameters on the device characteristics were investigated using the modelling software. The final geometrical parameters were chosen for operation between 8 and 30 GHz with actuation voltages below 35 V. Figure 8 shows a SEM micrograph of a fabricated device with WL = 80 µm and WC = 120 µm. The thickness of the beam and its initial height was designed for low voltage operation. Coupled electro-mechanic analysis was performed to optimize the device performance. The thickness of the membrane was set to 1.2 µm for allowing a reliable fabrication while keeping the actuation voltage below 35 V. The initial switch gap was set to 5 µm attending to a trade-off between actuation voltage and on-state insertion losses which were lower than -0.4 dB @ 30 GHz.

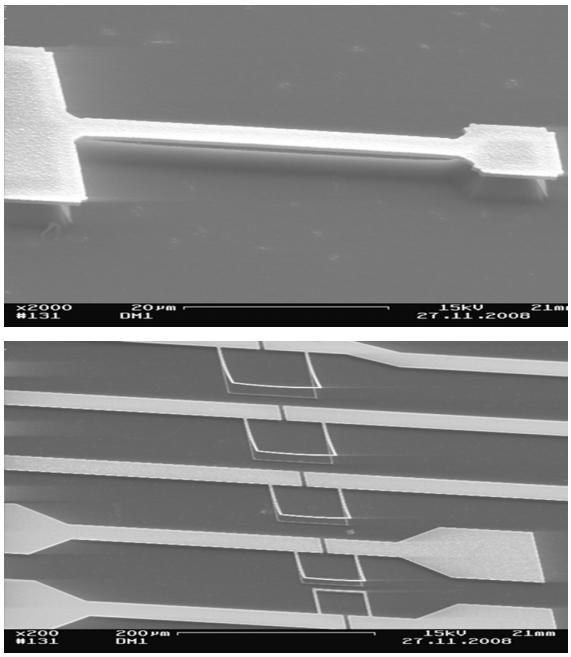

***Figure 9.** (a) SEM micrograph of a nanocrystalline diamond freestanding double-clamped beam for static loading experiments with L = 30 µm. (b) SEM micrograph of an array of U-frame resonators, used to determine the dynamic acoustic velocity, with W = L. The observed out-of-plane deflection is due to the large tensile residual stress in the metal layer covering the structure.*

Moreover, two complementary measurement techniques have been used for a precise static and dynamic mechanical characterization of freestanding nano-crystalline diamond micromachined structures [14]. The micromachined structures used for the mechanical characterization were fabricated as follows. First, the as grown Si/NCD wafers were metallized with a Ti/Au/Ni (10 nm/100 nm/80 nm) etch mask which was patterned by lift-off. An H_2:O_2 (4:1) RIE plasma etching at 500 V dc

bias was employed for the pattern transfer to the NCD layer. Then, the freestanding structures were released by means of a front-side silicon sacrificial etch using the NCD/metal structure as an etch mask. Finally, for the static mechanical characterization the metal was removed using an HF (10%) wet chemical etching. NCD-based singly and doubly clamped beams have been actuated and characterized in AFM and doubly clamped beams and resonant U-frames have been tested in a magnetomotive setup in order to extract the mechanical parameters of the material (Fig. 9). The derived value of the Young's modulus was as high as 947 ± 40 GPa, resulting in an acoustic velocity of 17283 ± 232 ms^{-1} for flexural resonators. High-frequency modes have been excited close to 10 MHz with quality factors as high as 2200. The vibrating devices exhibit excellent mechanical propertieswhich enable a high frequency of resonance and the appearance of high-order harmonics. A numerical model has been developed in order to include the imperfections of the fabrication process. For asymmetrically clamped U-frame resonators, where the residual stress is relieved, the fit to the numerical model is excellent and the stress stiffening phenomena have not been observed.

In summary, the work carried out in the ISOM involves the design, fabrication and characterization of surface acoustic wave devices based on *c*-axis oriented AlN films grown on different substrates. Films were grown in ISOM´s home built reactive sputter deposition system. We have demonstrated how nitride-based SAW filters can be directly integrated into MMICs based on AlGaN/GaN high electron mobility transistors. Both bandwidth and insertion-loss depend on film thickness, since it determines the acoustic propagation and the total absorption at a certain wavelength. Signal to noise ratio was also included in our design considerations to obtain reasonable values of insertion-loss and bandwidth. RF MEMS switches with III-V technology have been fabricated and characterized. Moreover, static and dynamic determination of the mechanical properties of nanocrystalline diamond micromachined structures has been done.

References

[1] G. F. Iriarte, "AlN Thin Film Electroacoustic Devices". PhD Thesis, Univ. Uppsala (2003).

[2] F. Calle, J. Pedrós, T. Palacios, J. Grajal, "Acoustic wave devices on III-V nitrides", Phys. Stat. Sol. (c) **2**, 976 (2005).

[3] Y. Satoh, T. Nishihara, T. Yokoyama, M. Ueda, T. Miyashita, "Development of piezoelectric thin film resonator and its impact on future wireless communication systems", Jap. J. Appl. Phys. (rev.) **44**, 2883 (2005).

[4] G.F. Iriarte, J. Bjurstrom, J. Westlinder, F. Engelmark, I.V. Katardjiev, IEEE Transactions on Ultrasonics Ferroelectrics and Frequency Control, **52,** 1170 (2005).

[5] G.F. Iriarte, E. Sillero, J.G. Rodríguez, A. Navarro, J. Pedrós, F. Calle, "E-beam lithography of nano IDT on insulating, semiconducting and conducting substrates", Proc. 33rd Workshop on Compound Semiconductor Devices and Integrated Circuits, WOCSDICE (2009).

[6] G.F. Iriarte, "Structural characterization of highly textured AlN thin films grown on titanium", Journal of Materials Research, **25**, 3 (2010).

[7] G.F. Iriarte, "The influence of the magnetron on the growth of aluminium nitride thin films deposited by reactive sputtering", Journal of Vacuum Science and Technology A, **28(2)** (2010).

[8] J.G. Rodríguez, G.F. Iriarte, F. Calle, "Optimization of c-axis oriented reactive sputter deposited AlN films", Proc. 18th European Workshop on Heterostructure Technology (2009).

[9] J. Grajal, F. Calle, J. Pedrós, J.L. Martínez-Chacón, A. Jiménez, "AlGaN/GaN-based SAW delay-line oscillators", Microwave and Optical Technology Letters **50**, 2967 (2008).

[10] J. Pedrós, Y. Takagaki, T. Ive, M. Ramsteiner, O. Brandt, U. Jahn, K.H. Ploog, F. Calle, "Exciton impact-ionization dynamics modulated by surface acoustic waves in GaN", Physical Review B**75**, 115305 (2007).

[11] P.D. Grant, M.W. Denhoff, and R.R. Mansour, “A Comparison Between RF MEMS Switches and Semiconductor Switches”Proceedings of the 2004 International Conference on MEMS, NANO and Smart, (2004).

[12] E. Sillero, D. López-Romero, F. Calle , M. Eickhoff, J.F. Carlin, N. Grandjean, M. Ilegems, “Selective etching of AlInN/GaN heterostructures for MEMS technology”, Microelectronic Engineering **84,** 1152 (2007).

[13] E. Sillero, D. López-Romero, A. Bengoechea, M.A. Sánchez-García, F. Calle, “Fabrication and stress relief modelling of GaN based MEMS test structures grown by MBE on Si(111)”, Phys. Stat. Sol. (c) **5**, 1974 (2008).

[14] E. Sillero, O.A. Williams, V. Lebedev, V. Cimalla, C-C. Röhlig, C.E. Nebel, F. Calle, “Static and dynamic determination of the mechanical properties of nanocrystalline diamond micromachined structures”, J. Micromech. Microeng. **19**, 115016 (2009).

6.4 Light emitting devices based on novel quantum dot structures for telecom applications[4]

One of the research lines of the ISOM is focused on the development of efficient optoelectronic devices for telecom applications. In particular, a strong effort is dedicated to the growth, fabrication and characterization of light emitting diodes (LED) and laser diodes (LD) based on novel semiconductor cero-dimensional nanostructures. Modified capping processes and novel materials, like (Al)GaAsSb(N) alloys, are used to tune the optical properties of quantum dots (QD) grown on GaAs. This requires a deep knowledge of the physics of the nanostructures used and in particular of the relationship between the optical and structural properties.

One recent approach towards efficient telecom emitters is based on the possibility of extending the emission wavelength of self-assembled InAs/GaAs QDs to the 1.3 and 1.55 μm regions by using a GaAsSb capping layer [1-4]. The strong observed red shift has been typically attributed to a type-II band alignment for high Sb contents, with the hole wavefunction being localized out of the QD in the GaAsSb capping layer [3]. Nevertheless, not much attention has been paid to the evolution of the optical properties of GaAsSb-capped InAs/GaAs QDs with the amount of Sb in the capping layer. Moreover, the effect that different Sb contents could have in the structural properties of the QDs is still unknown. The fact that GaAsSb acts as a strain reducing layer for InAs/GaAs QDs, together with the surfactant effect of Sb, could lead to an altered capping process that could modify the final size and/or shape of the QDs. These structural changes are of crucial relevance because they will strongly affect the optical properties of the QD system. Therefore, detailed information about the QD-capping layer structure as a function of the Sb content and its relationship with the optical properties would be very useful in order to understand the physics of GaAsSb-capped QDs and to fully exploit these structures for telecommunication wavelength applications.

The samples were grown by solid source MBE on n^+ Si doped (100) GaAs substrates. A series of eleven samples containing a single QD layer was grown for PL studies. In all these samples, 2.7 monolayers (ML) of InAs were deposited at 450 °C and 0.04 ML/s on an intrinsic GaAs buffer layer. The QDs were subsequently capped with a nominally 4.5 nm-thick $GaAs_{1-x}Sb_x$ layer grown at 470 °C. The Sb content was nominally changed from 0 to 25 %. 200 – 250 nm of GaAs grown at 580 ºC were finally deposited on top of the GaAsSb capping. A layer of similar uncapped QDs was also grown on the surface of every sample for AFM measurements. Four of the GaAsSb-capped QD layers with different Sb contents were reproduced in a single sample (separated from each other by 50 nm of GaAs) for X-STM measurements (done at the Photonic and Semiconductor Nanophysics group of the Technical University of Eindhoven).

Optical properties

As shown in figure 1 (a), by gradually increasing the Sb content in the capping layer the emission wavelength of the QDs can be red shifted, reaching almost 1.5 μm. All the QDs in these samples are grown under the same conditions and have a similar size before capping (7.5 ± 0.5 nm height and 26 ± 2 nm baselength), as measured by AFM in surface QDs. This means that the differences giving rise to the red shift are originated during the capping process. The emission wavelength can therefore be controllably tuned within a very wide region (1150 – 1500 nm) by exclusively increasing the Sb content in the capping layer. However, two clear different optical regimes (regimes I and II) are observed as the Sb content is increased (Fig. 1(b)). For low Sb contents, the PL emission is progressively improved (reduced full width at half maximum (FWHM) and increased integrated intensity), reaching its optimum at a peak wavelength of ~ 1280 nm. For higher wavelengths (higher Sb contents) the PL is gradually degraded with increasing Sb, becoming very broad for the longest wavelengths. Indeed, the presence of the first regime allows to obtain

[4] *Contact person: José María Ulloa jmulloa@die.upm.es and Adrián Hierro ahierro@die.upm.es*

PL emission at 1.3 µm with significantly improved optical properties compared to the shorter wavelength PL of the reference GaAs-capped InAs/GaAs QDs.

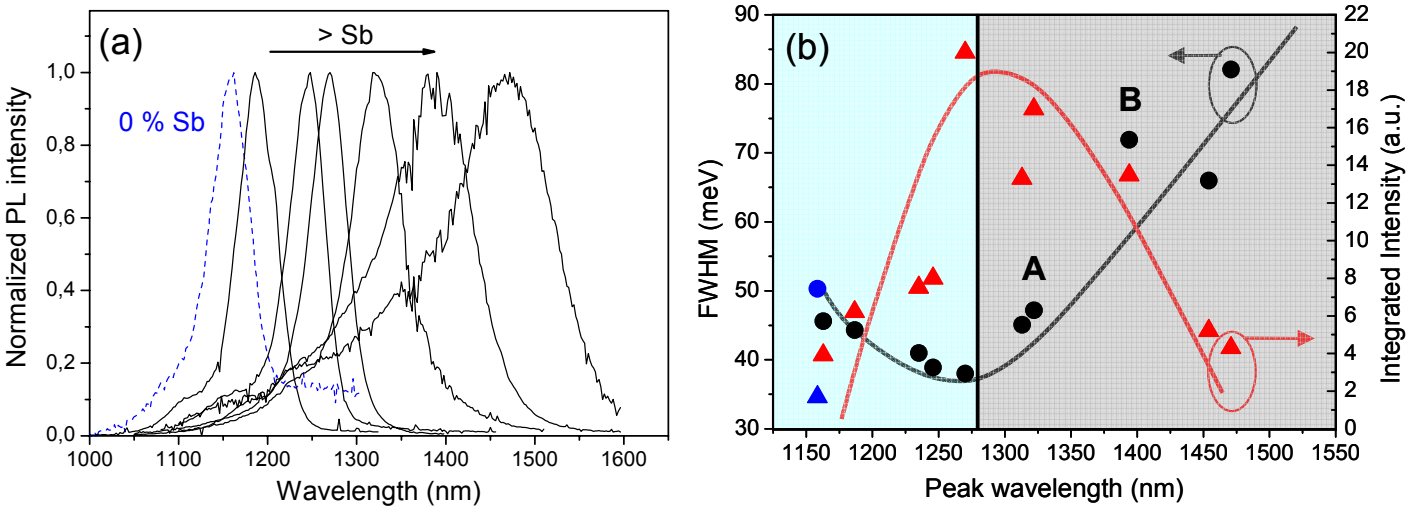

***Figure 1**. (a) Normalized room temperature PL spectra from a selection of the QD layers with increasing amount of Sb in the capping layer. (b) FWHM and integrated PL intensity dependence on the peak wavelength. The blue symbols correspond to the 0% Sb case. Lines are guides to the eye. The two different background colors indicate the two different optical regimes.*

Previous works have assigned the Sb-induced changes in the optical properties to the reduced strain and the transition from a type-I to a type-II band alignment (holes are confined in the capping layer) [1-3]. However, the evolution of the PL spectra with the Sb content within these two optical regimes cannot be explained by only considering these mechanisms. From PL measurements as a function of excitation power (not shown) we see that the transition from a type-I to a type-II alignment happens at a longer wavelength (~ 1350 nm) than the onset for the degradation of the optical properties (~ 1280 nm). Indeed, sample B is the first sample to show a clear type-II band alignment behavior that is also present in all the QD layers emitting at longer wavelengths. This is evident from the observed blue shift of the PL peak energy with excitation power in those samples, which is not present in the shorter wavelength layers. The observed evolution of the PL spectra must therefore be related also to structural changes.

Structural properties

An X-STM large scale topography image of the sample with four QD layers is shown in figure 2 (left). The Sb content in the capping layer was different in each layer, starting from 0 % (reference GaAs-capped QDs) in the first layer. Only three layers (from now on L0, L1 and L2) are visible in the image. The last layer, with the highest Sb content, could not be analyzed due to bad cleavage, probably due to too much accumulated strain. Nevertheless, a layer with high Sb content grown in another sample could be measured successfully (from now on called L3). From these high voltage (-3 V) images, the Sb content in the capping layer can be deduced by analyzing the outward relaxation of the cleaved surface. Under high voltage conditions, the electronic contrast is strongly suppressed and the measurements reflect mainly the topographic contrast, which is due to the outward relaxation of the cleaved surface due to the compressive strain stemming from the QDs and the wetting layer (WL) [5]. In our case, since the GaAsSb capping layer is also compressively strained, it will also contribute to the outward relaxation. The relaxation of the layer far from a QD (averaged over a ~ 80 nm wide region to avoid any possible effect of alloy fluctuations) was compared to calculations from continuum elasticity theory (Fig. 2 right). A finite element calculation was performed to solve the 3D problem, in which an isotropic material is considered. Both the wetting layer and the capping layer were considered in the calculation and In and Sb segregation were also included. The measured thickness of the GaAsSb layer (4.0 ± 0.5 nm) is introduced in the model and the composition is

changed until a good fit to the experimental profile is obtained. From the fits shown in figure 2, the Sb content is deduced to be 0, 7, 11 and 22 % for L0, L1, L2 and L3, respectively.

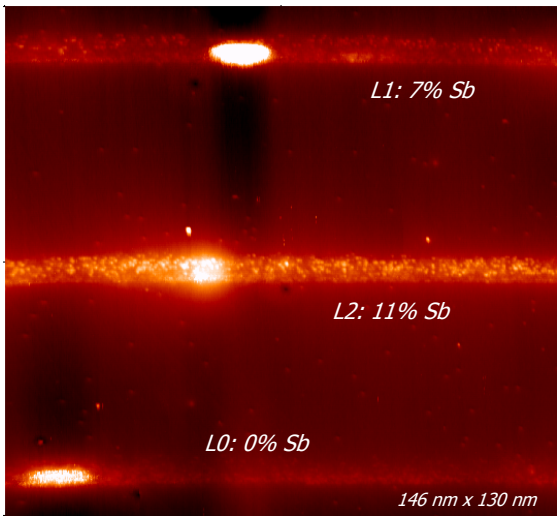

***Figure 2**. Left: X-STM topography image (V= -3 V) of the first three layers of the sample designed for X-STM measurements. The GaAsSb layer with higher amount of Sb appears brighter in the image. Right: Measured (solid line) and calculated (dotted line) outward relaxation profiles of the four different layers studied by X-STM. The amount of Sb deduced was 0, 7, 11 and 22 % (figures (a), (b), (c) and (d), respectively).*

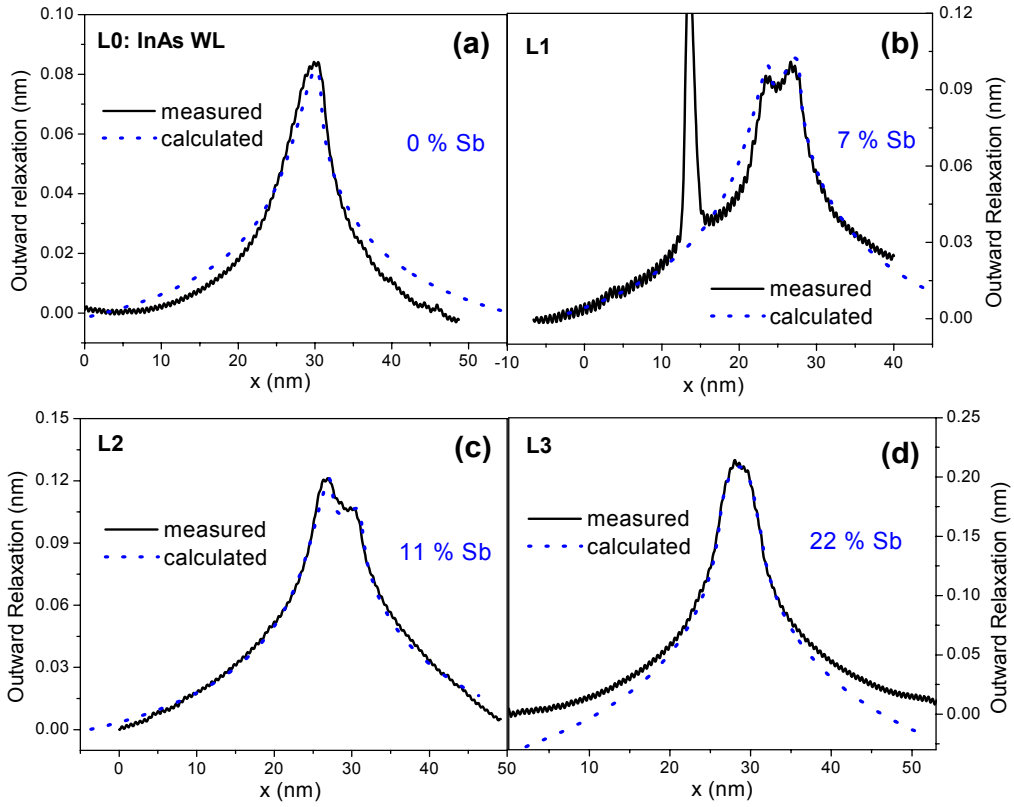

***Figure 3.** Measured (solid line) and calculated (dotted line) outward relaxation profiles of the four different layers studied by X-STM. The amount of Sb deduced was 0, 7, 11 and 22 % (figures (a), (b), (c) and (d), respectively).*

A high resolution image of a QD in L0 and L3 can be seen in figures 3 (a) and (b), respectively. The measurement conditions (negative voltage) allow imaging group V elements so that the bright spots in image (b) represent individual Sb atoms in the As matrix (due to the different size and bonding configuration, Sb atoms appear brighter than As atoms). The bright spots in image (a) represent individual In atoms, which are visible through their distortion of the surrounding As atoms. From local mean equalization filtered images we conclude that there is no Sb inside the QDs.

Significant differences between the QDs in the different layers are already clear from these images. The size and shape of the QDs in each layer can be deduced by a statistical analysis of the relationship between the height and the base length in a large number of QDs. After analyzing ~ 15 QDs in each layer, a linear dispersion, similar to that obtained in [6], is found, indicating that the QDs have an ellipsoidal or lens shape (also apparent from Fig. 3) with a base diameter of 24 ± 1 nm. This correlates very well with the 26 ± 2 nm diameter measured by AFM in similar surface QDs.

However, the capped QD height increases with the Sb content, as shown in figure 3 (c), in which the QD height normalized to the height of surface uncapped QDs is plotted as a function of the Sb content in the capping layer. The height differences must be originated during the capping process: the strong QD decomposition that takes place during capping with GaAs is reduced by the presence of Sb [7]. Moreover, the reduction is proportional to the amount of Sb in the capping layer. The result is that the QD height is progressively increased when the amount of Sb in the capping layer increases. The dissolution process is found to be completely suppressed for a Sb content of 22 % (the QD height measured by X-STM is the same that the one measured by AFM in uncapped QDs) but the linear regression in the figure shows that QD dissolution stops completely for a smaller Sb content of ~14%. For higher Sb contents, no further change in the QD height is expected. It is possible, therefore, to controllably tune the height of the InAs QDs by changing the Sb content in the capping layer between 0 and ~14 %.

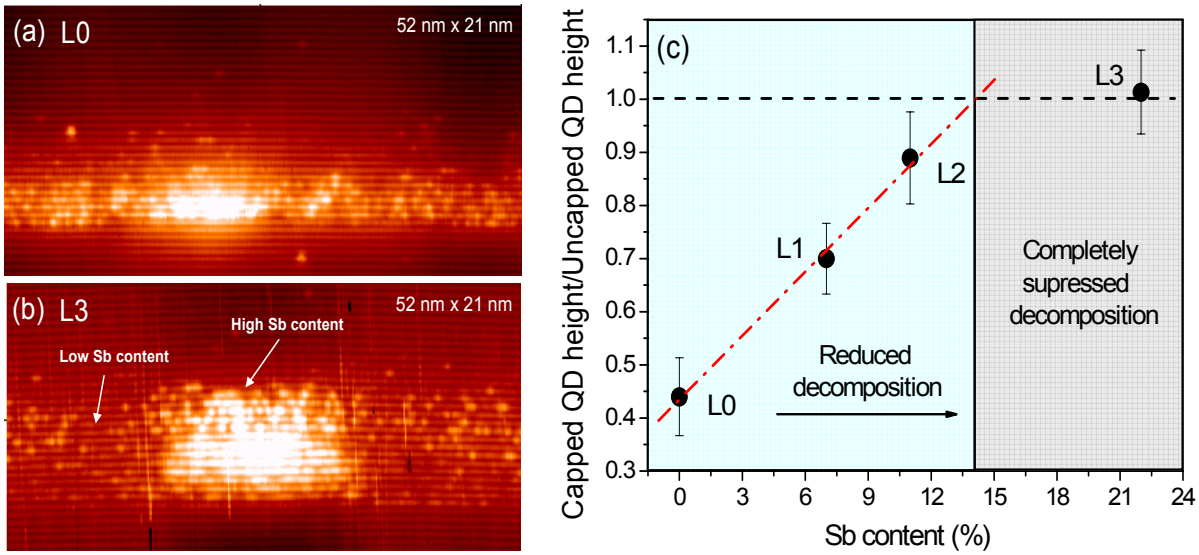

Figure 4. *Left: Filled states topography images of a QD in (a) L0 and (b) L3. In image (a) the bright spots correspond to In atoms. In image (b) the bright spots correspond to Sb atoms in the As matrix. Right: QD height normalized to the height of the equivalent uncapped QDs as a function of the Sb content in the four different layers studied by X-STM. A value of 1.0 indicates a completely suppressed decomposition process. The red dash-dot line is a linear fit to the values of L0, L1 and L2. The two different background colors indicate the two different regimes.*

Regime I: from 1150 to 1280 nm

As we just showed, the QD height progressively increases with the Sb content and can be more than doubled by adding 14 % Sb (the baselength is found to be unaffected by the amount of Sb). This should strongly affect the optical properties, not only by red-shifting the wavelength but also by increasing the PL intensity due to stronger carrier confinement. The resulting enhancement of the electron-hole wavefunction overlap is likely the reason for the improved PL integrated intensity obtained when the Sb content is initially increased. Moreover, since the dependence of the energy of the confined levels on QD size decreases when the QD size increases, taller QDs will show less dispersion in the effective band gap energy for the same size

fluctuations within the ensemble. This could explain the observed initial narrowing of the PL with the Sb content (Fig. 1 (b)). The RT PL peak wavelength of L2 (11 % Sb) is 1268 nm, very close to the ~ 1280 nm wavelength of the optimum PL spectrum. This means that regime I takes place for Sb contents up to ~ 11-12 %, coinciding with the region of progressively increased QD height (up to ~ 14% Sb). Therefore, the region of improved PL characteristics can be directly correlated to an increased QD height.

The presence of Sb in the growth front must have the effect of reducing the In-Ga intermixing, the main reason for QD decomposition during capping, and this reduction is proportional to the amount of Sb within regime I. This phenomenon is likely due to the surfactant effect of Sb, which reduces the adatom surface diffusion on the growth front. Since intermixing takes place from the very initial stages of the capping process, we can further confirm the X-STM results by an AFM analysis of surface QDs in which only 3 ML of GaAs(Sb) are deposited. Once the thin capping layer is deposited, the sample is kept for 30 s under As_4 and then it is quickly cooled down. Fig. 4 shows AFM images of uncapped QDs (Fig. 4 (a)) and the same QDs capped with 3 ML of GaAs (Fig. 4 (b)) or 3 ML of GaAsSb (Fig. 4 (c)). When capping with GaAs, a strong intermixing occurs and the QDs are strongly dissolved, resulting in an InGaAs thin layer. This is why they are not visible in the image (only the few very big QDs initially present are still visible). The situation is very different when capping with GaAsSb. The QDs are still visible indicating a strong reduction of In-Ga intermixing and In segregation out of the QDs. Moreover, if the amount of Sb in the 3 ML of GaAsSb is increased, the height of the QDs increases (see Fig. 4 (d)), confirming the correlation between the amount of Sb and the degree of reduced decomposition during capping (or the degree of increased QD height).

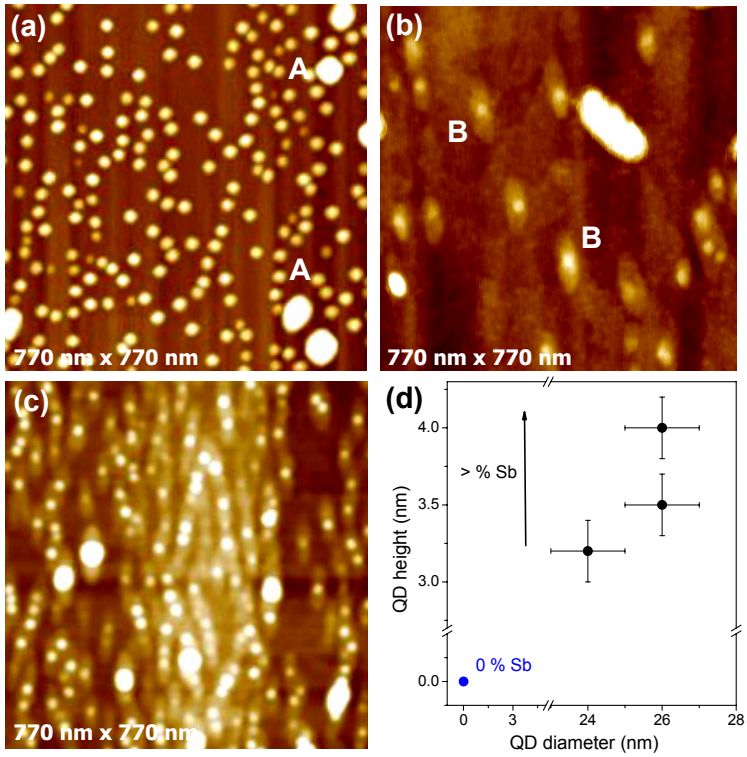

***Figure 5**. AFM images of (a) uncapped QDs, (b) QDs capped with 3 ML GaAs, and (c) QDs capped with 3ML GaAsSb. The z range is 20 nm in (a), and 10 nm in (b) and (c). Image (d) shows the QD height and baselength measured by AFM in QDs with different amounts of Sb in the 3 ML capping.*

Regime II: from 1280 to 1500 nm

The previous results can explain the initial improvement in the PL spectra, but not the subsequent degradation. A second mechanism, competing with the first one, is likely responsible for this second optical regime. This mechanism is found to be related to alloy fluctuations in the capping layer. Figure 5 shows filled states high voltage images of L1 (Fig. 5 (a)) and L3 (Fig. 5 (b)). While in L1 there is no significant difference in brightness along the layer, in L3 some clearly brighter regions appear. As explained before, in

high voltage images the relaxation is proportional to the strain and, therefore, to the Sb content: the brighter regions are Sb-rich regions and the darker ones Sb-poor regions. The Sb distribution is quite homogeneous in low Sb content samples, but for high Sb contents, Sb-rich clusters with a lateral size between 10 and 20 nm appear in the capping layer (see the arrows in Fig. 5 (b)). This strong composition modulation could be due to the large miscibility gap of GaAsSb. By comparing the outward relaxation profile between Sb-rich and Sb-poor regions, the absolute value of the Sb fluctuations can be estimated to be 2, 4 and 12 % in L1, L2 and L3, respectively. The alloy fluctuations are very small for low Sb contents but they increase with Sb, becoming very strong for Sb contents of 22 %.

The observed clusters can act as GaAsSb/GaAs QDs, trapping holes and reducing the carrier injection efficiency in the InAs QDs, which would reduce the PL integrated intensity. Moreover, the composition modulation can be enhanced by the strain field of the QDs which propagates into the matrix. Since GaSb has a very similar lattice constant to InAs, from the point of view of the strain it will be favorable for Sb to accumulate on top of the partially relaxed InAs QDs (a similar process has been observed for InGaAs capping and columnar QD growth). This is clearly observed in the X-STM measurements of L3, in which the amount of Sb on top of the QDs is much higher than around them (see Fig. 3 (b)). In the low Sb content samples, in which alloy fluctuations are very small, there is no Sb accumulation on top of the QDs. In this case, all of the QDs are covered by a very similar and uniform layer and therefore they have the same strain state and band-offsets. The result is that the PL of the ensemble is narrow. When the Sb content is increased, the composition modulation becomes significant, introducing inhomogeneities in the composition of the capping layer on top of a single QD and between different QDs, which results in a PL broadening. The PL broadening is enhanced for the high Sb content type-II samples. In this case, the hole wavefunction is confined in the capping layer on top of the QDs and, therefore, different Sb contents on top of the QDs will have a much stronger impact on the hole energy levels. This is likely the reason for the strong increase in the FWHM of the type-II samples compared to the type-I ones. The observed PL degradation in regime II can therefore be explained by the presence of alloy fluctuations in the capping layer and strain-induced Sb accumulation on top of the QDs, together with the transition to a type-II band alignment.

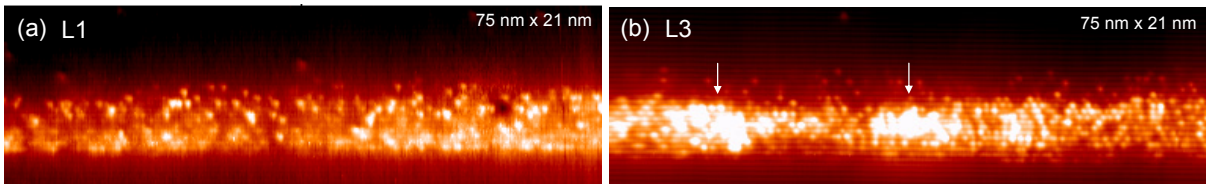

***Figure 6**. Filled states topography images of the WL and capping layer of (a) L1 and (b) L3. A clear contrast inhomogeneity is present in L3 in which Sb-rich clusters (indicated by the arrows) are formed.*

It must be noticed that, despite the presence of alloy fluctuations and the type-II band alignment, the integrated intensity of the longest wavelength samples is still slightly larger than that of the reference sample, indicating that these samples could still be very useful for applications in which a broad spectral range luminescence can be an advantage, like in semiconductor optical amplifiers.

Conclusions and future work

We have shown how the structural and optical properties of InAs QDs can be strongly modified by changing the capping material, in particular by adding Sb to the capping layer. We can extend the emission wavelength up to 1.55 μm, which would allow using GaAs-based technology for telecom applications. The impact of other new alloys on the QD properties is currently being investigated. Small amounts of N are being added to the GaAsSb layer with the goal of reaching 1.55 μm while preserving a type-I band alignment. The addition of Al, which could reduce the composition modulation in the capping layer due to the presence of the stronger Al-Sb bond, is also being explored. The fact that the capping process can be used to control the structure of the QDs is of a general nature and can be transferred to other QD systems.

References

[1] K. Akahane, N. Yamamoto, and N. Ohtani, Physica E, Amsterdam **21**, 295 (2004).

[2] H.Y. Liu, M.J. Steer, T.J. Badcock, D.J. Mowbray, M.S. Skolnick, P. Navaretti, K.M. Groom, M. Hopkinson, and R.A. Hogg, Appl. Phys.Lett. **86**, 143108 (2005).

[3] J.M. Ripalda, D. Granados, Y. González, A.M. Sánchez, S.I. Molina, and J.M. García, Appl. Phys. Lett. **87**, 202108 (2005).

[4] J.M. Ulloa, R. Gargallo-Caballero, M. Bozkurt, M. del Moral, A. Guzmán, P.M. Koenraad and A. Hierro, accepted on Phys. Rev. **B** (2010)

[5] D.M. Bruls, J.W.A.M. Vugs, P.M. Koenraad, H.W.M. Salemink, J.H. Wolter, M. Hopkinson, M.S. Skolnick, F. Long, and S.P.A. Gill, Appl. Phys. Lett**. 81**, 1708 (2002).

[6] J.H. Blokland, M. Bozkurt, J. M. Ulloa, D. Reuter, A.D. Wieck, P.M. Koenraad, P.C.M. Christianen and J.C. Maan, Appl. Phys. Lett. **94**, 023107 (2009).

[7] J.M. Ulloa, I.W.D. Drouzas, P.M. Koenraad, D.J. Mowbray, M.J. Steer, H.Y. Liu, and M. Hopkinson, Appl. Phys. Lett. **90**, 213105 (2007).

6.5 IR detectors based on In(Ga)As(N) quantum nanostructures[5]

Since 2004 the ISOM has an active line of research based on the study of quantum dot (QD) layers to be used as the active regions of IR detectors. The physical properties of these zero dimensional (0D) structures are of great interest, in particular to achieve detection at room temperature and normal incidence. The selection rules associated with intersubband transitions in quantum wells predict no absorption when the electric field of the light has components parallel to the wafer surface. The latter makes necessary to employ light coupling techniques like tilting the detector, incidence of the light through a 45º polished edge or (most used) the definition of a diffraction grating on top of the detector. Besides, the high dark current imposed by the need of high doping levels in the QWs make very difficult to obtain good responsivity at temperatures above 77K where the detector shows a high conductivity and it is very difficult to separate the dark current from the photosignal. The QD IR detectors have been proposed as a potential solution to overcome these problems since in theory, they should have a lower dark current and a higher photoresponse resulting from longer carrier capture and relaxation times. The normal incidence absorption should be also possible due to the different selection rules behind intersubband transitions in QD.

The so-called Quantum Dot IR Photodetectors (QDIP), based on InAs/(In)GaAs QD have been studied during the last 10 years as a possible alternative to replace both, the known uncooled far-infrared detectors such as bolometers and pyroelectric detectors, as well as the cooled ones based on InSb or HgCdTe for instance. The high fragility of their mechanical properties makes very difficult to fabricate a large-area two-dimensional array to be used as active devices in IR cameras or night vision systems. The maturity of the GaAs processing must help in the development of high yield focal plane arrays. However, even though some QDIPs operating at room temperature have been demonstrated, up to now, this technology is restricted to a research level, focused in the second and third atmospheric transmission windows (3-5 and 8-12 μm respectively) and with no clear industrial interest.

The ISOM, is very interested in developing QDIPs for a practical operation at room temperature extending their absoprtion peak to the first window in 1.55 μm (optical fiber communication wavelength). One way to extend the emission wavelength is the incorporation of N into the QDs, i.e. the growth of InAsN/InGaAs dot-in-a-well (DWELL) structures. The addition of a small mole fraction of N (1-3%) into the QD lattice, leads to a strong reduction in the bandgap of the III–V semiconductors. Moreover the incorporation of N into the QDs allows us to decrease the lattice parameter of the QDs, leading to a reduction of the compressive strain. Similarly, we could avoid low growth rates to obtain large QDs and thus, In segregation, since N allows us to extend QDs' emission wavelength without the need for increasing their dimensions. Moreover, the growth of InAsN QDs can help in overcoming some disadvantages related to the increase in the dimensions of these nanostructures such as the formation of dislocations inside the QDs due to the huge strain accumulated in them. Thus, the incorporation of N into the InAs QDs of DWELL structures seems to be an advantageous option to shift the absorption wavelength to values as high as 1.55μm, due to the strong reduction in the bandgap and in the compressive strain in the QDs.

The samples are fabricated using self-organized Stranski-Krastanov growth mode. This mode is an intermediate case in between the island growth and the layer by layer growth modes. After forming a few monolayers of material (in our case In(Ga)AsN on GaAs), subsequent layer growth is highly strained, and thus, islands are formed on top of this intermediate layer (normally called "*wetting layer*"). The most important point is to control the first nucleation of these islands on the wetting layer in order to achieve self-ordered distribution of the QDs (Fig.1).

[5] *Contact person: Álvaro de Guzmán Fernández* guzman@die.upm.es

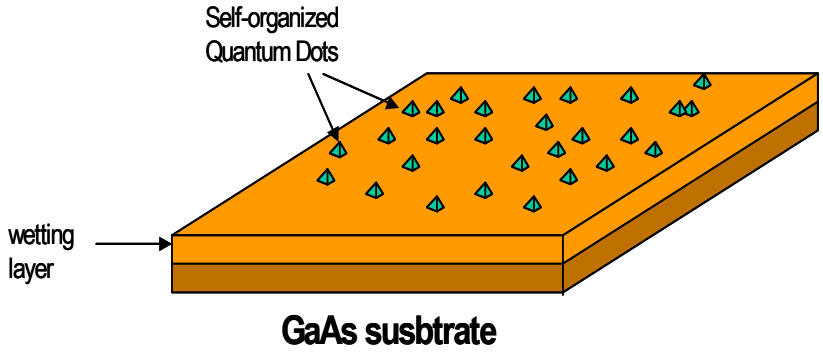

***Figure 1**. Stranski-Krastanov growth mode. InAsN quantum dots are formed on top of a InAs(N) wetting layer.*

The samples were grown on GaAs (100) substrates using a RIBER 32 Molecular Beam Epitaxial system equipped with a radiofrequency (RF) Oxford Applied N_2 Plasma Source. The active region of the detectors consists of several In(Ga)AsN QDs layers buried with InGaAs. The mentioned QDs were grown with a nominal thickness of 4ML at 0.15ML/s at a substrate temperature of 470ºC. Then, a capping layer of $In_{0.2}Ga_{0.8}As$ of 12 nm was used to cover the QDs at the same substrate temperature. The atomic N is generated by means of N plasma using 0.2 sccm of N_2 flux and a RF power of 65W. The active nitrogen is monitorized by an optical emission detector (OED) tuned at the main emission wavelength of the N plasma. In all the cases, the evolution of the growth was monitored by reflection high-energy electron diffraction (RHEED). This technique gives information about the surface allows observe in situ the transition from a 2D growth corresponding to the wetting layer to a 3D growth corresponding to the formation of the first islands. The QD layers were sandwitched between two 500 nm $Al_{0.3}Ga_{0.7}As$ barriers to block the dark current. This whole structure was grown between two GaAs layers highly doped with Si to $2x10^{18}$ cm^{-3} which were used as ohmic contacts (Fig 2a). Finally, to achieve the intraband transitions, it is necessary to fill with electrons the first confined level in the QD avoiding to fill the second one (which results in a reduction of the absorption). In this case, a very accurate knowledge of the surface density of QD is necessary, since we must ensure the existence of two electrons per QD. This can be done directly doping the QD layer, but it results in a non uniform distribution of the dopants and in the presence of ionized impurities in the QD which increases the linewidth due to scattering. In our case we use a modulation doping technique (Fig. 2b) where we introduce the dopant species in the GaAs barrier below the QD. A thin (3 nm) Si doped GaAs layer ($2{\cdot}10^{18}$ cm^{-3}) is separated from the QD by a spacer of 3 nm. This improves the surface distribution of the dopant, physically separating the impurities from the carriers. Furthermore, the presence of an assymetrical distribution of charge at both sides of the DWELL layer, gives rise to the existence of an internal electric field that helps the photogenerated carriers to be swept to the contacts, thus allowing the device to be operated in the photovoltaic mode (i.e. at 0 V bias).

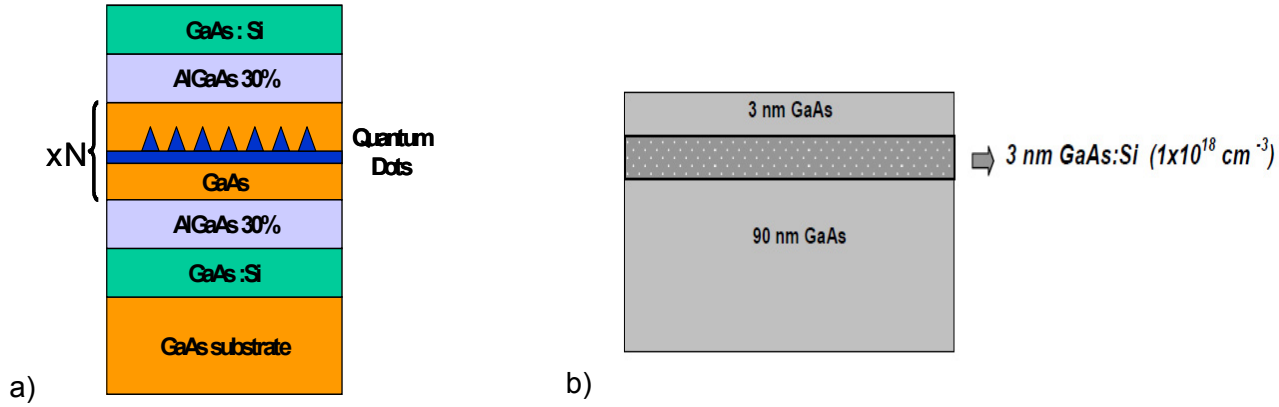

***Figure 2**. a) structure of a QDIP based on dilute nitrides QD, b)modulation doping scheme of the layer just below the QD.*

The photovoltaic detectors normally have a higher signal to noise ratio due to the strong reduction in the shot and 1/f noise (both of them depending on the bias current flowing through the detector). The first task was to improve the surface density and homogeneity of the QD layers and therefore, several samples were grown under different growth conditions. During these studies, an additional QD layer was grown on top of the structure, but without the capping to be further analyzed using Atomic Force Microscopy (AFM) imaging. In fig 3, we show some of these AFM images for different Ga/In content in the QD. We observed a suitable homogeneity together with a high density using a Ga/In ratio of 0.5. The N incorporation was also analyzed as a function of the In/Ga ratio [1] and the amount of ion species present in the N plasma [2]. The final N content was estimated growing a test quantum well under the same N plasma conditions and measuring the PL emission at low temperature [3]. With this procedure we estimated a N content of 1%.

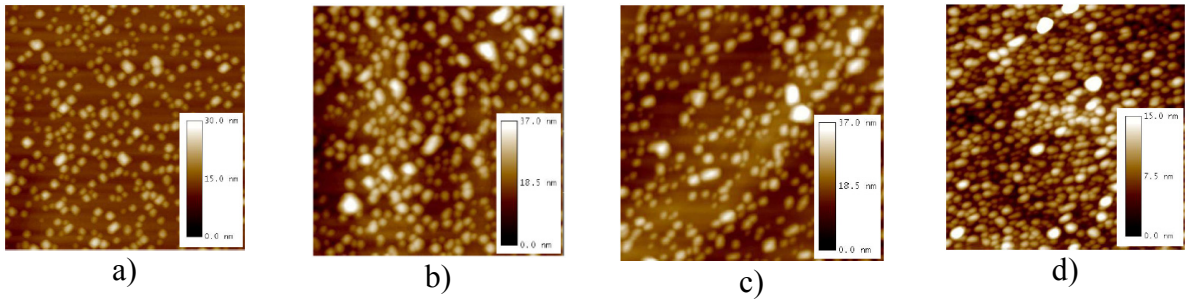

Figure 3. *AFM images(1μm x 1 μm) of several InGaAsN QD samples grown with different Ga contents. a) 0%, b) 15%, c) 30% and d) 50%*

Finally, a sample with 25 $In_{0.5}Ga_{0.5}AsN$ QD layers was processed into 200 μm diameter mesa photodetectors using standard photolithography and wet chemical mesa etching. A ring-shaped metallization using AuGe–Au was deposited on top of the mesas and then alloyed for the ohmic contacts. The bottom contact was chosen as the ground in all measurements. Figure 4, shows the I-V characteristics of the mentioned sample, as well as the normal incidence photocurrent spectra taken at different temperatures. From these curves, it can be observed the strong photovoltaic response as a consequence of the low dark current at 0V bias. The device has different response depending on the operating temperature. At low temperatures (below 70 K) it has a strong broad peak centered in 5.5 μm, but above this temperature, the detector has strong absorption in the band of the first atmospheric window revealing its potential application in telecommunications [4]. Moreover, this peak persists up to 240K, the highest temperature reported for QD devices operating in this range.

This is, to our knowledge, the first demonstration of QD intraband absorption in the region of 1-2 μm using dilute nitrides as the active region. Further improvements in the layer structure and the growth procedure are current in progress to achieve the desired operation at room temperature.

In conclusion we have fabricated QD intraband photodetectors to operate in the region of 1-2 μm using dilute nitrides in the active region. The optimization of the growth conditions, the careful selection of In/Ga ratio and the use of modulation doping allowed us to improve the photovoltaic properties of such devices and as a consequence, clear absorption peaks can be observed at temperatures as high as 240 K at 0 V bias. With these promising results, we are optimistic to reach the room temperature detection in the next future opening the possibility of a new generation of IR detectors to be used in focal plane arrays, sensors and other industrial and medical applications.

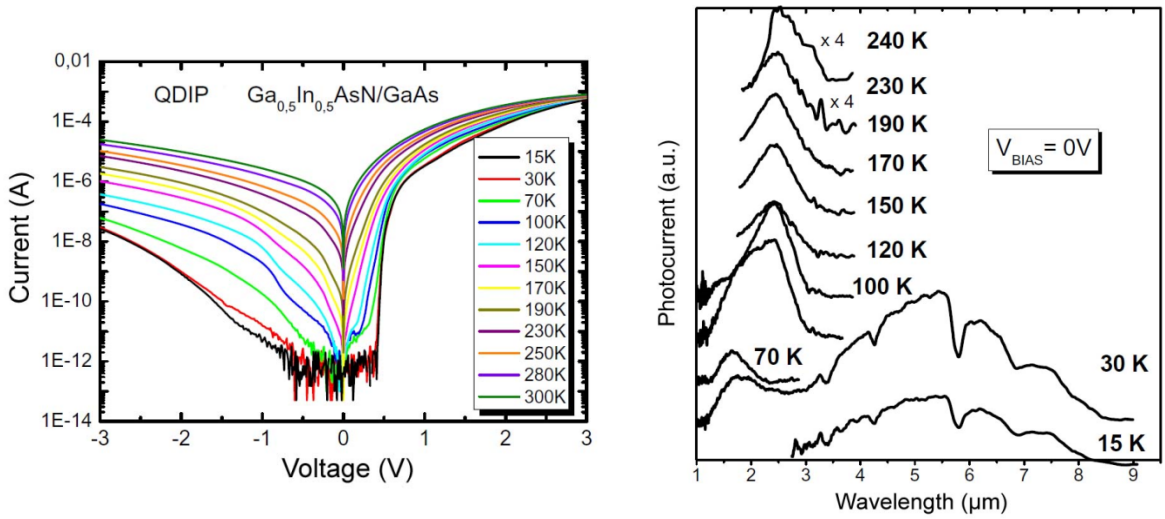

***Figure 4**. I-V characteristics and normal incidence photocurrent spectra of a QDIP with 25 layers of $In_{0.5}Ga_{0.5}AsN$ QD.*

References

[1] R. Gargallo-Caballero, Á.Guzmán, M. Hopkinson, J. M. Ulloa, A. Hierro and E. Calleja, Phys. Stat. Sol (c) **6** ,1441 (2009).

[2] R. Gargallo-Caballero, A.Guzmán, J. Miguel-Sánchez, A. Hierro and E. Muñoz, Materials Science and Engineering B **147**, 118 (2008).

[3] R Gargallo-Caballero, J Miguel-Sánchez, Á Guzmán, A Hierro and E Muñoz, Journal of Physics D: Applied Physics, **41** 065413 (2008).

[4] R. Gargallo-Caballero, A. Guzmán, M. Hopkinson, A. Hierro, J.M. Ulloa and E. Calleja. 15th European Molecular Beam Epitaxy Workshop, Zakopane (Poland), March 8-11 2009.

6.6 (In,GaAl)N photodetectors and applications in biophotonics[6]

Activities on photodetectors at ISOM have been devoted to the growth and fabrication of (In,Ga,Al)N devices working in the near UV and visible ranges for biophotonic applications, and to A-plane GaN devices as polarization sensitive photodetectors. Bulk InGaN regions and InGaN MQW as active layers, as well as GaN layers grown on polar surfaces have been investigated. These efforts have allowed some progresses in MBE growth and understanding of InGaN alloys in the whole range of In contents and about their p-type doping with Mg. Characterization by ion beam analysis has provided complementary information about phase separation and crystal quality as a function of In mole fraction. The benefits of GaN/InGaN MQW photodetectors have been confirmed by exploiting their internal intrinsic electric fields to obtain internal gain and photovoltaic response in n-i-n devices. The intrinsic limitations of MQW heterostructures due to the high recombination rates in the QWs or carrier collection deficiencies were overcome by designing, growing and fabricating optimized MQW structures by proper design of the barriers and studying the effect of electron blocking layers. Motivated by applications in biophotonics, the integration of filters and detectors has been pursued, and GaN surfaces have been functionalized, adding new possibilities for chemical sensing. Undoped *a*-plane GaN layers grown on sapphire showed a very high resistivity, allowing the fabrication of high responsivity MSM photodetectors as compared to Schottky photodetectors on *m*-plane layers.

InGaN layers and photodetectors

A set of $In_xGa_{1-x}N$ samples were grown by Plasma-Assisted MBE covering the whole range of In contents. Through XRD, optical transmittance/absorption, XPS, CL, Raman, PL and RBS experiments, including channelling measurements, band gap, alloy bowing parameter, crystal quality and localization problems were studied. Crystal quality lowers significantly for the $0.3<x<0.8$ range [1]. As part of an international multi-laboratory effort, some of our samples were used to determine the dependence of bandgap with hydrostatic pressure and In content. Phase separation and In segregation tend to make less abrupt absorption characteristics. Initial electrical assessment indicated surface electron accumulation, high residual concentrations, non-rectifying Schottky contacts and localization effects. All these issues become more pronounced when the In content increases. Figure 1 shows the photoresponse of a set of photoconductors illuminated from the substrate [1-3].

To circumvent above difficulties, metal-insulator-semiconductor (MIS) structures were fabricated. SiN deposited by PECVD and anodically-grown (In)GaO films were used as insulators. SiN based devices showed the best performance, and responsivities of 50 mA/W were obtained for up to 15% of In content, with good rectifying properties [4].

In order to improve rectifying properties of Schottky contacts on InGaN, compensation of high residual electron concentration by Mg doping was also studied. A detailed study of Mg doping of $In_{0.18}Ga_{0.82}N$ was carried out. A maximum carrier concentration of $2.6\times10^{19}cm^{-3}$ was obtained, reaching the state of the art for any growth technique. It was observed that, as for GaN, once a certain Mg flux is exceeded, carrier concentration decreases as the Mg in the layer increases and the structural quality of the sample lowers. Schottky barrier PD on these layers showed good responsivities (Figure 2). The activation energy of the Mg acceptors in $In_{0.18}Ga_{0.82}N$ has been determined by PL and Hall measurements as a function of temperature, obtaining a value of ~60meV [4].

[6] *Contact person: Elias Muñoz* elias@die.upm.es

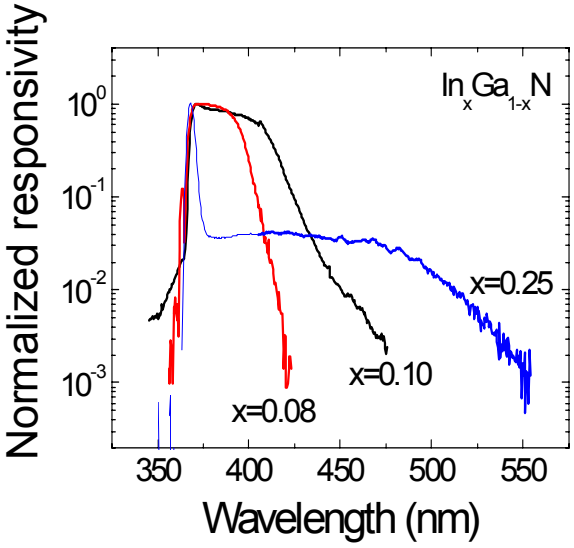

Figure 1. *Responsivity of InGaN phoconductors, back-illuminated, showing how the absorption edge becomes less abrupt with increasing In mole fractions.*

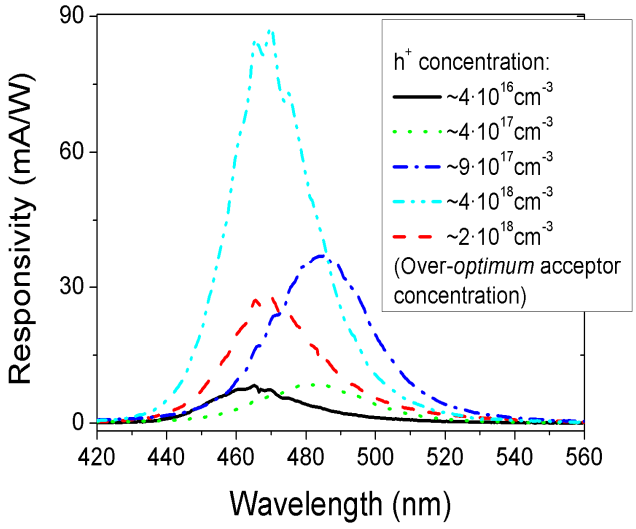

Figure 2. *Photoresponse of back-illuminated Schottky photodetectors fabricated in Mg-doped InGaN layers (In 18%) as a function of doping level.*

InGaN MQW photodetectors

MQW photodetectors offer an extra flexibility to tune the detection-edge by adjusting wells width and composition, presenting sharp abrupt detection edges, greater rejection ratios, allow the exploitation of polarization fields and gain mechanisms, and include the potential of monolithic integration of emitter and detector structures.

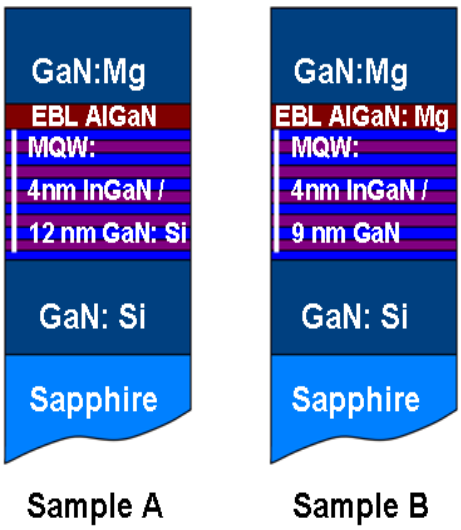

Figure 3.*Reference and improved InGaN/GaN MQW heterostructures used in the optimization experiment.*

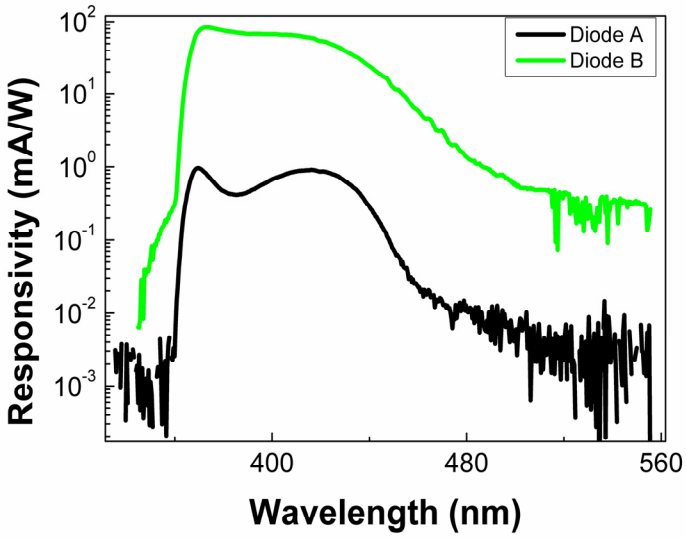

Figure 4. *Responsivity as a function of wavelength in diodes A and B.*

In a previous work, it was already pointed out that one of the limitations to reach high responsivity in MQW PD devices comes from the reduced number of QWs that remain in the device space charge layer, i.e. real active detecting layers. Following the experience with LED, experiments were conducted about the use of electron blocking layers (EBL) in SB PD. In these devices dark current was lowered when an EBL was used. To increase the number of QWs in the SCR, an optimization process for MQW photodetectors was performed, using initially computer simulations. Some of the parameters considered were, EBL composition

and width, barrier doping and thickness, and number of QWs. As an illustration of the final experiments to have more QW in the space charge region, figure 3 shows two structures fabricated by MOCVD, a reference structure (diode A) and an optimized one (diode B). Both have 4 nm QWs. While diode A has doped barriers, diode B has thinner-undoped barriers. In the reference diode the EBL layer was undoped, while the optimized diode has a Mg-doped EBL layer. For diode B responsivity is about 70 times greater, and its detectivity was about one order of magnitude larger (D*= 1.4×10^{12} cm.$Hz^{0.5}$/W). C-V measurements indicated that at least 2 QWs were outside the space charge region for the reference diode (A) while no QWs were observed outside this region in the case of diode B. Simulations showed that no QW were expected to be inside the space charge region for diode A and all of them were expected to be inside this region in the case of diode B. Figure 4 shows the photoresponses from both devices [5,6].

Schottky InGaN/GaN MQW detectors were fabricated showing very high internal gains, and this behaviour was modelled through the specific profile of the internal fields in the active MQW region. N-i-N devices showed photovoltaic response and asymmetric I-V characteristics due to the presence of polarization fields. P-I-N and N-I-P structures were designed and simulated, indicating the advantages of having a top n-type region to increase carrier collection due to the addition of polarization and junction fields in the QW in this configuration [4,7,8].

Applications in Biophotonics

Our participation in projects linked with biosensors and biophotonics (EU GaNano project and regional project Futursen) motivated that the above device technology was used to develop photodetectors suitable for fluorescence applications. Figure 5 indicates a general scheme for fluorescence measurements. Integration with emitters, filters and fluorophores was addressed. Efforts to grow custom InGaN filters below InGaN PD were not successful, due to the different decomposition of InN fraction at GaN growth temperatures. Instead, hybrid elements were fabricated by wafer bonding [4]. As an example of substance detection by optical measurements, Figure 6 shows the good fitting to the optical spectra of Alexa Fluor, used for protein and nucleic acid detection, by integration of a PIN MQW detector and an InGaN filter.

In such efforts to integrate devices and functionalities for chemical monitoring, surface functionalization of GaN with adequate luminescent molecular probes would enable integrated microcircuits with chemical sensing features. In collaboration with the Chemical Optosensors & Applied Photochemistry group (GSOLFA) in Universidad Complutense de Madrid, O_2 sensing was selected to prove the feasibility of such concept. Luminescent Ru(II) polyazaheterocyclic complexes reign among all blue-absorbing O_2 indicator dyes, due to their >150 nm Stokes' shift, 0.2-8 μs lifetimes. Covalent tethering of a Ru(II) dye to gallium nitride surfaces has been accomplished. A functionalization sequence based on n-GaN surface oxidation, silanization with 3-aminopropyltriethoxysilane (APTES) and final reaction with the sulfonyl chloride of the luminescent complex, leads to the sought covalent attachment of the O_2 indicator dye via formation of a strong sulfonamide bond. After functionalization of the GaN surface with the Ru complex, the XPS spectrum (Prof. C. Palacios, UAM) broadens and the maximum shifts to higher binding energies suggesting that, in addition to sulfonate groups, other sulfur species appear. In conclusion, the covalent binding of a luminescent indicator to a GaN surface has been demonstrated. This achievement paves the way to a new generation of integrateable ultracompact microsensors that combine semiconductor-probe assemblies [9,10].

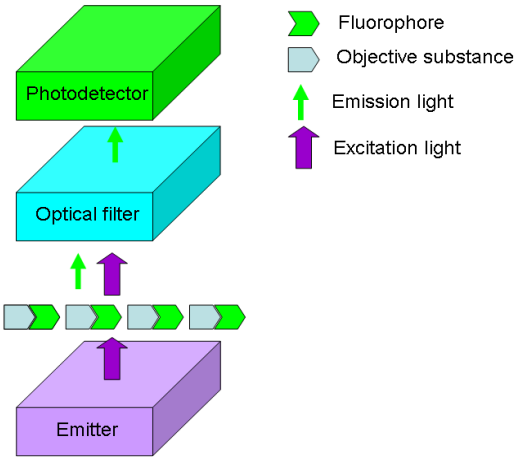

***Figure 5**. General scheme for fluorescence basic measurements*

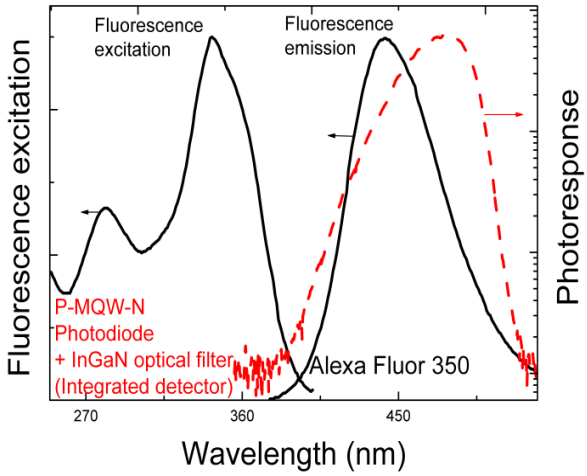

***Figure 6**. MQW InGaN + InGaN optical filter heterostructure photorresponse fitting Alexa Fluor fluorophore emisión and excitation*

A-plane GaN-based photodetectors for polarization-sensitive applications

A-plane GaN, as other nitride materials grown along nonpolar directions, has attracted much attention for its potential use in light-emitting devices and polarization-sensitive photodetectors (PSPD). The nonpolar nature of the surface and the in-plane crystal asymmetry can be exploited to enhance the intrinsic polarization sensitivity. Demanding applications are solid state light sources, optical storage, biophotonics, and polarized-light detection. In particular, PSPDs have been fabricated so far on *m*-plane GaN films grown on γ-$LiAlO_2$(100) substrates. In addition to purely polarization-sensitive applications, these photodetectors can be used for narrow band detection. However, some electrical performance limitations were present in these *m* -plane GaN PSPDs because of their large leakage currents even for low applied voltages. We present results on non-intentionally doped *a*-plane GaN PSPDs grown on sapphire substrates as an alternative to *m* -plane GaN PSPDs. The origin of the interesting properties of nitride materials grown along nonpolar directions as photodetectors is the reduced in-plane crystal symmetry. This reduced symmetry results in the complete in-plane polarization of the A-exciton, even for the case of unstrained GaN. The effect of strain induces further changes in the in-plane polarization selection rules and the valence band (VB) splitting. Theoretical studies for *m*-plane GaN have shown that transitions between the conduction and two uppermost VBs become completely linearly polarized for orthogonal in-plane directions in a certain range of in-plane strain values. At the same time, the splitting of the two uppermost VBs increases for this in-plane strain. These results can be similarly applied to the case of *a*-plane GaN material. Therefore, we expect an in-plane optical anisotropy in the vicinity of the energy gap for photodetection perpendicular (E ⊥c) and parallel to the *c*-axis (E ||c), thus allowing to extend the potential advantages of *m*-plane GaN PSPDs to *a*-plane GaN PSPDs. We denote T1 and T2 as the optical transitions from the conduction band into the two uppermost valence bands for an arbitrary induced strain. In the case of the *a*-plane GaN, we expect that transition T1 at lower energy is E ⊥c polarized, whereas T2 is E ||c polarized [11-15].

The PSPDs were fabricated on a *a* -plane GaN film grown at UCSB by low-pressure metal-organic vapor phase epitaxy on an *r*-plane sapphire substrate. The film thickness was determined to be about 1 μm by means of SEM and the out-of-plane dilation was extracted from X-ray diffraction (XRD). The XRD also showed that the sample was under biaxial compressive strain. The resulting in-plane strain was determined and the normalized oscillator strengths for T1 and T2 were calculated.

The high resistivity found in the *a*-plane GaN material led to study some electrical properties of this material using metal-semiconductor-metal (MSM) devices. These devices were fabricated by thermal deposition of 100-nm-thick Ni interdigitated electrodes both submicron and micro size periods. The spectral response for different in-plane polarization angles was measured (see Fig. 7). We can observe a spectral

separation of approximately 2 nm between the response curves corresponding to E ||c (i.e., R⊥) and E ||c (i.e., R||), leading to a maximum polarization sensitivity contrast for a single photodetector of R⊥ ~ R|| = 1.8. These devices can be used in a two- or four-photodetector differential configuration as explained in the introduction. In this case, the signal of interest is obtained as R⊥~R||, with a peak responsivity around 20% of the R⊥ maximum and a full width at half-maximum of the polarization sensitive region of 8.5 nm, as shown in the inset of figure 7. The ultraviolet–visible contrast was found to be higher than 10^3, limited by the experimental set up. The highest responsivity reached before the dark current becomes comparable to the photocurrent is approximately 2 A/W. This large responsivity value seems to indicate the presence of photoconductive gain [16].

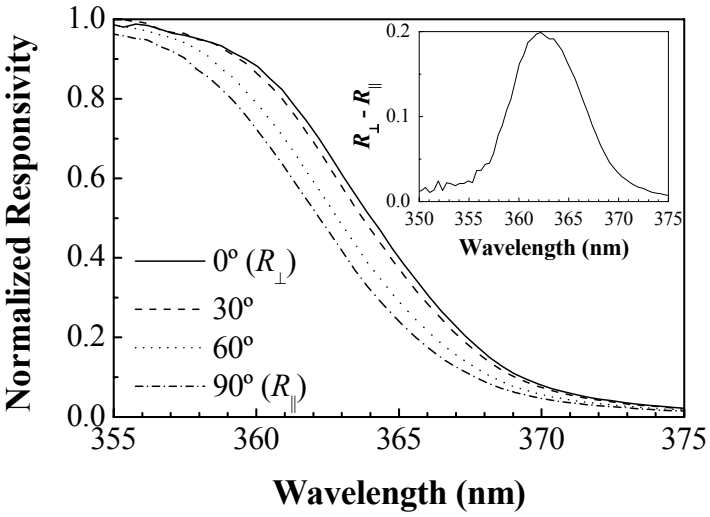

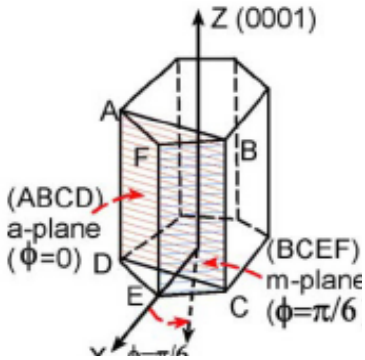

***Figure** 7. Normalized spectral response for different light polarizations for a-plane photodetector. Response of the photodetector system in a differential configuration (inset) [16]. Some crystal planes in wurtzite.*

Compared to previously reported results on *m*-plane layers grown on γ-LiAlO2 substrates, this technology allows the use of sapphire substrates, with reduced cost and simplicity. A-plane layers also showed very high resistivity, and improved electrical performance was obtained. The intrinsic responsivity contrast for a single-photodetector falls from 7.25 (M-plane GaN) to 1.8 (*a*-plane GaN), probably due to the fact that *m*-plane GaN layers are under a higher anisotropic strain. Theoretical calculations confirm a reduction in the expected oscillator strength ratio for E ⊥c and E ||c by a factor of ~ 4 for *a*-plane versus *m*-plane GaN. In order to improve the intrinsic polarization sensitivity for *a* -plane GaN, we should design devices fabricated on thinner active layers. However, when *a* -plane PSPDs are used in a differential configuration, this reduction can be compensated by their higher detectivity, offering a better performance even in terms of polarization sensitivity [16].

Acknowledgements

This work was partially supported by GaNano (EU STREP 505641-1 project, 2005-07) and by Regional Project CM P-AMB-000374-0505 FUTURSEN.

References

[1] G. Franssen, I. Gorczyca, T. Suski, A. Kamińska, J. Pereiro, E. Muñoz, E. Iliopoulos, A. Georgakilas, S.B. Che, Y. Ishitani, A. Yoshikawa, N.E. Christensen, and A. Svane, J. Appl. Phys. **103**, 033514 (2008).

[2] J. Pereiro, J.L. Pau, C. Rivera, A. Navarro, E. Muñoz, R. Czernecki, G. Targowski, P. Prystawko, M. Krysko, M. Leszczynski and T. Suski, in *Nitrides and Dilute Nitrides: Growth, Physics and Devices,* J. Miguel, Ed., Research Signpost, Singapore, 2007.

[3] L.R. Bailey, T.D. Veal, P.D.C. King, C.F. McConville, J. Pereiro, J. Grandal, M.A. Sánchez-García, E. Muñoz and E. Calleja, J. Appl. Phys. **104**, 113716 (2008).

[4] J. Pereiro, PhD Thesis, UPM, Madrid (2009).

[5] C. Rivera, E. Muñoz, O. Brandt, and H.T. Grahn, Appl. Phys. Lett. **91**, 203514 (2007).

[5] C. Rivera, P. Misra, J.L. Pau, E. Muñoz, O. Brandt, H.T. Grahn, and K.H. Ploog, Phys. Stat. Sol. c **4**, 2548 (2007).

[6] J. Pereiro, C. Rivera, A. Navarro, E. Muñoz, R. Czernecki, S. Grzanka and M. Leszczynski, IEEE J. Quantum Electron. **45**, 617 (2009).

[7] C. Rivera, PhD Thesis, UPM, Madrid (2007).

[8] C. Rivera and E. Muñoz Appl. Phys. Lett. **92**, 233510 (2008).

[9] A. Arranz, C. Palacio, D. García-Fresnadillo, G. Orellana, A. Navarro and E. Muñoz, Langmuir, ***24***, 8667 (2008).

[10] J. Lopez-Gejo, A. Arranz, A. Navarro, C. Palacio, E. Muñoz and G. Orellana, J. Am. Chem. Soc., **132**(6), 1746 (2010).

[11] S. Ghosh, O. Brandt, H.T. Grahn and K. H. Ploog, Appl. Phys. Lett. **81**, 3380 (2002).

[12] S. Ghosh, P. Waltereit, O. Brandt, H.T. Grahn and K.H. Ploog, Phys. Rev. B **65**, 075202 (2002).

[13] C. Rivera, J.L. Pau, E. Munoz, P. Misra, O. Brandt, H.T. Grahn and K.H. Ploog, Appl. Phys. Lett., **88**, 213507 (2006).

[14] S. Ghosh, C. Rivera, J.L. Pau, E. Muñoz, O. Brandt, and H.T. Grahn, Appl. Phys. Lett. **90**, 091110 (2007).

[15] C. Rivera, P. Misra, J.L.Pau and E. Muñoz, O. Brandt, H.T. Grahn and K.H. Ploog, J. Appl. Phys. **101**, 053527 (2007).

[16] A. Navarro, C. Rivera, J. Pereiro, E. Muñoz, B. Imer, S.P. DenBaars and J.S. Speck, Appl. Phys. Lett. **94**, 213512 (2009).

6.7 Nanophotonic Biosensors[7]

The ISOM has started a new research line focused on the development of novel photonic devices for biochemical sensing. Optical sensors are remarkable tools for analyte detection in biochemical, health and environmental applications. The use of photons for sensing makes possible multi-dimension (intensity, wavelength, phase, and polarization) and remote interrogation, immunity to electromagnetic interferences, multiplexed detection, and availability of well-established technologies from communication industries: e.g. lasers of almost any wavelength, detector arrays, micro-/nano-machining, waveguides, and high speed links. In addition, optical frequencies coincide with a wide rage of physical properties of bio-related materials in Nature.

Slot-waveguide microring resonator based biochemical sensors

Slot-waveguides allow light to be guided and strongly confined inside a nanometer-scale region of low refractive index. Thus stronger light-analyte interaction can be obtained as compared to that achievable by a conventional waveguide, in which the propagating beam is confined to the high-refractive-index core of the waveguide. In addition, slot-waveguides can be fabricated by employing CMOS compatible materials and technology, enabling miniaturization, integration with electronic, photonic and fluidic components in a chip, and mass production. These advantages have made the use of slot-waveguides for highly sensitive biochemical optical integrated sensors an emerging field [1].

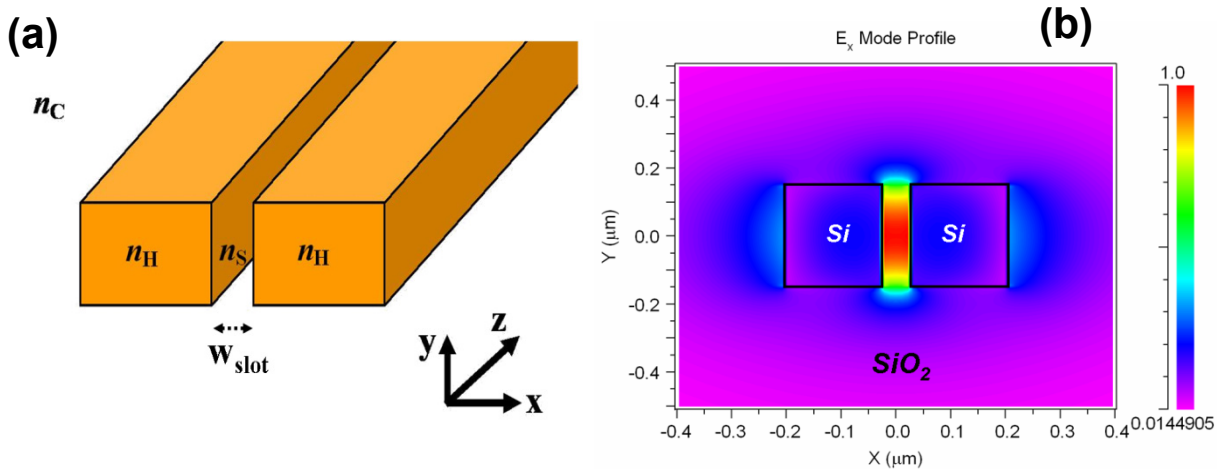

Figure 1. *(a) Schematic view of a slot-waveguide. (b) Calculated E_x profile of the quasi-TE eigenmode in a Si (n_H = 3.45)/SiO_2 (n_S = n_C = 1.44) slot-waveguide at a wavelength of 1.55 μm. E-field is enhanced in the nanoscale slot-region of refractive index n_S.*

ISOM participates as a partner in a European Project entitled "Ultrahigh sensitivity slot-waveguide biosensor on a highly integrated chip for simultaneous diagnosis of multiple diseases" (SABIO). This is a multidisciplinary project involving the emerging fields of micro-nano technology, photonics, fluidics and bio-chemistry, targeting to contribute to the development of intelligent diagnostic equipment for the healthcare of the future. SABIO addresses this objective through the demonstration of a compact polymer-based and silicon-based CMOS-compatible micro-nano system. It integrates optical biosensors for label-free biomolecular recognition based on a novel photonic structure named slot-waveguide with immobilised biomolecular receptors on its surface. This structure offers the possibility of confinement and guidance of light in a nanometer-size void channel enhancing the interaction between an optical probe and biomolecular complexes (antibody-antigen).

[7] *Contact Person: Carlos Angulo Barrios: carlos.angulo.barrios@upm.es*

The first experimental demonstration of a slot-waveguide based biochemical sensor was achieved at ISOM by C.A. Barrios et al. for both liquid (bulk) and biomolecule (surface) sensing [2,3]. These authors employed a vertical (slot/rail interface is normal to the substrate) slot-waveguide ring resonator made of Si_3N_4 on silicon dioxide. The use of Si_3N_4 as high-index material (instead of higher-index Si) enables the definition of a wider slot region while maintaining single-mode operation [4]. The main purpose of having a wider slot region is to facilitate filling it with liquids for sensing and optofluidic applications. The device sensor was probed at a wavelength around 1.3 μm, which is typically used in telecomm applications (O-band) and leads to lower water optical absorption than that at the other common telecom wavelength, 1.55 μm.

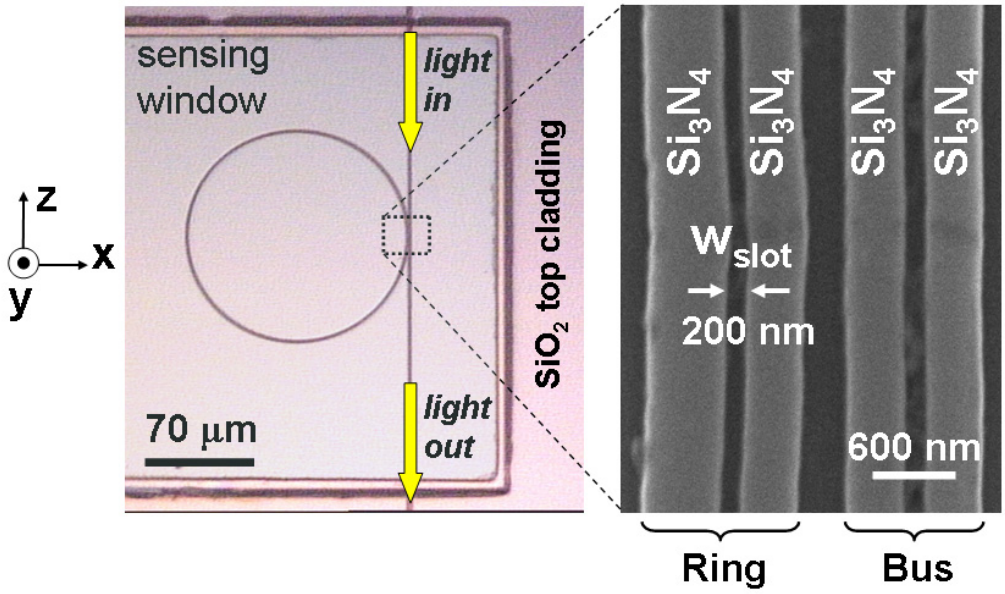

Figure 2. *Left: Top view photograph of a 70-μm-radius Si_3N_4 slot-waveguide microring resonator. Right: Scanning electron microscope image of the coupling region.*

A spatial discriminating chemical treatment to selectively Si_3N_4 nitride versus SiO_2 was designed for the attachment of biomolecules only to the nitride area of the sensing surface [5]. The effectiveness of the selective surface modification procedure was supported by comparing experimental and numerical calculations [6] of the optical performance of a label-free Si_3N_4/SiO_2 slot-waveguide ring resonator.

A Si_3N_4 microring array with a PDMS microfluidic network was integrated on a Si single chip, enabling accurate multiplexed assays in labs-on-chip [7]. Details on the implementation and characterization of the final SABIO biochip were published in *Lab on a Chip* [8] and featured on the inside front cover of the printed edition (Fig. 3).

A Si_3N_4 slot-waveguide microring resonator was also used to demonstrate optofluidic device reconfigurability [9]. It was observed that small amounts of organic liquids were trapped, due to capillary and wetting forces, inside the slot-nanochannel, modifying dramatically the microring resonator optical response. Potential optofluidic applications of this effect include permanent and rewriteable photonic configurations, process monitoring, *in-situ* chemical detection, and study of liquid-solid interfacial forces at the nanoscale.

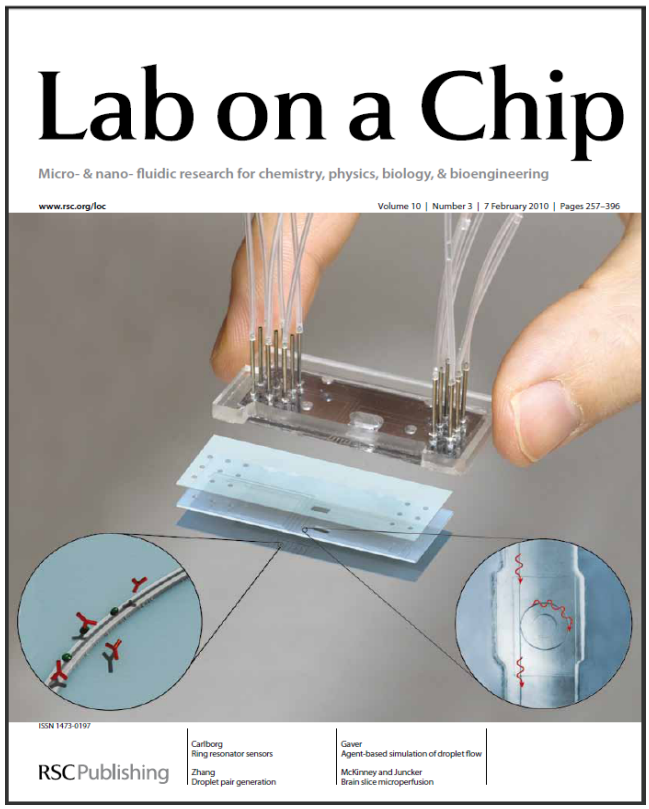

Figure. 3. *The SABIO device is featured on the inside front cover of the printed edition of the journal Lab on a Chip.*

Nano-opto-fluidic structures for biochemical sensing based on advance high sensitivity optical techniques

ISOM also participates as a partner in a Spanish project entitled "**Nano-opto-fluidic structures for biochemical sensing based on advance high sensitivity optical techniques (*BIOPSIA*).** The aim of this project is to develop a high sensitive optical sensing system for label-free bioassays. The key benefits and features of the BIOPSIA sensing system rely on a holistic approach that combines both: unique optical technologies capabilities and CMOS compatible bio-photonic structures for a new generation of a high value optical biosensing system. By means of the simultaneously observation of the reflectivity profile of three complementary enhanced sub-micron spot size optical technologies, and the magnification for label-free biosensing due to the interferometric micro-nano photonic structures, BIOPSIA will make possible to determine with more reliability and sensitivity the biomolecular interaction with the receptor biomolecules attached in the sensing areas. It is also a target of the project to investigate the fluidic phenomena in nano-channels, nano-slots and in micro-nano holes applied to metrology, in which a clear research line is currently open under the European Metrology Research Programme (EMRP) to investigate both: measure of small fraction of volumes and advanced flow measuring techniques. In both cases BIOPSIA proposes a system that make advance in solutions in these research fields as well. The BIOPSIA sensing system uses a tightly focused beam that allows measuring in situ of sub-micron size geometries, making possible a high integration of bio-photonic sensing areas. Furthermore, BIOPSIA also offers an inexpensive solution for packaging (an important issue identified in the European Technology Platform Photonics 21) because it overcomes the need for using complex systems for light coupling such as inverted tapers or grating couplers because the sensor evaluation is done measuring vertically collecting the reflected light of the bio-photonic sensing areas. It will also demonstrate that routine screening will be more cost-effective and suitable for performing hundred of assays on a sample for multi-single or multi-parameter measurements. The simultaneous use of three different techniques in less than 5 seconds allows the systems to achieve a high sensitivity, throughput, reliability and productivity in comparison with other analytical techniques.

We have fabricated periodic lattices of SU-8 nano-pillars as bio-cells [10], where the following immunoassay was carried out: a monolayer of BSA (Bovine Serum Albumin) was immobilized on the surface of the bio-cells and then the lattice was infiltrated with a buffer solution containing different concentrations of anti-BSA protein. The affinity reaction generated changes in the bio-cell refractive index, and thus in the position of the reflectance interference peaks, which are the source of information to evaluate the anti-BSA recognition to obtain the biosensing response. Detection limits on the order of 1 ng/ml where measured.

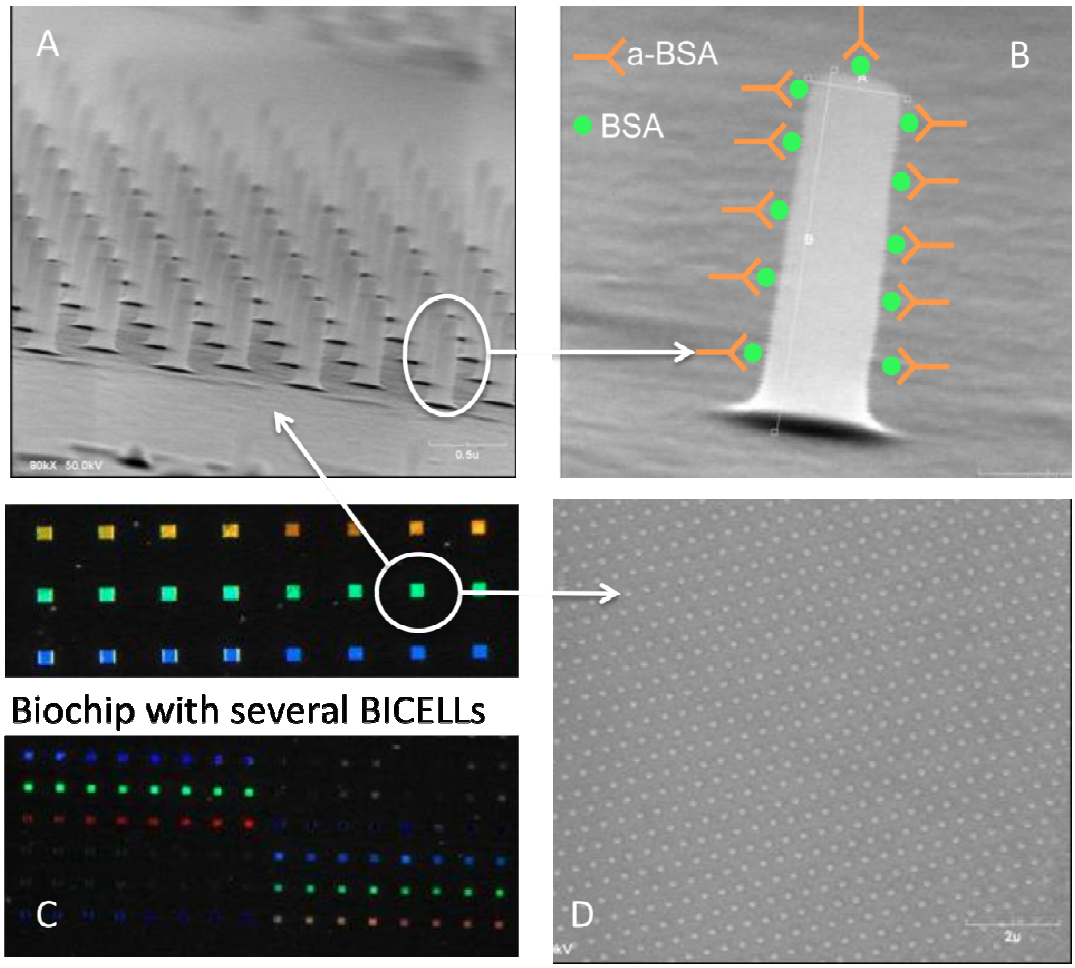

Figure 4. *A) SEM micrograph of a SU8-based BICELL, B) SEM micrograph of one single nano-pillar and a schematic representation of BSA immobilization and aBSA recognition. C), Optical image of a biochip with an array of BICELLs, D) SU8-BICELL top-view SEM micrograph.*

References

[1] C.A. Barrios, "Optical Slot-Waveguide based Biochemical Sensors", Sensors, **9**, 6, 4751 (2009).

[2] C.A. Barrios, K.B. Gylfason, B. Sánchez, A. Griol, H. Sohlström, M. Holgado, and R. Casquel, "Slot-waveguide biochemical sensor", Optics Letters, **32,** 21, 3080 (2007).

[3] C.A. Barrios, M.J. Bañuls, V. Gonzalez-Pedro, K.B. Gylfason, B. Sánchez, A. Griol, A. Maquieira, H. Sohlström, M. Holgado and R. Casquel, "Label-free optical biosensing with slot-waveguides", Optics Letters, **33,** 7, 708, 2008.

[4] C.A. Barrios, B. Sánchez, K.B. Gylfason, A. Griol, H. Sohlström, M. Holgado, and R. Casquel, "Demonstration of slot-waveguide structures on silicon nitride/silicon oxide platform", *Optics Express*, **5**, 11, 6846 (2007).

[5] M.J. Bañuls, V. González-Pedro, C.A. Barrios, R. Puchades and A. Maquieira, "Selective chemical modification of silicon nitride/silicon oxide nanostructures to develop label-free biosensors", Biosensors and Bioelectronics, **25**, 1460 (2010).

[6] C.A. Barrios "Analysis and modeling of a silicon nitride slot-waveguide microring resonator biochemical sensor", *Proc. of SPIE*, vol**. 7356**, 735605(1-9) (2009).

[7] K.B. Gylfason, C.F. Carlborg, A. Kazmierczak, F. Dortu, H. Sohlström, L. Vivien, C.A. Barrios, W. van der Wijngaart and G. Stemme, "On-chip temperature compensation in an integrated slot-waveguide ring resonator refractive index sensor array", Optics Express, **28**, 4, 3226 (2010).

[8] C.F. Carlborg, K.B. Gylfason, A. Kaźmierczak, F. Dortou, M.J. Bañuls Polo, A. Maquieira Catala, G. M. Kresbach, H. Sohlström, T. Moh, L. Vivien, J. Popplewell, G. Ronan, C.A. Barrios, G. Stemme and W. van der Wijngaart, "A packaged optical slot-waveguide ring resonator sensor array for multiplex label-free assays in labs-on-chips", Lab Chip, **10,** 281 (2010).

[9] C.A. Barrios, M. Holgado, O. Guarneros, B. Sánchez, K.B. Gylfason, R. Casquel, and H. Sohlström, "Reconfiguration of microring resonators by liquid adhesion", Applied Physics Letters, **93**, 20, 203114 (2008).

[10] D. López-Romero**,** C.A. Barrios, M. Holgado, M.F. Laguna, and R. Casquel, "High aspect-ratio SU-8 resist nano-pillar lattice by e-beam direct writing and its application for liquid trapping" Microelectronic Engineering, **87,** 663 (2010).

6.8 ZnO-based micro- and nanophotonics[8]

The driving force for this research line is the stability of the ZnO free exciton, with a binding energy of 60 meV in bulk material, and even higher in confined structures. Indeed, the binding energy is more than twice that of the GaN free exciton (25 meV), quite significant since nitrides are the semiconductors mostly used for UV and blue optoelectronic applications and the ZnO bandgap (3.37 eV at room temperature) is comparable to that of GaN. Moreover, the availability of fairly high quality larger area bulk substrates, at much cheaper prices and with lower threading dislocations densities could make this technology very competitive compared to nitrides. ZnO also has the advantage over other compound semiconductors, and specifically over nitrides, that it can be grown rather easily into one-dimensional structures with various shapes including nanowires, nanoneedles, nanobelts, nanotubes, rings, combs, or tetrapods, which opens new doors to optoelectronic devices with very efficient light extraction/coupling schemes and high quality crystal structures leading to high radiative efficiencies. Our goal is to identify the physical origin of the dominant electrically active defects that are present in these structures, the impact they have on the electrical and transport properties, and ultimately on photonic devices [1].

Among the devices currently being developed, photoconductors, Schottky and MSM photodiodes covering the UV to VIS region are included [1], where ZnMgO or ZnCdO are used to tune the detection wavelength either in bulk layers or in quantum wells (QWs). Additionally, and with the final goal of achieving bipolar photonic devices (such as LEDs or laser diodes), the identification of the mechanisms limiting p-type doping in these oxides is being investigated focusing on deep level formation and paying particular attention to polarity and alloy composition. Indeed, we have recently shown that ZnMgO is heavily compensated and thus is quite amenable to p-type doping [2], and that the acceptor-like levels are responsible for the huge responsivities present in ZnMgO UV-photodetectors [3].

Towards p-type in ZnMgO

We have performed a systematic analysis with the Mg content of the formation and concentration of deep levels found throughout the lower half of the bandgap of a-plane ZnMgO [2]. A combination of deep level optical spectroscopy (DLOS) and lighted capacitance-voltage profiling (LCV) are used since they allow the quantification of the energies and concentrations of the deep levels found in the lower half of the bandgap of n-type material, i.e., deep levels that may act as acceptors.

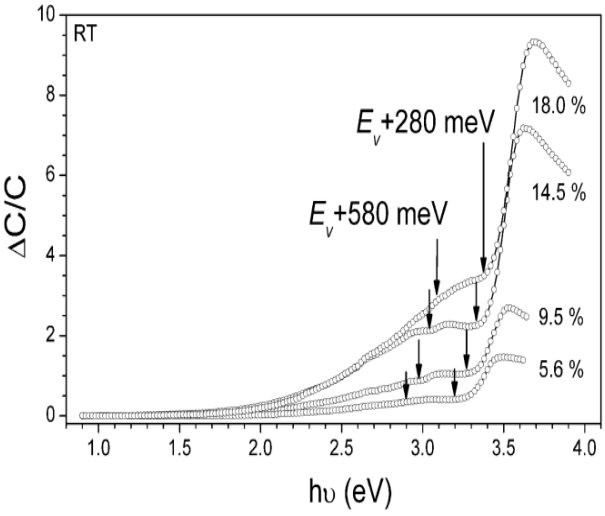

***Figure 1**: Steady state photocapacitance spectra of ZnMgO, where two acceptor-like states are observed close to the valence band.*

In this work non-polar *a*-plane ZnMgO films grown at the University of Shizuoka (Japan) have been used. The films were grown on *r*-plane sapphire by remote plasma enhanced metal-organic chemical vapor depositionunder O-rich conditions.

It is clearly observed that the presence of Mg in ZnMgO can result in the formation of two deep levels at E_v+580 and E_v+280 meV (figure 1) whose concentrations increase linearly with the Mg content, accounting for the observed decrease in the net electron concentration (Table 1). The formation of these deep levels, specially the E_v+280 meV one (N_t~1x10^{18} cm^{-3} at 18.0 % Mg), can explain the strong carrier compensation effect observed at higher Mg contents, the large series resistance of the Schottky diodes, being

[8] *Contact person: Adrián Hierro* ahierro@die.upm.es

likely at the origin of the amenability to p-type doping typically observed in ZnMgO.

UV Schottky photodiodes

Using *a*-ZnMgO bulk films grown on *r*-sapphire (University of Shizuoka, Japan), semitransparent 100 Å thick Au Schottky photodiodes using circular structures of 200 and 400 μm diameters have been optimized in a lateral geometry co-planar to 1000 Å-thick Ti/Al/Ti/Au extended ohmic contacts [4]. The surface is typically passivated with H_2O_2. Figure 2 shows the dark *I-V* curves of the Schottky photodiodes, which present very low saturation currents and an excellent rectifying behavior.

Mg Content (%)	N_d-N_a (cm^{-3})	E_v+280 meV (cm^{-3})	E_v+580 meV (cm^{-3})
5.6	$8.02x10^{16}$	$1.08x10^{17}$	$1.66x10^{16}$
9.5	$1.98x10^{16}$	$3.44x10^{17}$	$1.54x10^{16}$
14.5	$1.47x10^{16}$	$8.62x10^{17}$	$2.27x10^{16}$
18.0	$1.27x10^{16}$	$1.01x10^{18}$	$5.23x10^{16}$

***Table 1**: Effective carrier concentration (N_d-N_a) and deep level concentration in ZnMgO films.*

The spectral response of the photodiodes has been analyzed in photovoltaic mode and under a -1.5 V reverse bias (Fig. 3). Under reverse biases, the Au-ZnMgO Schottky photodiodes present absorption edge energies tunable from 3.35 to 3.58 eV as the Mg content is increased from 5.6 to 18.0 %, and UV/VIS spectral rejection ratios of up to 5 orders of magnitude (Fig. 3). In contrast, under photovoltaic mode the spectral rejection ratio is much lower, between one and two orders of magnitude. These rejection ratios are much larger than those typically reported in AlGaN Schottky photodiodes for similar biases, and are accompanied by very large responsivities ($\mathcal{R}$) above bandgap (Table 2). For the photodiodes with low Mg concentration $\mathcal{R}$ is as high as 185 A/W at -1.5 V, while increasing the Mg concentration to 18 % leads to a reduction down to 32 A/W. Under photovoltaic conditions, $\mathcal{R}$ ranges from $5.9x10^{-5}$ to $3.3x10^{-5}$ A/W. Both under photovoltaic mode and reverse biases, $\mathcal{R}$ decreases at higher Mg concentrations, correlating well with the increase in the series resistance (R_s) of the diodes. Thus, the decreased responsivities at high Mg contents may be ascribed to the fact that the material is highly compensated.

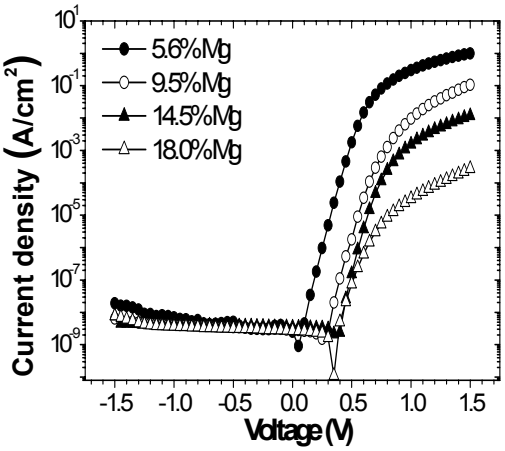

***Figure 2**: IV characteristics of the Au-ZnMgO Schottky photodiodes.*

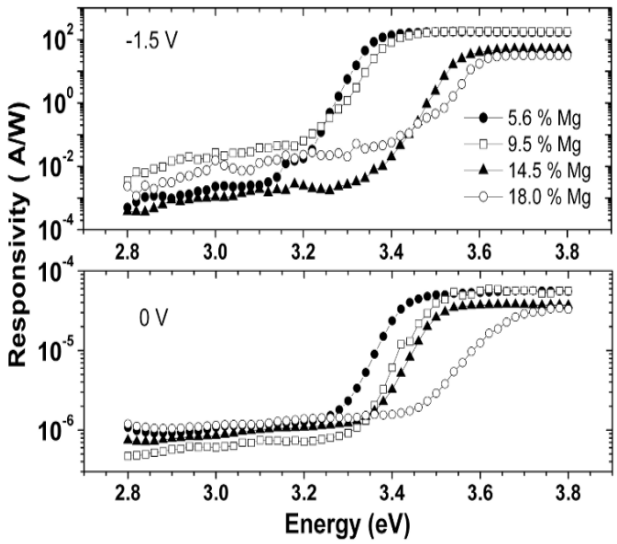

***Figure 3**: Responsivity at -1.5 and 0 V of ZnMgO Schottky photodiodes.*

However, the giant ~10^5 A/W responsivities observed under reverse biases yield quantum efficiencies (η) much greater than 1, which implies that there must be an internal gain mechanism responsible for these

large responsivities. To understand the origin of this large internal gain, the I-V characteristics of the Schottky photodiodes were analyzed during illumination with above band-gap light (Fig. 4). As shown in the figure, the photodiodes become completely non-rectifying and present an ohmic-like behavior, with large saturation currents and ideality factors much greater than 2, behavior that is present for all the different Mg contents. Moreover, the I-V curves measured under illumination are highly sensitive to the photon flux. Taking the 14.5 % Mg photodiode as an example, a change of the photon flux by 4 orders of magnitude, from 7.0×10^{12} to 5.9×10^{16} $s^{-1}cm^{-2}$, produces a degradation of the ideality factors from 1.2 to 3.5, and most of all, an increase in the current at -1.5 V by more than 8 orders of magnitude (Fig. 4). This implies that the measured responsivity is a function of the photon flux (see inset of Fig. 4), and so is the internal gain.

% Mg content	-1.5 V		0 V	
	$\mathcal{R}$ (A/W)	ηg	$\mathcal{R}$ (A/W)	ηg
5.6	173	609	5.5×10^{-5}	1.9×10^{-4}
9.5	185	651	5.9×10^{-5}	2.2×10^{-4}
14.5	49	180	3.7×10^{-5}	1.4×10^{-4}
18.0	32	108	3.3×10^{-5}	1.2×10^{-4}

***Table 2**: Responsivity and internal quantum efficiency-gain product for ZnMgO Schottky photodiodes.*

Using Capacitance-Voltage (CV) profiling we observe that the total electron concentration increases from ~3.5×10^{16} cm^{-3} under dark conditions, up to ~8.2×10^{17} cm^{-3} for the highest photon flux. Consistent with this large increase in electron concentration, the depletion region width shrinks from ~0.24 μm in the dark down to ~0.06 μm under high photon fluxes. Thus, it is clear that there is a large redistribution of space charge as a result of illumination, and a progression from a highly compensated material in the dark to a highly conductive material under illumination, which implies that the electron quasi-Fermi level shifts to much higher energies.

Thus, during illumination the Schottky photodiodes become highly ohmic due to the large contribution of tunneling, whose primary origin is the photoexcitation of trapped carriers at acceptor-like deep levels, which is dominated by a level at E_v+280 meV discussed in the previous section. This tunnel current yields a high saturation current and high ideality factor of the diodes, and while at 0 V it has no effect, under large forward or reverse biases the current flowing is determined by this saturation current. Thus, at 0 V, the photodiode responsivities are very low, i.e., there is no internal gain and $\eta g \cong \eta$. However, applying a reverse bias of -1.5 V allows the tunnel-dominated saturation current to emerge, i.e., there is a large internal gain, which is a function of the photon flux. This internal gain mechanism can also explain why the spectral rejection ratio is so large under reverse biases. Illumination with energies smaller than E_g-280 meV has little impact on the conduction band carrier population, i.e., on the *I-V* characteristics and the measured photocurrent is low. However, when the excitation energy is equal to or greater than E_g-280 meV, the E_v+280 meV level is photoionized in parallel to the generation of *e-h* pairs, and the photocurrent rises to high values via the previously discussed mechanism.

In parallel to the development of Schottky UV photodetectors that use bulk layers grown by MOCVD, non-polar ZnO/ZnMgO QWs grown by MBE on different substrates, including sapphire and ZnO, are also being used to tune the detection wavelength, as well as to analyze their potential as polarization sensitive photodetectors. This work is currently being pursed under a collaboration with Centre de Recherche sur l'Hétéro-Epitaxie et ses Applications (CRHEA)-CNRS, in France.

Nanocolumns as photodetectors

Two different approaches are being pursued to develop nanophotodetectors [1]: a bottom-up approach where ZnCdMgO nanocolumns (NC) grown on sapphire are removed, re-deposited on an insulating substrate (typically SiO_2/Si), geometrically organized, and contacted with metal pads; and a top-bottom approach, where instead of using self-organized NCs, thin films containing either ZnO bulk layers or ZnO/ZnMgO QWs are used as the basis, on which through nanolithography followed by anisotropic etching, patterned NCs are defined, providing control over geometry.

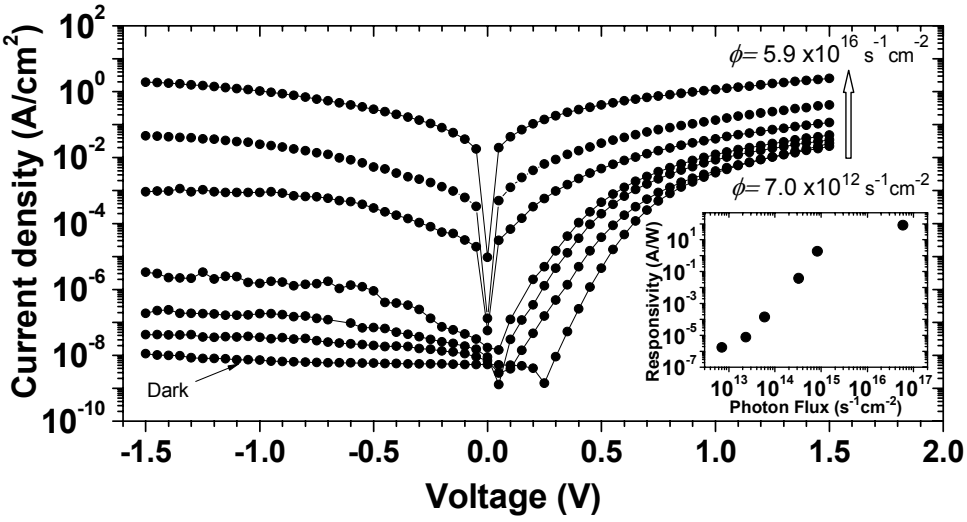

***Figure 4**: IV characteristics as a function of incident photon flux for the ZnMgO Schottky photodiode with 14% Mg at -1.5 V.*

Through the first bottom-up approach, single ZnO NCs from Univ. of Shizuoka have been contacted with Au/Ti layers (Fig. 5), with which a nanophotoconductor sensitive to light with E>3.4 eV (or λ<365nm) is obtained. Figure 6 shows the *I-V* characteristics of this nanophotoconductor, both in the dark and when excited with above bandgap energy. It is clear that the responsivity contrast between dark and illumination conditions is between one and two orders of mangnitude.

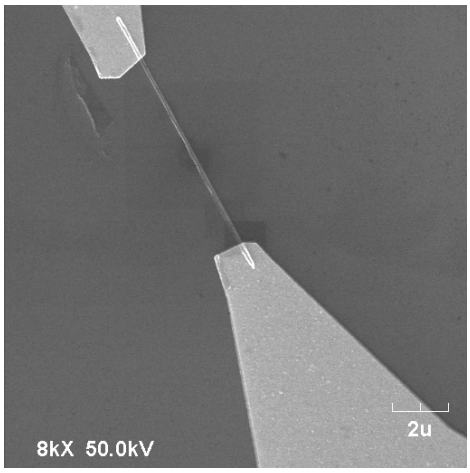

***Figure 5**: Image of a single ZnO nanocolumn electrically contacted.*

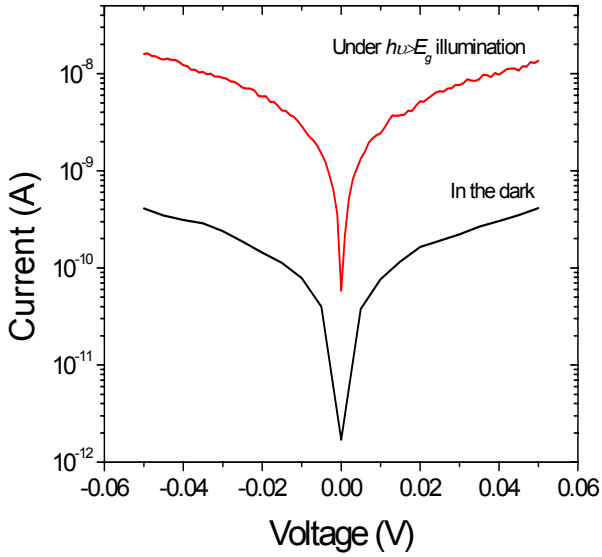

***Figure 6**: IV characteristics in the dark and under illumination for a single ZnO nanocolumn photoconductor.*

This responsivity can be spectrally tailored through proper choice of the NC alloy, and the gain can be controlled through deposition of a metal gate producing a nano-phototransistor, currently being developed. The technology to allow contacting tens of NCs on a single processing step has also been optimized, and will allow the future development of matrices of aligned NCs.

Through the second top-bottom approach, thin films grown at CRHEA-CNRS are being patterned with nanolithography followed by Ar milling, with the goal of defining arrays of patterned ZnO NCs. The NCs can be defined with lateral dimensions below 100 nm (Figure 7). With this approach, the goal is to have precise control of the nanophotodetector geometry, allowing the definition of custom-controlled arrays of NCs, which will be used to control parameters such as light coupling efficiency, sensitivity to light polarization, gain, etc.

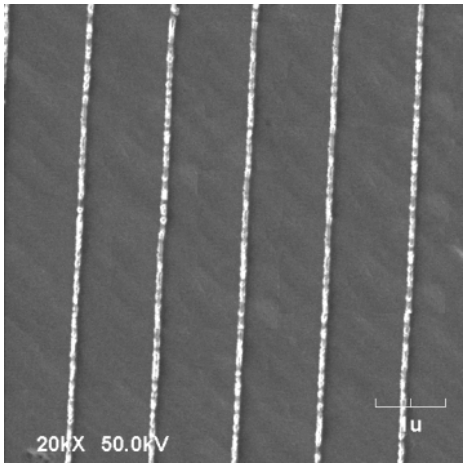

Figure 7*: Image of an array of patterned nanowires, 100nm-wide and 200 nm-high, made of ZnO.*

References

[1] *ZnO-based Micro- and nanosensors for UV and H2 detection*, project funded by Spanish ministry for Science and Innovation, 2009-2012, PI: Adrian Hierro.

[2] A. Hierro, G. Tabares, J.M. Ulloa, E. Muñoz, A. Nakamura, T. Hayashi, and J. Temmyo, *Carrier compensation by deep levels in $Zn_{1-x}Mg_xO$/sapphire*, Applied Physics Letters **94**, 232101 (2009).

[3] G. Tabares, A. Hierro, J.M. Ulloa, A. Guzman, E. Muñoz, A. Nakamura, T. Hayashi, J. Temmyo, *High responsivity and internal gain mechanisms in Au-ZnMgO Schottky photodiodes*, Applied Physics Letters, in press, 2010.

[4] A. Nakamura, T. Hayashi, A. Hierro, G. Tabares, J. M. Ulloa, E. Muñoz and J. Temmyo, *Schottky barrier contacts formed on polar-, nonpolar-$Mg_xZn_{1-x}O$ film grown by remote plasma enhanced MOCVD*, Physica Status Solid c, in press, 2010.

6.9 Al(Ga)N/GaN Solution Gate Field Effect Transistors for sensor application[9]

Wide bandgap materials such as diamond or GaN are prime candidates for a variety of sensor applications, particularly at high temperatures and in harsh environments. On one hand, the large bandgap ensures minimal problems due to unwanted optical or thermal generation of charge carriers, of special interest in the field of 'solar blind' UV detectors [1-3], and high temperature gas sensors [4]. On the other hand, the strong chemical bonding between the constituent atoms gives rise to an exceptional mechanical, thermal, and chemical stability of this class of materials.

The achievement of optimised sensors, as in any other competitive electronic device, requires a certain maturity in the deposition, processing and customization of the base materials. The remarkable progress made in the last decade in the growth and processing of GaN-related materials has opened up new possibilities not only in optoelectronics and high power/high frequency devices, but also for novel sensors and complex integrated systems featuring embedded sensor functions.

Many different designs for III-nitride based sensors are possible, but the work performed at ISOM has focused on those based in AlGaN/GaN heterostructures like that shown in figure 1. More importantly, the same heterostructure can also be used for the fabrication of high frequency/high power high electron mobility transistors (HEMTs) [5] as well as passive surface acoustic wave (SAW) devices [6], which opens up a possible route for monolithic integration of both, sensor functions and analog as well as digital data processing and transmission. In this way, integrated devices with multifunctional sensor capability, on-chip amplification and computation capability, and even remote wireless readout capability would be possible by suitable technological processes.

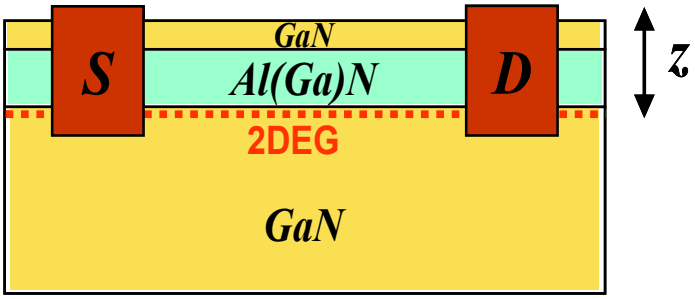

***Figure 1**. Schematic of a typical HEMT structure based on AlGaN/GaN. A 2-dimensional electron gas (2DEG) channel is formed at the AlGaN/GaN interface. Source and drain contacts are also shown.*

A particular field of application of this type of sensor has been the pH detection [7]. According to the site-binding model [8], the pH-sensitivity is due to amphoteric hydroxyl groups, in this case from the thin Ga_xO_y surface layer formed after wet chemical oxidation or even after a simple exposure to atmosphere. In addition, the oxidic surface of group III-nitride devices allows the covalent immobilization of biomolecules after silanization [9], [10], and makes the surface naturally biocompatible [11]-[13], which allows the application of these devices to detect ion currents through cell membranes in general and of action potentials of neuron cells in particular [12].

[9] *Contact person: Miguel Ángel Sánchez sanchez@die.upm.es*

In the HEMT structures (like the one shown in Figure 1), the conductivity of a two-dimensional electron gas (2DEG), located typically 20 nm to 30 nm beneath the surface, is affected by chemically induced changes of the surface potential. In order to enhance the transducive sensitivity of devices based on AlGaN/GaN electrolyte gate FETs, some works have demonstrated the use of nanostructures (ZnO nanorods) on the gate area [14]. But from the HEMT heterostructure point of view, only the application of N-face polarity heterostructures, with a significantly reduced 2DEG-to-surface distance (*z* in Figure 1), has recently been proposed [15]. However, this approach presents two drawbacks: (i) it leads to structures with lower chemical stability, as compared to (0001)-oriented surfaces [16], and (ii) the growth procedure of N-face heterostructures has been well established just recently, and it is not easy to obtain high quality material [17]. For these reasons, the application of AlN/GaN heterostructures as an alternative can be considered as a more promising approach. Due to the high difference in spontaneous and piezolectric polarizations between the GaN and AlN layers in these structures, 2DEGs with high electron concentration and mobility can be achieved employing a very thin AlN barrier. In spite of the obvious benefit that the reduction of barrier thickness has on the transconductance of transistors, and therefore on the device performance, sensor applications of AlN/GaN-based HEMT structures have not yet been studied.

The work performed at the ISOM recently has focused on the design, fabrication and characterization of an AlN-barrier solution-gate field effect transistor (SGFET) that, compared with standard SGFETs, exhibits much higher transconductivity at lower gate-drain voltages.

For this purpose, the performance of three pH-sensitive transistor structures (differing by the distance *z*) is compared. Sample A is a GaN/AlN/GaN heterostructure with z = 7.5 nm, sample B consists of a GaN/$Al_{0.27}Ga_{0.73}$N/GaN layer sequence with z = 19 nm and sample C is a GaN/$Al_{0.23}Ga_{0.77}$N/GaN heterostructure with z = 23 nm. Samples A and B were grown by plasma-assisted molecular beam epitaxy (PAMBE) on semi-insulating GaN:Fe templates, while sample C was grown by metal organic chemical vapor deposition (MOCVD) on *c*-plane sapphire (more details in [10]). For a better comparison, the thickness of the GaN capping layer, grown to prevent oxidation of the Al(Ga)N barrier, was set to 3 nm in all the samples, while the thickness of the respective Al(Ga)N barrier was 4.5 nm in sample A, 16 nm in sample B and 20 nm in sample C. Capacitance-voltage characterization of the as-grown samples was performed in order to confirm *z* values along with the carrier concentration in the 2DEG.

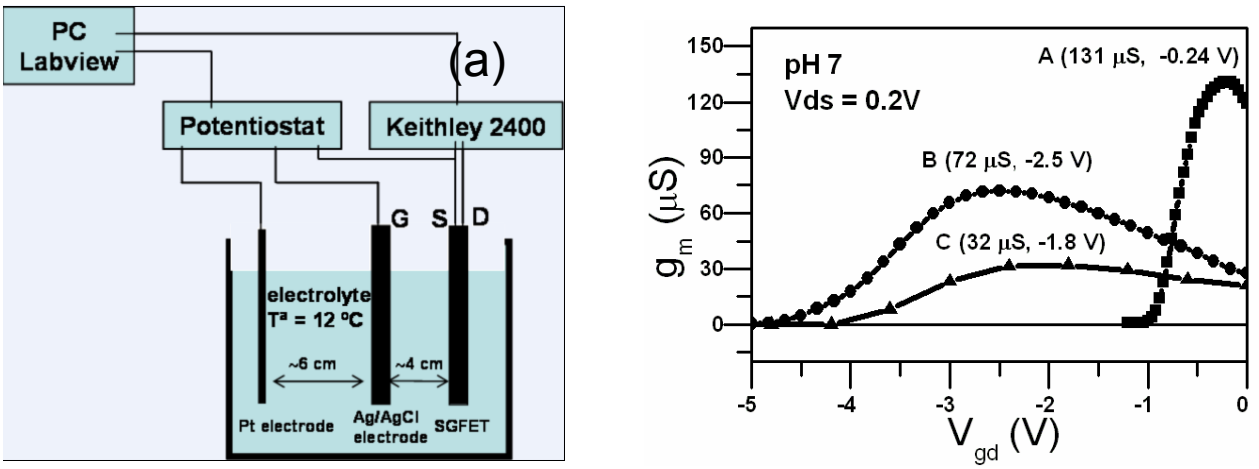

***Figure 2**. (a) Three-electrodes measurement set-up. For clarity, pH monitoring, temperature control and titriation are not shown. (b) Transconductance characteristics for samples A, B and C, recorded at pH 7 and V_{ds} = 0.2V. Maximum g_m values changes from 131 □S in the case of sample A, to 72 □S for sample B and 32 □S in the case of sample C. At the same time, g_m^{max} is shifted to much lower voltages in the case of sample A (-0.24 V).*

The typical processing steps of a device include H_2O_2:H_2SO_4 (1:3) cleaning, ohmic contacts deposition followed by a rapid thermal annealing treatment, and mesa isolation leading to channel dimensions of W = 0.5 mm (channel width) and L = 1.2 mm (channel length). After wire bonding of the ohmic contacts to metal pads, encapsulation with epoxy resin is accomplished by hand.

The electrochemical characterization was carried out in a three-electrode cell described elsewhere [10], and schematically depicted in figure 2a. The electrolyte was 10 mM N-2–Hydroxyethylpiperazine-N8-2–ethanesulfonic acid (HEPES) containing 1 M sodium chloride, titriated with buffered HCl and NaOH solutions. The solution was kept at 0 V with respect to the Ag/AgCl electrode by a Voltalab 40 potentiostat. During the measurements, the SGFET drain contact (working electrode) was offset relative to this zero point by the bias voltage V_{gd}. All measurements shown in this work were taken with a drain-source voltage V_{ds} = 200 mV. The solution temperature during the characterization was kept at 12 ºC, leading to a theoretical Nernstian surface potential sensitivity of 56.5 mV/pH.

Figure 2b shows the dependence of the transconductance (g_m) on V_{gd} at pH 7 for the three samples. The maximum transconductace (g_m^{max}) equals

$$(dI_{ds} / dV_{gd})^{\max} = (W / L)V_{ds}\mu^{\max}C_i \qquad (1)$$

where C_i is the capacitance per unit area between the electrolyte and the 2DEG channel $C_i = (\varepsilon \cdot \varepsilon_0)/z$, and μ^{max} the maximum electron mobility. Leaving post-growth design parameters (W/L) and V_{ds} aside, μ/z is the main key parameter to obtain a high transconductance value and therefore, high transducive sensitivity. Very recent improvements in the PAMBE growth of AlN/GaN structures allow this reduction in *z* without significant reduction of mobility [18]. Besides the increase of the magnitude of g_m, due to the reduction of the distance *z*, the shift of the maximum value of g_m towards lower V_{gd} values in the case of sample A (V_{gd} = -0.24 V) should be noted.

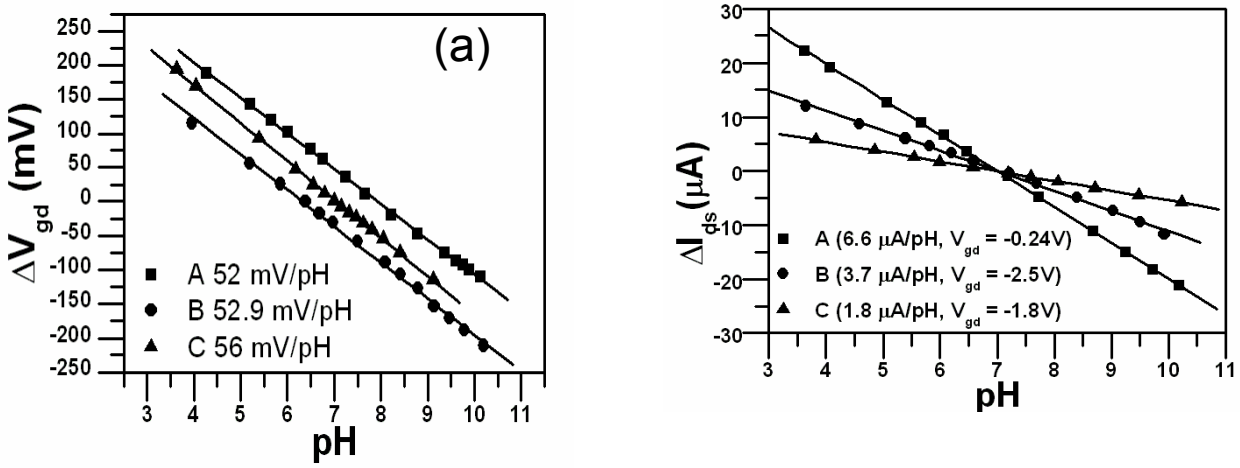

Figure 3. *(a) Variation of the surface potential with pH at 12°C. The linear regression of the experimental data reveals 52 mV/pH, 52.9 mV/pH and 56 mV/pH for samples A, B and C, respectively; (b) Changes in Ids related with pH for samples A, B and C. The device transducive sensitivity increases with decreasing barrier thickness.*

pH-induced changes in the surface potential are evaluated for the three samples by monitoring $\Delta V_{gd}/\Delta pH$ when the SGFET is regulated to keep a constant I_{ds}. The responses between pH 4 and pH 10 are depicted in figure 3a. For sample C, the pH related surface sensitivity (56 mV/pH) is close to the Nernstian limit value at 12 ºC (56.5 mV/pH), whereas for samples A and B, slightly lower pH sensitivities arise (52 and 52.9 mV/pH, respectively). The different pH-sensitivity of device C compared to devices A and B can be attributed to the different growth techniques. pH-sensitivity is caused by oxidized surface sites [7], which can vary in density and distribution with the applied growth method. On the other hand, all the samples exhibit good chemical stability and reproducibility in the measurements performed.

Whereas $\Delta V_{gd}/\Delta pH$ mainly depends on the chemical characteristics of the device surface, the pH-dependence of I_{ds} ($\Delta I_{ds}/\Delta pH$) at constant V_{gd} is strongly affected by the electrical characteristics of the 2DEG, and therefore by g_m. figure 3b shows ΔI_{ds} as a function of the pH, for samples A, B and C. In each case the measurements are taken at the V_{gd} value corresponding to the g_m^{max} of each sample. A linear dependence is found for all the samples, but a significant increase (by a factor of 3.7) of the transducive sensitivity (given by the slope $\Delta I_{ds}/\Delta pH$) is observed upon reduction of the distance *z*, from sample C (1.8 μA/pH) to sample A (6.6 μA/pH), despite of the slightly lower pH-related surface sensitivity $\Delta V_{gs}/\Delta pH$ found for sample A.

The importance of the shift of g_m^{max} to lower V_{gd} values is apparent in figure 4a. Real time I_{ds} measurements are represented in figure 4a, for samples A and B, when droplets of buffer solutions (pH 4, 7 and 10) are applied into the gate region by means of pasteur pipettes, and without the use of reference electrode. Figure 4b represents ΔI_{ds} as a function of the pH, derived from measurements depicted in Fig. 4a. Transducive sensitivities are calculated and, in the case of sample A, this value falls down from 6.6 μA/pH to 5.4 μA/pH (18.2 % drop). This result indicates that sample A could operate without a reference electrode, leading to a small decrease in its transducive sensitivity. On the other hand, for sample B this drop is much more drastic, from 3.7 μA/pH to 1.2 μA/pH (67.6% drop).

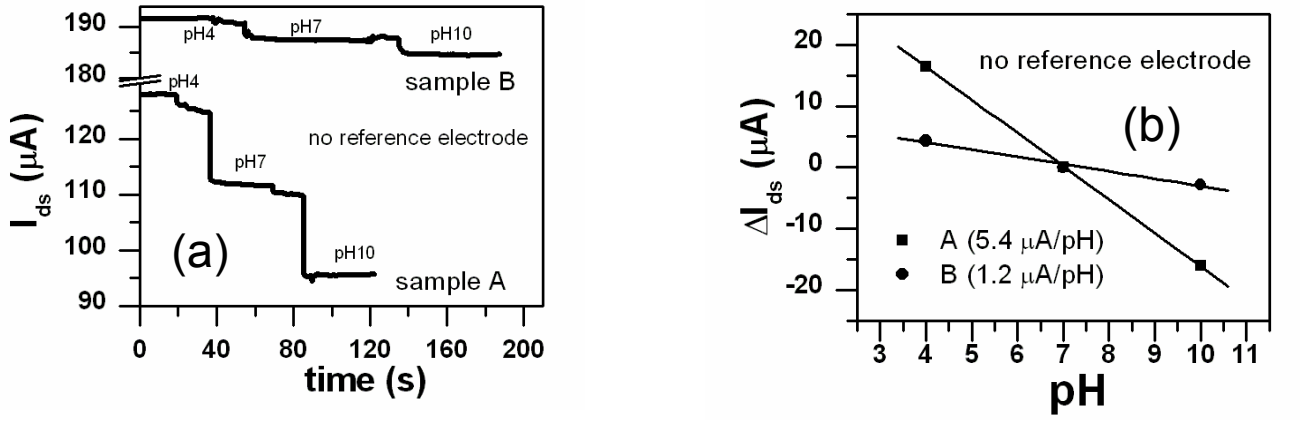

Figure 4. *(a) Transient behaviours of samples A and B, when pH is changed by means of droplets of buffer solutions (pH 4, 7 and 10), without reference electrode; (b) Linear regresions derived from (a) yielding transducive sensitivities*

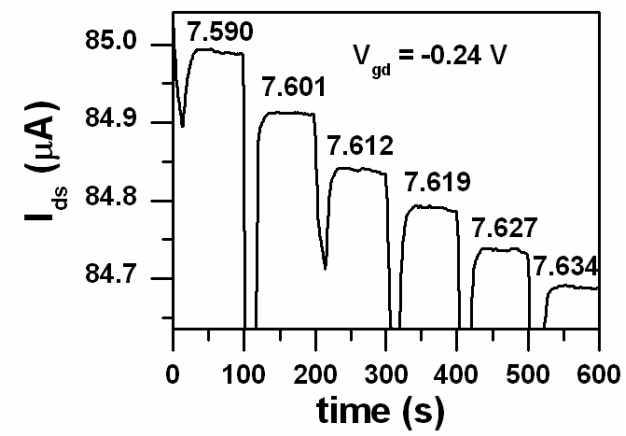

Figure 5. *Transient behaviour of sample A in a very narrow pH range, with Vgd = -0.24 V. Numbers on steps are values measured by a commercial pH-meter. Steps less than 0.01 pH are visible, and resolution is estimated to be better than 0.005 pH.*

Finally, figure 5 presents the transient pH-response of I_{ds} in a very narrow pH range for sample A, when

biased at maximun transconductance (V_{gd} = -0.24 V). Steps lower than 0.01 pH can be clearly resolved and a resolution better than 0.005 pH can be estimated. Valleys features are not always present, and they are not clearly attributed to any phenomenon, but might be related with feedback parameters or pH stabilization of the electrolyte.

In summary, we have demonstrated the sensing application of GaN/AlN/GaN HEMT structures, in the present case with a 2DEG-to-surface distance of 7.5 nm, as a pH-sensitive SGFET. Although the pH-sensitivity of the surface potential is very similar to the one obtained from standard AlGaN/GaN structures, the ultrathin AlN-barrier HEMT exhibits a significantly higher value for $\Delta I_{ds}/\Delta pH$ than structures with thicker barriers (as expected due to the $g_m^{max} \propto 1/z$), operating at V_{gs} values close to 0 V. These facts, together with the improvements on growth by PAMBE, offers a new opportunity for the realization of SGFET-sensors with enhanced transducive sensitivity and eventually, no need of reference electrode in less demanding applications.

References

[1] M. Razeghi, A. Rogalski, J. Appl. Phys. **79**, 7433 (1996).
[2] H.J. Looi, M.D. Whitfield, R.B. Jackman, Appl. Phys. Lett. **74,** 3332 (1999).
[3] U. Karrer, A. Dobner, O. Ambacher, M. Stutzmann, J. Vac. Sci. Technol. B**18,** 757 (1999).
[4] A. Lloyd-Spetz, A. Baranzahi, P. Tobias, I. Lundstrom, Phys. Stat. Sol. (a) **162**, 493 (1997).
[5] A. Jiménez,Z. Bougrioua, J.M. Tirado, A.F. Braña, E. Calleja, E. Muñoz, I. Moerman, Appl. Phys. Lett. **82,** 4827 (2003)
[6] J. Pedrós, F. Calle, R. Cuerdo, J. Grajal, Z. Bougrioua, Appl. Phys. Lett. **96,** 123505 (2010).
[7] G. Steinhoff, M. Hermann, W.J. Schaff, L.F. Eastman, M. Stuztmann, M. Eickhoff, Appl. Phys. Lett. **83,** 177 (2003).
[8] W.M. Siu, R.S.C. Cobbold, IEEE Trans. Electron Devices ED-26, 1805 (1979).
[9] B. Baur, G. Steinhoff, J. Hernando, O. Purrucker, M. Tanaka, B. Nickel, M. Stutzmann, M Eickhoff, Appl. Phys. Lett. **87,** 263901 (2005).
[10] B. Baur, J. Howgate, H.-G von Ribbeck, Y. Gawlina, V. Bandalo, G. Steinhoff, M. Stutzmann, M. Eickhoff, Appl. Phys. Lett. **89,** 183901 (2006).
[11] G. Steinhoff, O. Purrucker, M. Tanaka, M. Stutzmann, M. Eickhoff, Adv. Func. Mat. 13, (2003) 841.
[12] G. Steinhoff, B. Baur, G. Wrobel, S. Ingebrandt, A. Offenhäusser, A. Dadgar, A. Krost, M. Stutzmann, M. Eickhoff, Appl. Phys. Lett. **86,** 033901 (2005).
[13] I. Cimalla, F. Will, K. Tonisch, M. Niebelschütz, V. Cimalla, V. Lebedev, Sensors & Act. B **123** 740 (2007).
[14] B.H. Chu, B.S. Kang, F. Ren, C.Y. Chang, Y.L. Wang, S.J. Pearton, A.V. Glushakov, D.M. Dennis, J. W. Johnson, P. Rajagopal, J.C. Roberts, E.L. Piner, K.J. Linthicum, Appl. Phys. Lett. **93,** 042114 (2008).
[15] M. Bayer, C. Uhl, P. Vogl, J. Appl. Phys. **97**, 033703 (2005).
[16] J.L. Rouviere, J.L. Weyher, M. Seelmann-Eggebert, S. Porowski, Appl. Phys. Lett. **73,** 668 (1998).
[17] M.H. Wong, Y. Pei, R. Chu, S. Rajan, B.L. Swenson, D.F. Brown, S. Keller, S.P. DenBaars, J. S. Speck, U. K. Mishra, IEEE Electron Device Lett. **29,** 1101 (2008).
[18] A.M. Dariban, A.M. Wowchak, A. Osinsky, J. Xie, B. Hertog, B. Cui, D.C. Look, P.P. Chow, Appl. Phys. Lett. **93**, 082111 (2008).

6.10 Dense systems of athermal chain molecules[10]

During the last four years, a major theoretical and simulation effort at ISOM has been devoted to the investigation of the fundamental, and until recently still unresolved question of crystallization in the simplest molecular model of polymer molecules.Other things being equal, nature favors more randomness, but sometimes an orderly pattern lets a system increase its total disorder. Our recent work has shown that a large group of spheres favors a crystalline arrangement over a disorderly arrangement, even when the spheres are linked into polymer-like chains. Although our computer simulation is idealized, we believe it provides lessons for real polymers and other large molecules, including proteins. Individual particles such as atoms often arrange into a crystal because their mutual attraction lowers their total energy. In contrast, randomness, or entropy, usually favors a disordered arrangement, like that of molecules in a liquid. But researchers long ago found, in simulations and experiments that spheres without any attraction also crystallize when they are packed densely enough. This entropy-driven crystallization occurs because the crystal leaves each sphere with some space to rattle around. In contrast, a random arrangement becomes "jammed" into a rigid network of spheres in contact with their neighbors. The entropy of the few "rattlers" that are still free to move can't make up for the rigidity of the rest of the spheres.

But many researchers thought that connecting the spheres like beads on a string to simulate polymers would restrict their motion so much that the extra wiggle room in the crystal wouldn't help; random arrangements would prevail. To test this idea, we simulated an idealized model in which spheres in the same chain must stay in contact but can otherwise move freely. With no resistance to bending or twisting at these connection points, and no other inter-sphere forces, the simulation was similar to the case of uncharged single spheres, in that any transition to a crystal was entirely entropy driven.

One practical challenge was that densely packed chains become entangled and take an non-practical long time to rearrange into a crystal, even if that structure is preferred. To speed things up, we allowed the spheres in their simulation to swap from one chain to another. Although this is not true dynamics, we were able to sample configuration space orders of magnitude faster. The simulations showed that the individual spheres form a crystalline arrangement, as unconnected spheres do, although the chains do not form any regular pattern. The crystallization of polymers occurs for the same reasons as it does with unconnected spheres. It shows that it is possible for entropy to drive the crystallization, he says, although more realistic models of polymers would also include the influence of forces such as the mutual attraction of spheres and the resistance to bond bending and twisting. In addition to improving the understanding of polymer crystallization, the results may also relate to protein molecules, which are biological polymers. The relevance for proteins is not for crystallization, but for the natural folding of a protein into a three-dimensional structure, where the interactions among parts of the molecule are analogous to those among crystallizing polymers.

Compared with random packings of spheres, very little attention has been devoted to the investigation of dense assemblies of freely-jointed chains of tangent hard spheres, although they are considered as the second type of ideal amorphous solids assemblies of hard spheres being the ideal amorphous solids of the first kind. In spite of chains of hard spheres being the simplest and most fundamental model system for synthetic and biological polymers, neither experiments nor simulations to determine their density and structure at their MRJ state had been forthcoming. This impasse was due, on the one hand to the difficulty of constructing laboratory mechanical models, and on the other hand to their computational intractability. It was only very recently that the problem of determining the MRJ state of chain molecules could be solved through extensive Monte Carlo (MC) simulations. While very large (up to a million spheres) systems of dense random packings of single hard spheres can be generated almost routinely nowadays, the determination of the MRJ state for hard-sphere chains required the combined use of several advanced off-lattice MC algorithms in order to efficiently sample their multi-chain configuration space.

[10] *Contact person: Manuel Laso mlaso@etsii.upm.es*

The maximally random jammed state of hard-sphere chains

Thanks to our MC scheme, it has been possible to accurately determine the local structure and dimensions of freely-jointed chains of tangent hard spheres in the entire range of volume fraction up to the MRJ state. Since the computational efficiency of the MC algorithm in equilibrating the long-range system characteristics is affected by neither the average molecular length, nor the packing density, it was possible to simulate from relatively short macromolecules all the way into the asymptotic, infinite-chain regime. As a consequence, conclusive evidence has been collected about generic features such as their MRJ state, the universal scaling of chain dimensions, and the degree of local ordering with increasing packing density. To start with, it was found that hard-sphere chains reach their MRJ state at the same volume fraction as packings of single spheres do (within statistical uncertainty), regardless of chain length. At the MRJ state the pair radial distribution function of chain systems closely resembles that of single-sphere ones, although the double tangency conditions has a small but noticeable effect especially at distances close to the sphere diameter.

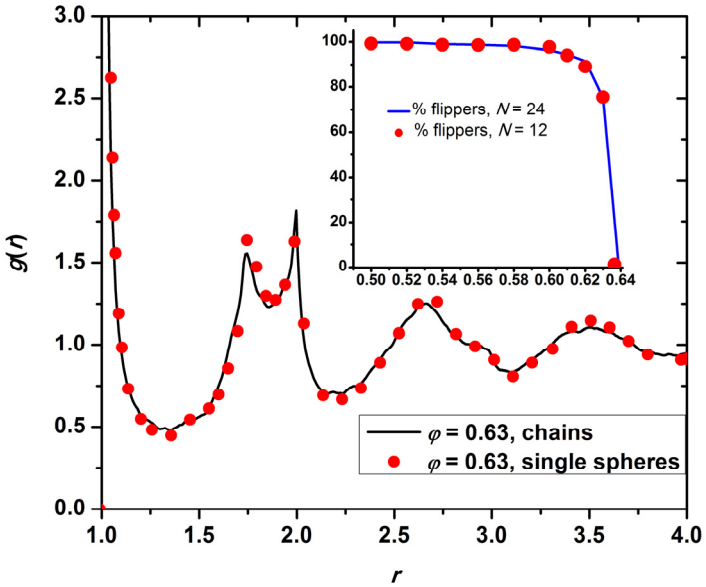

Figure 1. *Radial distribution function for hard-sphere chains and single hard spheres at packing density of Inset: Percentange of "flipper" hard spheres as a function of packing density.*

While it is trivial to prove that jamming density for chains cannot be higher than for single spheres, a rigorous proof, although tantalizingly close, is still missing. The MRJ state for chain molecules is characterized by the system becoming jammed, in the sense that it is not possible to displace any sphere by an arbitrarily small "flip"(or "minimal crankshaft") movement, without either incurring in overlaps with other spheres, or violating the connectivity of the chains. The inset of Figure 1 shows clearly how the fraction of "flipper"spheres declines sharply as the MRJ state is approached, in a way entirely analogous to that of "rattlers"for single hard spheres. The question is thus settled that neither chain length nor the tangency/connectivity constraint, which were responsible in the past for the computational untractability, hinder the packing of chains with respect to single spheres. Figure 2 gives an illustrative impression of the extreme packing conditions at the MRJ state, and highlights the difficulty of devising efficient configuration sampling algorithms.

Universal scaling behavior of chain dimensions

Chain connectivity is the key distinguishing feature of chain packings with respect to packings of single spheres. It endows dense systems of chains of hard spheres with a richer structure physical behavior. In addition, thanks to the simplicity of their geometry and of the interactions between spheres, hard-sphere chains turn out to display universal features with maximal clarity. In this respect, our MC numerical

experiments have shown that hard-sphere chains are the first system for which the full range of universal static scaling laws can be observed as packing density increases up to the MRJ state.

The exploration of the entire volume fraction range has revealed that chain dimensions display four clearly distinct scaling behaviors. These four regimes, often described as “dilute”, “semi-dilute”, “marginal”, and “concentrated”, are characterized by a regime-specific power dependence of chain size on volume fraction as displayed in Figure 3 with unprecedented clarity.

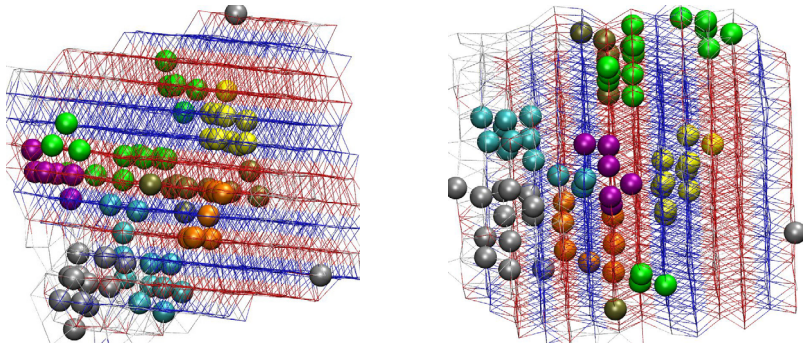

Figure 2. *System configuration of hard-sphere chains at where the majority of sites possess a highly ordered local environment. Spheres belonging to individual chains have the same color. The wireframe grid indicates the underlying crystalline structure. Bonds (“wires”) are colored according to whether their immediate environment is predominantly FCC or HCP*

The values found in the four regimes fully confirm theoretical predictions. Furthermore, the established equality of jamming density for single spheres and for hard-sphere chains at the MRJ state has also allowed a correspondence to be established between configurations of single spheres and of chains. This correspondence can be exploited by means of graph theoretical methods to predict the cross-over volume fractions between the high-concentration regimes. Both the marginal to concentrated and semidilute to marginal crossovers are predicted to be chain-independent to leading order, in agreement with the values shown in Figure 3. It is remarkable how faithfully the full range of expected behaviors is captured by this simplest possible molecular model. Although the first order behavior of had been conjectured qualitatively it is the identification of the MRJ state for hard-sphere chains that has made it possible to determine the exact forms of prefactors and coefficients.

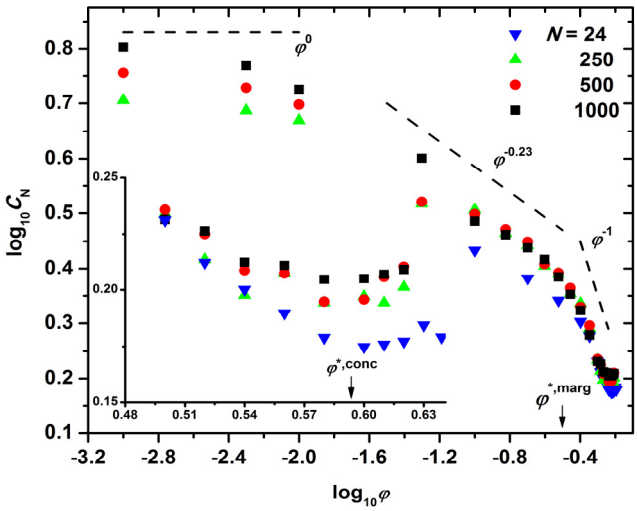

Figure 3. *Double logarithmic plot of the characteristic ratio C_N, as a function of packing density, φ. Lines with characteristic slopes are drawn as a guide to the eye. Inset: logarithm of characteristic ratio versus (linear) volume fraction in the marginal and concentrated regimes. $\varphi^{*,marg}$ and $\varphi^{*,conc}$ mark the predicted crossovers for the transitions from semi-dilute to marginal, and from marginal to concentrated regimes, respectively*

Topological constraints: entanglements and knots

A great deal of the unique dynamical and rheological behavior of polymers stems from the uncrossability of chains, which has been traditionally analyzed in terms of "entanglements", the heart of modern theories of polymer dynamics. As a consequence of the desire to enrich such approaches with atomistic information, work on the developments of algorithms for the determination of entanglements in atomistic or coarse-grained polymer systems is now being pursued at a frantic pace by various groups. It is well established that all different topological algorithms based either on the original annealing process or on the newer (direct or stochastic) geometric approaches provide very similar results for the underlying primitive path (PP) topology and entanglement statistics.

The extreme simplicity of hard-sphere chains makes them an ideal statistical mechanics model on which to analyze universal entanglement behavior. In particular, the analysis of primitive path networks as representation of states of polymers from solutions to jammed amorphous solids is an area of great current relevance.

Primitive paths were extracted from the corresponding hard-sphere chains by means of the state-of-the-art Z1 algorithm. This algorithm solves the problem of the shortest multiple disconnected path by minimizing the Euclidean length, subject to constraints arising from the initial (parent) state. By transforming the Doi-Edwards physical concept of entanglements into a mathematical problem, the Z1 algorithm provides an approximate but still accurate geometrical solution. Figure 5 shows the transformation through the Z1 code of the parent hard-sphere chains (panel b) to the corresponding primitive paths (panel d).

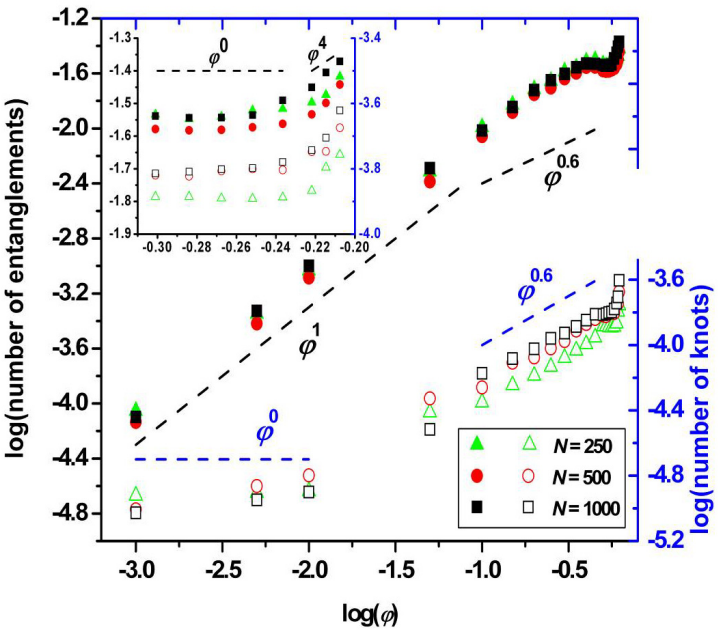

Figure 4. *Double logarithmic plot of the (left axis) average number of segments of the primitive path and (right axis) fraction of knotted chains for the hard-sphere chain system.Lines with characteristic slopes are drawn as guides to the eye. Inset: zoom into the marginal and concentrated regimes.*

The evolution of entanglement density with polymer volume fraction is of particular interest, since the complex, non-intuitive dependence of the number of entanglements on gives rise to the very different types of rheological behavior which have been observed experimentally as concentration increases up to the melt. Results of the topological analysis leading to the primitive paths for the asymptotically long hard-sphere multi-chain system up to the MRJ state are shown in Figure 4. Again, four easily distinguishable scaling regimes, characterized by specific scaling exponents, can be observed for the dependence of the average number of entanglements per chain, more precisely, the number of segments of the primitive path, on packing density. In particular, a very strong growth in the number of entanglements per chain takes place as the MRJ is approached.

While entanglements have been at the root of modern theories of polymer dynamics since its inception, the interest in knots as an alternative analysis pathway of topological constraints is quite recent. In the present work, knots were identified by the technique proposed by Mansfield. The results of such a knotting

analysis for the same long, hard-sphere, multi-chain system up to the MRJ state are also included in Figure 4, allowing for a direct comparison with the corresponding scaling behavior of entanglements.

The similarity, within the statistical uncertainty, of the scaling exponents for entanglements and knots is a most unexpected result, for a very simple reason: entanglements are, by definition, a multi-chain construct, while knotting is primarily a single-chain phenomenon. Thus, knotting is a purely intramolecular characteristic, whereas entanglements are a purely intermolecular measure of topological hindrance. Furthermore, entanglements seem to be localized in space, whereas knotting is a global, "delocalized"property of a chain. Yet the evidence we have collected on the hard-sphere chains strongly suggests that, in a very general sense, knots must be equivalent to entanglements. In other words, the multi-chain phenomenon of entanglement leaves an unequivocally recognizable imprint on the shape of individual chains: once the scale factor between knots and entanglements is found, it should be possible to determine the dependence of the number of entanglements on volume fraction from the dependence of the number of knots on volume fraction, by analyzing the knotting of single chains extracted from the multi-chain ensembles over the volume fraction range.

This remarkable finding may actually have a simple explanation. While the original concept of an entanglement is a dynamic one (as beautifully shown in the pioneering simulations of Grest and Kremer), all current algorithms for determining entanglements are based on static, basically geometric arguments. In very simplistic terms, entanglement detection algorithms find entanglements by holding the ends of all chains fixed, and by simultaneously "tightening"the chains as if they were retractable rubber bands, until a minimum overall length, compatible with chain uncrossability, is reached.

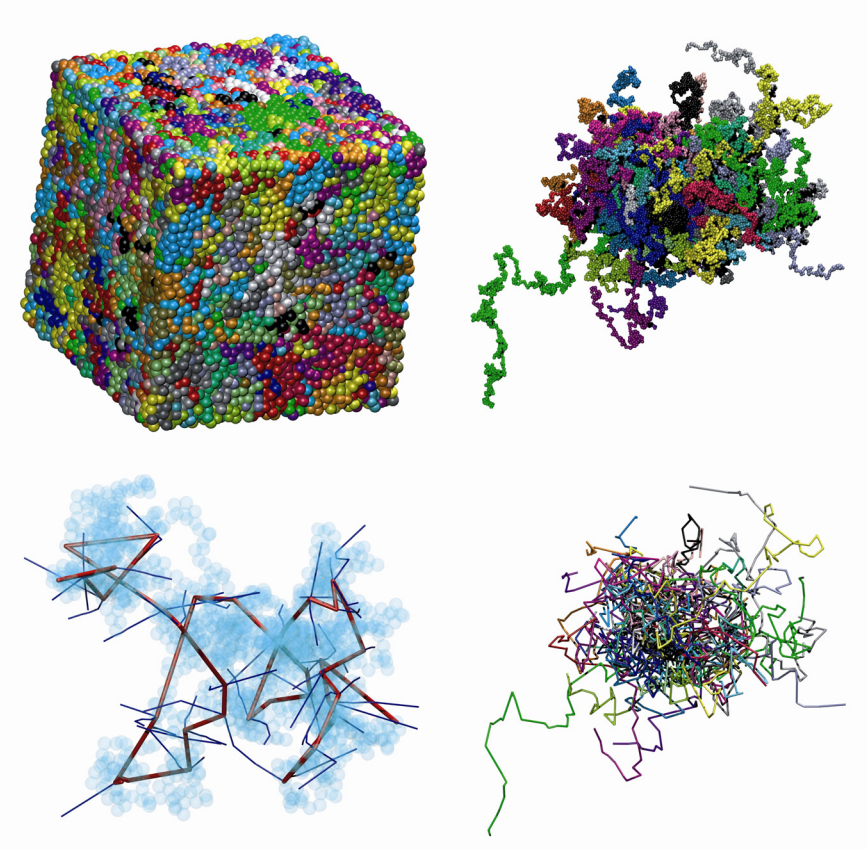

Figure 5.*Clockwise from top left: Representative configuration of 54-chain, hard-sphere system of molecular length 1000 in the vicinity of the MRJ state, with coordinates of sphere centers (a) wrapped, subject to three-dimensional periodic boundary conditions and (b) fully unwrapped in space. (d) The underlying primitive path network, after the application of the Z1 topological algorithm (see also Figure 6), with entanglement coordinates unwrapped in space. (c) An arbitrary selected single chain of high knotting complexity (10.153) with constituent sites shown as transparent spheres. Also shown is the corresponding primitive path, and segments of other primitive paths with which it is entangled.*

On the other hand, knotting algorithms start by connecting the ends of a given chain, and then determine the type of knot based on a number of different knot invariants (Gauss winding number, or the Alexander, Jones, or HOMFLY polynomials) . Although the two approaches seem to be unrelated at first sight, the essential information both of them ultimately require is basically contained in the succession of over- and under-crossings of two-dimensional projections of the chains (single chain in the case of a knot analysis).

Thus, in an ensemble average sense, single, highly knotted chains are proper class representatives of highly entangled, homogeneous multi-chain systems. This similarity may lead to a refinement, and revised evaluation of current methods of characterization of entanglements: once the entanglements of a particular system have been determined, additional information such as spacing between entanglements, reptation tube diameter, etc. is obtained in a kind of "post-processing"analysis. A knotting analysis however yields basically "delocalized"information: the number and the complexity (type) of knots. No further information can be extracted. If however, the basic information content of knots and entanglements is the same, as Figure 4 strongly suggests, the natural question is then to what extent the "post-processing"step imposes a structure on the results which is not contained in the original system, but which stems from explicit or implicit assumptions (e.g. freezing of dynamic degrees of freedom, Gaussian behavior of primitive paths, type of distribution of entanglements along chains, etc.).

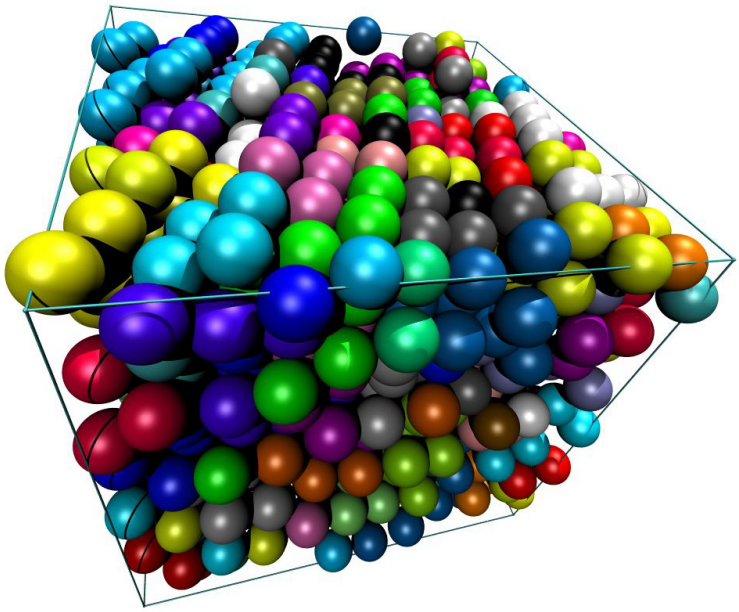

***Figure 6**. Individual hard-sphere chains within the entropy-crystallized system, showing their disordered embedding in the crystal. Each chain is characterized by a different color.*

Entanglement, knotting and aggregation in biophysics.

In practice, the observation that both measures of topological constraints for chain systems scale with identical universal exponents may open up a new and potentially very powerful avenue for the understanding of complex biological problems which are out of reach nowadays. A prominent example is the long-established correspondence between human neurodegenerative diseases and the genetic expansion of a chromosomal trinucleotide repeat sequence. In Huntington's disease, pathogenesis is known to be caused by a polyglutamine sequence of more than 36 aminoacids. Such expanded sequences lead to aggregation and to the ultimate appearance of protein inclusions in affected neurons. The nucleation event for aggregation involves folding within a single chain. A great effort is currently being devoted to the modeling of this single-chain folding event for sequences of moderate length (up to approx. 50 residues). These investigations make use of advanced simulation methods, like steered Molecular Dynamics, Transition Path Sampling replica exchange MD and massive large-scale computational resources. Such detailed analyses at the level of single chain are at the current limit of feasibility, even for relatively small polypeptide sequences. A similar approach to the collective entanglement behavior of a multi-polypeptide system to form an aggregate is a

rather hopeless undertaking, and will remain so for the foreseeable future. However, the universal character of the similarity between entanglement and knotting suggests that a great deal of information about the emergence and evolution of very large, computationally intractable, polypeptide aggregates such as those responsible for Huntington's disease, could be rigorously gleaned from the analysis of single polypeptide chains.

Conclusions and potential applications

The recent determination and understanding of the hitherto unknown structure of dense random packings of hard-sphere chains up to their MRJ state has answered several long-standing questions in the physics of polymers, complex fluids, statistical mechanics and thermodynamics. Furthermore, an analysis of chain topological hindrance has uncovered a profound connection between entanglements and knots. This connection deserves urgent, deeper investigation, as it may open a new avenue for the analysis of the very complex collective behavior of multi-chain, biomolecular systems. Our current efforts focus on the extension of the simulation studies to model polymer systems of varied molecular architecture (branched, stars and rings) either in the bulk or at interfaces (nanofillers, confined geometries and solid surfaces). There is every reason to expect that the universal aspects displayed by the hard-sphere chain model system will also apply to chemically realistic chains.

References

[1] N. Karayiannis, M. Laso, Phys. Rev. Lett., **100**, 050602 (2008).
[2] N. C. Karayiannis, M. Laso, Macromolecules, **41**, 1537 (2008).
[3] M. Laso, N.C. Karayiannis, J. Chem. Phys., **128**, 174901 (2008).
[4] K. Foteinopoulou, N.Ch. Karayiannis, M. Laso, M. Kröger, Phys. Rev. Lett., **101**, 265702 (2008).
[5] N. Karayiannis, K. Foteinopoulou, M. Laso, M. Kröger, J. Phys. Chem. B**113**, 442 (2009).
[6] N. Karayiannis, K. Foteinopoulou, M. Laso, J. Chem. Phys. **130**, 074704 (2009).
[7] M. Laso, N. Ch. Karayiannis, K. Foteinopoulou, M. Kröger, Soft Matter **5,** 1762 (2009).
[8] N. Karayiannis, K. Foteinopoulou, M. Laso, Phys. Rev. E **80**, 011307 (2009).
[9] N. Karayiannis, K. Foteinopoulou, M. Laso, Phys. Rev. Lett., **103**, 045703 (2009).

6.11 Detection system of magnetic nanoparticles in the brain and in biological tissues with a Magneto-encephalograph[11]

During the last 4 years ISOM has made a big effort to design and implement a new set-up for the production of magnetic nanoparticles (MNPs) by sputtering [1]. MNPs have a great interest in biomedicine areas, due to their direct applications [2-6], both for diagnosis and therapy. Keeping this in mind, we have collaborated with end users, such as Hospitals and another bio-related research centers. In fact, we have participated in the project MADR.IB (Ref: S2006/SAL-0312), funded by Comunidad de Madrid. Other partners in such project are bio-related (from Universities and Hospitals: UPM, UCM, Hospital Universitario Ramón y Cajal, Hospital Universitario Puerta de Hierro de Madrid). As a result of this collaboration, a first application has been developed by combining nanoparticles produced in our lab with Magnetoencephalography (MEG) technique at UCM. We have developed a new method to detect nanoparticles in the brain and in biological tissues. Biological samples have been provided by Hospital Ramón y Cajal. This method has been registered as a patent [7] and a related paper has been submitted.

Although MNPs are currently used as Magnetic Resonance Imaging (MRI) contrast enhancement [8-10], their detection in "in vivo"samples is, until now an open problem. Traditional methods to detect magnetic particles, commonly used in magnetic material characterization, are not adequate to be used for "in vivo"specimens. On the other hand, Magnetoencephalography (MEG) [11] is a non-invasive functional imaging technique that enables the description of the temporal and spatial patterns of brain activity in resting conditions or related to different basic cognitive processes, by detecting the weak magnetic fields generated by currents in the neurons. One major advantage of MEG is its ability to measure brain activity with fine temporal resolution, on the scale of milliseconds [11]. MEG systems are able to measure magnetic fields in the range of 10^{-14} T and are mainly used for neurological research or as an additional method for diagnosis of diseases of neurological nature, such as brain tumors, Alzheimer, schizophrenia, epilepsy and others. MEG technique is appropriate to detect alternating magnetic fields with frequencies in the range of 1-2000 Hz (typical values for brain signal oscillations).

However, MEG systems are not currently being used for the detection of MNPs in biological tissues. Although MNPs generate a magnetic field strong enough to be detected by the MEG system, such field is taken as a background signal by the MEG, because the magnetic field produced by MNPs changes very slowly with time, following an exponential decay, which is not a periodical signal suitable to be measured by MEG system.

Experimental

The system is designed to detect the presence of MNP in biological samples, by means of a commercial MEG system, with the addition of a pneumatic actuator able to produce a controlled (both, frequency and amplitude) alternating movement of the biological tissues. The mechanical vibration produces an effective amplitude modulation of the magnetic field created by the nanoparticles that is detected by the MEG. In order to reduce the noise signal as much as possible, the actuator part inside the MEG-shielded room is completely metal free. The vibration system is mechanical, so it is free from possible electric noise sources. The pneumatic system is based on a 4-meter long flexible tube, with both ends closed by latex membranes. The outer side membrane is connected to an electric DC motor by a mechanical transmission which transforms rotation movement into linear motion. Nanoparticle samples are attached to the inner side membrane with double sided adhesive tape. In order to regulate the movement amplitude an air vent is implemented in parallel connection in the system. By increasing the valve opening, less pressure is transmitted between the membranes and the oscillation amplitude may be decreased to approximately 0.5

[11] *Contact Person: Maria del Mar Sanz Lluch* mmsanz@die.upm.es

mm; by reducing it, the pressure transmitted increases, and the oscillation amplitude may reach 2.3 mm. The frequency is regulated by using a voltage-controlled power supply. Recordings were done using a 148 magnetometer whole-head system housed in a shielded room. The system response was characterized with nickel MNP produced in our laboratory. Animal experiments were performed in accordance with *Hospital Ramon y Cajal´*s Animal Welfare Institutional Committee. The detection of MNP in biological tissues was performed in formalin fixated rat liver and brain cylindrical samples (ca. 1.5 mm diameter, 10 mm long) taken from animals that were euthanized and perfused 24 hours after slow intravenous (i.v.) injection by tail vein of dextran based, 100 nm magnetite commercial NPs. In control animals, saline was i.v. injected. Samples were kept in micro-eppendorf vials. Brain samples originated four different types of recordings, depending on whether the brain tissue was or was not lesioned by a glass micropipette in combination with MNP injection or not, as described below.

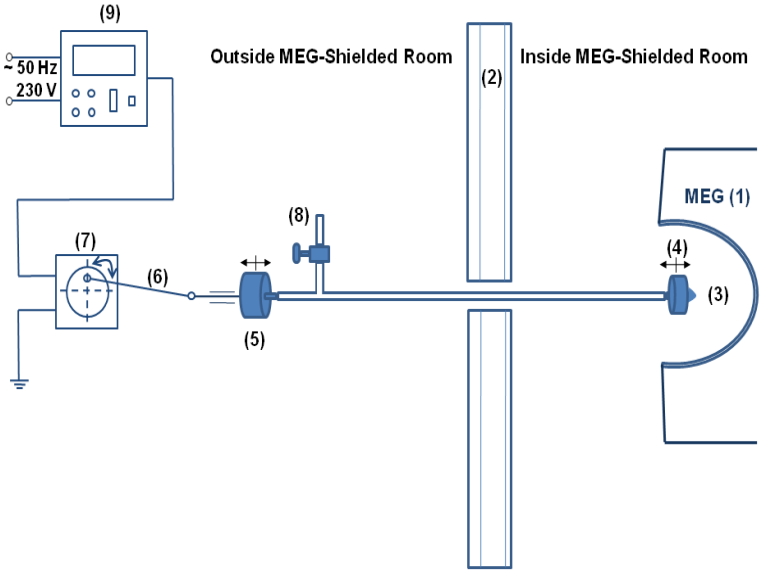

Figure 1. *Experimental Set-up. Simple non-metallic actuator vibrates biological tissue inside MEG shielded room allowing detection of modulated magnetic field created by MNP. See description in experimental section. (1) MEG, (2) Magnetic shield, (3) MNP sample, (4) Inner pneumatic membrane, (5) Outer id., (6) Mechanical transmission, (7) DC motor, (8) Air vent, (9) DC Power supply*

The sample, one MNPs cluster with magnetic moment m, is vibrated at low frequency, as explained above. Then, the magnetic field generated by the vibrating MNPs in the MEG sensors is given by:

$$B = \frac{\mu_0 m}{2\pi}\left(\frac{2}{r^3} + \frac{3\Delta l \sin(\omega t)}{r^4}\right) \qquad (1)$$

Where Δl is the vibration amplitude of the nanoparticles cluster, r is the distance between the MNP and the point where the magnetic field is detected (the MEG sensors), and ω is the pulsation of the mechanical vibration provided by the pneumatic system.

The signal due to the sinusoidal component of the magnetic field,

$$\Delta B = \frac{3\mu_0 m}{2\pi r^4}\Delta l \sin(\omega t) \qquad (2)$$

is measured by the MEG, whereas the signal from the constant magnetic field, $\mu_0 m/\pi r^3$, would not be appraised by the signal processing system of the MEG.

Figure 2 shows the experimental values of ΔB (dots) recorded with our system from nickel MNPs located at different distances (r) from the detector, and the best fitting curve (solid line) versus r. Data are

the *rms*-value from one of the MEG channels, when varying the distance, *r*, from sample to the base of the arrays of sensors. As it is shown in Figure 2a, fitting parameters correspond to:

$$a = \frac{3\mu_0 m}{2\pi}\Delta l \qquad (3)$$

and *b* is the distance from the selected sensor to the base of the arrays of sensors.

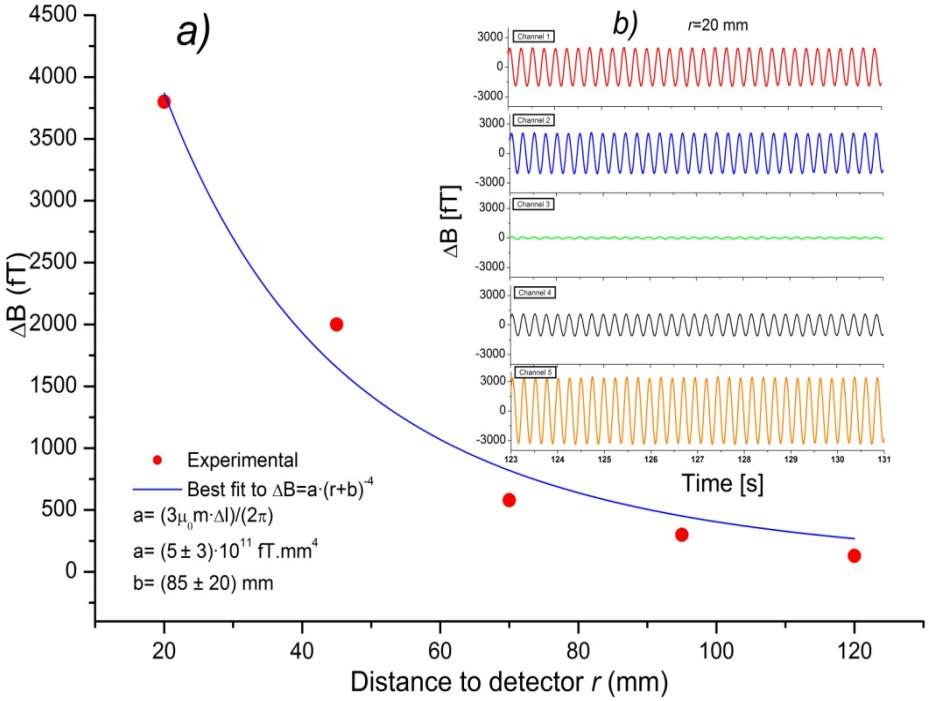

Figure 2. *Dependence of the magnetic signal generated by the MNPs and recorded with our method, with the distance to the detector. Different channels correspond to five representative sensors. Dots in* ***part a)*** *correspond to peak-to-peak value of the signal in Channel 1 averaged during 5 seconds, for a Nickel MNPs sample (20 nm), at different distances from the detector.* ***Part b)*** *in the figure shows a typically recorded signal from 5 channels of the MEG system, placing the sample at a distance of 20 mm from the base of sensors arrays. Samples were magnetized before measurements in all figures.*

To perform the measurement, we have used a set of Ni MNPs produced in our laboratory by sputtering [11], with an *m* value of 800 μemu, measured by VSM. Taking Δl= 1mm (the vibration amplitude of the MNP cluster), the *a* value is $4{,}8.10^{-11}$ fT.mm^4, in good agreement with the value obtained by the fitted curve. In this, and the following figures, samples were magnetized before measurement.

The sensitivity of this system depends on the product $m \cdot \Delta l$. By increasing Δl (the vibration amplitude of the MNP cluster), the sensitivity for *m* detection can be very high, hence allowing the system to be able to measure very low values of *m*. However, there is a practical limit for the maximum value of Δl. If we intend to use this system for biomedical application, we must follow the European Directive for safety at work regarding risks from mechanical vibration during their work (European Directive 2002/44/EG). In our system, the sample is vibrating following a sine wave function given by: $s = \Delta l \sin \omega t$. Then, the maximum value for the acceleration will be given by $\ddot{s} = \omega^2 \cdot \Delta l$. Typical working frequencies have been lower than 4 Hz, hence, the maximum amplitude Δl that we can use will be lower than 2 mm, which will give the maximum limit for the amplitude modulation in our system.

Assuming the MEG sensitivity of 100 fT and taking an amplitude of 1 mm, the minimum detectable *m* value is about 10 μT. Translating this information into mass values, if we take, as an example, ferrite nanoparticles, the minimum detectable mass will be around 0.1 μg, well under the typical working conditions.

With respect to biomedical applications, it is well known that upon intravenous injection, magnetic nanoparticles can be captured by the monocyte-macrophage system before being cleared from the circulating bloodstream by the liver and the spleen. Macrophages are among the major cells mediating inflammatory responses to foreign substances, including nanoparticles, through phagocytosis and secretion of proinflammatory cytokines. The size, chemical property, and the surface charge of the particles are the major factors determining their impact on the function of macrophages. In the case of MNPs, macrophages capture them, but they are not able to phagocyte them, remaining in the macrophage for a period of time. Their capacity to phagocyte particles and compounds and to migrate to sites of inflammation has provided the rationale for *in vivo* labeling and monitoring of macrophages [9]. In normal cases, though, when no injury or inflammatory process takes place, MNPs will accumulate in the reticuloendothelial system such as the liver and spleen.

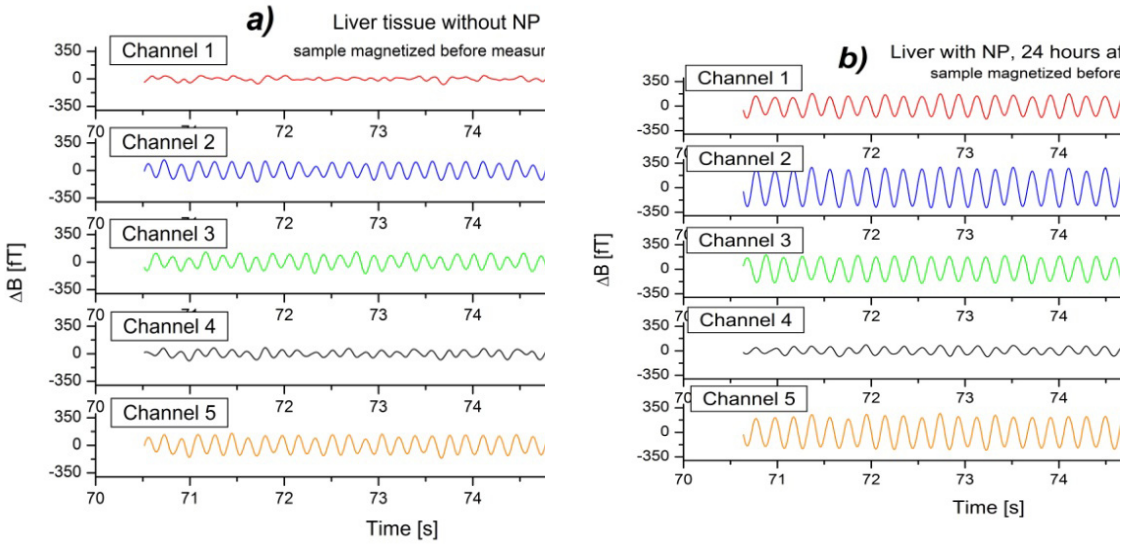

Figure 3. *Some signal channels from the MEG system with the new method developed in this work. Samples are tissues from rat liver. In a) the tissue is MNP free (saline injected), whereas in b) the tissue was taken from a rat perfused 24 hours after MNPs injection, instead.*

Therefore, to test the validity of the new method to detect MNPs in biological tissues, the first trials were performed with samples taken from the liver of a rat previously injected with MNPs. When MNPs are injected in the bloodstream, the part of the body with higher concentration of such MNP is expected to be the liver. The feasibility of the system to detect the presence of MNPs can be observed in Figure 3, where some channels of the MEG signals for non MNPs injected and MNPs injected rat liver tissues are plotted.

It is also well known that nanoparticles are able to cross the blood brain barrier (BBB)[10]. In fact, there are already companies devoted to develop nanoparticles based technology which allows or improves the transport of pharmaceutical active compounds loaded into nanoparticles (NP) across the BBB. On the other hand, macrophage tracking by magnetic resonance imaging (MRI) with iron oxide nanoparticles has been developed during the last decade for numerous diseases of the Central Nervous System (CNS), being good marker agents for clinical diagnosis. Keeping this in mind, the new method developed in our laboratory will be useful to detect the presence of MNPs in the brain tissue. Given the high sensitivity of the method, even very weak signals coming from very low MNPs concentration, can be detected. Therefore, we can detect the presence of injuries or disorders in the brain cells, by detecting the presence of macrophages “in vivo”.

In order to check the use of the system for this purpose, we performed several measurements (as shown in Figure 4) with rat brain tissue from:

(a) healthy rat brain with no injury and no MNPs injected in the bloodstream
(b) healthy rat brain perfused 24 hours after MNPs injection

(c) injured rat brain without MNPs injection
(d) injured rat brain perfused 24 hours after MNPs injection

When there is no injury in the brain tissue, difference between the MNPs injection or not in the rat body, is almost negligible. Therefore, there is no sink place for MNPs in a healthy brain. However, in micro-injured brains, we can notice some differences: in the first place, the signal plotted in fig4c) shows higher amplitude signal than those shown in fig4a) and b). This is probably due to the presence of blood clots, than naturally contain small amounts of ferromagnetic nanoparticles from hemoglobin. Figure 4d) shows the response from injured brain tissue previously injected with MNPs. (case d)). It is clear that there is a large signal increase in almost all channels. Therefore, the system seems to be sensitive enough to detect the presence of MNPs in injured brain.

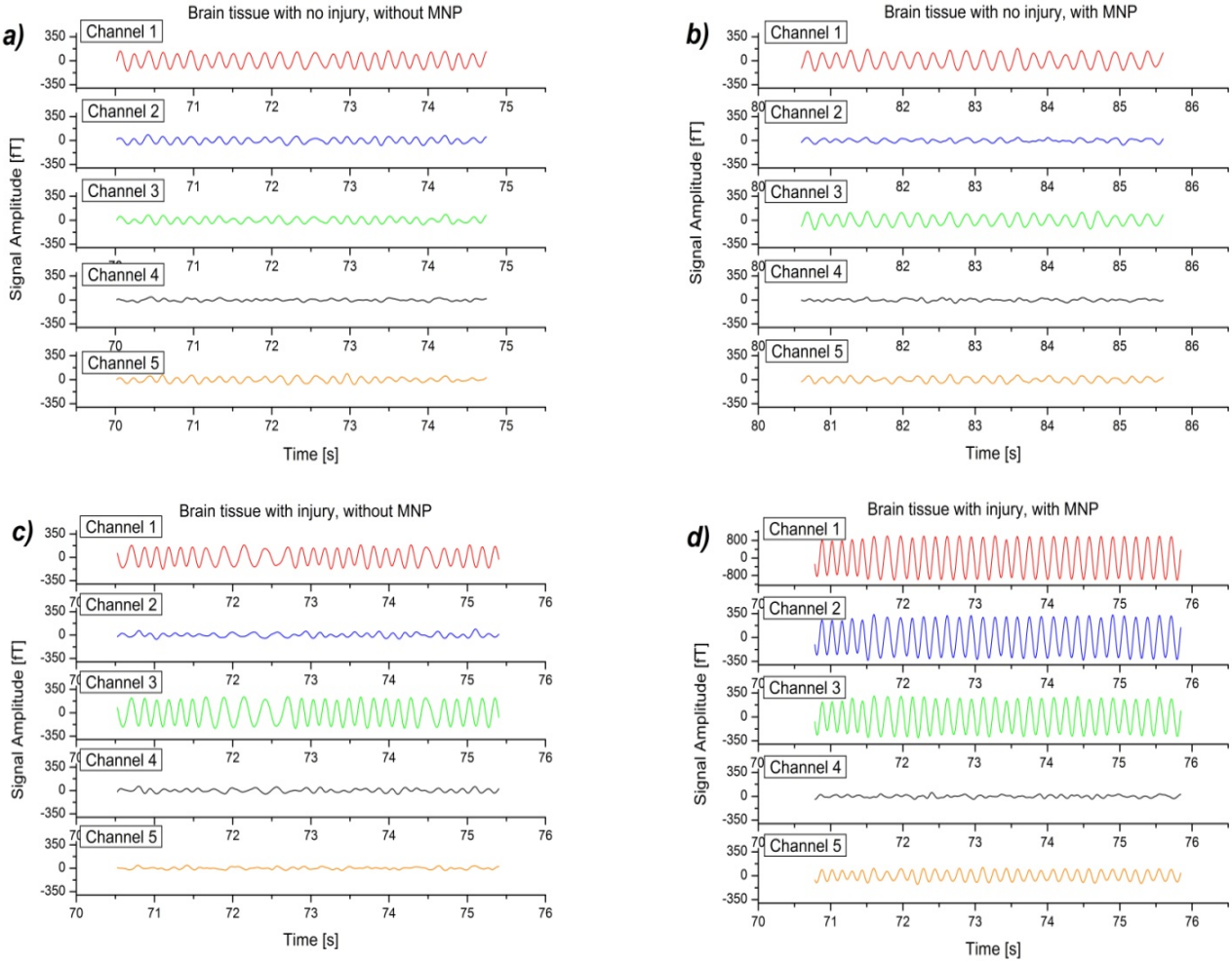

Figure 4. *Comparison of signal channels from the MEG system obtained from rat brain tissues, in two different cases: with and without injury. In all cases, tissues were taken from a rat perfused 24 hours after saline or MNP injection.*

This method can help to detect in a more precise way, cerebral pathological conditions that cannot be detected with MRI. It opens new ways for the MEG-system to be used for biomedical research, and points to the design of vibrated SQUID detectors for macroscopic samples or objects contaminated with MNPs. Although there is still a long way up to the real practical application to human beings, research uses may be immediate.

References

[1] Partially funded by NANOPUCEL project (MAT2007-65965-C02-01/ MEC) and NANOMAG project (UCM-CM R05-11885 (2006))

[2] Q.A. Pankhurst, J. Connolly, S.L. Jones and J. Dobson, J. Phys. D.: Appl. Phys**. 36,** R167 **(**2003).

[3] Q.A. Pankhurst, N.K.T. Thanh, S.K. Jones and J. Dobson, J. Phys. D: Appl. Phys. **42**, 224001 (2009).

[4] P. Tartaj, M.P. Morales, S. Veintemillas-Verdaguer, T. González-Carreño and C.J. Serna, J. Phys. D.: Appl. Phys., **36**, R182 (2003).

[5] A.G. Roca, R. Costo, A.F. Rebolledo, S. Veintemillas-Verdaguer, P. Tartaj, T. González-Carreño, M P. Morales and C.J. Serna, J. Phys. D: Appl. Phys. **42**, 224002 (2009).

[6] B. Thiesen and A. Jordan, Int. J. Hyperthermia, 1-8, iFirst (2008).

[7] "Sistema y procedimiento de detección de nanopartículas magnéticas mediante magneto-encefalografía" (Ref.: P200901528).

[8] G.Stoll and M.Bendszus, Neuroscince, 158(3), 1151 (2009).

[9] K.G. Petry, C. Boiziau, V. Dousset and B. Brochet, Neurtherapeutics: The Journal of the American Society for Experimental NeuroTherapeutics, **4**, 434 (2007).

[10] V. Rousseau, B. Denizot, D. Pouliquen, P. Jallet, and J.J. Le Jeune, MAGMA, **5**, 213 (1997).

[11] D. Cohen, Science, **161**, 784 (1968).

[12] M. Maicas, M. Sanz, H.Cui, C. Aroca, P. Sánchez, *submitted to* J. Magn. Magn. Mater, (2009).

6.12 Magnetic properties and morphology of Ni nanoparticles synthesized in the gas phase [12]

During the last years ISOM is working in the synthesis of magnetic nanoparticles by the gas aggregation technique using magnetron sputtering sources. This equipment allows the growing of nanoparticles made of pure elements with stronger magnetic properties than traditional products based on iron oxides. We have focused on the synthesis of Ni nanoparticles and have studied the influence of the growing parameters on their structure, morphology and magnetic properties.

Experimental

Ni nanoparticles are fabricated using a sputtering system with a free-jet source configuration. The source has ∅2in DC planar magnetron covered by a removable cylindrical chamber with selectable nozzle apertures and length. Nickel targets had a thickness of 1.5mm and were located 45mm from the nozzle orifice. The magnetron growing power was 40W and Ar was used as inert gas injected directly into the aggregation chamber at pressures ranging from 0.2mbar to 2mbar. The samples were deposited on 4x5mm Si substrates for magnetic measurements (VSM) and field emission scanning electron microscopy (FE-SEM). AFM observations were performed by depositing the nanoparticles directly on freshly cleaved mica substrates [1] and measurements were carried out in tapping mode using standard 10nm radius tips. Mass measurements were made using a commercial microbalance with a sensitivity of 0.1μg. Typical deposition mass obtained for a 10 min. growing was in the range of 10-100 micrograms.

Results

The main parameter for the nanoparticle formation is a high growing gas pressure. The inert gas is injected into the aggregation chamber and transports the particles to the main chamber through the nozzle orifice. The atoms ejected from the target, due to the small mean free path for the given pressure, are involved in multiple collisions producing agglomeration that leads to nanoclusters. The geometry of the nozzle controls the flow and pressure of the carrier gas. The nanoparticles deposited are highly focalized on the substrate. Typical deposits exhibit a maximum thickness at the beam axis (figure 1) that decreases with radial distance from it. In the outer areas, where the thickness is smaller, it is possible to see a ring pattern with dark fringes of nanoparticles separated by a distance in the range of tenths of millimeters [2]. Figure 2 shows an AFM image of nanoparticles deposited at 0.4 mbar using a ∅2mm nozzle with 20mm length. The nanoparticles are well isolated on the substrate. Their height is close to 10nm which is smaller than the apparent size due to AFM tip convolution [1].

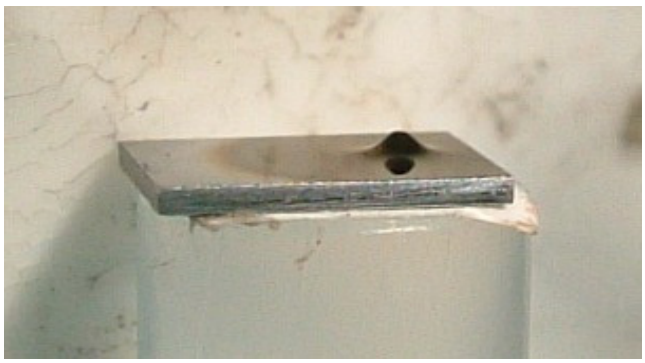

Figure 1. *Typical nanoparticles deposit*

[12] *Contact Person: Marco Maicas* maicas@fis.upm.es

Magnetic measurements show a good control on coercive field with the growing pressure. Figure 3 shows the coercive fields for three different nozzle appertures as a function of the Ar pressure. The measurements were performed in the sample plane. Coercivities fall below 1 Oe for pressures under 0.4 mbar, corresponding to a small particle size with a nearly superparamagnetic behaviour. Perpendicular to the plane loops are similar but exhibit a little lower susceptibility and coercivity which reveals an interaction between the particles in the deposit that avoids a complete superparamagnetic behaviour. In the range of 0.4-0.8 mbar the coercive field increases to a maximum of 145 Oe due to a decrease on the mean free path and so a promotion of the cluster aggregates. Similar values are found by other authors with a maximum coercivity of 148 Oe for 60nm Ni nanoparticles grown by chemical synthesis [3]. In this range particles are ferromagnetic with a monodomain structure. The coercive field shows a maximum at 0.8-0.9 mbar and begins to decrease at higher pressures.

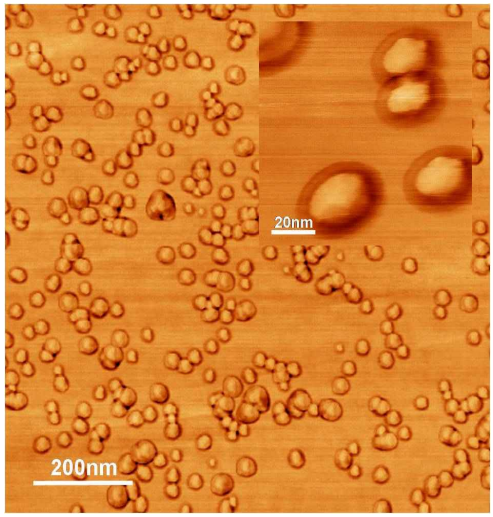

Figure 2. *Ni nanoparticles synthesized at 0.4mbar*

Nanoparticle size ranges from nearly 10nm for P_{Ar}=0.4mbar to 50nm at 0.9mbar with a size dispersion of about 13% (figure 3), very close to that reported for other materials grown in sputtering sources [4]. This behaviour can be associated to an increase in particle size that leads to ferromagnetic processes based on non-coherent magnetization rotations or multidomain dynamics. In the range 0.9-1.6mbar (∅1mm orifice) we find that the origin of coercive field reduction is associated to a small decrease in particle size. This reduction is associated to a larger Ar flow, necessary to increase the pressure in the aggregation chamber. While the increasing pressure promotes bigger aggregates the increasing flow makes the particles remain in the aggregation chamber for a shorter time reducing the aggregation time. These two effects should be considered and from 0.9mbar and up the effect of the larger Ar flow predominates and the size of the aggregates begins to decrease [5]. This effect can also be observed when working with different nozzle apertures. Considering three apertures used (1, 1.5 and 2mm) the resulting coercivity is very sensitive to the nozzle diameter. The behaviour with the Ar pressure is similar in all of them but the coercivities are smaller as the aperture size increases. In this case the increase in the aperture size produces larger fluxes reducing the particle size.

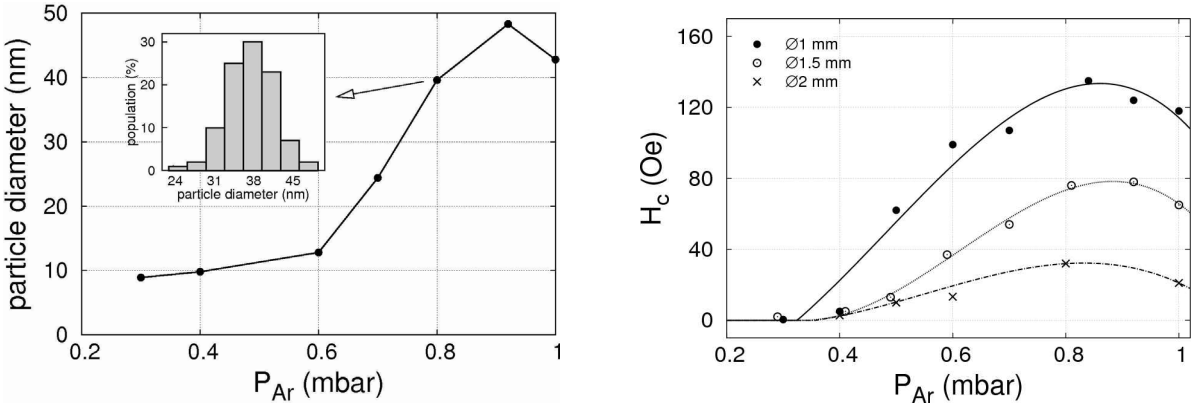

Figure 3. *Influence of the growing pressure on: left) coercive field, right) particle size*

The specific magnetic moment of Ni nanoparticles depends on particle size and thus on coercive field. Figure 4 shows the specific magnetic moment of Nickel as a function of sample coercivity (all values were taken at a saturating field of 1000 Oe). The magnetic moment of bigger particles gets close to that of Ni bulk magnetization (55.8 emu/g). For smaller coercivities and particle diameters the specific magnetization

decreases to nearly 15 emu/g which corresponds to particles in the limit of superparamagnetic behaviour (about 10nm). In contrast to pure Fe [4] the reduction of the specific moment is more pronounced on Ni.

The nanoparticles are expected to be covered by a thin NiO layer when the sample is taken out from the sputtering chamber and brought into air. The relative volume of the NiO layer with respect to the whole particle becomes larger for the smaller particles. For the applied field (< 1000 Oe) NiO layer contributes with a nearly zero magnetic moment [6] thus decreasing notably the total magnetic moment of the particle. The amount of material synthesized is also strongly dependant on the growing pressure, being a maximum at pressures about 0.6-0.7mbar. A large reduction in the nanoparticle production is found below 0.2mbar and over 1.5mbar, the former due to the decrease of carrier capacity of the inert gas and the latter due to the reduction in the sputtering rate. For pressures over 1.5mbar the particle size continues increasing and in the range of 1.6-1.8 mbar it is observed a major change to diameters over 100nm. The resulting particles have low dispersion in size and appear to be made from aggregates of smaller particles (figure 5). The free-jet nanoparticle source has shock waves associated to the expansion of the carrier gas in the low pressure deposition chamber. The origin of this further aggregation may be associated to collisions of particles at the supersonic shock waves that appear over the substrate [7].

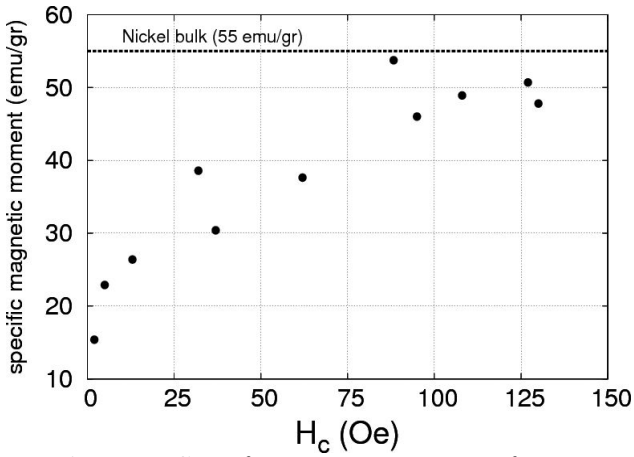

Figure 4. *Specific magnetic moment of Ni nanoparticles as a function of their coercivity*

The Ni nanoparticles obtained have either spherical or cubic shape being the population of spherical particles much larger than that of cubic particles in our system. In the case of high pressures (over 1.8 mbar) particles with diameters over 100nm can also exhibit cubic shape or are made from small particle aggregates. The two different morphologies found are shown in figure 6. This cubic shape appears compatible with a fcc crystal structure. The fcc-Ni nanoparticles exhibit stronger magnetic features when compared to hcp phase [3,8] which is supported by the large specific magnetic moment measured for the bigger particles. Similar

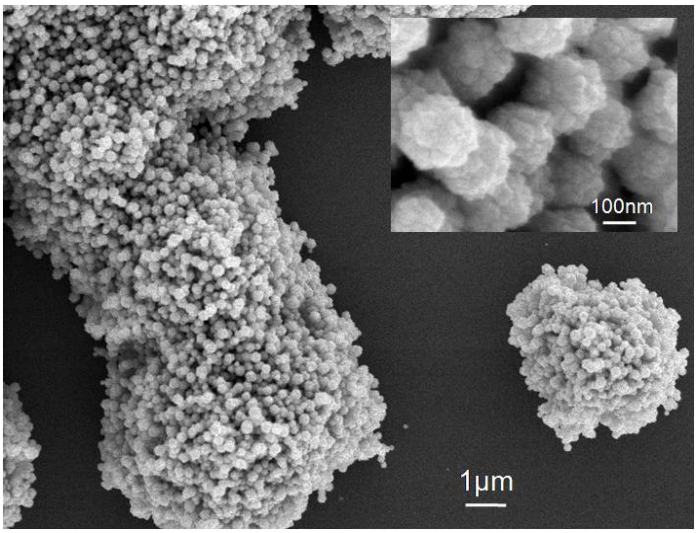

Figure 5. *Nanoparticles deposited at 1.8mbar*

crystal morphologies in particles obtained by sputtering can also be found in other materials like Fe [4], FePt [9] and FeCo [10]. The techniques used to obtain those crystals are based on in-flight thermal annealing [11] or based on particular designs to control the magnetic field and inert gas flow just above the target [9]. In our system there is no cooling of the aggregation chamber so nanoparticle crystallization is promoted by the

heated walls of the aggregation chamber resulting in a small but appreciable population of crystal shape nanoparticles.

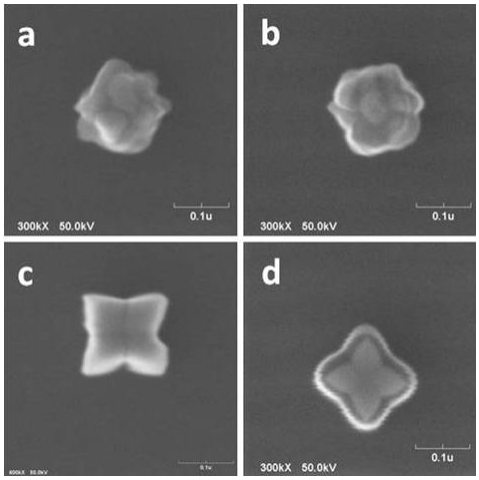

Figure 6. *Different particle morphologies: a-b) agglomerates, c-d) crystals*

References

[1] M. Rasa, B. W. M. Kuipers and A. P. Philipse, J. Colloid Interface Sci. **250,** 303 (2002).

[2] C. Chiappini, P. Piseri, S. Vinati and P. Milani, Rev. Sci. Instrum. **78,** 066105 (2007).

[3] H. Wang, X. Kou, L. Zhang, J. Li, Materials Research Bulletin **43,** 3529 (2008).

[4] Y. Qiang, J. Antony, A. Sharma, J. Nutting, D. Sikes and D. Meyer, J. Nanoparticle Research **8**, 489 (2006).

[5] A.N. Banerjee, R. Krishna and B. Das, Appl. Phys. A **90**, 299 (2008).

[6] Y. Ichiyanagi, N. Wakabayashi, J. Yamazaki, S. Yamada, Y. Kimishima, E. Komatsu and H. Tajima, Physica B **329-333**, 862 (2003).

[7] A. Zare, O. Abouali and G. Ahmadi, J. Aero Sci. **38**, 1015 (2007).

[8] S. Mourdikoudis, K. Simeonidis, A. Vilalta-Clemente, F. Tuna, I. Tsiaoussis, M. Angelakeris, C. Dendrinou-Samara and O. Kalogirou, J. Magn. Magn. Mat. **321**, 2723 (2009).

[9] J.M. Qiu and J.P. Wang, Appl. Phys. Letters **88,** 192505-1-3 (2006).

[10] J. Bai, Y.H. Xu and J.P. Wang, IEEE Trans. on Magn, **43**, 7, 3340 (2007).

[11] Y. H. Xu, J. M. Qiu, J. Bai, J. H. Judy and J. P. Wang, J. Appl. Phys. **97**, 10J305 (2005).

6.13 Influence of the substrate stiffness on the crystallization process of sputtered TbFe2 thin films [13]

During the last few years, great attention has been paid to magnetostrictive materials in order to develop new magnetomechanical sensors at ISOM. Our works on FeCoB have shown the possibility to control the anisotropy and coercivity on sputtered magnetostrictive thin films[1-2]. Nevertheless, the magnetostriction constant of this material system can appear as a drawback for some applications.

Bulk $TbFe_2$ is the material with the highest magnetostriction constant, 4400 ppm at 0 K and 2500 ppm at room temperature[3]. Nevertheless, $TbFe_2$ has not yet made any impact in sensor technology due to the difficulties of obtaining high-quality thin films. Crystalline $TbFe_2$ and its Laves phase can also be obtained through thermal post-deposition annealing that can potentially be more effective than high temperature deposition[4]. Additionally, for practical applications the choice of substrate it is indeed an issue, as it has to be either very thin or made from a material with a very low Young modulus, so it can allow the deformation of the magnetostrictive $TbFe_2$ film. Although there is some previous work on the effect of annealing on films deposited by sputtering on different substrates, an exhaustive study of the influence of the substrate on the $TbFe_2$ crystallization process is still missing. We have analyzed thoroughly the structural and magnetic properties of as-deposited and annealed $TbFe_2$ films deposited on different substrates and different buffer layers[5].

Samples were deposited by DC magnetron sputtering at Room Temperature on different substrates: Si(100) 0.5 mm thick, glass 120 μm thick, kapton 20 μm thick and mica 100 μm thick. We have also investigated the effect of different buffer layers: Mo, Pt, Al and Cu on the crystallization process of $TbFe_2$ during post-deposition annealing. Thermal treatments were conducted in Ar atmosphere at 400° C during 1 hour. In order to prevent oxidation the same buffer material was also used as capping layer, or Mo if no buffer was used.

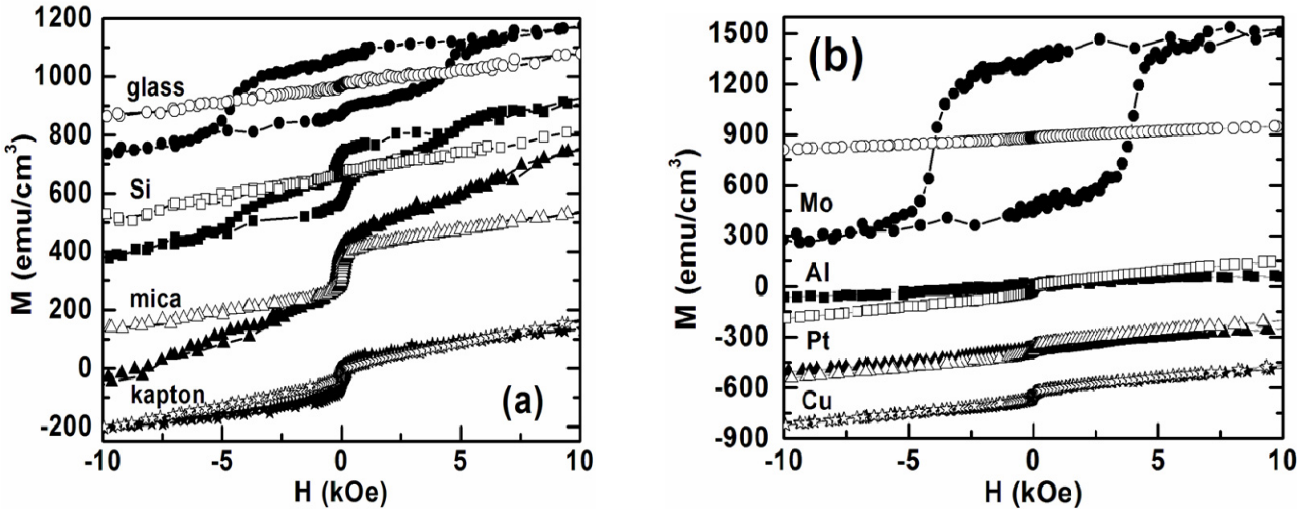

Figure 1. *a) Hysteresis loops for $TbFe_2$ films before annealing (open symbols) and after annealing (solid symbols), directly deposited on different substrates: glass (circles), Si(100) (squares), mica (triangles) and kapton (stars). (b) Hysteresis loops for $TbFe_2$ films before (open symbols) and after annealing (solid symbols) grown on Si(100) substrates on different buffer layers: Mo (circles), Al (squares), Pt (triangles) and Cu (stars). Curves are vertically shifted for clarity.*

[13] *Contact Person: Rocío Ranchal rociran@fis.ucm.es and Claudio Aroca caroca@fis.upm.es*

First we show the magnetic characteristics of the films deposited directly on different substrates in figure 1a, for both before and after annealing. The samples show very small magnetic signal prior to the

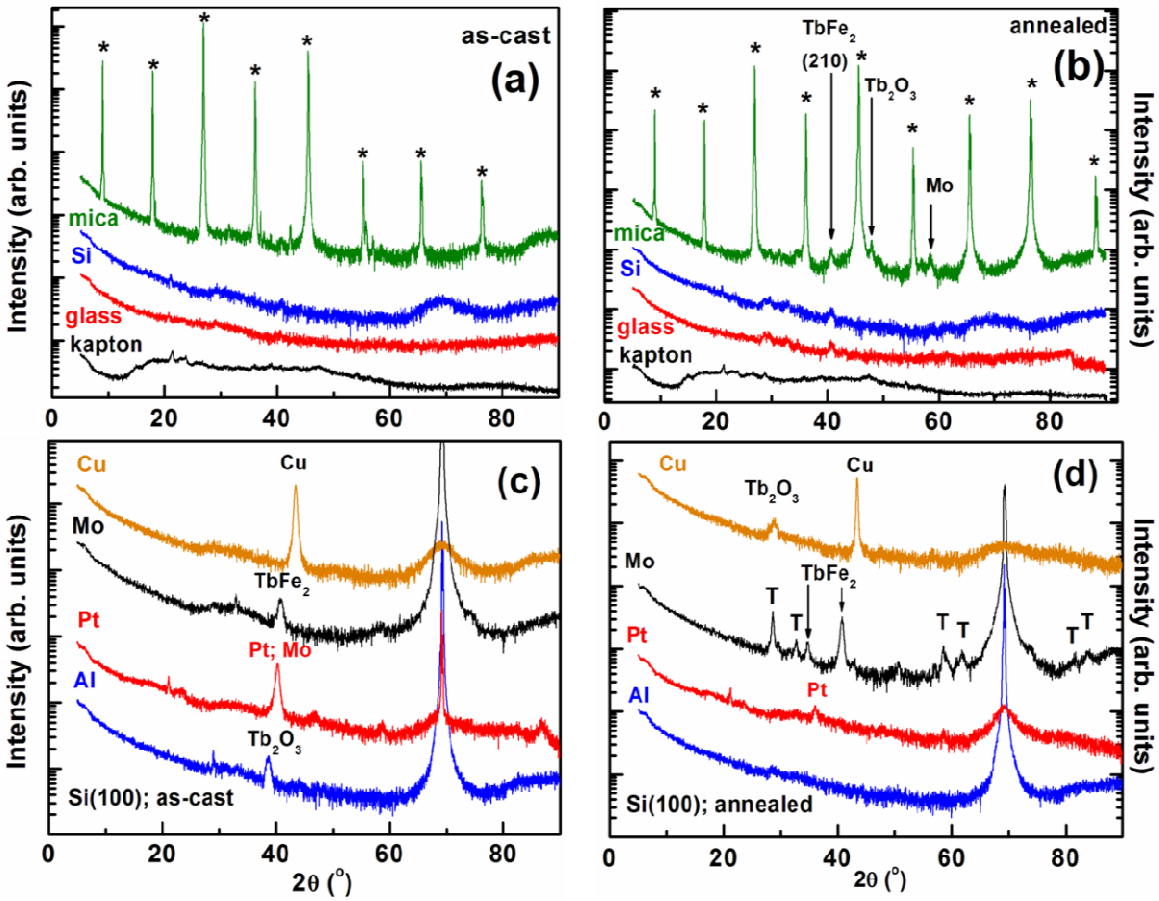

Figure 2. *(a) θ-2θ diffraction scans of as-deposited $TbFe_2$ layers directly deposited on different substrates. (b) θ-2θ diffraction scans of annealed $TbFe_2$ layers directly deposited on different substrates. Peaks related to the mica substrate are labeled with an asterisk (*). (c) θ-2θ diffraction scans of as-deposited $TbFe_2$ layers deposited on different buffer layers: Cu, Mo, Pt and Al. (d) θ-2θ diffraction scans of annealed $TbFe_2$ layers deposited on different buffer layers: Cu, Mo, Pt and Al. Peaks related to the Tb-α phase are labeled with a T. In all cases, curves are shifted for clarity.*

annealing on any substrate. Upon annealing, all of them show an enhancement of the magnetic signal and some of them show a large increase in the coercivity. In $TbFe_2$, high coercivity (Hc) is usually associated to the formation of the highly magnetostrictive Laves Phase[6]. Additionally, with the magnetostriction measurements for all the samples, we have seen that in our samples, large coercivity always indicates large magnetostriction.

Therefore, judging by the coercivity values, the substrate that promotes better properties on the annealed $TbFe_2$ is amorphous glass, even better than Si (100), while layers deposited on kapton or mica do not show a significant increase of H_C upon annealing. Although Si has a lattice parameter (5.431 Å) close to that of $TbFe_2$ (5.207 Å), the higher coercivity obtained for layers deposited on amorphous glass, indicates that crystallinity of the substrate is not essential to promote the formation of crystalline $TbFe_2$ in the annealing.

The structure of these samples is shown in figures 2a and 2b. $TbFe_2$ films directly grown on the substrates, without any buffer, do not show any distinct diffraction peak revealing a low structural quality, in agreement with the magnetic results. After the thermal treatment, low intensity peaks related to the $TbFe_2$ appear, indicating an incomplete crystallization (Fig 2b). Additionally, the bad results obtained on flexible substrates like kapton and thin mica might indicate that mechanical properties could have some influence in the crystallization process.

In order to find out what are the properties of the substrate that promote the formation of the Laves phase during annealing, we have investigated the influence of different buffer layers, Cu, Al, Pt and Mo on the properties of the $TbFe_2$ deposited on top. Figure 1b shows that the pre-annealed $TbFe_2$ films deposited on any of these buffer layers still have very small magnetic signal. After the thermal treatment, the film deposited on Mo shows a huge increase of the coercivity (Fig. 1b) while the rest of the buffers promote only marginal changes.

Structurally, prior annealing only the samples deposited on Mo show a diffraction peak related to $TbFe_2$ (Fig. 2c) and the situation is very similar after annealing: only Mo promotes an enhancement of the intensity peak related to $TbFe_2$, together with the crystallization of the Tb-α phase (Fig. 2d). Aluminium buffer produces oxidation of the Tb even before annealing, and Cu buffer also gives oxidation problems during annealing. The positive influence of the Mo buffer layer cannot be related to its capacity to prevent Tb oxidation, as Pt can equally prevent oxidation but does not improve the magnetic or structural properties of the $TbFe_2$ deposited on top.

Interestingly, if we introduce a 20 nm-thick Mo layer between a Pt buffer and the $TbFe_2$ film grown on Si, the properties of the annealed $TbFe_2$ improve again dramatically (Fig. 3a). X-ray diffraction scan for this sample (not shown) confirms that the introduction of the Mo buffer between the Pt and the $TbFe_2$ layers promotes the $TbFe_2$ crystallization. This crystalline $TbFe_2$ gives rise to the increase of both magnetization and H_C (Fig. 3a). The magnetostriction also improves largely upon introduction of the Mo buffer layer (Fig. 3b) and this is also a clear indication of the presence of the crystalline Laves phase. Similar results have been obtained in the rest of the samples studied: the higher the coercivity, the higher the magnetostriction.

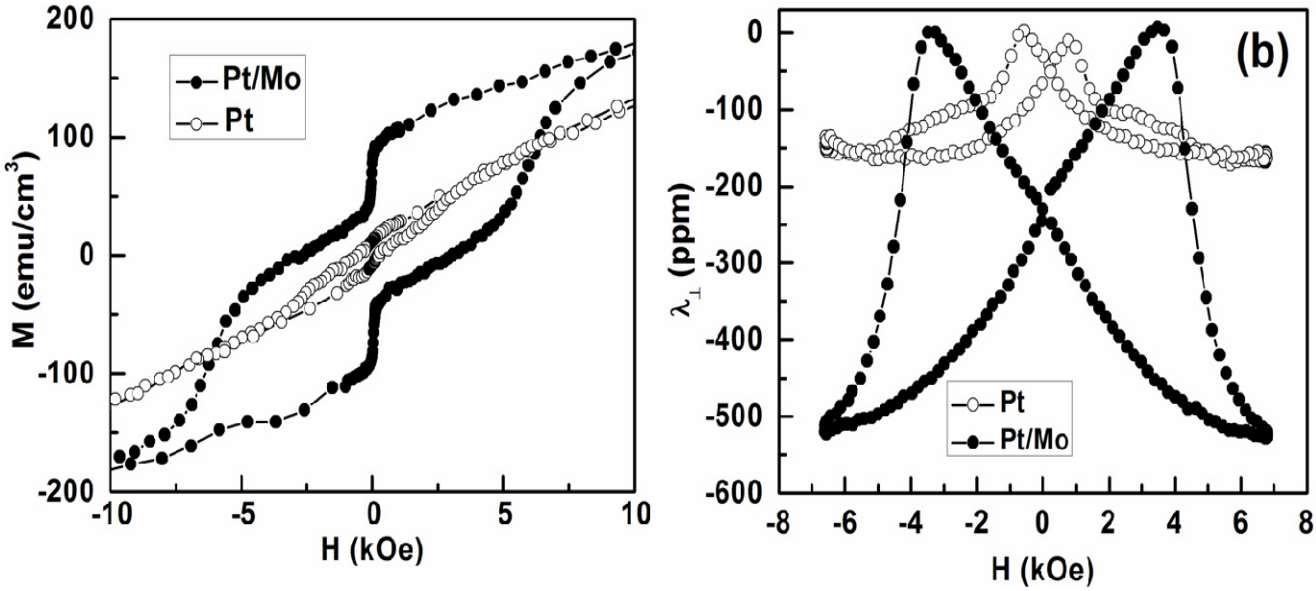

Figure 3. *(a) Hysteresis loops of annealed $TbFe_2$ films grown on Si(100) substrates on different buffer layers: Pt/Mo (●), Pt (○). (b) Transversal magnetostriction of the same samples. The applied magnetic field is perpendicular to the sample axis.*

Our results have shown that a post deposition annealing promotes the ferromagnetic behavior of the $TbFe_2$ layer, which is clear in the hysteresis loop of most of the annealed samples (Fig. 1). This ferromagnetism comes in two distinct phases: one showing a soft magnetic behavior and a second one with much larger coercivity. The low coercivity phase gives no magnetostriction. The high coercivity phase comes together with peaks of $TbFe_2$ in the diffractograms and it always gives large magnetostriction, so it is very likely caused by the Laves phase.

The fact that both rigid substrates (Si and amorphous glass) and the Mo buffer layer are clearly beneficial, and that crystallinity or purity against oxidation do not seem to have a determining role, suggests that the reason behind this positive effect could be purely mechanical.

Usually, the difference between the thermal expansion coefficients (α) of film and substrate is the only mechanical parameter that is taken into account to explain induced stresses during a thermal treatment. The difference between the α values of Mo and $TbFe_2$ is higher than the one comparing $TbFe_2$ and Pt, but the crystallization is better with Mo. Therefore we also have to take the Young modulus of the substrate and buffer into account. This has been previously done in order to explain the properties of amorphous magnetostrictive layers deposited by sputtering[2].

Let us use the ratio between Young modulus and thermal expansion (Y/α) as the parameter that can quantitatively describe the deformation of the substrate (and/or the buffer layer) during the annealing process, either by the temperature increase (α) or by the stress induced by the $TbFe_2$ layer: the higher the Y/α ratio is, the lower the substrate deformation. If we summarize the values of Y/α for every substrate and buffer layer used in this work[7], we can instantly see that Si, glass and Mo have the highest Y/α, and they are in fact the best substrates. This can be seen graphically in figure 4, where we plot the coercivity after annealing (Fig. 4a) and the transversal magnetostriction (Fig. 4b) versus the parameter Y/α for all substrates. In the same plot we can also see the positive effect of adding a Mo buffer layer, which has the highest Y/α out of all materials used and one of the highest in the periodic table.

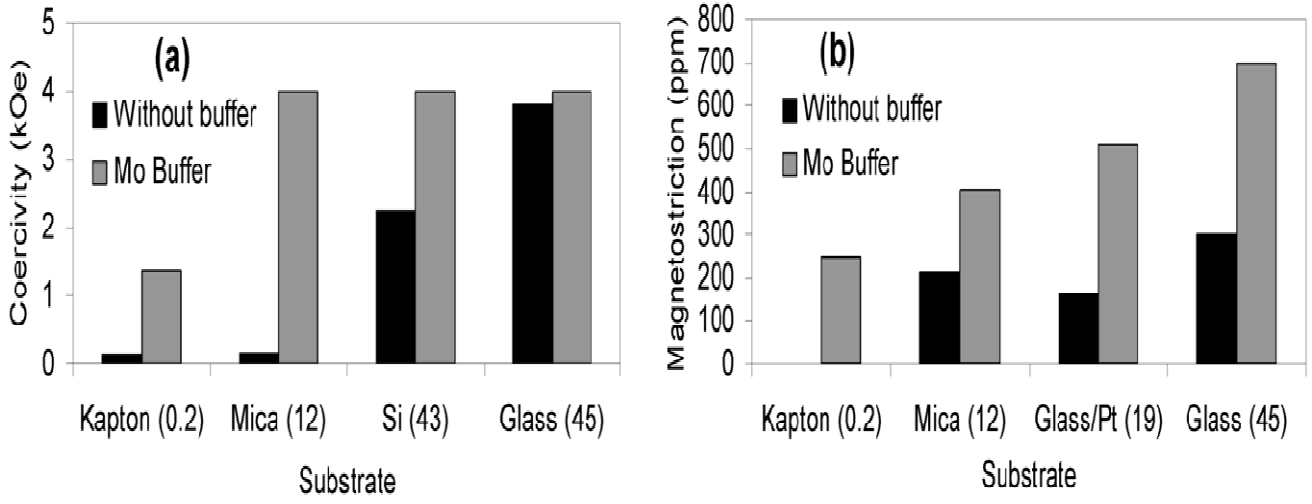

Figure 4. *(a) Bar diagrams showing the coercivity of annealed $TbFe_2$ films deposited on different substrates and with a Mo buffer layer. (b) Transversal magnetostriction measured with the applied magnetic field perpendicular to the sample axis. In the horizontal axis, the number between brackets for each substrate is the factor Y/α * 10^6 GPa·K. Note that Si substrate is not present as the magnetostriction cannot be measured properly in such a thick hard substrate. The Y/α values for all the materials are:* ***kapton*** *= 0.2 × 10^6 GPa·K;* ***Al*** *= 3 × 10^6 GPa·K;* ***Cu*** *= 7 × 10^6 GPa·K;* ***mica*** *= 12 × 10^6 GPa·K;* ***Pt*** *= 19 × 10^6 GPa·K;* ***Si*** *= 43 × 10^6 GPa·K;* ***glass*** *= 45 × 10^6 GPa·K;* ***Mo*** *= 71 × 10^6 GPa·K.*

The buffers not represented in figure 4 do not promote a significant enhancement of the coercivity or magnetostriction in the $TbFe_2$ layer deposited on top and therefore the Laves phase either nucleates in a negligible fraction of the $TbFe_2$ volume or it does not nucleate at all. As it was mentioned before, even with buffers that do not give a particular coercivity enhancement like Pt, when a Mo layer is added on top (Pt 20nm-Mo 20nm buffer layer) the coercivity and the magnetostriction is recovered. For instance the coercivity on annealed Si/Pt/$TbFe_2$ is 0.04 kOe, while on Si/Pt/Mo/$TbFe_2$ is 2 kOe, and for Glass/Pt/$TbFe_2$ is 0.03 kOe while for Glass/Pt/Mo/$TbFe_2$ is 3 kOe. On the contrary, the insertion of buffer layers with lower Y/α factors than the substrates reduces the $TbFe_2$ crystallization. For instance, adding a Pt buffer onto the Si sample is detrimental and reduces the coercivity of the annealed sample by a factor of 10.

It is important to remark that the best results are related to a high Y/α factor in the substrate or buffer and not to a Y/α close to that of $TbFe_2$. The poor results for Kapton are probably caused by the irreversible macroscopic deformation that the thermal treatment produces in this substrate. This deformation partially overrules the effect of the buffer, although the Mo can still improve the properties of the $TbFe_2$ deposited on Kapton (Fig. 4).

Another possibility could be that the Mo is stopping the diffusion of elements into the $TbFe_2$ and that is why is so beneficial. We believe this is not the case as many of the materials used should not have any tendency to diffuse into the $TbFe_2$. A clear example is the noble metal Pt that should not have any chemical tendency to diffuse into the $TbFe_2$ layer and still a Mo layer improves its efficiency promoting crystalline $TbFe_2$ during annealing.

In conclusion, we have shown that promoting the formation of the Laves phase in $TbFe_2$ films during the post-deposition annealing, does not seem to depend on the crystallinity of the substrate but rather on its mechanical properties. An amorphous phase with low coercivity and zero magnetostriction forms when the substrate and the buffer allow the deformation of the $TbFe_2$ during annealing. If this deformation is partially restricted by the rigidity of the substrate or the buffer, the highly magnetostrictive Laves phase is promoted. The very positive effect of a Mo buffer layer opens the possibility to further research using other rigid elements like Ru, Ir or Rh as buffers, which could lead to highly magnetostrictive $TbFe_2$ films on a wide variety of substrates.

References

[1] M. González-Guerrero, J.L. Prieto, D. Ciudad, P. Sánchez, and C. Aroca, Appl. Phys. Lett. **90**, 162501 (2007).

[2] M. González-Guerrero, J.L. Prieto, P. Sánchez, and C. Aroca, J. Appl. Phys. **102**, 123903 (2007).

[3] A.E. Clark and H. S. Belson, Phys. Rev. B**5**, 3642 (1972).

[4] P. Farber, and H. Kronmüller, J. Magn. Magn. Mater. **214**, 159 (2000).

[5] R. Ranchal, J. L. Prieto, P. Sánchez, and C. Aroca (submitted).

[6] A. E. Clark, Appl. Phys. Letters **23**, 642 (1973).

[7] **Kapton**: Y = 4 GPa; $\alpha = 19 \times 10^{-6}$ K^{-1}; $Y/\alpha = 0.2 \times 10^{6}$ GPa·K. **Aluminum**: Y = 70 GPa; $\alpha = 23 \times 10^{-6}$ K^{-1}; $Y/\alpha = 3 \times 10^{6}$ GPa·K. **Copper**: Y = 119 GPa; $\alpha = 16 \times 10^{-6}$ K^{-1}; $Y/\alpha = 7 \times 10^{6}$ GPa·K. **Mica**: Y = 180 GPa; $\alpha = 15 \times 10^{-6}$ K^{-1}; $Y/\alpha = 12 \times 10^{6}$ GPa·K. **Platinum**: Y = 168 GPa; $\alpha = 9 \times 10^{-6}$ K^{-1}; $Y/\alpha = 19 \times 10^{6}$ GPa·K. **Glass**: Y = 90 GPa; $\alpha = 2 \times 10^{-6}$ K^{-1}; $Y/\alpha = 45 \times 10^{6}$ GPa·K. **Silicon**: Y = 170 GPa; $\alpha = 4 \times 10^{-6}$ K^{-1}; $Y/\alpha = 43 \times 10^{6}$ GPa·K. **Molibdenum**: Y = 329 GPa; $\alpha = 5 \times 10^{-6}$ K^{-1}; $Y/\alpha = 71 \times 10^{6}$ GPa·K. **$TbFe_2$**: Y = 76 GPa; $\alpha = 12 \times 10^{-6}$ K^{-1}; $Y/\alpha = 6 \times 10^{6}$ GPa·K. The values for mica were obtained from E McNeil and, M. Grimsditch, J Phys: Condens Matter **5**, 1681 (1993) and Y.B Chen and, J.R.G. Evans; Scripta Materialia **54**, 1581 (2006).

6.14 Spintronics in the ISOM: from GMR multilayers to Magnetic Domain Walls in nanowires[14]

In the last two years, the Group of Magnetic Devices of the ISOM (GDM) has started an active research in the field of Spintronics. At the end of 2007 we had a new home made sputtering system with 7 magnetron targets, specially designed for the very precise deposition of metallic multilayers. Additionally, thanks to our new nanolithography facility (CRESTEC CABL 9500C) we are able to pattern our magnetic samples in small wires and devices and study the interaction of the current and the field with confined magnetic Domain Walls. Here we give examples of some of the complicated structures we deposit and of some of the measurements we are currently doing with magnetic domain walls in patterned nanowires.

Spin valves with a thin layer of Gd

It is well known that rare-earth make a negative effect in the magnetoresistance of the spin-valves [1]. On the other hand, there have been very interesting studies using rare-earth and transition metal compounds, where negative magnetoresistance can be achieved [2]. Very recently a new application of rare-earth came into play. As the size of the reading heads in magnetic hard drives shrink in size, the measuring current creates Spin Transfer Torque instabilities [3] and it seems that some rare earth impurities in the main matrix or even deposited as a capping layer can increase the critical current of the structure (the maximum current that can flow through the structure without creating any spin transfer instabilities) [4].

Although Gadolinium as an impurity does not increase the Gilbert damping (parameter that it is proportional to the critical current) [5], we believe its effect might be different when it is inserted in the structure as a thin layer, as it could effectively increase the Gilbert damping due to the Gd strong magnetic moment. A thin layer of Gd might make an especially strong effect when in a sandwich with Fe, as the interface is very good and the iron promotes strong ferromagnetism in the Gd even at Room Temperature.

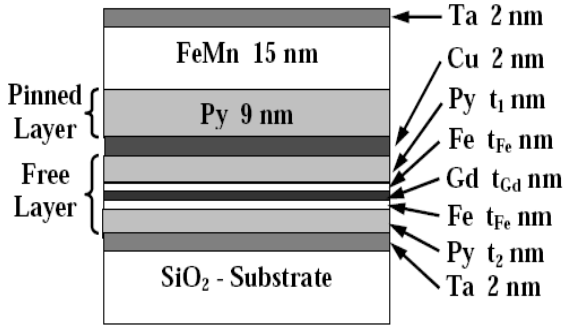

***Figure 1**. Schematic of the multilayer stack composition. The total thickness of the Py free layer is constant (t_1+t_2= 9 nm). Note that when t_1 changes its value, effectively we are only displacing the Gd layer or the Fe/Gd/Fe trilayer within the thickness of the free layer. t_{Fe}=1 nm for all the samples with a trilayer Fe/Gd/Fe inserted and t_{Fe}=0 nm for the samples with a layer of Gd only inserted.*

We began the study of the effect of the Gd layers on Spin Valve structures with current in-plane measurements, following the structure of figure 1. In first place we study the effect of inserting a sole Gd layer in the free Py layer (t_{Fe}=0 and t_{Gd}=1-2 nm). Due to the large resistance of a Gd layer (or even of a GdNi alloy layer, which is more likely the case given the natural interdiffusion between Ni and Gd), in a CIP configuration, the conduction electrons can be reflected in that dirty layer and the effect of Gd on the MR might be difficult to evaluate. In order to interpret the results correctly, test samples were deposited for

[14] *Contact Person: José Luis Prieto - joseluis.prieto@upm.es*

comparison, where all the layers below the Py t_1 nm layer are removed (t_{Fe}, t_{Gd} and t_2 all are zero in the test samples).

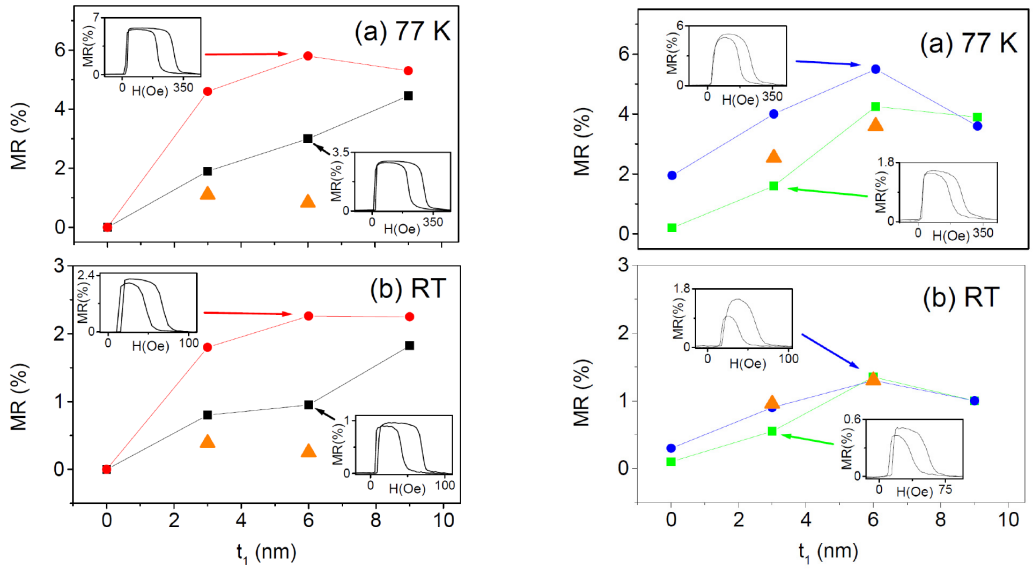

***Figure 2**. (LEFT) Magnetoresistance values for samples with a 1 nm Gd layer inserted in the free layer (squares) at t_1 nm of the Cu spacer, compared with the test sample (circles) where t_{Fe}, t_{Gd} and t_2 all equal to zero. Triangles represent samples where a 2 nm Gd layer is inserted in the free layer at t_1 nm of the Cu spacer. The insets show selected MR loops. (a) Measurements at 77 K and (b) at Room Temperature. (RIGHT) Magnetoresistance values for samples with a Fe(1 nm)/Gd(1 nm)/Fe(1 nm) trilayer inserted in the free layer at t_1 nm of the Cu spacer (squares), compared with the test sample (circles) where the Gd is removed from the inserted trilayer (t_{Gd}=0). Triangles represent samples with a Fe(1 nm)/Gd(2 nm)/Fe(1 nm) trilayer inserted in the free layer at t_1 nm of the Cu spacer. The insets show selected MR loops. (a) Measurements at 77 K and (b) at Room Temperature.*

Figure 2-LEFT shows the MR values for the spin valves with a thin layer of Gd inserted in the free layer, both at RT and at 77 K. The insets show selected MR loops. As can be seen in the figure, even the smallest (1 nm) contamination at the interface of the free layer with the Cu (t_1=0), completely destroys the MR at any temperature. Although SV based on rare-earths give little MR, it is still striking how just a trace of Gd at the interface of the free layer with the Cu, can kill completely the giant magnetoresistance effect. On the other hand, good MR values are quickly restored once the Gd is inserted further away from the interface with Cu, at t_1 larger than the Py spin diffusion length (~5 nm). The fact that a decrease of MR occurs even when the Gd is inserted at 9 nm from the Cu, suggests that the Py is diffusing through the Gd layer , and indeed samples with a 2 nm Gd layer (triangles in Fig. 2-LEFT) show even lower MR values.

Although the diffusion of Gd within Py is quite significant, this diffusion can be stopped by adding a thin layer of Fe on both sides of the Gd . Figure 2-RIGHT shows the results when a layer of Fe/Gd/Fe is inserted in the free Py layer (t_{Fe}=1 nm and t_{Gd}=1-2 nm) at both RT and 77 K. Another test sample is also deposited for comparison to evaluate the effect of the Fe layer, where t_{Gd}=0 nm and t_{Fe}=1 nm (2 nm of Fe in total, see Fig. 1). The insets show selected MR loops. Looking first at the low temperature measurements in figure 2-RIGHT-a, it is clear that Gd is still detrimental to the MR when it is inserted close to the Cu spacer, even in a sandwich with Fe. Again good values of MR can be restored when the trilayer is inserted at t_1>5 nm and these values are larger than those for the equivalent samples without Fe at 77 K (Fig. 2-LEFT-a). The effect of Fe on the MR values at low temperature is negligible as the test sample of Fig. 2-RIGHT (only Fe inserted), shows similar low temperature MR values to the test sample of figure 2-LEFT (with no layer inserted). Increasing the thickness of the Gd layer to 2 nm (triangular symbols in Fig. 2-RIGHT) does not seem to have a significant effect when it is in a sandwitch with Fe, although the MR values for these samples are again larger than those for the equivalent samples without Fe.

The picture is different at room temperature in figure 2-RIGHT-b, where both the test sample (only Fe inserted) and the sample with Fe/Gd/Fe, show very similar MR values, which are smaller than those of the

test sample in figure 2-LEFT-b (no layer inserted). This different behaviour at room temperature could be due to the Gd going paramagnetic (unlikely as it is only 1-2 nm of Gd and it is surrounded by Fe) or due the Fe introducing additional roughness to the structure, as it is explained below.

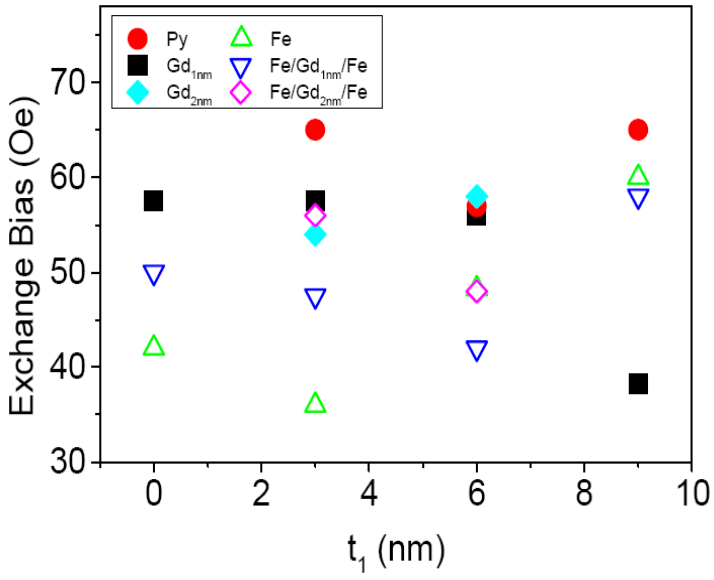

Figure 3. *Exchange bias field values at Room Temperature for all the samples used in this study. The values are smaller for most samples with a Fe layer inserted in the structure (empty symbols).*

The insets to figure 2-RIGHT-b show that the MR loops with Fe show no clear resistance plateau associated with a well-defined anti-parallel state. This is not observed in samples without Fe (Fig. 2-LEFT). The lack of a defined plateau at R_{AP} values is typical from samples were there is a strong coupling between the free and the pinned layer. As this happens for all samples with Fe, even if it is deposited far away from the Cu, it cannot be caused by an enhanced direct exchange coupling through the Cu. Looking at the values of the exchange bias field of all the samples in this study in figure 3, it is clear that most samples with Fe (empty symbols) show a reduced exchange bias field in comparison with the samples without Fe (filled symbols), independently on the position of the Fe within the structure. This fact indicates that the Fe layer might be introducing some additional roughness to the structure, which decreases the exchange bias of the pinned layer. In these reduced exchange bias conditions, irregularities or defects are more likely to affect the MR value when the pinned layer is switched against its natural exchange bias direction (lower MR value for the returning R_{AP} branch of the MR loop). At low temperatures though, the exchange bias is largely increased but not so much the effect caused by irregularities or the direct exchange between free and pinned layer, so the effect of the roughness introduced by the Fe layer is less obvious (see Fig. 2-RIGHT-a).

In conclusion, we have studied the effect of inserting a thin Gd layer in the free layer of a Py based spin valve. Gd shows a detrimental effect on the MR when it is close to the Cu spacer, although good values can be regained if the Gd is inserted at larger distance than ~5 nm from the Cu spacer. At a glance, the effect of depositing a stabilizing Fe layer on both sides of the Gd might not seem to help sustaining the MR values. A deeper look shows that if the Fe/Gd/Fe trilayer is inserted at t1 > 5 nm, the low temperature MR values are quite high. This fact suggests that Fe might have a positive effect once the roughness problem is solved.

As the Fe keeps the Gd ferromagnetic at high temperatures its introduction might be necessary for the best possible results increasing the critical current in spin valve structures. For future CPP measurements, the spin valves should be deposited with the FeMn at the bottom (so the roughness introduced by the Fe layers is no detrimental to the performance of the sensor) and with the Gd in a sandwich with Fe further than 5 nm from the non magnetic spacer.

Magnetic Domain Walls in nanowires

In the last few years, since the introduction of the Race-Track memory concept by Stuart Parkin at IBM [6], there has been a very active research on magnetic domain walls (DW) in ferromagnetic nano-wires. The concept of a Race-Track memory is based on the movement of DWs on a nanowire: i.e. moving the bits, rather than the magnetic disc as it is done actually. This concept is certainly very challenging and before being a true alternative, it requires to solve several non-trivial issues. First of all, the DW has to be reliably created, pinned and depinned all with electrical currents and not with magnetic fields, so the integration is possible. This opens several active lines of research, like the study of the spin transfer on DW, the study of the pinning or depinning of a DW in a engineered defect or the study of the velocity of the DW and its structure as it is moving.

Thanks to the extraordinary precision of our nanolithography facility, we can study defects in patterned nanowires with a precision that other groups cannot match. For instance, we can see in Figure 4 an example of a nanowire of permalloy fabricated in the ISOM. On the right we can see some different shapes of defects artificially created in the nanowire and the depinning statistics for each of them.

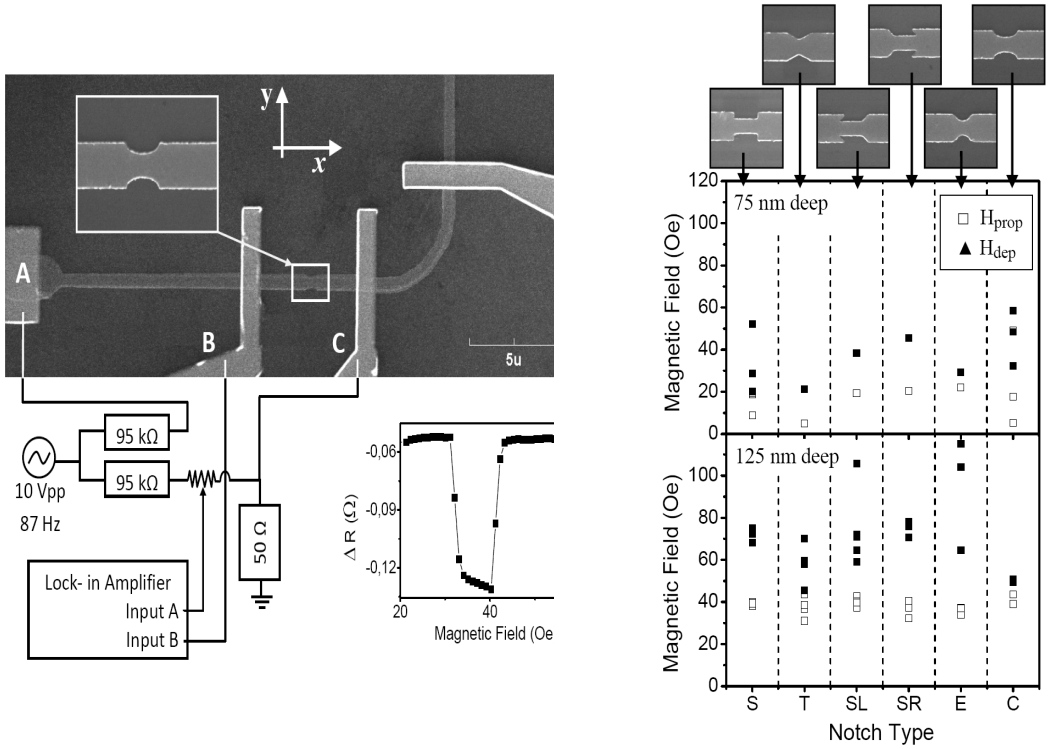

***Figure 4**. SEM photographs of permallow nanowires and notches. Diagram for AMR measurement of the DW (left) and statistics of depinning on the right.*

Although there are plenty studies on pinning and depinning of a DW in notches, they are usually done in triangular or square notches and other shapes have not been explored. There are also very few stochastic studies. Most importantly, when the depinning is achieved by an electrical current, it is very difficult to know how much the local heating is affecting the process. It is usually assumed that the depinning current density is uniform through the DW in the notch, but for instance, in a triangular notch the peak holds higher current density and it can likely trigger the depinning of the DW because of local heating. In order to explore this effect we are currently studying the depinning magnetic field for different notches and we will compare the results with the depinning current density and COMSOL simulations of the current distribution around the notch. This comparison should give us some inside in the true spin transfer contribution in the depinning process.

Additionally our group is trying to measure the speed of DW in nanowires by anisotropic magnetoresistance. These measurements are challenging and require high frequency techniques. To date,

these measurements have been performed only at IBM and they require averaging thousands of resistance measurements with a high frequency oscilloscope. In the measuring set up, a current pulse creates the domain wall that is pushed by the field towards the wire. While the domain wall is in the wire, there is a small (but measurable) change in the resistance of the wire, which is measured (through thousands of averages) in the digital oscilloscope.

Of course, these measurements can only work if the domain wall is always created with the current pulse. We are currently performing probability maps were we can measure how easily a domain wall is created for a given current pulse and a given field. In figure 5, there is an example of one of these maps for a current pulse of 100 ns. The current density flowing through the current line is $1.94 \cdot 10^7$ A/cm^2 per volt of the pulse. As one can see in the figure, the domain wall can be created even for zero magnetic field and also, the probability is not necessarily higher for higher fields. This does not necessarily mean that the domain wall is not created at large fields, because these plot actually reflect the probability of "seeing" the domain wall (as it could be created but not pinned in the notch, in which case it would not be detected.

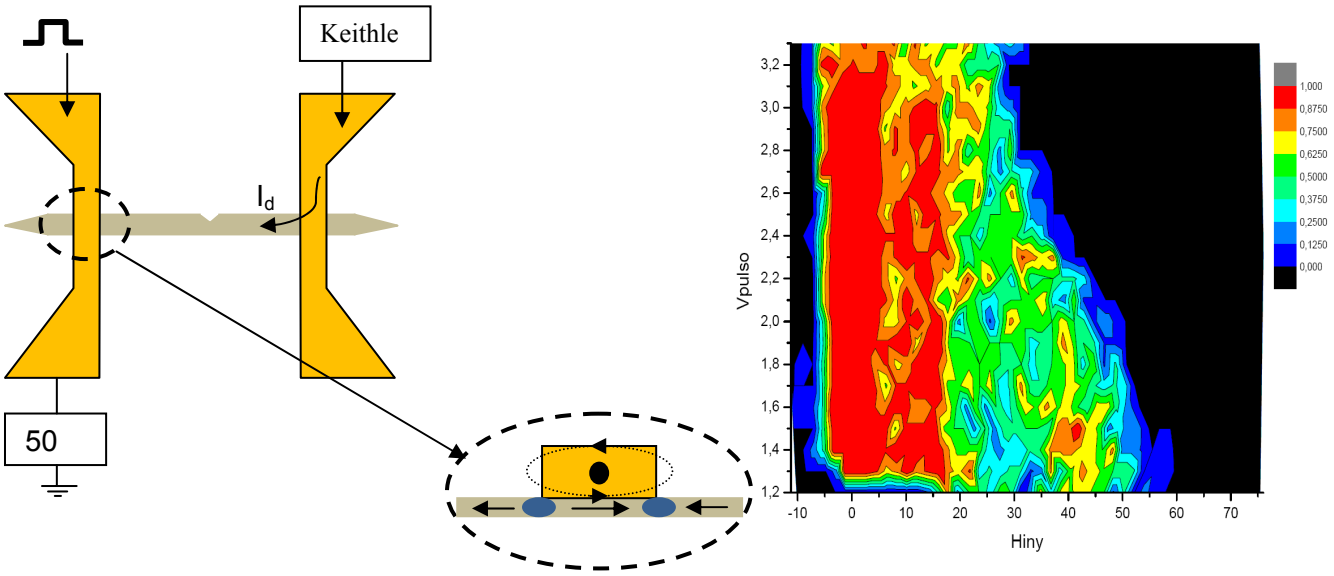

***Figure 5**. Set-up for the measurement of the probability of creating (and pinning) a domain wall in a magnetic nanowire (permalloy). On the left the set-up with a close up of the area where the domain wall is created and on the right the actual probability (color coded) for each pulse voltage and injection field.*

References

[1] A.T. Hindmarch and B.J. Hickey, Phys. Rev. Lett. **91**, 116601 (2003).
[2] C. Bellouard, H.D. Rapp, B. George, S. Mangin, G. Marchal and J.C. Ousset, Phys. Rev. B **53**, 5082 (1996).
[3] F.E. Stanley, M. Perez, C.H. Marrows, S. Langridge and B.J. Hickey, Europhys. Lett, **49**, 528 (2000).
[4] J.G. Zhu and X. Zhu, IEEE Trans. Magn. **40**, 182 (2004).
[5] G. Woltersdorf et al. Phys. Rev. Lett. **102**, 257602 (2009).
[6] Stuart S. P. Parkin, *et al.* Science, **320**, 190 (2008).

7 RESEARCH PROJECTS

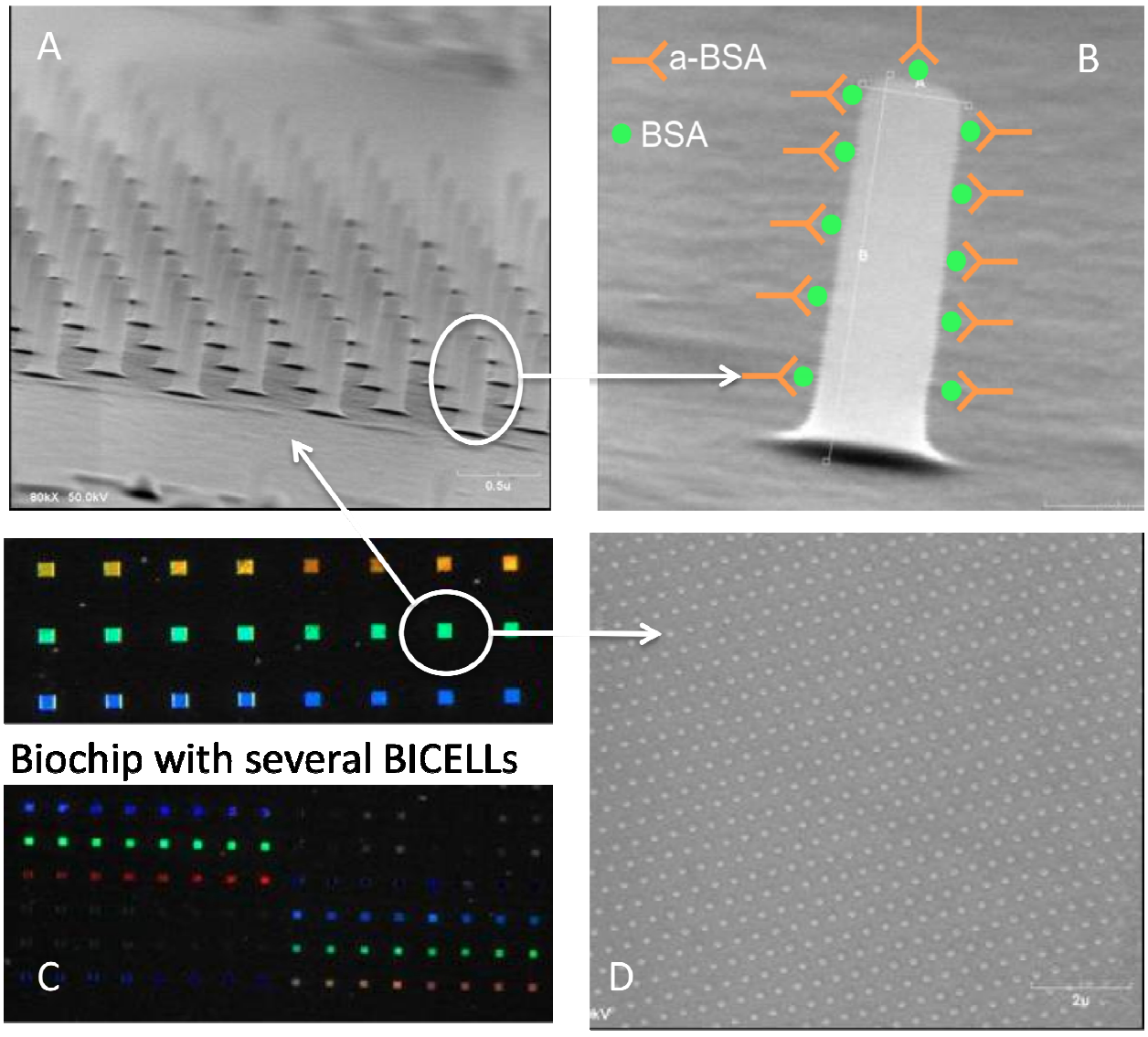

A) SEM micrograph of a SU8-based BICELL, B) SEM micrograph of one single nano-pillar and a schematic representation of BSA immobilization and aBSA recognition. C), Optical image of a biochip with an array of BICELLs, D) SU8-BICELL top-view SEM micrograph.

7.1 International Public Funding

Europe:

"Key Organisation for Research on Integrated Circuits in GaN Technology (KORRIGAN)"
European Understandings for Research Organisation, European Defense Agency
Contract nº 04/102.052/032 (2005-2009)
Principal Investigator: Elías Muñoz

"Ultrahigh sensitivity Slot-wAveguide BIOsensor on a highly integrated chip for simultanous diagnosis of multiple diseases (SABIO)"
European Comission STREP, Contract nº 026554 (2006-2009)
Principal Investigator: Carlos Angulo

"Designing dyes and pigments for inkjet technology breakthrough (DEDYPINK)"
European Academy of Sciences (EAS) (2006-2008)
Principal Investigator: Manuel Laso

"High quality Material and intrinsic Properties of InN and In rich Nitride Alloys (The Rainbow ITN"
European Comission: 213238- PITN-GA-2008-213238 (2008-2012)
Principal Investigator: Miguel Ángel Sánchez

"Directed Assembly of Polymeric Materials Nanofabrication (DAPOMAN)"
DG Research: PIIF-GA-2009-236797 (2009-2010)
Principal Investigator: Manuel Laso

"Smart Nanostructured Semiconductors for Energy-Saving Light Solutions (SMASH)"
European Comission: Código: Nº 228999, FPT-NMP-2008-LARGE 2 (2009-2012)
Principal Investigator: Enrique Calleja

"MBE regrowth of a laterally-biased double quantum well tunable detector"
European Office of Aerospace Research and Development. FA8655-09-1-3047(2009-2010)
Principal Investigator: Álvaro de Guzmán Fernández.

Integrated Actions (travel and stage funding):

"High frequency nanoresonators by MEMS technologies"
HISPANO-ALEMANA (Fraunhofer Institute for Applied Solid State Physics IAF, DE2009-0015 (2010-2011)
Principal Investigator UPM: Fernando Calle, IP Fraunhofer IAF: Volker Cimalla.

7.2 National and Regional Public Funding

"Fabrication of AlGaN/GaN High Mobility Transistors grown on Si(111) and SiC/Si(111) Substrates"
CSIC-CNM-BARNA, Acuerdo Hispano-Canadiense NRC-SEPOCYT (2005-2007)
Principal Investigator: Elías Muñoz (ISOM)

"Desarrollo de láseres horizontales y de cavidad vertical para la banda de 1.35 a 1.55 micras basados en pozos cuánticos de GaInNAs/GaAs"
Min. Educación y Ciencia, TEC2005-03694/MIC (2005-2008)
Principal Investigator: Adrián Hierro

"Nanoestructuras de Semiconductores como Componentes para la Información Cuántica (NANIC)"
Min. Educación y Ciencia, Acción Estratégica en Nanotecnología. NAN2004-09109-C04-02 (2005-2008)
Principal Investigator: Enrique Calleja

"(Bio)sensores químicos avanzados para medida in-situ de la calidad de aguas basados en elementos específicos de reconocimiento y lectura "multifuncional integrada"
Com. de Madrid- Univ. Politécnica de Madrid. Ref: S-0505/AMB/0374 (2005-2009)
Principal Investigator: Guillermo Orellana / Miguel Angel Sánchez (ISOM-UPM)

"Fabricación de substratos nanoestructurados de SiO2 para crecimiento epitaxial de emisores eficientes de Luz Blanca con Nitruros del Grupo-III"
Min. Educación y Ciencia, PROFIT- 2006. FIT-330100-2006-139 (2006-2007)
Principal Investigator: Enrique Calleja

"Ayuda financiera para la mejora de las Infraestructuras Científicas y Tecnológicas Singulares y para el acceso a las mismas"
Ministerio de Educación y Ciencia (ICTS-2006-01) (2006-2008)
Principal Investigator: Pedro Sánchez

"Nanoestructuras de semiconductores como componentes para la información cuántica (NANOCOMIC)"
Com. de Madrid (IV PRICYT-) Univ. Politécnica de Madrid. Ref: S-0505/ESP-0200 (2006-2009)
Principal Investigator: Enrique Calleja

"Tecnologías de Información Basadas en Optica Cuántica"
Ministerio de Educacion y Ciencia. Programa Consolider-Ingenio CSD2006-19 (2006-2011).
Principal Investigator: Jürgen Eschner. Fundación Privada Instituto de Ciencias Fotónicas.
Principal Investigator ISOM-UPM: Enrique Calleja

"Fabricación de substratos nanoestructurados de SiO2 para crecimiento Epitaxial de emisores eficientes de Luz Blanca con Nitruros del Grupo-III"
Ministerio de Industria, Turismo y Comercio, PROFIT- 2007. FIT-330100-2007-134, (2007-2008).
Principal Investigator: Enrique Calleja

"Demostrador de un conmutador Microelectromecánico operando en altas frecuencia"
Ministerio de Industria, Turismo y Comercio, PROFIT- 2007. FIT-330100-2007-66 (2007-2008)
Principal Investigator: Fernando Calle

"Microscopio de barrido de capacidad para caracterización de nanoestructuras"
Min. Educación y Ciencia, UNPM06-33-037 (2007)
Principal Investigator: Miguel Ángel Sánchez

"Sistema de caracterización óptica avanzada multifuncional"
Min. Educación y Ciencia, UNPM06-33-038 (2007-2007)
Principal Investigator: Miguel Ángel Sánchez

"Ultrahigh sensitivity Solot-wAveguide BIOsensor on a highly integrated chip for simultaneous diagnosis of multiple diseases (SABIO)"
Min. Educación y Ciencia, EC-2006-28117-E (2007-2007)
Principal Investigator: Carlos Angulo

"Desarrollo matriz de detectores multiespectral en el infrarrojo 3-5 micras"
Ministerio de Industria, Turismo y Comercio FIT-330101-2007-11 (2007-2009)
Principal Investigator: Álvaro de Guzmán Fernández

"I+D de Micro y Nanosistemas basados en Nitruros III-V para comunicaciones y sensores (MINANI)"
Min. Educación y Ciencia, TEC-2007-67065/MIC (2007-2010)
Principal Investigator: Fernando Calle

"Obtención y caracterización de nanoestructuras magnéticas obtenidas por pulverización catódica y nanolitografía por haz de electrones"
Ministerio de Educación y Ciencia (MAT2007-65965-C02-01) (2007-2010)
Principal Investigator: Marco Maicas

"Programa de investigación en ingeniería biomédica. MADRID, IB-CM"
Com. de Madrid -Univ. Politécnica Madrid, Ref. S-SAL ORDEN 6892/2006 (2007-2011)
Coordinator: D. Francisco del Pozo Guerrero, Principal Investigator UPM: Claudio Aroca

"Ayudas financieras para la mejora de las infraestructuras científicas y tecnológicas singulares y para el acceso a las mismas"
Ministerio de Ciencia e Innovación. Ref: ICTS-2008-29 (2008-2009)
Principal Investigator: Enrique Calleja

"Multiscale Modeling of Nanostructured Interfaces for Biological Sensors (MNIBS)"
Min. Educación y Ciencia, MAT2005-25569-E/ (2006-2008)
Principal Investigator: Manuel Laso

"Ayudas para apoyar las líneas de I+D en el programa de creación y consolidación de grupos de investigación de la Universidad Politécnica de Madrid"
Com. de Madrid – Univ. Politécnica Madrid. Ref. CCG07-UPM/000-3220 (2007-2008)
Principal Investigator: Elías Muñoz

"Obtención de nanopartículas magnéticas por pulverización catódica"
Min. Educación y Ciencia, MAT2007-65965-C02-01/ (2007-2010)
Principal Investigator: Marco Maicas

"Ayudas para apoyar las infraestructuras de laboratorios de investigación en virtud del programa de infraestructura y gestión de calidad del contrato-programa I+D entre la CAM y la UPM"
Com. de Madrid -Univ. Politécnica Madrid (2007-2007)
Principal Investigator: Marco Maicas

"Ayudas para apoyar las líneas de I+D en el programa de creación y consolidación de grupos de investigación de la UPM (Resolución de 3 de julio de 2008)"
Comunidad de Madrid-Univ. Politécnica de Madrid. Ref: CCG07-UPM/00-03 (2007-2009)
Principal Investigator: Elías Muñoz

"Ayudas para apoyar las líneas de I+D en el programa de creación y consolidación de grupos de investigación de la UPM"
Comunidad de Madrid – Univ. Politécnica de Madrid. Ref: CCG07-UPM/000-3316, (2007-2009)
Principal Investigator: Pedro Sánchez/Claudio Aroca

"Síntesis y caracterización de nanopartículas magnéticas funcionarizadas y estables en medios biológicos (NANOMAG)"
Ministerio de Sanidad y Consumo, Ref: CIBER-BBN (2008-2009)
Coordinator: D. Francisco del Pozo Guerrero/ Claudio Aroca (ISOM-UPM)

"Estudio de la transferencia de espín en paredes y nanosistemas magnéticos. Aplicación a sensores y memorias magnéticas alternativas (MAGWALLMEN)"
Min. Educación y Ciencia, MAT2008-02770/NAN (2008-2011)
Principal Investigator: José Luis Prieto

"Desarrollo de Micro y Nanocavidades incluyendo regiones activas de Puntos Cuánticos de Nitruros-III: aplicaciones a emisores de luz en azul y UV (QUADONIC)"
Min. Educación y Ciencia, MAT2008-04815 (2008-2011)
Principal Investigator: Enrique Calleja

"Desarrollo de estructuras nano-opto-fluídicas (BIOPSIA-3)"
Min. Educación y Ciencia, TEC2008-06574-C03-03/TEC (2008-2011)
Principal Investigator: Carlos Angulo

"Nano- y microdispositivos basados en ZnO para la detección de H2 y UV (THINKOXIDE)"
Min. Educación y Ciencia, TEC2008-04718 (2008-2011)
Principal Investigator: Adrián Hierro

"Ayuda para apoyar las infraestructuras de laboratorios del contrato Programa con la Comunidad de Madrid, para el Instituto de Sistemas Optoelectrónicos y Microtecnología"
Com. de Madrid – Univ. Politécnica Madrid. Ref: 200700051799 (2008-2008)
Principal Investigator: Carlos Angulo

"Células solares de heterounión InGaN y alta eficiencia crecidas por MBE"
Ministerio de Ciencia e Innovación. PLE2009-0023 (2009-2012)
Principal Investigator: Enrique Calleja

"Nanodispositivos eficientes de luz clásica y cuántica (Q&CLight)"
Com. de Madrid – Univ. Politécnica Madrid. Ref: S-0505/ESP-0200 (2009-2014)
Principal Investigator: Luis Viña / Enrique Calleja (ISOM-UPM)

"Microsistemas de control térmico en aplicaciones industriales (T-MEMS)"
Com. de Madrid – Univ. Politécnica Madrid. Ref: S-2009/DPI-1572 (2009-2014)
Principal Investigator: Ángel Velázquez/ Gonzalo Fuentes (ISOM-UPM)

"Advanced Wide Band Gap Semiconductor Devices for Rational Use of Energy", RUE (Dispositivos Avanzados de Gap Ancho para el uso racional de la energía)".
Ministerio de Ciencia e Innovación: CSD2009-00046 (2009-2014)
Principal Investigator: Fernando Calle

7.3 Funding from Companies and Institutions

"Asistencia técnica para el control y caracterización de las matrices tricolor del demostrador SIRIO"
CIDA- Univ. Politécnica Madrid, Ref: Coincidente – SIRIO DN8644 (2006-2007)
Principal Investigator: Álvaro de Guzmán Fernández

"Asistencia Técnica: Desarrollo de un conmutador microelectromecánico operando en altas frecuencias"
INDRA-CIDA- Univ. Politécnica de Madrid, Ref: Coincidente DN8644 (2006-2007)
Principal Investigator: Fernando Calle

"Asistencia Técnica: Depósito y caracterización de capa antidifusora sobre acero CENIT-CETICA"
ACCIONA ENERGÍA SOLAR- Univ. Politécnica de Madrid. Ref: P080920B883 (2008-2009)
Principal Investigator: Fernando Calle

"Asistencia Técnica: Estudio de la degradación en amplificadores con MMIC con PHEMT de GaAs"
ISOM-INDRA SISTEMAS SA.-Univ. Politécnica de Madrid. Ref: P090920B152, (2009-2009)
Principal Investigator: Fernando Calle

"Contrato con la Fábrica Nacional de Moneda y Timbre"
Real Fábrica de Moneda y Timbre- Univ. Politécnica de Madrid. Ref: P080920B659
(2008-2009)
Principal Investigator: José Luis Prieto

"Estudio y modelización del comportamiento de los campos magnéticos en una subestación eléctrica"
Metro de Madrid- Univ. Politécnica de Madrid, Ref: P08 0920B1116 (2008)
Principal Investigator: Marco César Maicas

"Estudio del comportamiento de los campos magnéticos en la subestacion eléctrica de Sainz de Baranda"
Metro de Madrid-Univ. Politécnica de Madrid, Ref: P090920B466 (2009)
Principal Investigator: Marco César Maicas

"Realización de Antenas Ópticas"
Departamento de Óptica de la Univ. Complutense de Madrid-Univ. Politécnica de Madrid
Ref: P090920B153 (2009)
Principal Investigator: José Luis Prieto

8 DISEMINATION OF THE SCIENTIFIC ACTIVITY

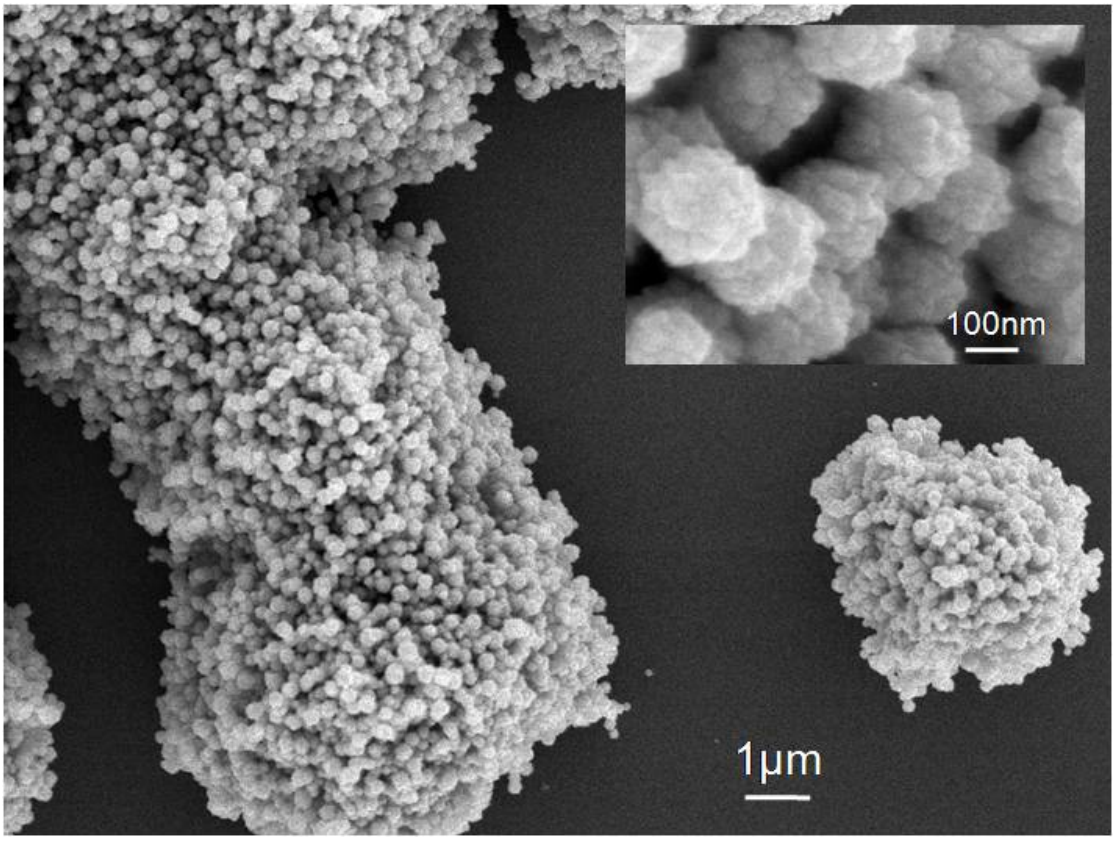

Scanning Electron Microscope of conglomerates of magnetic Ni nanoparticles deposited by Sputtering. This deposition technique allows the deposition of enough material for biological applications and allows the control of the size and the composition. ISOM is currently working on medical applications of magnetic nanoparticles.

8.1 Papers in Scientific Journals and Books

2007

C.A. BARRIOS, B. SÁNCHEZ, K.B. GYLFASON, A. GRIOL, H. SOHLSTRÖM, M. HOLGADO, R. CASQUEL
"Demonstration of slot-waveguide structures on silicon nitride/silicon oxide platform"
Optics Express, 15, 11, 6846 (2007)

C.A. BARRIOS, K.B. GYLFASON, B. SÁNCHEZ, A. GRIOL, H. SOHLSTRÖM, M. HOLGADO, R. CASQUEL
"Slot-waveguide biochemical sensor"
Optics Letters, 32, 21,3080 (2007)

Z. BOUGRIOUA, P. GIBART, E. CALLEJA, U. JAHN, A. TRAMPERT, J. RISTIC, M. UTRERA, G. NATAF
"Growth of free-standing GaN using Pillar-Epitaxial Lateral Overgrowth from GaN nanocolumns"
Journal of Crystal Growth, 309, 113 (2007)

E. CALLEJA, J. GRANDAL, M.A. SÁNCHEZ-GARCÍA, M. NIEBELSCHÜTZ, V. CIMALLA, O. AMBACHER
"Evidence of electron accumulation at non-polar surfaces of InN nanocolumns"
Applied Physics Letters, 90, 262110 (2007)

E. CALLEJA, J. RISTIĆ, S. FERNÁNDEZ-GARRIDO, L. CERUTTI, M. A. SÁNCHEZ-GARCÍA, J. GRANDAL, A. TRAMPERT, U. JAHN, G. SANCHEZ, A. GRIOL, B. SANCHEZ
"Growth, morphology and structural properties of group-III-nitride nanocolumns and nanodisks"
Physica Status Solidi (b), 244, 2816 (2007)

J.M. CALLEJA, S. LAZIĆ, J. SANCHEZ-PÁRAMO, F. AGULLÓ-RUEDA, L. CERUTTI, J. RISTIĆ, S. FERNÁNDEZ-GARRIDO, M.A. SÁNCHEZ-GARCIA, J. GRANDAL, E. CALLEJA, A. TRAMPERT, U. JAHN
"Inelastic light scattering spectroscopy of semiconductor nitride nanocolumns"
Physica Status Solidi (b), 244, 2838 (2007)

F. CHINESTA, A. AMMAR, A. FALCÓ, M. LASO
"On the reduction of stochastic kinetic theory models of complex fluids"
Modelling and Simulation in Materials Science and Engineering, 15, 639 (2007)

D. CIUDAD, J.L.PRIETO, I. LUCAS, C. AROCA, P. SÁNCHEZ
"Optimization of magnetic properties of electrodeposited CoP for sensor applications"
Journal Applied Physics, 101, 043907-1 (2007)

R. CUERDO, J. PEDRÓS, A. NAVARRO, A.F. BRAÑA, J.L. PAU, E. MUÑOZ, F. CALLE
"High temperature assessment of nitride-based devices"
Journal of Materials Science: Materials in Electronics,19,189 (2007)

W. EERENSTEIN, F.D. MORRISON, F. SHER, J.L. PRIETO, J.P. ATTFIELD, J.F. SCOTT, N.D. MATHUR
"Experimental difficulties and artefacts in multiferroic and magnetoelectric thin films of BiFeO3, Bi0.6Tb0.3La0.1FeO3 and BiMnO3"
Philosophical Magazine Letters, 87, 3-4, 249 (2007)

W. EERENSTEIN, M. WIORA, J.L. PRIETO, J.F. SCOTT, N.D. MATHUR
"Giant sharp and persistent converse magnetoelectric effects in multiferroic epitaxial heterostructures".
Nature Materials, 6, 347 (2007)

S. FERNÁNDEZ-GARRIDO, E. CALLEJA, A. REDONDO-CUBERO, R. GAGO, J. PEREIRO, F. GONZÁLEZ-POSADA, E. MUÑOZ
"Properties and growth by Plasma Assisted Molecular Beam Epitaxy of Quaternary III-nitrides"
Nitrides and dilute nitrides: Growth, physics and devices, editors: Javier Miguel Sánchez-Transworld Research Network (2007)

S. GHOSH, C. RIVERA, J. L. PAU, E. MUÑOZ, O. BRANDT, H.T. GRAHN
"Very narrow-band ultraviolet photodetection based on strained M-plane GaN films"
Applied Physics Letters, 90, 091110 (2007)

M. GONZÁLEZ-GUERRERO, J.L PRIETO, P. SÁNCHEZ, C. AROCA
"Influence of the deposition-induced stress on the magnetic properties of sputtered magnetostrictive amorphous (Fe80Co20)80B20"
Journal of Applied Physics, 102, 123903 (2007)

M. GONZÁLEZ-GUERRERO, J.L. PRIETO, D. CIUDAD, P. SÁNCHEZ, C. AROCA
"Engineering the magnetic properties of amorphous (Fe80Co20)80B20 with multilayers of variable anisotropy direction"
Applied Physics Letters, 90, 162501-1 (2007)

F. GONZÁLEZ-POSADA, J.A. BARDWELL, S. MOISA, S. HAFFOUZ , H. TANG, A.F. BRAÑA, E. MUÑOZ
"Surface cleaning and preparation in AlGaN/GaN-based HEMT processing as assessed by X-ray photoelectron spectroscopy"
Applied Surface Science, 53, 14, 6185 (2007)

J. GRANDAL, M.A. SANCHEZ-GARCIA, E. CALLEJA
"Characterization of In-polar indium nitride layers grown by molecular beam epitaxy on Si (111) substrates"
Nitrides and dilute nitrides: Growth, Characterization and devices, Research SignPost, editor: Javier Miguel Sánchez, ISBN: 978-81-7895-250-5 (2007)

J. GRANDAL, M.A. SANCHEZ-GARCIA , E. CALLEJA, E. LUNA, A. TRAMPERT
"Accommodation mechanism of InN nanocolumns grown on Si (111) substrates by molecular beam epitaxy"
Applied Physics Letters, 91, 021902 (2007)

A. HIERRO, J.M. ULLOA, J. MIGUEL-SÁNCHEZ, A. GUZMÁN, A. TRAMPERT, E. TOURNIE
"Photo- and Electro-luminescence from GaInAsN/GaAs single quantum wells and light emitting diodes"
Nitrides and dilute nitrides: Growth, Characterization and devices, Research SignPost, editor: Javier Miguel Sánchez, ISBN: 978-81-7895-250-5 (2007)

U. JAHN, J. RISTIC, E.CALLEJA
"Cathodoluminescence of GaN/(Al,Ga)N nanocolumns containing quantum disks"
Applied Physics Letters, 90, 161117 (2007)

M.A. KHADERBAD, S. DHAR, L. PÉREZ, K.H. PLOOG, A. MELNIKOV, A.D. WIECK
"Effect of annealing on the magnetic properties of Gd focused ion beam implanted GaN"
Applied Physics Letters, 91, 072514 (2007)

G. KOBLMÜLLER, J.S. SPECK , S. FERNANDEZ–GARRIDO, E. CALLEJA
"In situ investigation of growth modes during plasma–assisted molecular beam epitaxy of (0001) GaN"
Applied Physics Letters, 91, 161904 (2007)

G. KOBLMÜLLER, F. WU, T. MATES, J.S. SPECK, S. FERNANDEZ-GARRIDO, E. CALLEJA
"High electron mobility GaN grown under N–rich conditions by plasma–assisted molecular beam epitaxy"
Applied Physics Letters, 91, 221905 (2007)

S. LAZIĆ, E. GALLARDO, J.M. CALLEJA, F. AGULLO-RUEDA, J. GRANDAL, M.A. SANCHEZ-GARCIA, E. CALLEJA, E. LUNA, A. TRAMPERT
"Phonon-plasmon coupling in electron surface accumulation layers in InN nanocolumns"
Physical Review B, 76, 205319 (2007)

I. LUCAS, L.PEREZ, M.PLAZA, O.DE ABRIL, M.C.SANCHEZ
"Pinning field and coercivity in CoP alloys"
Journal of Magnetism and Magnetic Materials 316, 462 (2007)

J. MIGUEL-SÁNCHEZ, A. GUZMÁN, U. JAHN, A. TRAMPERT, J. M. ULLOA, E. MUÑOZ, A. HIERRO
"Role of ionized nitrogen species in the optical and structural properties of GaInNAs/GaAs quantum wells grown by plasma-assisted molecular beam epitax"
Journal of Applied Physics, 101,1035261 (2007)

E. MUÑOZ
"(Al,In,Ga,Al)N- based photodetectors. Some materials issues"
Physica Status Solidi (b), 244, 2683 (2007)

A. NAVARRO, C. RIVERA, R. CUERDO, J.L. PAU, J. PEREIRO, E. MUÑOZ
"Low frequency noise in InGaN/GaN MQW-based photodetector structures"
Physica Status Solidi (a), 204, 262 (2007)

M. NIEBELSCHÜTZ, V. CIMALLA, O. AMBACHER, T. MACHLEIDT, K.H. FRANKE, J. RISTIC, J. GRANDAL, M.A. SÁNCHEZ-GARCÍA, E. CALLEJA
"Electrical characterization of Group III-Nitride nanocolumns with Scanning Force Microscopy"
Modern Research and Educational Topics in Microscopy, Eds. A. Méndez-Vilas, J. Díaz. Formatex, 560-567 (2007)

F. OMNES, E. MONROY, E. MUÑOZ, J.L. REVERCHON
"Wide bandgap UV photodetectos: a short review of devices and applications"
Proceedings Spie The International society for optical engineering, 6473, 64730E (2007)

L. OUATTARA, J. M. ULLOA, A. MIKKELSEN, E. LUNDGREN, P. M. KOENRAAD, M. BORGSTRÖM, L. SAMUELSON, W. SEIFERT
"Correlation lengths in stacked quantum dot systems: Experiment and Theory"
Nanotechnology, 18,145403 (2007)

D. PASTOR, J. IBAÑEZ, R.CUSCO, L. ARTUS, G. GONZALEZ-DIAZ, E. CALLEJA
"Crystal damage assessment of Be+-implanted GaN by UV Raman scattering"
Semiconductor Sci. & Technolology, 22, 70 (2007)

J.L. PAU, R. MCCLINTOCK, K. MINDER, C. BAYRAM, P. KUNG, M. RAZEGUI, E. MUÑOZ, D. SILVERSMITH
"Geiger-mode operation of back-illuminated GaN avalanche photodiodes"
Applied Physics Letters, 91, 041104 (2007)

J. PEDRÓS, Y. TAKAGAKI, T. IVE, M. RAMSTEINER, O. BRANDT, U. JAHN, K.H. PLOOG, F. CALLE
"Exciton impact-ionization dynamics modulated by surface acoustic waves in GaN"
Physical Review B 75, 115305 (2007)

J. PEREIRO, J.L. PAU, C. RIVERA, A. NAVARRO, E. MUÑOZ, R. CZERNECKI, G. TARGOWSKI, P. PRYSTAWKO, M. KRYSKO, M. LESZCZYNSKI, T. SUSKI
"InGaN growth applied to the fabrication of photodetector devices"
Nitrides and dilute nitrides: Growth, physics and devices, J.Miguel-Sanchez editor, Research Signpost, ISBN 978-81-7895-250-5, 265-288 (2007)

L. PÉREZ, J.L. PRIETO
"B*reve historia de la magnetorresistencia gigante: de Fert y Grünberg a la Espintrónica actual"*.
Revista Española de Física 21, 4, 61 (2007)

M. PLAZA, L. PEREZ, M.C. SANCHEZ
"Reducing the losses in sintered permalloy by addition of ferrite"
The Journal of Magnetism and Magnetic Materials, 309, 207 (2007)

J.L. PRIETO.
"Hopes for growth in Spain".
Nature 449, 1086 (2007)

R. RANCHAL, C. AROCA, M. MAICAS, E. LOPEZ.
"Temperature dependence of the magnetic and electrical properties of Permalloy/gadolinium/Permalloy thin films"
Journal of Applied Physics 102, 053904-1 (2007)

C. RIVERA, U. JAHN, T. FLISSIKOWSKI, J.L. PAU, E. MUÑOZ, H.T. GRAHN.
"Strain-confinement mechanism in mesoscopic quantum disks based on piezoelectric materials"
Physical Review B (selected by the Virtual Journal of Nanoscale Science & Technology), 75, 0453163 (2007)

C.. RIVERA, P. MISRA, J. L. PAU, E. MUÑOZ, O. BRANDT, H.T. GRAHN, K.H. PLOOG
"Electrical and optical characterization of M-plane GaN films grown on LiAlO2 substrates"
Physica Status Solidi (c), 4, 2548 (2007)

C. RIVERA, P. MISRA, J. L. PAU, E. MUÑOZ, O. BRANDT, H.T. GRAHN, K. H.PLOOG.
"Intrinsic photoluminescence of M-plane GaN films on LiAlO2 substrates"
Journal of Applied Physics, 101, 053527 (2007)

C. RIVERA, P. MISRA, J.L. PAU, E. MUÑOZ, O. BRANDT, H.T. GRAHN, K.H. PLOOG
"M-plane GaN-based dichroic photodetectors"
Physica Status Solidi (c), 4, 86 (2007)

C. RIVERA, E. MUÑOZ, O. GRANDT, H.T. GRAHN
"Detection of the optical polarization angle with bandplass characteristics based on M-plane GaN photodetectors"
Applied Physics Letters 91, 203514 (2007)

E. SILLERO, D. LÓPEZ-ROMERO, F. CALLE, M. EICKHOFF, J. F. CARLIN, N. GRANDJEAN, M. ILEGEMS
"Selective etching of AlInN/GaN heterostructures for MEMS technology"
Microelectronic Engineering 84, 1152 (2007)

J.M. ULLOA, C. ÇELEBI, P.M. KOENRAAD, A. SIMON, E. GAPIHAN, A. LETOUBLON, N. BERTRU, I. DROUZAS, D.J. MOWBRAY, M.J. STEER, M. HOPKINSON
"Atomic scale study of the impact of the strain and composition of the capping layer on the formation of InAs quantum dots"
Journal of Applied Physics, 101, 081707 (2007)

J. M. ULLOA, I. W. D. DROUZAS, P.M. KOENRAAD, D.J. MOWBRAY, M.J. STEER, H. Y. LIU, M. HOPKINSON
"Suppression of InAs/GaAs quantum dot decomposition by the incorporation of a GaAsSb capping layer"
Applied Applied Physics Letters 90, 213105 (2007)

J.M. ULLOA, P.M. KOENRAAD, E. GAPIHAN, A. LÉTOUBLON, N. BERTRU
"Double capping of MBE grown InAs/InP quantum dots studied by cross-sectional scanning tunneling microscopy"
Applied Physics Letters, 91, 073106-073109 (2007)

A. WIERTS, J.M. ULLOA, C. ÇELEBI, P.M. KOENRAAD, H. BOUKARI, L. MAINGAULT, R. ANDRÉ, H. MARIETTE
"Cross-sectional scanning tunnelling microscopy study on II-VI multilayer structures"
Applied Physics Letters, 91, 161907 (2007)

2008

A. ARRANZ, C. PALACIO, D. GARCÍA-FRESNADILLO, G. ORELLANA, A. NAVARRO, E. MUÑOZ
"Influence of Surface Hydroxylation on 3-Aminopropyltriethoxysilane Growth Mode during Chemical Functionalization of GaN Surfaces: An Angle-Resolved X-ray Photoelectron Spectroscopy Study"
Langmuir, 24, 8667 (2008).

L.R. BAILEY, T.D. VEAL, P.D.C. KING, C.F. McCONVILLE, J. PEREIRO, J. GRANDAL, M.A. SÁNCHEZ-GARCÍA, E. MUÑOZ, E. CALLEJA
"Band bending at In-rich InGaN surfaces"
Journal of Applied Physics 104, 113716 (2008)

C.A. BARRIOS, M.J. BAÑULS, V. GONZALEZ-PEDRO, K.B. GYLFASON, B. SÁNCHEZ, A. GRIOL, A. MAQUIEIRA, H. SOHLSTRÖM, M. HOLGADO, R. CASQUEL
"Label-free optical biosensing with slot-waveguides"
Optics Letters, 33, 7, 708 (2008)

C.A. BARRIOS, M. HOLGADO, O. GUARNEROS, B. SÁNCHEZ, K. GYLFASON, R. CASQUEL, H. SOHLSTRÖM
"Reconfiguration of microring resonators by liquid adhesion"
Applied Physics Letters, 93, 20, 203114 (2008)

K. BEJKA, P.R. EDWARDS, R. W. MARTIN, S. FERNÁNDEZ-GARRIDO, E. CALLEJA
"Composition and luminescence properties of AlInGaN layers grown by plasma-assisted molecular beam epitaxy"
Journal of Applied Physics 104, 073537 (2008)

R.CASQUEL, M. HOLGADO, A. LAVIN, C.A. BARRIOS, C. MOLPECERES, M. MORALES, J.L. OCAÑA.
"Vertical resonant microcavities based on pillars analyzed by beam profile ellipsometry and reflectometry"
Eurosensors XII,1577-1580, ISBN: 978-3-00-025217 (2008)

D. CIUDAD RIO-PEREZ, P.C. ARRIBAS, C.AROCA, P. SÁNCHEZ
"Testing Thick Magnetic Shielding Effect on a New Low Frequency RFIDs System"
IEEE Transactions on Antennas and Propagation 8, 56, 12, 3838 (2008)

F. COLDREN, K. FOTEINOPOULOU, D. CARROLL, M. LASO
"Modeling the effect of cell-associated polymeric fluid layers on force spectroscopy measurements. Part I: model development"
Langmuir, 24, 9575 (2008)

F. COLDREN, K. FOTEINOPOULOU, W. VERBEETEN, D. CARROLL, M. LASO
"Modeling the effect of cell-associated polymeric fluid layers on force spectroscopy measurements. Part II: model development"
Langmuir, 24, 9588 (2008)

R. CUERDO, F. CALLE, A.F. BRAÑA, Y. CORDIER, M. AZIZE, N. BARON, S. CHENOT, E. MUÑOZ
"High temperature behavior of GaN HEMT devices on Si(111) and sapphire substrates"
Physica Status Solidi (c), 5, 1971 (2008)

R. CUERDO, J. PEDRÓS, A. NAVARRO, A.F. BRAÑA, J.L. PAU, E. MUÑOZ, F. CALLE
"High temperature assessment of nitride-based devices"
Journal of Materials Science – Materials in Electronics 19, 189 (2008)

R. CUERDO, Y. PEI, F. RECHT, N. FICHTENBAUM, S. KELLER, S. P. DENBAARS, F. CALLE, U.K. MISHRA
"Temperature-dependent High-Frequency Performance of Deep Submicron Ion-Implanted AlGaN/GaN HEMTs"
Physica Status Solidi (c), 5, 2994 (2008)

S. FERNÁNDEZ-GARRIDO, E. CALLEJA, A. REDONDO-CUBERO, R. GAGO, J. PEREIRO, F. GONZÁLEZ-POSADA, E. MUÑOZ
"Properties and growth by Plasma Assisted Molecular Beam Epitaxy of Quaternary III-nitrides"
Nitrides and dilute nitrides: Growth, physics and devices, editors: Javier Miguel Sánchez-Transworld Research Network (2008)

S. FERNÁNDEZ-GARRIDO, Z. GACEVIC, E. CALLEJA
"A comprehensive diagram to grow InAlN alloys by plasma-assisted molecular beam epitaxy"
Applied Physics Letters 93, 191907 (2008)

S. FERNÁNDEZ-GARRIDO, G. KOBLMÜLLER, E. CALLEJA, J.S. SPECK
"**In-situ GaN decomposition analysis by quadrupole mass spectrometry and reflection high-energy electron diffraction"**
Journal of Applied Physics, 104, 033541 (2008)

S. FERNÁNDEZ-GARRIDO, J. PEREIRO, F. GONZÁLEZ-POSADA, E. MUÑOZ, E. CALLEJA, A. REDONDO-CUBERO, R. GAGO
"Photoluminiscence enhancement in quaternay III-nitrides alloys grown by molecular beam epitaxy with increasing Al content"
Journal of Applied Physics, 103, 4, 046104-1/3 (2008)

S. FERNÁNDEZ-GARRIDO, A. REDONDO-CUBERO, R. GAGO, F. BERTRAM, J. CHRISTEN, E. LUNA, A. TRAMPERT, J. PEREIRO, E. MUÑOZ, E. CALLEJA
"Effect of the growth temperature and the AlN mole fraction on In incorporation and properties of quaternary III-nitride layers grown by molecular beam epitaxy"
Journal of Applied Physics 104, 083510 (2008)

K. FOTEINOPOULOU, N. CH. KARAYIANNIS, M. LASO, M. KRÖGER, M. MANSFIELD
"Universal Scaling, Entanglements, and Knots of Model Chain Molecules"
Physical Review Letters, 101, 265702 (2008)

G. FRANSSEN, AL. GORCZYCA, T. SUSKI, A. KAMINSKA, J. PEREIRO, E. MUÑOZ, E. LLIOPOULOS, A. GEORGAKILAS, S.B. CHE, Y. ISHITANI, A. YOSHIKAWA, N.E. CHRISTENSEN, A. SVANE
"Bowing of the band gap pressure coefficients in InGaN alloys"
Journal of Applied Physics, 103, 033514 (2008)

E. GALLARDO, S. LAZIC, J.M. CALLEJA, J. MIGUEL SÁNCHEZ, M. MONTES, A. HIERRO, R. GARGALLO-CABALLERO, A. GUZMAN, E. MUÑOZ, A.M. TEWELDEBERHAN, S. FAHY
"Local vibration modes and nitrogen incorporation in AlGaAs: N layers"
Physica status solidi (c), 5, 2345 -2348 (2008)

E. GALLARDO, S. LAZIC, J.M. CALLEJA, J. MIGUEL-SÁNCHEZ, M. MONTES, A. HIERRO, R. GARGALLO-CABALLERO, A. GUZMÁN, E. MUÑOZ, A.M. TEWELDEBERHAN, S.FAHY
"Resonant Raman study of local vibrational modes in AlGaAsN layers"
Physica E 40, 2084 (2008)

R. GARGALLO-CABALLERO, J. MIGUEL-SÁNCHEZ, Á.GUZMÁN, A. HIERRO, E. MUÑOZ
"The effect of rapid thermal annealing on the photoluminescence of InAsN/InGaAs dot-in-a-well structures"
Journal of Physics D: Applied Physics, 41, 065413-1 (2008)

R. GARGALLO-CABALLERO, J. MIGUEL-SÁNCHEZ, Á.GUZMÁN, A. HIERRO, E. MUÑOZ
"The effect of the individual species of the N plasma on the characteristics of InAsN quantum dots grown by MBE"
Materials Science and Engineering B 147,118 (2008)

P. GESTOSO, N. KARAYIANNIS
"Molecular simulation of the effect of temperature and architecture on polyenthylene barrier properties"
The Journal of Physical Chemistry B, 5646 (2008)

S. GHOSH, C. RIVERA, J.L. PAU, E. MUÑOZ, O. BRANDT, H.T. GRAHN
"Narrow-band photodetection based on M-plane GaN films"
Physica status solidi (a) 205, 1100 (2008)

J. GRAJAL, F. CALLE, J. PEDRÓS, J.L. MARTÍNEZ-CHACÓN, A. JIMÉNEZ
"AlGaN/GaN-based SAW delay-line oscillators"
Microwave and Optical Technology Letters 50, 2967 (2008)

A. HIERRO, J.M. ULLOA, J. MIGUEL-SÁNCHEZ, A. GUZMÁN, A. TRAMPERT, E. TOURNIÉ
"Photo- and Electro-luminescence from GaInNAs/GaAs single quantum wells and light emitting diodes"
Nitrides and Dilute Nitrides: Growth, Physics and Devices. Editors: Transworld Research, 77-98, *ISBN* 978-81-7895-250-5, (2008)

J. IBAÑEZ, S. HERNÁNDEZ, E. ALARCON-LLADÓ, R. CUSCÓ, L. ARTÚS, S. V. NOVIKOV, C.T. FOXON, E. CALLEJA
"Far-infrared transmission in GaN, AlN and AlGaN thin films grown by molecular beam epitaxy"
Journal of Applied Physics, 104, 033544 (2008)

F. ISHIKAWA, A. GUZMÁN-FERNÁNDEZ, O. BRANDT, A. TRAMPERT, K. H. PLOOG
"Impact of carrier localization on the photoluminescence characteristics of (Ga,In)(N,As) and (Ga,In)(N,As,Sb) quantum wells"
Journal of Applied Physics, 104, 11, 113502 (2008)

C. ISRAEL, L. GRANJA, T.M. CHUANG, L.E. HUESO, D. SÁNCHEZ, J.L. PRIETO, P. LEVY, A. DE LOZANNE, N.D. MATHUR
"Translating reproducible phase-separated texture in manganites into reproducible two-state low-field magnetoresistance: An imaging and transport study".
Physical Review B 78, 054409 (2008)

U. JAHN, E. CALLEJA, J. RISTIC, A. TRAMPERT, C. RIVERA
"Spatially Resolved Luminescence Spectroscopy of Single GaN/(Al,Ga)N Quantum Disks"
Physica status solidi (c), 2164 (2008)

N. KARAYIANNIS, M. LASO
"Monte Carlo Scheme for Generation and Relaxation of Dense and Nearly Jammed Random Structures of Freely Jointed Hard-Sphere Chains"
Macromolecules, 41, 1537 (2008)

N. KARAYIANNIS, M. LASO
"Dense and nearly jammed random packings of freely jointed chains of tangent hard spheres"
Physical Review Letters 100, 5, 050602 (2008)

M. LASO
"Modeling Smart Materials"
Smart Materials, M. Schwartz, editors, CRC Press, 190-197 (2008)

M. LASO, N. KARAYIANNIS
"Flexible chain molecules in the marginal and concentrated regimes: universal static scaling laws and cross-over predictions"
Journal of Chemical Physics, 128, 174901 (2008)

S. LAZIĆ, E. GALLARDO, J.M. CALLEJA, F. AGULLO-RUEDA, J. GRANDAL, M.A. SANCHEZ-GARCIA, E. CALLEJA
"Raman scattering by coupled plasmon-LO phonons in InN nanocolumns"
Physica Status Solidi (c), 5, 6,1562 (2008)

S. LAZIĆ, E. GALLARDO, J.M. CALLEJA, F. AGULLO-RUEDA, J. GRANDAL, M.A. SANCHEZ-GARCIA, E. CALLEJA
"Raman scattering by longitudinal optical phonons in InN nanocolumns grown on Si(111) and Si(001) substrates"
Physica E: Low-Dimensional Systemas & Nanostructures, 40, 2087 (2008)

E. LUNA, A. TRAMPERT, J. MIGUEL-SÁNCHEZ, A. GUZMÁN, K.H. PLOOG
"Vertical composition fluctuations in (Ga,In)(N,As) quantum wells grown on vicinal (1 1 1)B GaAs"
Journal of Physics and Chemistry of Solids, 69, 343 (2008)

M. MAICAS, R. RANCHAL, C. AROCA, P. SÁNCHEZ, E. LÓPEZ
"Magnetic properties of permalloy multilayers with alternating perpendicular anisotropies"
European Physical Journal B 62, 267 (2008)

J. MIGUEL-SÁNCHEZ
"Nitrogen in seminconductors"
Nitrides and dilute nitrides: Growth, physics and devices, J.Miguel-Sanchez editor, Transworld Research Signpost, ISBN 978-81-7895-250-5, 265-288 (2008)

J. MIGUEL-SANCHEZ, A. GUZMAN, A. HIERRO, E. MUÑOZ, U. JAHN, A. TRAMPERT
"Impact of Nitrogen Ion Density on the Optical and Structural Properties of MBE Growh GaInAs/GaAs (100) and (111)B Quantum Wells"
Dilute III-V Nitride Semiconductors and Material Systems Physics and Technology, Series: Springer Series in Materials Science, vol. 105, Editors. Erol, Ayse, ISBSN: 978-3-540-74528-0 (2008)

M. MONTES, A. HIERRO, J. M. ULLOA, A. GUZMAN, B. DAMILANO, M. HUGUES , M. AL KHALFIOUI, J.Y. DUBOZ, J. MASSIES
"Analysis of the characteristic temperatures of (Ga,In)(N,As)/GaAs laser diodes"
Journal of Physics D: Appl. Phys. 41, 155102-1 (2008)

A. NAKAMURA, T. AOSHIMA, T. HAYASHI, S. GANGIL, J. TEMMYO, A. NAVARRO, J. PEREIRO, E. MUÑOZ
"Growth of Nitrogen-Doped MgxZn1−xO for Use in Visible Rejection Photodetectors"
Journal of the Korean Physical Society, 53, 5, 2909 (2008)

M. NIELBELSCHÜTZ, V. CIMALLA, O. AMBACHER, T. MACHLEIDT, K.-H. FRANKE, J. RISTIC, J. GRANDAL, M.A. SANCHEZ-GARCÍA, E.CALLEJA
"Space charged region in GaN and InN nanocolumns investigated by Atomic Force Microscopy"
Physica status solidi (c), 5, 6, 1609 (2008)

R. RANCHAL, C. AROCA, E. LÓPEZ
"Domain walls and exchange-interaction in Permalloy/Gd films"
New Journal of Physics 10,1, 013013 (2008)

A. REDONDO-CUBERO, R. GAGO, F. GONZALEZ-POSADA, U. KREISSIG, M.-A. DI FORTE POISSON, A.F. BRAÑA, E. MUÑOZ
"Aluminium incorporation in AlGaN/GaN heterostructures: a comparative study by ion beam analysis and X-ray diffraction"
Thin Solid Films, 516, 8147 (2008)

A. REDONDO-CUBERO, R. GAGO, M. F. ROMERO, A. JIMÉNEZ, F. GONZÁLEZ-POSADA, A.F. BRAÑA, E. MUÑOZ
"Study of SiNx:Hy passivant layers for AlGaN/GaN high electron mobility transistors"
Physica Status Solidi (c*), 5, 2, 518* (2008)

J. RISTIC, E. CALLEJA, S.FERNÁNDEZ-GARRIDO, L. CERUTTI, A.TRAMPERT, U. JAHN, K.H. PLOOG
"On the mechanisms of spontaneous growth of III-nitride nanocolumns by plasma-assisted molecular beam epitaxy"
Journal Crystal Growth, 310, 4035 (2008)

C. RIVERA
“Photodetectors based on quantum-well structures: theory, properties and novel concepts”
Quantum Wells: Theory, Fabrication and Applications, 1-44. *Nova Science Publishers, Inc. Hauppauge*, NY, Estados Unidos (2008)

C. RIVERA, E. MUÑOZ
"Observation of giant photocurrent gain in highly doped (In,Ga)N/GaN MQW-based photodiodes"
Applied Physics Letters, 233510 (2008)

M.F. ROMERO, A. JIMENEZ, J. MIGUEL-SANCHEZ, A.F. BRAÑA, F. GONZÁLEZ-POSADA, R. CUERDO, F. CALLE, E. MUÑOZ
“Effects of N2 plasma pre-treatment on the SiN Passivation of AlGaN/GaN HEMT"
IEEE Electron Devices Letters, 29, 3, 209 (2008)

M.A. SÁNCHEZ-GARCÍA, M. GARRIDO, M. LOPEZ-VALLEJO, J. GRAJAL
“Implementing FFT-based digital channelized receivers on FPGA platforms”
IEEE Transactions on Aerospace and Electronic Systems, 44, 4, 1567-1585, ISSN: 0018-9251 (2008)

E. SILLERO, D. LÓPEZ-ROMERO, A. BENGOECHEA, M.A. SÁNCHEZ-GARCÍA, F. CALLE
“Fabrication and stress relief modelling of GaN based MEMS test structures grown by MBE on Si(111)”
Physical Status Solidi (c) 5, 1974 (2008)

A.M. SÁNCHEZ, R. PRIETO, M. LASO, T. RIESGO
"A Piezoelectric Minirheometer for Measuring the Viscosity of Polymer Microsamples"
IEEE Transactions on Industrial Electronics, 55, 427 (2008)

M.M. SANZ, I. TANARRO
“Plasma basic concepts and nitrogen containing plasmas”
Nitrides and dilute nitrides: Growth, physics and devices. Research Signpost, ISBN 81-7895-250-5, 15-46 (2008)

J. SEGURA, N. GARRO, A. CANTARERO, J. MIGUEL-SÁNCHEZ, A. GUZMÁN, A. HIERRO
"Photoluminescence and magnetophotoluminescence studies in GaInNAs/GaAs quantum wells"
AIP Conf. Proc, 893, 425-426 (2008). Physics of Semiconductors: 28th International Conference on the Physics of Semiconductors (2008)

A.M. TEWELDEBERHAN, G. STENUIT, S. FAHY, E. GALLARDO, S. LAZIC, J.M. CALLEJA, J. MIGUEL-SÁNCHEZ, M. MONTES, A. HIERRO, R. GARGALLO-CABALLERO, A. GUZMAN, E. MUÑOZ
“Resonant Raman-active localized vibrational modes in AlyGa{1-y}NxAs{1-x} alloys: Experiment and first principles calculations”
Physical Review B 77, 155208 (2008)

J M. ULLOA, S. ANANTATHANASARN, P.J. VAN VELDHOVEN, P.M. KOENRAAD, R. NÖTZEL
“Influence of an ultrathin GaAs interlayer on the structural properties of InAs/InGaAsP/InP (100) quantum dots investigated by cross-sectional scanning tunneling microscopy”
Applied Physics Letters, 92, 083103-1 (2008)

J.M. ULLOA, P.M. KOENRAAD, D. FUSTER, L. GONZÁLEZ, Y. GONZÁLEZ, M.U. GONZÁLEZ
“Non-Stranski-Krastanov growth of stacked InAs/InP quantum wires studied by cross-sectional scanning tunnelling microscopy and in situ stress measurements during growth”
Nanotechnology 19, 445601 (2008)

J.M. ULLOA, P.M.KOENRAAD, M. HOPKINSON
“Structural properties of GaAsN/GaAs quantum wells studied at the atomic scale by cross-sectional scanning tunnelling microscopy”
Applied Physics Letters, 93, 083103 (2008)

J.M. ULLOA, P.OFFERMANS, P.M.KOENRAAD
“InAs quantum dot formation studied at the atomic scale by cross-sectional scanning tunneling microscopy”
Self-Assembled -Assembled semiconductor Nanostructures for new Devices in photonics and Electronics, ISBN: 978-0-08-046325-4 Ed. Elsevier (2008)

2009

C. ALEMÁN, N. KARAYIANNIS, D. CURCO, K. FOTEINOPOULOU, M. LASO
"Computer Simulations of Amorphous Polymers: from Quantum Mechanical Calculations to Mesoscopic Models"
Journal of Molecular Structure: THEOCHEM 898, 62–72 (2009)

A. AMMAR, F. CHINESTA, D. RYCKELYNCK, M. LASO
"Reduced Numerical Modeling of Flows Involving Liquid-Crystalline Polymers"
Journal of Non-Newtonian Fluid Mechanics, 160, 140-165 (2009)

C.ANGULO BARRIOS
"Optical Slot-Waveguide based Biochemical Sensors"
Sensors, 9, 6, 4751-4765 (2009)

C. ANGULO BARRIOS
"Analysis and modeling of a silicon nitride slot-waveguide microring resonator biochemical sensor"
Optical Sensors, Proceding of SPIE, 7356, 735605 (1-9) (2009)

A . BENGOECHEA ENCABO, J. HOWGATE, M. STUTZMANN, M. EICKHOFF, M.A. SÁNCHEZ-GARCÍA
"Ultrathin GaN/AlN/GaN solution-gate field effect transistor with enhanced resolution at low source-gate voltage"
Sensors and Actuators B, 142, 304 (2009)

J.H. BLOKLAND, M. BOZKURT, J.M. ULLOA, D. REUTER, A.D. WIECK, P.M. KOENRAAD, P.C.M. CHRISTIANEN, J.C. MAAN
"Ellipsoidal InAs quantum dots observed by cross-sectional STM"
Applied Physics Letters, 94, 023107 (2009)

P. CORFDIR, P. LEFEBVRE, J. RISTIĆ, P. VALVIN, E. CALLEJA, J.D. GANIÈRE, B. DEVEAUD-PLÉDRAN,
"Time-resolved spectroscopy on GaN nanocolumns grown by plasma assisted molecular beam epitaxy on Si substrates"
Journal of Applied Physics, 105, 013113 (2009)

R. CUERDO, Y. PEI, Z. CHEN, S. KELLER, S. P. DENBAARS, F. CALLE, U. K. MISHRA,
"The Kink Effect at Cryogenic Temperatures in Deep Submicron AlGaN/GaN HEMTs"
IEEE Electron Device Letters, 30, 209 (2009)

R. CUERDO, E. SILLERO, M. F. ROMERO, M. J. UREN, M.-A. DI FORTE POISSON, E. MUÑOZ, F. CALLE
"High Temperature Microwave Performance of Submicron AlGaN/GaN HEMTs on SiC"
IEEE Electron Device Letters, 30, 808 (2009)

P.R. EDWARDS, R.W. MARTIN, K. BEJTKA, K.P. O´DONNELL, S. FERNÁNDEZ-GARRIDO, E. CALLEJA.
"Correlating Composition and Luminescence Variations in AlInGaN epilayers"
Superlattices and Microstructures 45, 151-1 (2009)

S. FERNÁNDEZ-GARRIDO, J. GRANDAL, E. CALLEJA, M.A. SÁNCHEZ-GARCÍA, D. L. ROMERO
"A growth diagram for plasma-assisted molecular beam epitaxy of GaN nanocolumns on Si(111)"
Journal of Applied Physics, 106, 126102 (2009)

K. FOTEINOPOULOU, N. KARAYIANNIS, M. LASO, M. KRÖGER
"Structure, dimensions, and entanglement statistics of long linear polyenthylene chains"
The Journal of chemical Physics B, 113, 442 (2009)

K. FOTEINOPOULOU, N. KARAYIANNIS, M. LASO, M. KRÖGER, M. MANSFIELD
"Universal Scaling, Entanglements, and Knots of Model Chain Molecules"
Virtual Journal of Biological Physics Research, 17,1 (2009)

K. FOTEINOPOULOU, N. KARAYIANNIS, M. LASO, M. KRÖGER, M. MANSFIELD
"Universal Scaling, Entanglements, and Knots of Model Chain Molecules"
Virtual Journal of Quantum Information, 9, 1 (2009)

Ž. GAČEVIĆ, S. FERNÁNDEZ-GARRIDO, E. CALLEJA, E. LUNA, A. TRAMPERT
"Growth and characterization of lattice-matched InAlN/GaN Bragg reflectors grown by plasma assisted molecular beam epitaxy"
Physica status Solidi (c), 6, S2, S643 (2009)

R. GARGALLO-CABALLERO, Á.GUZMÁN, M. HOPKINSON, J. M. ULLOA, A. HIERRO, E. CALLEJA
"Dependence of N incorporation into (Ga)InAsN QDs on Ga content probed by rapid thermal annealing"
Physica status solidi (c), 6,6, 1441 (2009)

T.E. GÓMEZ ALVAREZ-ARENAS, P.YU. APEL, O.L. ORELOVITCH, M. MUÑOZ
"New ultrasonic technique for the study of the pore shape of track-etched pores in polymer films"
Radiation Measurements, 44, 1114 (2009)

F. GONZÁLEZ-POSADA FLORES, A. REDONDO, A.BENGOECHEA, A.JIMENEZ, R.GAGO, A.F.BRAÑA, E. MUÑOZ.
"High-resolution hydrogen profiling in AlGaN/GaN heterostructures grown by different epitaxial methods"
Journal of Physics D, 42(5), 055406 (2009) .

F. GONZÁLEZ-POSADA FLORES, C. RIVERA, E.MUÑOZ.
"The effects of processing of high-electron-mobility transistors on the strain state and the electrical properties of AlGaN/GaN structures"
Applied Physics Letters 95, 203504 (2009)

J. GRANDAL, M.A. SÁNCHEZ-GARCÍA, E. CALLEJA, E. GALLARDO, J.M. CALLEJA, E. LUNA, A. TRAMPERT, U. JAHN,
"InN nanocolumns grown by plasma-assisted molecular beam epitaxy on A-plane GaN templates"
Applied Physics Letters, 94, 221908 (2009)

A. GUZMÁN, E. LUNA, F. ISHIKAWA, A. TRAMPERT
"The role of Sb and N ions on the morphology and localization of (Ga,In) (N,As) quantum wells"
Journal of Crystal Growth, 311, 1728 (2009)

V. HAXHA, I. DROUZAS, J.M. ULLOA, M. BOZKURT, P.M. KOENRAAD, D.J. MOWBRAY, H.Y. LIU, M.J. STEER, M. HOPKINSON, M.A. MIGLIORATO
"Role of Segregation in InAs/GaAs Quantum Dot Structures Capped with a GaAsSb Strain Reduction Layer"
Physical Review B 80, 165334 (2009)

V. HAXHA, R. GARG, M.A. MIGLIORATO, I.W. DROUZAS, J.M. ULLOA, P.M. KOENRAAD, M.J. STEER, H.Y. LIU, M.J. HOPKINSON, D.J. MOWBRAY
"Empirical bond order potential calculations of the elastic properties of epitaxial InGaSbAs layers"
Microelectronics Journal 40, 533 (2009)

A .HIERRO, G. TABARES, J.M. ULLOA, E. MUÑOZ, A. NAKAMURA, T. HAYASHI, J. TEMMYO
"Carrier compensation by deep levels in Zn1−xMgxO/sapphire"
Applied Physics Letters, 94, 232101 (2009)

R.S. HOY, K. FOTEINOPOULOU, M. KROGER
"Topological analysis of polymeric melts: Chain-length effects and fast-converging estimators for entanglement length"
Physical Review E 80, 031803 (2009)

N. KARAYIANNIS, K. FOTEINOPOULOU, M. LASO
"Entropy-driven crystallization in dense systems of athermal chain molecules"
Physical Review Letters, 130, 164908 (2009)

N. KARAYIANNIS, K. FOTEINOPOULOU, M. LASO
"The structure of random packings of freely jointed chains of tangent hard spheres"
Journal of Chemical Physics 130, 164908 (2009)

N. KARAYIANNIS, K. FOTEINOPOULOU, M. LASO
"Contact network in nearly jammed disordered packings of hard-sphere chains"
Physical Review E 80, 011307 (2009)

N. KARAYIANNIS, K. FOTEINOPOULOU, M. LASO
"The characteristic crystallographic element norm: a descriptor of local structure in atomistic and particulate systems"
Journal of Chemical Physics, 130, 074704 (2009)

N. KARAYIANNIS, M. KROGER
"Combined molecular algorithms for the generation, equilibration and topological analysis of entangled polymers: methodology and performance"
International Journal of Molecular Sciences, 5054 (2009)

N. KARAYIANNIS, M. LASO, M. KRÖGER
"Detailed atomistic molecular-dynamics simulations of α-conotoxin AuIB in water"
Journal of Physical Chemistry B, 113, 5016 (2009)

D.R. KHANAL, W. WALUKIEWICZ, J. GRANDAL, E. CALLEJA, J. WU,
"Determining surface Fermi level pinning position of InN nanowires using electrolyte gating"
Applied Physics Letters, 95, 173114 (2009).

M. LASO, N. KARAYIANNIS, K. FOTEINOPOULOU, M. KRÖGER, M. MANSFIELD
"Random Packing of Model Polymers: Local Structure, Topological Hindrance and Universal Scaling"
Soft Matter 5, 1762 (2009)

V. MLINAR, M. BOZKURT, J.M. ULLOA, M. EDIGER, G. BESTER, A. BADOLATO, P.M. KOENRAAD, R.J. WARBURTON, A. ZUNGER
"Structure of quantum dots as seen by excitonic spectroscopy versus structural characterization: Using theory to close the loop"
Physical Review B 80, 165425 (2009)

M. MONTES, A. HIERRO, J.M. ULLOA, A. GUZMÁN, M. AL KHALFIOUI, M. HUGUES, B. DAMILANO, J. MASSIES
"Electroluminescence analysis of 1.3-1.5 μm InAs quantum dot LEDs with (Ga,In)(N,As) capping layers"
Physical Status Solidi (c), 6, 6, 1424 (2009)

F.B.NARANJO, M.GONZÁLEZ-HERRÁEZ, S.VALDUEZA-FELIP, H.FERNÁNDEZ, J.SOLIS, S. FERNÁNDEZ, E.MONROY, J.GRANDAL, M.A.SÁNCHEZ
"Non-linear properties of nitride-based nanostructures for optically controlling the speed of light at 1.5 μm"
Microelectronics Journal 40, 349 (2009)

A. NAVARRO, C. RIVERA, J. PEREIRO, E. MUÑOZ, B. IMER, S.P. DENBAARS, J.S. SPECK.
"High responsivity A-plane GaN-based metal-semiconductor-metal photodetectors for polarization-sensitive applications"
Applied Physics Letters, 94, 213512 (2009)

E. PAWEL, J.J. MALINOWSKI, J.Y. DUBOZ, G. HELLINGS, A. LORENZ, J.G. RODRIGUEZ MADRID, CH. TURDEVANT, K. CHENG, M. LEYS, J. DERLUYN, J. DAS, M. GERMAIN, K. MINOGLOU, P. DE MOOR, E. FRAYSSINET, F. SEMOND, J-F. HOCHEDEZ, B. GIORDANENGO, R. MERTENS
"Bakside-Illuminated GaN-on-Si Schottky Photodiodes for UV Radiation Detection"
IEEE Electron Device Letters, 30,12, 1308 (2009)

J. PEREIRO, C. RIVERA, A. NAVARRO, E. MUÑOZ, R. CZERNECKI, S. GRZANKA, M. LESZCZYNSKI
"Optimization of InGaN/GaN MQW photodetector structures for high responsivity performance"
IEEE Journal of Quantum Electronics, 45, 617 (2009)

A. REDONDO-CUBERO, K. LORENZ, N. FRANCO, S. FERNÁNDEZ-GARRIDO, R. GAGO, P.J.M. SMULDERS, E. MUÑOZ, E. CALLEJA, E. ALVES
"Influence of steering effects on strain detection in AlGaInN/GaN heterostructures by ion channelling"
J. Phys. D: Appl. Phys., 42 (6), 065420-1/8 (2009)

A. REDONDO-CUBERO, K LORENZ, R GAGO, N FRANCO, S. FERNÁNDEZ-GARRIDO, P.J.M. SMULDERS, E. MUÑOZ, E. CALLEJA, I.M. WATSON, E. ALVES
"Breakdown of anamalous channeeling with ion energy for accurate strain determination in GaN-based heterostructures"
Applied Physics Letters, 95, 051921 (2009)

C. RIVERA, E. MUÑOZ
"The role of electric field-induced strain in the degradation mechanism of AlGaN/GaN high-electron-mobility transistors"
Applied Physics Letters 94, 053501 (2009).

M. ROMERA, M. MUÑOZ, P. SÁNCHEZ, C. AROCA, J. L. PRIETO
"Influence on the magnetoresistance of a spin valve due to the insertion of an ultrathin Gd layer in the free layer"
Journal of Applied Physics, 106, 023922 (2009)

E. SILLERO, O.A. WILLIAMS, V. LEBEDEV, V. CIMALLA, C. C. RÖHLIG, C. E. NEBEL, F. CALLE
"Static and dynamic determination of the mechanical properties of nanocrystalline diamond micromachined structures"
Journal of Micromechanics and Microengineering 19, 115016 - 6 (2009)

N. SOFIKITI, N. CHANIOTAKIS, J. GRANDAL, M. UTRERA, M.A. SANCHEZ-GARCIA, E. CALLEJA, E. ILIOPOULOS, A. GEORGAKILAS,
"Direct immobilization of enzymes in GaN and InN nanocolumns: The urease case study"
Applied Physics Letters 95, 113701 (2009)

V. TASCO, A. CAMPA, I. TARANTINI, A. PASSASEO, F. GONZÁLEZ-POSADA, A. REDONDO-CUBERO, K. LORENZ, N. FRANCO, E. MUÑOZ
"Investigation of different mechanisms of GaN growth induced on AlN and GaN nucleation layer"
Journal of Applied Physics, 105, 063510 (2009)

J. M. ULLOA, M. BOZKURT, P. M. KOENRAAD
"Intrinsic and Mn doped InAs quantum dots studied at the atomic scale by crossectional scanning tunnelling microscopy"
Solid State Comunications, R, 149, 1410 (2009)

F. YAKUPHANOGLU, R. MEHROTRA, A. GUPTA, M. MUÑOZ
"Nanofiber organic semiconductors: The effects of nanosize on the electrical charge transport and optical properties of bulk polyanilines"
Journal of Applied Polymer Science, 114, 794 (2009)

8.2 Conferences and Meetings

2007

S. BARBET, R. AUBRY, D. DERESMES, M-A. POISSON, T. MÉLIN, D. THÉRON, F. ROMERO, E. MUÑOZ, A. JIMÉNEZ
"Kelvin force Microscopy on Gan Material and Devices"
16th European Workshop on Heterostructure Technology "HETECH 2007"
Frejus (France), 2007

C.A.BARRIOS
"Ultrasensitive Nanomechanical Photonic Microsensor"
SPIE Europe, Microtechnologies for the new millennium 2007
Gran Canaria (Spain), 2007

C.A. BARRIOS
"Nanomechanical Photonic Microsensor for Ultrasensitive Explosive Detection"
Nato-Research & Technology Organization. Set-117 specialists' meeting on prediction and detection of improvised explosive devices (ied).
Toledo (Spain), 2007

C.A. BARRIOS, K.B. GYLFASON, B. SANCHEZ , H. SOHLSTRÖM, A. GRIOL, R. CASQUEL, M. HOLGADO.
"Integrated Si_3N_4/SiO_2 Slot-Waveguide Microresonators"
33rd European Conference and Exhibition on Optical Communication (ECOC 2007)
Berlín (Germany), 2007

K. BEJTKA, R.W. MARTIN, S. FERNÁNDEZ-GARRIDO, A. REDONDO-CUBERO, F. GONZÁLEZ-POSADA, E. CALLEJA
"Composition and luminescence of AlInGaN layers grown by MBE"
14th European Molecular Beam Epitaxy Workshop 2007
Sierra Nevada, Granada (Spain), 2007

K. BEJTKA, R.W. MARTIN, S. FERNÁNDEZ-GARRIDO, E. CALLEJA, A. REDONDO-CUBERO, F. GONZÁLEZ-POSADA
"Composition and luminescence of AlInGaN layers grown by PA-MBE"
United Kingdom Nitride Consortium 2007
Cambridge (U.K), 2007

J.H. BLOKLAND, J.M. ULLOA, U. ZEITLER, P.C.M. CHRISTIANEN, P.M. KOENRAAD, D. REUTER, A.D. WIECK, J.C. MAAN
"Shell-filling and correlation effects of holes in InAs quantum dots"
International Conference on Electronic Properties of Two-dimensional Systems and Modulated Semiconductor Structures (EP2DS 17 – MSS 13)
Genova (Italy), 2007

E. CALLEJA
"Self-assembled MBE growth of III-Nitride Nanocolumnar Heterostructures on Si substrates"
European Materials Research Society Meeting (E-MRS) 2007
Estrasburgo (France), 2007

R. CUERDO, F. CALLE, A. F. BRAÑA, Y. CORDIER, M. AZIZE, N. BARON, S. CHENOT, E. MUÑOZ
"High temperature behaviour of AlGaN/GaN HEMTs on Si(111) and sapphire substrates"
7th International Conference on Nitride Semiconductors (ICNS07)
Las Vegas (USA), 2007

R. CUERDO, F. CALLE, A. F. BRAÑA, E. MUÑOZ, Y. CORDIER, M. AZIZE, N. BARON, S. CHENOT
"High temperature DC performance of nitride HEMTs with different gate length"
16th European Workshop on Heterostructures Technology
Frejus (France), 2007

I.W.D. DROUZAS, J.M. ULLOA, P.M. KOENRAAD, D.J. MOWBRAY, M.A. MIGLIORATO, M.J. STEER, H.Y. LIU, M. HOPKINSON
"InAs self-assembled quantum dots capped with a GaAsSb strain reducing layer: Morphology of a nanostructure with novel optical properties"
UK Compound Semiconductors 2007
Sheffield (UK), 2007

I. W.D. DROUZAS, J. M. ULLOA, P. M. KOENRAAD, D. J. MOWBRAY, M. STEER, H. Y. LIU, M. HOPKINSON
"InAs self-assembled quantum dots with a GaAsSb strain reducing layer: Structural and compositional analysis by cross sectional scanning tunnelling microscopy"
One day Quantum Dot Meeting 2007
Nottingham (UK), 2007

I. W. D. DROUZAS, J. M. ULLOA, P. M. KOENRAAD, D. J. MOWBRAY, M. A. MIGLIORATO, M. J. STEER, H.Y. LIU, M. HOPKINSON
"InAs self-assembled quantum dots capped with a GaAsSb strain reducing layer: Morphology of a nanostructure with novel optical properties"
International Conference on Electronic Properties of Two-dimensional Systems and Modulated Semiconductor Structures (EP2DS 17 – MSS 13)
Génova (Italy), 2007

S. FERNÁNDEZ-GARRIDO, E. CALLEJA, F. BERTRAM, J. CHRISTEN, E. LUNA, A. TRAMPERT
"Photoluminescence enhancement through carrier localization in Inalgan layers grown by MBE"
14th European Molecular Beam Epitaxy Workshop 2007
Sierra Nevada, Granada (Spain), 2007

S. FERNÁNDEZ-GARRIDO, G. KOBLMÜLLER, E. CALLEJA, J. S. SPECK
"**In-Situ Gan Decomposition Analysis By Quadrupole Mass Spectrometry And Reflection High-Energy Electron Diffraction"**
14th European Molecular Beam Epitaxy Workshop 2007
Sierra Nevada, Granada (Spain), 2007

G. FRANSEN, T. SUSKI, J. RISTIC, E. CALLEJA
"Anomalous Hydrostatic Pressure Dependence Of Pl In Pambe-Grown Nanocolumnar Gan And GaN/AlGaN Qdiscs"
14th European Molecular Beam Epitaxy Workshop 2007
Sierra Nevada, Granada (Spain), 2007

E. GALLARDO, S. LAZIC, J. M. CALLEJA, J. MIGUEL-SÁNCHEZ, M. MONTES, A. HIERRO, R. GARGALLO-CABALLERO, A. GUZMÁN, A.M. TEWELDEBERHAN, S. FAHY
"Local vibration modes and nitrogen incorporation in AlGaAs:N layers"
7th International Conference on Nitride Semiconductors (ICNS07)
Las Vegas (Nevada, USA), 2007

R. GARGALLO-CABALLERO, Á.GUZMÁN, J. MIGUEL-SÁNCHEZ, A. HIERRO.
"Role of N plasma species on the morphology and luminescence of InAsN quantum dots grown by MBE"
European Materials Research Society Meeting (E-MRS) 2007
Estrasbourg (France), 2007

R. GARGALLO-CABALLERO, J. MIGUEL-SÁNCHEZ, Á. GUZMÁN, A. HIERRO, E. MUÑOZ.
"Structural and optical study of InAsN quantum dots grown on GaAs(100) and buried with different materials"
14th European Molecular Beam Epitaxy Workshop 2007
Sierra Nevada, Granada (Spain), 2007

R. GARGALLO-CABALLERO, M.SANZ, Á.GUZMÁN, E.CALLEJA, E.MUÑOZ
"High Temperature Multiquantum Dot Infrared Photodetectors Using Inas Self-Assembled Quantum Dots"
6th Spanish Conference on Electronic Devices "CDE-07"
El Escorial, Madrid (Spain), 2007

R. GARGALLO-CABALLERO, M. SANZ, Á. GUZMÁN, E. CALLEJA, E. MUÑOZ
"Quantum Dot Infrared Photodetector for mid-infrared detection at high temperatures"
6th Spanish Conference on Electronic Devices "CDE-07". *IEEE Proceedings, ISBN: 1-4244-0868-7 (2007)*
El Escorial, Madrid (Spain), 2007

S. GHOSH, C. RIVERA, J. L. PAU, E. MUÑOZ, O. BRANDT, H. T. GRAHN
"Narrow-Band Photodetection Based on M-Plane Gan"
7th International Conference on Nitride Semiconductors (ICNS07)
Las Vegas (Nevada, USA), 2007

F. GONZÁLEZ-POSADA, A. F. BRAÑA, D. L. ROMERO, M. F. ROMERO, E. MUÑOZ, C. PALACIO, A. JIMÉNEZ, J. A. BARDWELL.
"Effects of Surface Cleaning And Treatments In 2DEG Characteristics of Gan HEMT Structures"
31st Workshop on compound Semiconductor devices and Integrated circuits "WOCSDICE-2007"
Venecia (Italy), 2007

F. GONZÁLEZ-POSADA, A. F. BRAÑA, D. L. ROMERO, M. F. ROMERO, A.JIMENEZ, A.ARRANZ, C. PALACIO, E. MUÑOZ
"2DEG Characteristics improvement by N2 plasma exposure in HEMT heterostructures"
6th Spanish Conference on Electronic Devices "CDE-07". IEEE, Electron Devices, 154 – 157, ISBN: 978-1-4244-2838-0
El Escorial, Madrid (Spain), 2007

J. GRANDAL, A.BENGOECHEA, M.A. SÁNCHEZ-GARCÍA, E. CALLEJA, E. LUNA, A. TRAMPERT, M. NIEBELSCHÜTZ, V. CIMALLA
"Structural Characterization of InN-Based Layers Grown on Si (111) and Si (001) Substrates By MBE"
14th European Molecular Beam Epitaxy Workshop 2007
Sierra Nevada, Granada (Spain), 2007

J. GRANDAL, M.A. SÁNCHEZ-GARCÍA, E. CALLEJA, S. LAZIC, J.M. CALLEJA, E. LUNA, A. TRAMPERT
"Characterization of Inn Nanocolumns Grown On Si (001) Substrates by Plasma Assisted Molecular Beam Epitaxy"
European Material Research Society Spring Conference 2007
Estrasbourg (France), 2007

J. GRANDAL, M.A. SÁNCHEZ-GARCÍA, E. CALLEJA, S. LAZIC, J.M. CALLEJA, E. LUNA, A. TRAMPERT
"Structural and optical characterization of Inn/Ingan multiple quantum wells grown by plasma assisted-MBE"
7th International Conference on Nitride Semiconductors (ICNS07)
Las Vegas (NV), USA, 2007

Á. GUZMÁN, F. ISHIKAWA, A. TRAMPERT, K.H. PLOOG
"Effect of Sb on the optical properties of GaInNAs and GaInNAsSb Quantum Wells grown by MBE"
14th European Molecular Beam Epitaxy Workshop 2007
Sierra Nevada, Granada (Spain), 2007

Á. GUZMÁN, E. LUNA, J. HERNANDO, E. MUÑOZ
"Quantum well Infrared photodetectors (QWIP), basics and current activities at UPM University"
19th NATO/RTO Sensors and Electronics Technology Panel Business Meeting
Toledo (Spain), 2007

A. HIERRO
"Diluted Nitrides for IR lasing applications"
31st Workshop on Compound Semiconductor Devices and Integrated Circuits, WOCSDICE 2007
Venecia (Italy), 2007

U. JAHN, E. CALLEJA, J. RISTIC, A. TRAMPERT, C. RIVERA
"Spatially resolved luminescence spectroscopy of single GaN/(Al,Ga)N quantum disks"
7th International Conference on Nitride Semiconductors (ICNS)
Las Vegas (Nevada, USA), 2007

G.KOBLMUELLER, S. FERNANDEZ-GARRIDO, J. S. BROWN, E.CALLEJA, J. S. SPECK
"Improved growth mode diagram for plasma–assisted MBE growth of (0001) GaN"
14th European Molecular Beam Epitaxy Workshop 2007
Sierra Nevada, Granada (Spain), 2007

M. LASO, J. RAMIREZ, K. FOTEINOPOULOU et AL.
"Molecule-based micro-macro methods for complex fluids"
10th ESAFORM Conference on Material Forming, AIP Conference Proceedings 907, 1490-1495 (2007)
Zaragoza (Spain), 2007

S. LAZIĆ, E. GALLARDO, J. M. CALLEJA, F. AGULLÓ-RUEDA, J. GRANDAL, M. A. SÁNCHEZ-GARCÍA, E. CALLEJA, A. TRAMPERT, E. LUNA
"Raman Scattering by Coupled Plasmon-Lo Phonons in InN Nanocolumns"
7th International Conference on Nitride Semiconductors (ICNS07)
Las Vegas (NV), USA, 2007

S. LAZIĆ, E. GALLARDO, J.M. CALLEJA, F. AGULLÓ-RUEDA, J. GRANDAL, M.A. SÁNCHEZ-GARCIA, E. CALLEJA
"Raman Scattering By Longitudinal Optical Phonons In InN Nanocolumns Grown On Si(111) And Si(001) Substrates"
13th International Conference on Modulated Semiconductor Structures (MSS-13)
Génova (Italy), 2007

S. LAZIĆ, E. GALLARDO, J.M. CALLEJA, F. AGULLO-RUEDA, M.A. SANCHEZ-GARCIA, J. GRANDAL, E. CALLEJA, A. TRAMPERT
"Coupled longitudinal optical phonon-plasmon modes in InN nanocolumns"
European Material Research Society Spring Conference 2007. AIP Conference Proceedings 893, 287
Strasbourg (France), 2007

S. LAZIĆ, E. GALLARDO, J.M. CALLEJA, J. MIGUEL-SÁNCHEZ, M. MONTES, A. HIERRO, R. GARGALLO-CABALLERO, A. GUZMÁN, E. MUÑOZ, A.M TEWELDEBERHAN, S.FAHY
"Resonant Raman study of local vibrational modes in AlxGa1-xAs1-yNy layers"
13th International Conference on Modulated Semiconductor Structures (MSS-13)
Génova (Italy), 2007

S. LAZIĆ, J.M. CALLEJA, F.AGULLÓ-RUEDA, M.A. SÁNCHEZ-GARCÍA, J. GRANDAL, E. CALLEJA, A. TRAMPERT
"Inelastic light scattering by the longitudinal optical phonons in InN nanocolumns and compact layers"
Physics of Light-Matter Coupling in nanostructures
La Habana (Cuba), 2007

J. MIGUEL-SÁNCHEZ, M. HOPKINSON, Á. GUZMÁN, R. GARGALLO-CABALLERO, E. MUÑOZ.
"(In)GaAs(N) On GaAs (100) And (111)B Grown In A Low Pressure N2 Environment"
14th European Molecular Beam Epitaxy Workshop 2007
Sierra Nevada, Granada (Spain), 2007

J. MIGUEL-SÁNCHEZ, M. MONTES, A. HIERRO, R. GARGALLO-CABALLERO, A. GUZMÁN, E. MUÑOZ, S. LAZIC, E. GALLARDO, J. M. CALLEJA
"Growth and Characterization of AlGaAs(N) On GaAs"
14th European Molecular Beam Epitaxy Workshop 2007
Sierra Nevada, Granada (Spain), 2007

M. MONTES, A. HIERRO, J.M. ULLOA, B. DAMILANO, M. HUGUES, M. AL KHALFIOUI, J.-Y. DUBOZ, J. MASSIES
"Role of N plasma species on the morphology and luminescence of InAsN quantum dots grown by MBE"
European Materials Research Society (E-MRS) Spring Meeting
Estrasburgo (France), 2007

M. MONTES, A. HIERRO, B. DAMILANO, M. HUGUES, M. AL KHALFIOUI, J.-Y. DUBOZ, J. MASSIES
"Analysis of gain spectra and Fermi level pinning of GaInNAs/GaAs quantum well lasers with 0 to 3.3% N Content"
European Materials Research Society Meeting (E-MRS) 2007
Strasburgo (France), 2007

A. NAKAMURA, T. HAYASHI, S. GANGIL, J. TEMMYO, A. NAVARRO, J. PEREIRO, E. MUÑOZ
"Nitrogen-Doped Mgxzn1-Xo Growth towards visible rejection photodetetors"
13th International Conference on II-VI Compounds
Jeju (Korea), 2007

A. NAVARRO, C. RIVERA, R. CUERDO, J.L. PAU, J. PEREIRO, F. CALLE, E. MUÑOZ
"Noise study in photodiodes based on InGaN/GaN MQW"
6th Spanish Conference on Electronic Devices, CDE-07. *IEEE Proceedings 321-324, ISBN: 1-4244-0868-7*
El Escorial (Madrid, Spain), 2007

M. NIEBELSCHÜTZ, V. CIMALLA, O. AMBACHER, T. MACHLEIDT, J. RISTIC, J. GRANDAL, M. A. SÁNCHEZ-GARCÍA. E. CALLEJA
"Space Charged Region In Gan And Inn Nanocolumns Investigated By Atomic Force Microscopy"
7th International Conference on Nitride Semiconductors 2007
Las Vegas (NV), USA, 2007

Y. PEI, R. CUERDO, F. RECHT, N. FICHTENBAUM, S. KELLER, S.P. DENBAARS, F. CALLE, U.K. MISHRA
"Low temperature high-frequency performance of deep submicron AlGaN/GaN HEMTs"
34th International Symposium on Compound Semiconductors (ISCS'07)
Kyoto (Japan), 2007.

J. PEREIRO, C. RIVERA, J.L. PAU, A. NAVARRO, S. FERNANDEZ-GARRIDO, S. GRZANKA, M. LESZCZYNSKI, E. MUÑOZ
"Growth and Characterization of (In,Ga)N Based Photodetectors Designed By Internal Field Engineering"
14th European Molecular Beam Epitaxy Workshop 2007
Sierra Nevada, Granada (Spain) ,2007

J. PEREIRO, C. RIVERA, J.L. PAU, A. NAVARRO, S. FERNANDEZ- GARRIDO, S. GRZANKA, M. LESZCZYNSKI, E. MUÑOZ
"Design of InGaN based photodetectors by internal field engineering"
6th Spanish Conference on Electronic Devices "CDE-07"
El Escorial (Madrid, Spain), 2007

A. REDONDO-CUBERO, R. GAGO, F. GONZÁLEZ-POSADA, S. FERNÁNDEZ-GARRIDO, A. MUÑOZ-MARTÍN, A. F. BRAÑA, U. KREISSIG, D. GRAMBOLE, E. MUÑOZ
"Ion Beam Analysis of Ternary and Quaternary AlInGaN/GaN Heterostructures For High-Power Electronic Devices"
European Materials Research Society Meeting (E-MRS) 2007
Estrasburgo (France), 2007

A. REDONDO-CUBERO, M. F. ROMERO, R. GAGO, A. MUÑOZ-MARTÍN, A.F. BRAÑA, A. JIMÉNEZ, E. MUÑOZ
"Study of a-SiN:H passivant layers for GaN-based high electron mobility transistors"
European Materials Research Society Meeting (E-MRS) 2007
Estrasburgo (France), 2007

A. REDONDO-CUBERO, J.A. SÁNCHEZ-GARCÍA, R. GAGO, L. VÁZQUEZ, J. MUÑOZ-GARCÍA, M. CASTRO, R. CUERNO
"Surface nanodot patterning of amorphous silicon films by low-energy ion beam sputtering"
Nanopatterning via ions, photon beam and epitaxy
Sestri Levante (Italy), 2007

J. RISTIC, C. RIVERA, S. FERNÁNDEZ-GARRIDO, E. CALLEJA, A. TRAMPERT, K. H. PLOOG, M- POVOLOSKYI, A. DI CARLO
"Improved growth mode diagram for plasma-assisted MBE growth of (0001) GaN"
7th International Conference on Nitride Semiconductors
Bremen (Germany), 2007

C. RIVERA, P. MISRA, J.L. PAU, E. MUÑOZ, O. BRANDT, H.T. GRAHN, K.H. PLOOG
"Strained M-Plane GaN for Polarization-Sensitive Applications"
6th Spanish Conference on Electronic Devices "CDE-07"
El Escorial (Madrid, Spain), 2007

E. SILLERO, A. BENGOECHEA, M. A. SÁNCHEZ-GARCÍA, F. CALLE
"III-Nitride MEMS grown by MBE on Si(111): Fabrication and mechanical characterisation"
16th European Workshop on Heterostructures Technology
Frejus (France), 2007

E. SILLERO, D. LÓPEZ-ROMERO, A. BENGOECHEA, M. A. SÁNCHEZ-GARCÍA, F. CALLE
"Fabrication and stress relief modelling of GaN based MEMS test structures grown by MBE on Si(111)"
7th International Conference on Nitride Semiconductors (ICNS07)
Las Vegas (USA), 2007

V.SONI, J. ABILDSKOV, G. JONSSON, R. GANI, G. TSOLOU, N. KARAYIANNIS, V.G. MAVRANTZAS
"Integrating multilevel modelling aspects to predict gas permeability in polymers for the design of membranes"
11th International Conference on properties and phase equilibria
Hersonissos (Greece), 2007

J. M. ULLOA, C. ÇELEBI, P. OFFERMANS, P.M. KOENRAAD, A. SIMON, E. GAPIHAN, A. LETOUBLON, N. BERTRU, I. DROUZAS, D.J. MOWBRAY, M.J. STEER, M. HOPKINSON
"Capping of InAs quantum dots studied at the atomic scale by cross-sectional scanning tunneling microscopy"
Microscopy of Semiconducting Materials XV
Cambridge (UK), 2007

J. M. ULLOA, C. ÇELEBI, P. OFFERMANS, P.M. KOENRAAD, A. SIMON, E. GAPIHAN, A. LETOUBLON, N. BERTRU, I. DROUZAS, D.J. MOWBRAY, M.J. STEER, M. HOPKINSON
"Capping of InAs quantum dots studied at the atomic scale by cross-sectional scanning tunneling microscopy"
14th European Molecular Beam Epitaxy Workshop
Granada (Spain), 2007

J. M. ULLOA, P. M. KOENRAAD, E. GAPIHAN, A. LETOUBLON, N. BERTRU
"Double capping of InAs/InP (311)B quantum dots studied by cross-sectional scanning tunneling microscopy"
One day Quantum Dot Meeting 2007
Nottingham (UK), 2007

J.M. ULLOA, P.M. KOENRAAD, E. GAPIHAN, A. LETOUBLON, N. BERTRU, D. FUSTER, Y. GONZALEZ, L. GONZALEZ
"Atomic scale structural characterization of long wavelength InAs/InP quantum dots and wires"
International Workshop on Long Wavelenght Quantum Dots: Growth and Applications
Rennes (France), 2007

J.M. ULLOA, A. WIERTS, C. ÇELEBI, P.M. KOENRAAD, H. BOUKARI, L. MAINGAULT, H. MARIETTE
"Cross-Sectional Scanning Tunneling Microscopy on II-VI Semiconductor Multilayer Structures TIPO"
13th International Conference on II-VI Compounds
Jeju (Korea), 2007

M. UTRERA, J. RISTIĆ, S. FERNÁNDEZ-GARRIDO, L. CERUTTI, G. FUENTES, E. CALLEJA, A. TRAMPERT, U. JAHN, K. H. PLOOG
"Ordered growth of GaN Nanostructures on Si by MBE"
14th European Molecular Beam Epitaxy Workshop 2007
Sierra Nevada, Granada (Spain), 2007

S. VALDUEZA-FELIP, F.B. NARANJO, M. GONZÁLEZ-HERRÁEZ, H. FERNÁNDEZ, J. SOLIS, S. FERNÁNDEZ, F. GUILLOT, E. MONROY, J. GRANDAL, M.A. SÁNCHEZ-GARCÍA
"Novel nitride - based materials for nonlinear optical signal processing applications at 1.5 μm"
Inter. Symposium on Intelligent Signal Processing WISP 2007
Alcalá de Henares (Spain), 2007

2008

J. ÁLVAREZ, L. VIVIEN, D. MARRIS-MORINI, C.A. BARRIOS, D. HILL
"A theoretical comparison of strip and vertical slot-waveguide resonators in silicon nitride for sensing purposes"
Trends in Nanotechnology, TNT 2008
Oviedo (Spain), 2008

L. R. BAILEY, T. D. VEAL, P. D. C. KING, C. F. MCCONVILLE, J. PEREIRO, J. GRANDAL, M. A. SÁNCHEZ-GARCÍA, E. MUÑOZ, E. CALLEJA
"Photoemission and Optical Studies of Electron Accumulation at InN and In-rich InGaN Surfaces"
International Worshop on Nitride Semiconductor 2008
Montreux (Switzerland), 2008

C.A. BARRIOS, K.B. GYLFASON, B. SANCHEZ , A. GRIOL, R. CASQUEL, M. HOLGADO.
"Integrated slot-waveguide microresonator for biochemical sensing"
EUROPTRODE IX. Proceedings
Dublin (Ireland), 2008

M. BOZKURT, C. CELEBI, P.J. VAN VELDHOVEN, R. NOTZEL, P.M. KOENRAAD
"Mn and Fe doped InAs quantum dots studied by X-STM"
35th International Symposium on Compound Semiconductors (ISCS)
Rust (Germany), 2008

R. CASQUEL, M. HOLGADO, A. LAVIN, C. A. BARRIOS, C. MOLPECERES, M. MORALES, J. L. OCAÑA.
"Vertical resonant microcavities based on pillars analyzed by beam profile ellipsometry and reflectometry"
EUROSENSORS XXII, Proceedings,1577-1580
Dresden (Germany), 2008

P. CORFDIR, J. RISTIC, P. LEFEBVRE, E.CALLEJA, J.-D. GANIÈRE, B.DEVEAUD-PLÉDRAN
"Time-resolved photoluminescence of GaN nanocolumns grown by molecular beam epitaxy on Si"
International Workshop on Nitride Semiconductors (IWN 2008)
Montreux (Switzerland), 2008

R. CUERDO, E. SILLERO, M. F. ROMERO, M. UREN, E. MUÑOZ, F. CALLE
"DC and RF Performance of AlGaN/GaN HEMTs on SiC at High Temperatures"
International Workshop on Nitrides
Montreaux (Switzerland), 2008.

H.R. CUI, M. SANZ, M. MAICAS, C. AROCA
"Synthesis of Ni nanoparticles by DC magnetron sputtering"
IEEE International magnetics conference- Intermag-2008.
Madrid (Spain), 2008

P.R. EDWARDS, K. BEJTKA, I.M. WATSON, S. FERNÁNDEZ-GARRIDO, E. CALLEJA, R.W. MARTIN, K.P. O´DONNELL,
"Correlating Composition and Luminescence Variations in III-Nitride Semiconductor Alloys"
Microscopy & Microanalysis Meeting, 4 – 7.
Albuquerque, New Mexico, (USA), 2008

S. FERNÁNDEZ-GARRIDO, Z. GACEVIC, E. CALLEJA
"A diagram to grow InAlN layers on (0001)GaN by plasma-assisted molecular beam epitaxy"
International Workshop on nitrides Semiconductors 2008, 6-10 de Octubre 2008
Montreux, (Switzerland), 2008

S. FERNÁNDEZ-GARRIDO, G. KOBLMÄLLER, E. CALLEJA, J. S. SPECK
"In-situ GaN decomposition analysis by quadrupole mass spectrometry and reflection high-energy electron diffraction"
International Workshop on nitrides Semiconductors 2008, 6-10 de Octubre 2008
Montreux (Switzerland), 2008

Z. GACEVIC, S. FERNÁNDEZ-GARRIDO, E. CALLEJA, E.LUNA. A. TRAMPERT
"Growth and characterization of lattice-matched InAlN/GaN Bragg reflectors grown by plasma-assisted molecular beam epitaxy"
International Workshop on nitrides Semiconductors 2008, 6-10 de Octubre 2008. Conferences Proceedings.
Montreux (Switzerland), 2008

R.GARGALLO-CABALLERO, A. GUZMÁN, M. HOPKINSON, J. M. ULLOA, A. HIERRO, E. CALLEJA
"Enhancement of N incorporation into (Ga)InAsN quantum dots"
International Symposium on Compound Semiconductors (ISCS)
Friburgo (Germany), 2008

R. GARGALLO-CABALLERO, M. HOPKINSON, A. GUZMÁN, J. M. ULLOA, A. HIERRO, E. CALLEJA
"The influence of the Ga content on the N incorporation in InAsN and GaInNAs Quantum Dots"
7th International Workshop on Epitaxial Semiconductors on Patterned Substrates and Novel Index Surfaces (ESPS-NIS),
Les Arcenaulx, Marseille (France), 2008

K.B. GYLFASON, B. SANCHEZ, A. GRIOL, C.A. BARRIOS, H. SOHLSTROM, M.J. BANULS, V. GONZALEZ-PEDRO, A. MAQUIEIRA, M. HOLGADO, R. CASQUEL, D. HILL, G. STEMME
"Robust Hybridization of Nanostructured Buried Integrated Opticalwaveguide Systems with On-Chip Fluid Handling for Chemical Analysis"
12th International Conference on Miniaturized Systems for Chemistry and Life Sciences. ISBN: 978-0-9798064-1
San Diego, California (USA), 2008

F. GONZÁLEZ-POSADA FLORES
"Degradación y fiabilidad en transistores de alta movilidad electrónica (HEMT) basados en heteroestructuras AlGaN/GaN"
Proceeding Jornadas de Jóvenes Investigadores de la Universidad de Álcalá.
Madrid (Spain), 2008

J. GRANDAL, M.A. SÁNCHEZ- GARCÍA, E. CALLEJA, S. LAZIC, E. GALLARDO, J.M. CALLEJA, E. LUNA, A. TRAMPERT
"Growth of InN on Silicon substrates"
Mini-Symposium on Physics and Applications of InN and InGaN Semiconductor Materials
The Rank Prize Funds
Grasmere (U.K), 2008

J. GRANDAL, M.A. SÁNCHEZ-GARCÍA, E. CALLEJA, E. LUNA, A. TRAMPERT, U. JAHN, E. GALLARDO, J.M. CALLEJA
"Characterization of InN nanocolumns grown by PA-MBE on a-plane GaN/r-plane Al_2O_3 templates"
International Workshop on Nitride Semiconductor 2008
Montreux (Switzerland), 2008

J. GRANDAL, M.A. SÁNCHEZ-GARCÍA, E. CALLEJA, E. LUNA, A. TRAMPERT, U. JAHN, E. GALLARDO, J.M. CALLEJA
"Growth of InN nanocolumns on a-plane GaN templates"
15th International Conference on Molecular Beam Epitaxy
Vancouver (Canada), 2008

Á. GUZMÁN, F. ISHIKAWA, E. LUNA, A. TRAMPERT.
"The effect of ions and Sb on the carrier localization in GaInNAs quantum wells"
15th International Conference on Molecular Beam Epitaxy
Vancouver (Canada), 2008

K.B. GYLFASON, B. SÁNCHEZ, A. GRIOL, C.A. BARRIOS, H. SOHLSTRÖM, M.J. BAÑULS, V. GONZÁLEZ-PEDRO, Á. MAQUIEIRA, M. HOLGADO, R. CASQUEL, D. HILL, G. STEMME.
"Robust hybridization of nanostructured buried integrated optical waveguides systems with on-chip fluid handling for chemical analysis"
MicroTAS 2008. Proceedings
San Diego (USA), 2008

V. HAXHA, R. GARG, M.A. MIGLIORATO, I.W. DROUZAS, J. M. ULLOA, P. M. KOENRAAD, M. J. STEER, H. Y. LIU, M. HOPKINSON, D. J. MOWBRAY
"The use of Abel-Tersoff potentials in atomistic simulations of InGaAsSb/GaAs"
8th International Conference on Numerical Simulation of Optoelectronic Devices
Nottingham (UK), 2008

D. HILL, B. SANCHEZ, A. GRIOL, G.MAIRE, F.DORTU, L.VIVIEN, A.STRAGIER, D.MARRIS-MORINI, E. CASSAN, A. KAŹMIERCZAK, D. GIANNONE, K. B. GYLFASON, H.SOHLSTRÖM, M.JOSÉ BAÑULS, V. GONZÁLEZ-PEDRO5, A. MAQUIEIRA, C.A. BARRIOS, M. HOLGADO, R. CASQUEL
"Ultrahigh Sensitivity Slot-Waveguide Biosensor on a Highly Integrated Chip for Simultaneous Diagnosis of Multiple Diseases"
21st IEEE International Semiconductor Laser Conference
Sorrento (Italy), 2008

M. LASO
"Meshless stochastic simulation of micro-macro models arising from kinetic theory"
8th World Congress on Computational. Mechanics, WCCM8 8th World Congress on Computational. Mechanics, WCCM8
Venice (Italy), 2008

I. LUCAS, M. MAICAS, L. PÉREZ, M. DÍAZ-MICHELENA
"Magnetic properties of Sm2Co17 & Sm2Co7 sputtered and post-annealed thin films. Effect of Mo underlayer"
The Intermag 2008
Madrid (Spain), 2008

E. LUNA, E. GALLARDO, J.M. CALLEJA, J. GRANDAL, M.A. SÁNCHEZ-GARCÍA, E. CALLEJA, A. TRAMPERT
"Challenges In The Investigation Of III-V Nanocolumns (Ncs) Using Plan-View Transmission Electron Microscopy: Application To Inn Ncs Grown On Si Substrates"
33rd Workshop On Compound Semiconductor Devices And Integrated Circuits Wocsdice
Malaga (Spain), 2009

A. MAQUIEIRA, M.J. BAÑULS, R. PUCHADES, C.A. BARRIOS, M. HOLGADO.
"High sensitive label-free nano-biosensor"
II Workshop of Nanoscience and Analytical Nanotechnology
Tarragona (Spain), 2008

R.W. MARTIN, P.R. EDWARDS, K. BEJTKA, K.P. O´DONNELL, S. FERNÁNDEZ-GARRIDO, E. CALLEJA
"Correlating Composition and Luminescence Variations in AlInGaN epilayers"
9th International Workshop on Beam Injection Assessment of Microstructures in Semiconductors, 2008
Toledo (Spain), 2008

M.A.MIGLIORATO, V.HAXHA, R.GARG, I.W.DROUZAS, J.M.ULLOA, P.M. KOENRAAD , M.J.STEER, H.Y.LIU, M.HOPKINSON, D.J.MOWBRAY
"Atomistic Modelling of III-V Semiconductors: from a single tetrahedron to millions of atoms"
17th Heterostructure Technology Workshop
Venice (Italy), 2008

M. MONTES, A. HIERRO, J. M. ULLOA, A. GUZMÁN, M. AL KHALFIOUI, M. HUGUES, B. DAMILANO, J. MASSIES
"Electroluminescence analysis of 1.3-1.5 µm InAs quantum dot LEDs with (Ga,In)(N,As) capping layers"
35th International Symposium on Compound Semiconductors (ISCS)
Friburgo (Germany), 2008

A. NAVARRO, C. RIVERA, J. PEREIRO, E. MUÑOZ, B. IMER, S. P. DENBAARS, J. S. SPECK
"A-plane GaN polarization-sensitive photodetectors"
International Workshop on Nitride Semiconductors (IWN) 2008
Montreux (Switzerland), 2008

M. NIEBELSCHÜTZ, V. CIMALLA, O. AMBACHER, A. SCHOBER, J. GRANDAL, M. A. SÁNCHEZ-GARCÍA, E. CALLEJA
"Investigation and Manipulation of Space Charged Regions in GaN and InN Nanocolumns"
International Conference on Electronic Materials
Sydney, (Australia), 2008

J. PEREIRO, C. RIVERA, A. NAVARRO, J. L. PAU, E. MUÑOZ, R. GZERNECKI, S. GRZANKA, M. LESZCZYNSKI
"Optimization of InGaN/GaN MQW structures for high responsivity performance"
Workshop on Compound Semiconductor Devices and Integrated Circuits held in Europe (WOCSDICE) 2008
Leuven (Belgique), 2008

J. PEREIRO, C. RIVERA, A. NAVARRO, J. L. PAU, E. MUÑOZ, R. GZERNECKI, S. GRZANKA, M. LESZCZYNSKI
"Optimization of (Al,Ga,In)N-based MQW photodiodes for high responsivity performance in the visible and UV regions"
International Workshop on Nitride Semiconductors (IWN) 2008
Montreux (Switzerland), 2008

J.L.PRIETO, M. GONZÁLEZ-GUERRERO, D. CIUDAD, P.SÁNCHEZ, C. AROCA
"Magnetic softening of magnetostrictive (Fe80Co20)80B20 amorphous thin films with a thickness modulation of the magnetic anisotropy"
INTERMAG 2008
Madrid (Spain), 2008

A. REDONDO-CUBERO, K. LORENZ, N. FRANCO, S. FERNÁNDEZ-GARRIDO, R. GAGO, E.MUÑOZ, E. ALVES
"Influence of Steering Effects on Ion Channeling Determination of Strain in GaN-based Heterostructures"
51st Workshop, "Channeling 2008"
Erice (Trapani - Sicilia), Italy, 2008

C. RIVERA, C. SÁNCHEZ, E. MUÑOZ
"The Role of Strain in the Off-state Degradation Mechanism of AlGaN/GaN High Electron Mobility Transistors"
International Workshop on Nitride Semiconductors (IWN) 2008
Montreux (Switzerland), 2008

M. ROMERA, M. MAICAS, R. RANCHAL, D. CIUDAD, E. LÓPEZ, P. SÁNCHEZ
"Magnetic properties of sputtered permalloy/molibdenum multilayers "
IEEE International Magnetics Conference-Intermag-2008
Madrid (Spain), 2008

E. SILLERO, M. EICKHOFF, F. CALLE
"Nanoporous GaN by UV assisted electroless etching for sensor applications"
International Workshop on Nitrides
Montreaux (Switzerland), 2008

E. SILLERO, J. PEDRÓS, R. SAN ROMÁN, G. F. IRIARTE, F. CALLE
"**RF MEMS Switches with III-N Technology"**
32nd Workshop on Compound Semiconductors and Integrated Circuits, WOCSDICE 2008.
Lovaina (Belgique), 2008

2009

M.J .BAÑULS, J. ORTEGA, R. PUCHADES, A. MAQUIEIRA, M. HOLGADO, MARIAFE LAGUNA, R. CASQUEL, F. J. SANZ, C.A. BARRIOS, D. LOPEZ-ROMERO.
"Funcionalización de SU-8 para la construcción de un sistema de biosensado de alta sensibilidad"
III Workshop Nanociencia y Nanotecnología Analíticas
Oviedo (Spain), 2009

C. ANGULO BARRIOS
"Analysis and modeling of a silicon nitride slot-waveguide microring resonator biochemical sensor SPIE Europe Optics +Optoelectronics".
Optical Sensors. Proceedings
Praga (Czech Republic), 2009

A. BENGOECHEA, J. HOWGATE. M.STUTZMANN, M. EICKHOFF, M.A. SÁNCHEZ-GARCÍA
"Enhanced resolution with GaN/AlN/GaN solution gate field-effect transistor"
33rd Workshop on Compound Semiconductor Devices and Integrated Circuits, WOCSDICE
Málaga (Spain), 2009

B.R. BERMEJO, J. L. PRIETO, P. ILG, M. LASO,
"A stochastic semi-Lagrangian micro-macro model for liquid crystalline solutions"
Internacional Conference on Numerical Analysis and Applied Mathematics
Rethymno (Greece), 2009

R. CUERDO, F. CALLE
"Source and drain resistances behaviour as a function of temperature and drain current in AlGaN/GaN HEMTs"
8th International Conference of Nitride Semiconductors (ICNS-8)
Jeju (Korea), 2009

R. CUERDO, E. MUÑOZ, F. CALLE
"Characterisation of Nitride-based HEMTs at high temperatures"
ESA-MoD Workshop on GaN Microwave Component Technologies
Ulm (Germany), 2009

R. CUERDO, M. UREN, M.-A. DI FORTE POISSON, E. MUÑOZ, F. CALLE
"DC and microwave behaviour of AlGaN/GaN HEMTs on SiC at high temperature"
33rd Workshop on Compound Semiconductor Devices and Integrated Circuits (WOCSDICE'09)
Málaga (Spain), 2009

J. EROLES, A. BENGOECHEA, M.A. SANCHEZ-GARCIA, F. CALLE
"Characterization of a pH sensor based on an AlGaN/GaN transistor"
7th Spanish Conference on Electronic Devices "CDE-09". IEEE, Electron Devices, 258-261, ISBN: 978-1-4244-2838-0
Santiago de Compostela (Spain), 2009

S. FERNANDEZ-GARRIDO, Z. GACEVIC, E. CALLEJA, A. REDONDO-CUBERO, R. GAGO, E.MUÑOZ
"A Comprehensive Diagram to Grow InaIn Alloys By Plasma-Assisted Molecular Beam Epitaxy"
15th European Molecular Beam Epitaxy Workshop
Zakopane (Poland), 2009

Z. GACEVIC, S. FERNÁNDEZ-GARRIDO, E. CALLEJA
"Current status and further challenge in MBE growth of lattice-matched InAlN/GaN Bragg reflectors"
8th International Conference on Nitride Semiconductors (ICNS-8)
Jeju (Korea), 2009

Z. GACEVIC, S. FERNÁNDEZ-GARRIDO, E. CALLEJA
"New approach to grow high reflectivity Al(Ga)N bragg reflectors by plasma-assited molecular beam epitaxy"
8th International Conference on Nitride Semiconductors (ICNS-8)
Jeju (Korea), 2009

Z. GACEVIC, S. FERNÁNDEZ-GARRIDO, E. CALLEJA, E.LUNA, A. TRAMPERT
"Growth and characterization of lattice-matched InAlN/GaN Bragg reflectors grown by plasma assisted molecular beam epitaxy"
15th European Molecular Beam Epitaxy Workshop
Zakopane (Poland), 2009

R. GARGALLO-CABALLERO, A. GUZMÁN, M. HOPKINSON, A. HIERRO, J. M. ULLOA, E. CALLEJA
"Optoelectronic devices based on (Ga,In)(As,N) Quantum dots"
15th European Molecular Beam Epitaxy Workshop
Zakopane (Poland), 2009

J. GRANDAL, A. BENGOECHEA, M. A. SÁNCHEZ-GARCÍA, E. CALLEJA, E. LUNA, A. TRAMPERT, E. GALLARDO, J.M. CALLEJA
"InN/InGaN multiple quantum wells emitting at 1.5 μm"
15th European Workshop on Molecular Beam Epitaxy
Zakopane (Poland), 2009

K.B. GYLFASON, C.F. CARLBORG, A. KAŹMIERCZAK, F. DORTU, H. SOHLSTRÖM, L. VIVIEN, G. RONAN, C. A. BARRIOS, W. VAN DER WIJNGAART, G. STEMME.
"A packaged optical slot-waveguide ring resonator sensor array for multiplex assays in labs-on-chip"
MicroTAS 2009
Jeju (Korea) 2009

A. HIERRO, G. TABARES, J.M. ULLOA, E. MUÑOZ, A. NAKAMURA, T. HAYASHI, J. TEMMYO
"Carrier compensation by deep levels in a-plane MgxZn1-xO Schottky photodiodes grown by RPE-MOCVD"
Spring European Materials Research Society Conference 2009
Strasburg (France), 2009

A. HIERRO, G. TABARES, J.M. ULLOA, E. MUÑOZ, A. NAKAMURA, T. HAYASHI, J. TEMMYO
"Impact of acceptor states in MgxZn1-xO Schottky photodiodes"
Internacional Conference on II-VI Compounds
Saint Petersburg (Russia), 2009

M. HOLGADO, R.CASQUEL, M.F. LAGUNAS, C. A. BARRIOS, D. LÓPEZ-ROMERO, R. PUCHADES, M.J. BAÑULS, A. MAQUIEIRA.
"Performance comparison of biophotonic sensing cells for label-free biosensing"
European Material Research Society (E-MRS). Proceedings
Strasbourg (France), 2009

J. IBAÑEZ, S. HERNÁNDEZ, E. ALARCÓN LLADÓ, R. CUSCÓ, L. ARTÚS, E. CALLEJA, S. V. NOVIKOV, C.T. FOXON
"Far infrared Transmission in AlGaN Thin Films: Normal and Oblique incidence"
8th International Conference on Nitride Semiconductors (ICNS-8)
Jeju (Korea), 2009

G.F.IRIARTE, E. SILLERO, J.G. RODRÍGUEZ, A.NAVARRO, J. PEDRÓS, F.CALLE
"E-beam lithography of nano IDT on insulating, semiconducting and conductive substrates"
33rd Workshop on Compound Semiconductor Devices and Integrated Circuits, WOCSDICE
Málaga (Spain), 2009

F. KNÖBBER, E. SILLERO, C.-C. RÖHLIG, O.A. WILLIAMS, R.E. SAH, L. KIRSTE, V. CIMALLA, C.E.NEBEL, F. CALLE, V. LEBEDEV
"Piezoelectrically actuated AlN and Nanodiamond microstructures"
18th European Workshop on Heterostructures Technology
Ulm (Germany), 2009

J. MATEOS, S. PÉREZ, R. CUERDO, E. MUÑOZ, F. CALLE, T. GONZÁLEZ
"Monte Carlo Simulation of GaN HEMTs: Influence of GaN p-type Doping and High Temperature of Operation"
33rd Workshop on Compound Semiconductor Devices and Integrated Circuits (WOCSDICE'09)
Málaga (Spain), 2009

M. MONTES, A. HIERRO, J. M. ULLOA, A. GUZMÁN, M. AL KHALFIOUI, M. HUGUES, B. DAMILANO, J. MASSIES
"1.3-1.5 μm emitting InAs quantum dot LEDs with (Ga, In)(N,As) and Ga(As,Sb) capping layers: a comparison"
Spring European Materials Research Society Conference 2009
Strasburg (France), 2009

M. MONTES, A. HIERRO, J. M. ULLOA, M. AL KHALFIOUI, M. HUGUES, B. DAMILANO, J. MASSIES
"InAs/(Ga,In)(N,As) Quantum Dot LEDs Emitting at 1.3-1.5 μm"
7th Spanish Conference on Electron Devices 2009 "CDE-09".
Santiago Compostela (Spain), 2009

A. NAKAMURA, T. HAYASHI, J. TEMMYO, A. HIERRO, G. TABARES, J.M. ULLOA, E. MUÑOZ
"Schottky barrier contacts formed on polar-, nonporlar-MgxZn1-xO film grown by remote-plasma-enhanced MOCVD"
Internacional Conference on II-VI Compounds
Saint Petersburg (Russia), 2009

J. PEDRÓS, F. CALLE, J. GRAJAL, Z. BOUGRIOUA
"Voltage tunable SAW phase shifter on AlGaN/GaN"
2009 IEEE International Ultrasonics Symposium
Roma (Italy), 2009.

A. REDONDO-CUBERO, R. GAGO, K. LORENZ, N. FRANCO, E. MUÑOZ, M.-A. DI FORTE POISSON, E. ALVES
"Depth-resolved analysis of phase separation in AlInN by ion channeling"
19th International meeting on Ion Beam Analysis (IBA 2009)
Cambridge (UK), 2009

A. REDONDO-CUBERO, K. LORENZ, N. FRANCO, S. FERNÁNDEZ-GARRIDO, R. GAGO, P.J.M. SMULDERS, E. MUÑOZ, E. CALLEJA, I.W. WATSON, E. ALVES
"Accurate measurement of strain in semiconductor heterostructures by high-energy ion channeling: the influence of steering effects"
19th International meeting on Ion Beam Analysis (IBA 2009)
Cambridge (UK), 2009

A. REDONDO-CUBERO, J. PEREIRO, J. GRANDAL, K. LORENZ, N. FRANCO, R. GAGO, E. MUÑOZ, M. A. SÁNCHEZ-GARCÍA, E. CALLEJA, E. ALVES
"Structural study of the epitaxial growth in InGaN/GaN heterostructures by ion beam analysis"
33rd Workshop on Compound Semiconductor Devices and Integrated Circuits (WOCSDICE 2009)
Málaga (Spain), 2009.

C. RIVERA, F. GONZÁLEZ-POSADA, E. MUÑOZ
"Electric-field-Induced-strain effects on the degradation of III-Nitride-based HEMTs"
33rd Workshop on Compound Semiconductor Devices and Integrated Circuits (WOCSDICE 2009)
Málaga (Spain), 2009

C. RIVERA, F.GONZÁLEZ-POSADA FLORES, E. MUÑOZ.
"Strain-induced effects on the degradation of III-Nitride-based HEMTs"
33rd Workshop on Compound Semiconductor Devices and Integrated Circuits (WOCSDICE 2009)
Málaga (Spain), 2009

J.G. RODRÍGUEZ, G.F. IRIARTE, F. CALLE
"Optimization of c-axis oriented reactive sputter deposited AlN films"
18th European Workshop on Heterostructures Technology
Ulm (Alemania), 2009

M. F. ROMERO, A. JIMÉNEZ, C. PALACIO, D. DÍAZ, E. MUÑOZ
"Electrical and Microstructural Characteristics of Ohmic Contacts formation on AlGaN/GaN HEMT"
7th Spanish Conference on Electronic Devices "CDE-09". IEEE, Electron Devices, 258-261, ISBN: 978-1-4244-2838-0
Santiago de Compostela (Spain), 2009

M. F. ROMERO, M. J. UREN, A. JIMÉNEZ, R. CUERDO, C. DUA, F. CALLE, E. MUÑOZ
"Thermal storage effects in Ni/Au-gate"
7th Spanish Conference on Electronic Devices "CDE-09".IEEE Electron Device Letters, 258-261, ISBN: 978-1-4244-2838-0
Santiago de Compostela (Spain), 2009

J.G. RODRÍGUEZ, G.F. IRIARTE, F. CALLE
"Optimization of c-axis oriented reactive sputter deposited AlN films"
18th European Workshop on Heterostructures Technology
Ulm (Alemania), 2009

J.M. ROUTOURE, B. GUILLET, L. MÉCHIN, A. VILALTA-CLEMENTE, J. GRANDAL, M. A. SÁNCHEZ-GARCÍA, S. MARTÍN, F. CALLE, P. RUTERANA
"Low frequency noise measurements in InN films"
2009 E-MRS Fall Meeting, Symposium on Indium Nitride.
Warsaw (Poland), 2009

M. SANZ, I. TANARRO, C. AROCA, M. MAICAS, P. SÁNCHEZ
"Deposition patterns obtained with a nanoparticle sputtering gun"
International Conference on Magnetism (ICM 2009)
Karlsruhe (Germany), 2009

E. SILLERO, O.A. WILLIAMS, V. LEBEDEV, V. CIMALLA, C. C. RÖHLIG, C. E. NEBEL, F. CALLE
"Nanocrystalline diamond microelectromechanical resonators"
33rd Workshop on Compound Semiconductors and Integrated Circuits, WOCSDICE 2009.
Malaga (Spain), 2009

G.TABARES, A.HIERRO, J.M.ULLOA, E.MUÑOZ, A. NAKAMURA, T. HAYASHI, J. TEMMYO
"Responsivity and transient response of non-polar Au-MgXZn1-xO Schottky photodiodes"
Spring European Materials Research Society Conference 2009
Strasburg (France), 2009

I. TANARRO, MM. SANZ, M.F. ROMERO, E. MUÑOZ, A. JIMÉNEZ
"Plasma and surface diagnostics of silicon nitride thin film coatings"
International Symposium of Plasma Chemistry 19
Bochum (Germany), 2009

J.M. ULLOA, M. DEL MORAL, R. GARGALLO, M. MONTES, A. GUZMAN, A. HIERRO, M. BOZKURT, P.M. KOENRAAD
"1.3 – 1.5 µm GaAsSb-capped InAs quantum dots: effect of the Sb content on the structural and optical properties"
Spring European Materials Research Society Conference 2009
Strasbourg (France), 2009

J.M. ULLOA, M. DEL MORAL, R. GARGALLO, M. MONTES, A. GUZMAN, A. HIERRO, M. BOZKURT, P.M. KOENRAAD
"1.3 – 1.5 µm GaAsSb-capped InAs quantum dots: effect of the Sb content on the structural and optical properties"
15th European Molacular Beam Epitaxy Workshop
Zakopane (Poland), 2009

J.M. ULLOA , P.M. KOENRAAD, M. BONNET-EYMARD, A. LÉTOUBLON, D N. BERTRU
"Effect of a lattice-matched GaAsSb capping layer on the structural properties of InAs/InGaAs/InP quantum dots"
15th European Molacular Beam Epitaxy Workshop
Zakopane (Poland), 2009

S. VALDUEZA-FELIP, F.B. NARANJO, M. GONZÁLEZ-HERRÁEZ, L. LAHOURCADE, A. WIRTHMULLER, E. MONROY, S. FERNÁNDEZ
"Influence of deposition conditions on structual properties and surface morphology of InN thin films deposited by reactive radio frecuency sputtering"
33rd Workshop on Compound Semiconductors and Integrated Circuits, WOCSDICE 2009.
Malaga (Spain), 2009

8.3 Invited Talks

2007

F. CALLE
"Nanotecnología para la información y las comunicaciones"
Jornadas AUTOMEC, University Miguel Hernández.
Elche (Alicante, Spain), 2007

E. CALLEJA
"Self-assembled MBE growth of III-Nitride Nanocolumnar Heterostructures on Si substrates"
E-MRS 2007, Spring Meeting, Symposium B
Strasburg (France), 2007

Á. GUZMÁN, E. LUNA, J. HERNANDO, E. MUÑOZ
"Quantum Well Infrared Photodetectors (QWIP), Basics and current activities at UPM University"
19th NATO/RTO Sensors and Electronics Technology Panel Business Meeting
Toledo (Spain), 2007

A. HIERRO
"Diluted Nitrides for IR Lasing Applications"
31st Workshop on Compound Semiconductor Devices and Integrated Circuits, WOCSDICE 2007
Venecia (Italy), 2007

M. MAICAS
"Synthesis of Nanostructured Magnetic Materials By Sputtering"
XVI International Materials Research Congress
Cancún (Mexico), 2007

E. MUÑOZ
"UV detectors based on GaN and ZnO"
Inter-Academia 2007. University of Shizuoka
Shizuoka , Hamamatsu (Japan), 2007

E. MUÑOZ et al.
"Wide bandgap UV photodetectos: a short review of devices and applications"
Proceedings Spie The International society for optical engineering, 6473, 64730E, 2007
San José, California (USA), 2007

J.L. PRIETO
"Importante of the e-beam stability in modern nanolithography applications".
1st Spanish Workshop on Nanolithography
Zaragoza (Spain), 2007

J.L. PRIETO
"Advanced Magnetic Sensors"
16th European Workshop on Heterostructure Technology
Fréjus (France), 2007

J.L. PRIETO
"Sub 10nm e-beam lithography at the CT-ISOM
4th NanoSpain Workshop
Sevilla (Spain), 2007)

M.A. SÁNCHEZ-GARCÍA, J. GRANDAL, A. BENGOECHEA, D. LÓPEZ-ROMERO,E. CALLEJA, S. LAZIC, J.M. CALLEJA, E. LUNA, A. TRAMPERT, M. NIEBELSCHÜTZ, V. CIMALLA, O. AMBACHER
"MBE growth and characterization of InN on Silicon substrates"
European Materials Research Society Meeting (E-MRS) 2007
Symposium F (Novel Gain Materials and Devices based on III-N-V compounds)
Strasbourg (France), 2007

2008

E. CALLEJA et al.
"Spontaneous Growth of III-Nitride nanocolumns by Molecular Beam Epitaxy: Optical, Structural and Electrical Characterization"
Ecole Polytechnique Fédérale de Lausanne
Lausanne (Suiza), 2008

A. GUZMAN, E. LUNA, A. TRAMPERT, E. MUÑOZ
"Multicolor absorption using Quantum Well Infrared Photodetectors based on dilute nitrides"
Workshop on Frontier Optoelectronic Materials and Devices
Hakone (Japan), 2008

N. KARAYIANNIS
"Hierarchical Modeling of polymeric materials : structure-property predictions form atomistic simulations »
Seminarios de Fronteras de ciencia de materiales-UPM
Madrid (Spain), 2008

E. MUÑOZ et al.
"Optoelectrónica basada en semiconduc tores (Al,Ga,In)N"
Universidad de Chile, Facultad de Ingenieria
Santiago de Chile (Chile), 2008

E. MUÑOZ et al.
"Detectores de UV y VIS basados en AlGaN
Universidad Nacional de La Plata y Centro de Investigaciones Opticas (CIOP)
La Plata (Argentina), 2008

C. RIVERA
"Influence of Piezoelectric Effects on the Electrical and Optical Properties of GaN-based Quantum-Well and Quantum-Disk Structures"
Seminario invitado, Paul-Drude-Institut für Festkörperelektronik, 29 agosto de 2008
Berlín (Germany), 2008

M.A. SÁNCHEZ- GARCÍA, J. GRANDAL, A. BENGOECHEA, E. CALLEJA, S. LAZIC, E. GALLARDO, J.M. CALLEJA, E. LUNA, A. TRAMPERT
"MBE growth and characterization of InN-based layers and nanostructures"
Workshop on Frontier Photonic and Electronic Materials and Devices
Hakone, (Kanagawa, Japan), 2008

M.A. SÁNCHEZ-GARCÍA, J. GRANDAL, E. CALLEJA, S. LAZIC, J.M. CALLEJA, E. LUNA, A. TRAMPERT
"Growth and characterization of Nitrides-based (GaN, AlN, InN) nanostructures"
European Materials Research Society Meeting (E-MRS) 2008
Symposium G (Wide band gap semiconductor nanostructures for optoelectronic applications)
Estrasburgo (France), 2008

M.A. SÁNCHEZ- GARCÍA, J. GRANDAL, E. CALLEJA, S. LAZIC, E. GALLARDO,J.M. CALLEJA, E. LUNA, A. TRAMPERT, M. NIEBELSCHÜTZ, V. CIMALLA, O. AMBACHER
"Growth and characterization of Nitrides-based (GaN, AlN, InN) nanostructures"
Mini-Symposium on Physics and Applications of InN and InGaN Semiconductor Materials The Rank Prize Funds.
Grasmere (U.K), 2008

J.M. ULLOA et al.
"Atomistic Modelling of III-V Semiconductors: from a single tetrahedron to millions of atoms"
17th Heterostructure Technology Workshop
Venice (Italy), 2008

2009

E. CALLEJA et al.
"Recent Results on III-Nitride Nanorods and Inn Qws: Growth Mechanisms, Basics and Devices"
United Kingdom Nitride Consortium Annual Meeting
University of Oxford (England), 2009

E. CALLEJA et al.
"Characterization on In(Ga)N nanorods and MQWs grown by MBE"
UK Nitrides Consortium
Oxford (UK), 2009

E. CALLEJA et al.
"Self-Assembled and Ordered MBE Growth of III-Nitride Nanocolumns: Mechanisms, Characterization, And Nanodevices"
Spie Symposium on Opto: Integrated Optoelectronic Devices
San Jose (USA), 2009

E. CALLEJA et al.
"Recent progress in growth of III-N nanorods on polar and nonpolar orientation"
15th European Molecular Beam Epitaxy Workshop
Zakopane (Poland), 2009

E. CALLEJA et al.
"Recent progress on the growth of self-assembled and ordered III-N nanorods on polar and nonpolar substrates"
First European Workshop on MBE-Grown Nitride Nanowires
Berlin (Germany), 2009

E. CALLEJA et al.
"Spontaneous and ordered growth of III-N nanorods on polar and non-polar substrates"
European Materials Research Society (E-MRS) Fall Meeting 2009
Warsaw (Poland), 2009

E. CALLEJA et al.
"Progress on the spontaneous and ordered growth of III-N nanorods: model, growth on nonpolar substrates and applications"
2009 MRS Fall Meeting
Boston (USA), 2009

E. CALLEJA et al.
"Recent results on the spontaneous and ordered growth of III-N nanocolumns: growth on nonpolar substrates and applications to Optoelectronic Devices"
Worshop On frontiers in electronics, WOFE-09
Puerto Rico (USA), 2009

R. CUERDO, E. MUÑOZ, F. CALLE
"Performance of AlGaN-GaN HEMTS at high temperatura"
ESA-MoD Workshop on GaN Microwave Component Technologies.
Ulm (Germany), 2009

R. CUERDO, E. MUÑOZ, F. CALLE
"Characterisation of Nitride-based HEMTs at high temperatures".
ESA-MoD Workshop on GaN Microwave Component Technologies.
Ulm (Germany), 2009

G.F.IRIARTE et al.
"La Ciencia de Materiales en la Era Nano"
Universidad de la Habana
La Habana (Cuba), 2009

E.MUÑOZ et al.
"Recent Advances on AlGaN photodetectors"
University of Shizuoka, Research Inst. of Electronics
Tokyo (Japan), 2009

E.MUÑOZ et al.
"Materials and Strain Issues in AlGaN/GaN HEMT Degradation"
2009 International Conference on Solid State Devices and Materials (ISSDM 2009)
Tokyo (Japan), 2009

8.4 Ph.D. Thesis

Title:	**"Dispositivos SAW en estructuras de nitruros del grupo III: propagación y modulación óptica y electrónica"**
Author:	Jorge Pedrós Ayala
Director:	Fernando Calle Gómez
University:	University Politécnica de Madrid, E.T.S. Ing. de Telecomunicación, 2007
Grade:	Sobresaliente "Cum Laude"

Title:	**"Estudio de estructuras de baja dimensionalidad y avanzadas para detección de radiación visible y ultravioleta basadas en Nitruros del grupo III"**
Author:	Carlos Rivera de Lucas
Director/s:	Elías Muñoz Merino & JL. Pau Vizcaíno
University:	University Politécnica de Madrid, E.T.S. Ing. de Telecomunicación, 2007
Grade:	Sobresaliente "Cum Laude"

Title:	**"Modelización y monitorización de la calidad de la combustión en función de la información luminosa existente en la llama en calderas domésticas"**
Author:	Javier Anduaga Salvatierra
Director:	Elías Muñoz Merino
University:	University Politécnica de Madrid, E.T.S. Ing. de Telecomunicación, 2007
Grade:	Sobresaliente "Cum Laude"

Title:	**"Estudio de las propiedades magnéticas y magnetostrictivas de materiales magnéticos bandos desarrollados mediante tecnologías multicapa. Aplicación a detectores y dispositivos"**
Author:	David Ciudad Rio Pérez
Director/s:	Pedro Sánchez-Sánchez & Claudio Aroca Hernández-Ros
University:	University Politécnica de Madrid, E.T.S. Ing. de Telecomunicación, 2008
Grade:	Sobresaliente "Cum Laude"

Title:	**"Materiales Magnéticos modulados en el espesor. Aplicación en dispositivos"**
Author:	Miguel González-Guerrero Bartolomé
Director/s:	Pedro Sánchez Sánchez & José Luis Prieto
University:	University Politécnica de Madrid, E.T.S. Ing. de Telecomunicación, 2008
Grade:	Sobresaliente "Cum Laude"

Title:	**"Crecimiento y caracterización de nitruro de indio por epitaxia de haces moleculares para aplicaciones en el infrarrojo cercano"**
Author:	Javier Grandal Quintana
Director:	Miguel Ángel Sánchez García
University:	University Politécnica de Madrid, E.T.S. Ing. de Telecomunicación, 2009
Grade:	Sobresaliente "Cum Laude"

Title:	**"Crecimiento de nitruros del grupo III por epiaxia de haces moleculares para la fabricación de diodos electroluminiscentes en el rango visible-ultravioleta"**
Author:	Sergio Fernández Garrido
Director:	Enrique Calleja Pardo
University:	University Politécnica de Madrid, E.T.S. Ing. de Telecomunicación, 2009
Grade:	Sobresaliente "Cum Laude"

Title:	**"Aspectos estructurales, deformación y superficies en relación con la fiabilidad de transistores de alta movilidad electrónica basados en heteroestructuras de AlGaN/GaN"**
Author:	Fernando González- Posada Flores
Director:	Elías Muñoz Merino
University	University Politécnica de Madrid, E.T.S. Ing. de Telecomunicación, 2009
Grade:	Sobresaliente "Cum Laude"

Title:	**"Diseño, crecimiento, caracterización y fabricación de detectores de luz ultravioleta y visible basados en pozos cuánticos de nitruros del grupo III"**
Author:	Juan Pereiro Viterbo
Director:	Elías Muñoz Merino
University	University Politécnica de Madrid, E.T.S. Ing. de Telecomunicación, 2009
Grade:	Sobresaliente "Cum Laude"

8.5 B.Sc. Thesis

Title	**"Estudio de la oxidación electroquímica activada por luz de nitruros del grupo III"**
Author:	Pablo Tapia Reyero
Director/s:	José Luis Pau Vizcaíno & Elías Muñoz Merino
Date:	July 17th, 2007
Grade:	Matrícula de Honor, 10 p.

Title:	**"Automatización de las variables ambientales de una sala limpia"**
Author:	José Ramón Durán Retamal
Director:	Álvaro de Guzmán Fernández González
Date:	July 24th, 2007
Grade:	Sobresaliente, 9, 5 p.

Title:	**"Optimización de un sistema de sputtering para el depósito de películas delgadas de nitruro de aluminio"**
Author:	Rocío San Román Alonso
Director:	Gonzalo Fuentes Iriarte
Date:	July 18th, 2008
Grade:	Matrícula de Honor, 10 p.

Title:	**"Algunos aspectos de Fiabilidad y Degradación en transistores HEMT de GaN"**
Author:	Carolina Sánchez Muñoz
Director:	Elías Muñoz Merino
Date:	September 24th, 2008
Grade:	Sobresaliente, 9, 5 p.

Title**:**	**"Fabricación y caracterización de sensores de ph basados en nitruros y su control en la red"**
Author:	Javier Eroles Matallana
Director:	Fernando Calle
Date:	December 19th, 2008
Grade:	Matrícula de Honor, 10 p.

8.6 Patents

Inventors: David Ciudad Río-Pérez, Claudio Aroca Hernández-Ros, D. Pedro Sánchez Sánchez, D. Jose Luis Prieto Martin

Title: ***"Detector de campo magnético, mecánico y miniaturizable y su funcionamiento"***

Number of Request: P200703420

Country of Priority: Spain

Date of Priority: 2.007

Entidad titular: Universidad Politécnica de Madrid

Countries to which it has spread: Spain

Inventors: David Ciudad Río-Pérez, Claudio Aroca Hernández-Ros, Pedro Sánchez Sánchez

Title: ***"Gradiómetro de campo magnético, mecánico y miniaturizable y su funcionamiento"***

Number of Request: P200703421

Country of Priority: Spain

Date of Priority: 2.007

Entidad titular: Universidad Politécnica de Madrid

Countries to which it has spread: Spain

Inventors: David Ciudad Río-Pérez, Claudio Aroca Hernández-Ros, Pedro Sánchez Sánchez

Title: ***"Sistema de medida de gradiente de campo magnético***

Number of Request: P200703422

Country of Priority: Spain

Date of Priority: 2.007

Entidad titular: Universidad Politécnica de Madrid

Countries to which it has spread: Spain

Inventors: Carlos Rivera de Lucas, Elías Muñoz Merino, Holger T. Grahn

Title: ***"Sistema de detección de la polarización de la luz con respuesta paso de banda"***

Number of Request: P200701926

Country of Priority: Spain

Date of Priority: 2.008

Entidad titular: Universidad Politécnica de Madrid

Countries to which it has spread: Spain

Inventors: Alin Javorsky, Claudio Aroca Hernández-Ros, Francisco del Pozo Guerrero, María del Mar Sanz Lluch, José María Gaztelu Quijano, Fernando Maestu Unturbe, Marco C. Maicas Ramos, Javier García Pacios, Ceferino Maestu Unturbe, María Romero Vives, Juan Antonio Barios Heredero.

Title: ***"Procedimiento de detección de nanopartículas magnéticas mediante magnetoencefalografía"***

Number of Request: P200901528

Country of Priority: Spain

Date of Priority: 2.009

Entidad titular: Universidad Politécnica de Madrid - Fundación para la Investigación Biomédica del Hospital Ramón y Cajal (FIBio HRC)-Universidad Complutense de Madrid (UCM)

Countries to which it has spread: Spain

Inventors: Álvaro Navarro Tobar

Title: ***"Método y sistema de medida del tiempo de vida de fluorescencia en el dominio de la frecuencia con altos niveles de señal de fondo"***

Number of Request: P200901614

Country of Priority: Spain

Date of Priority: 2.009

Entidad titular: Universidad Politécnica de Madrid

Countries to which it has spread: Spain

Inventors: Julie Vincent Cros, Julie Grollier, Manuel Muñoz Sánchez, Albert Fert, Frederic Nguyen Van Dau

Title: ***"Spintronic devices with control by domain wall displacement induced by a current of spin-polarized carriers"***

Number of Request: US 2009/0273421 AI

Country of Priority: USA-FR

Date of Priority: 2.009

Entidad titular: Thales, Neuilly-Sur-Seine (FR)

Countries to which it has spread: USA-FR

9 R&D COLLABORATIONS, SERVICES AND SEMINARS

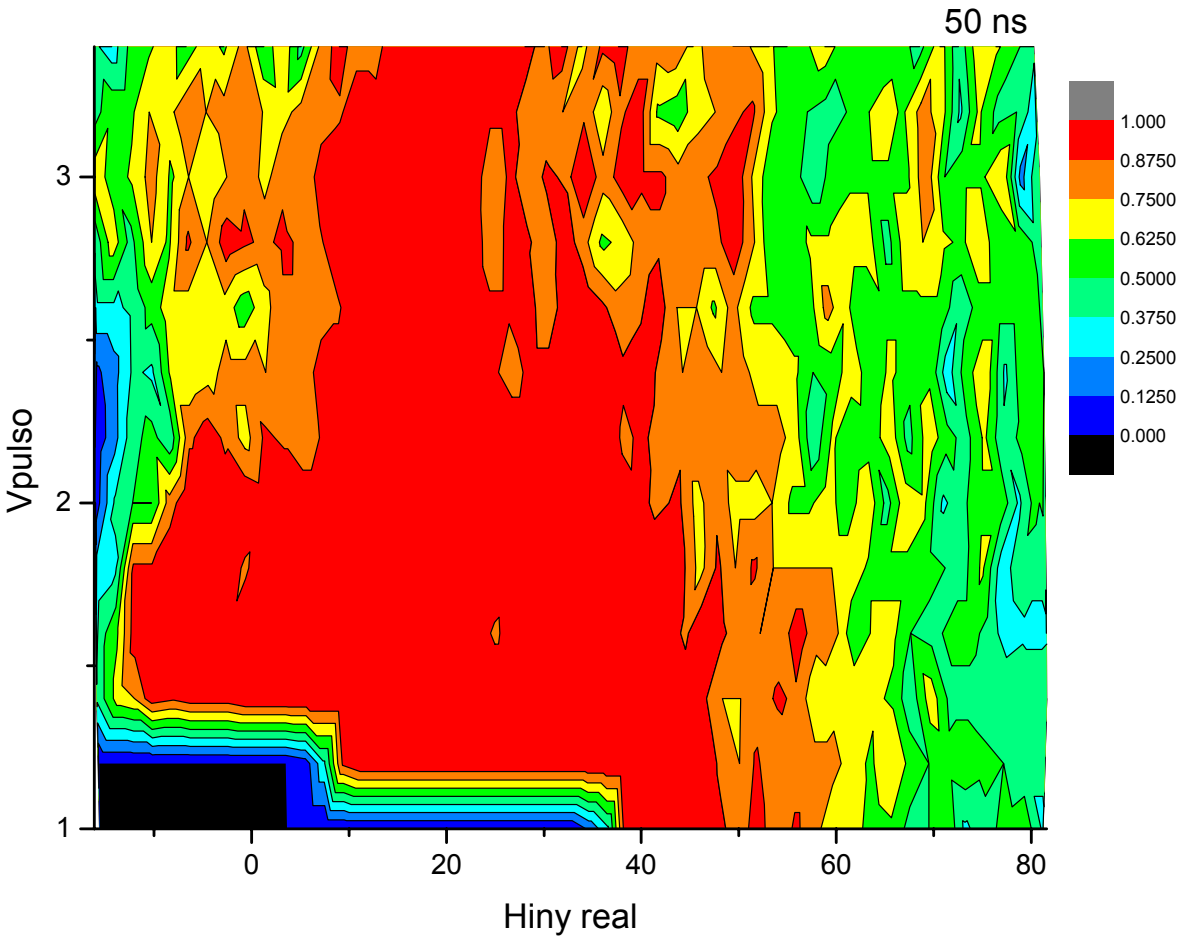

Probability map for the creation of a magnetic domain wall in a permalloy nanowire, with a short electrical pulse flowing through a current line on top. There are regions of probability one, even for zero magnetic field, which is very important for the implementation of future magnetic memories.

9.1 International Sientific Collaborations

- Walter Schottky Institute, Munich (Germany)
- Paul Drude Institute, Berlin (Germany)
- Ferdinand Braun Institute, Berlin (Germany)
- Fraunhofer IAF Institute, Friburg (Germany)
- University of Braunschweig (Germany)
- OSRAM gmbH, Regensburg (Germany)
- Centre de Recherche de L'Hetero-epitaxie, CNRS, Valbonne (France)
- National Microelectronics Research Center, Cork (Ireland)
- University of Queensland (Australia)
- University of Sheffield (UK)
- Lawrence Berkeley Labs. (USA)
- Santa Barbara California University (USA)
- Ohio State University, (USA)
- Cornell University (USA)
- MIT, Cambridge (USA)
- National Institute of Standards and Technology, NIST (USA)
- Ecole Politechnique Federale de Lausane (Switzerland)
- INTEC/IMEC, Leuven (Belgium)
- Technische Universiteit Eindhoven (The Netherlands)
- The University of Cambridge (UK)
- University Giessen (Germany)
- United Monolithic Semiconductors GmbH (Germany)
- Research Institute of Electronics, National University Corporation, Shizuoka University (Japan)
- Ritsumeikan University. Dept of Photonics (Japan)
- Kochi University of Technology (Japan)
- NTT, Basic Research Labs., Atsugi (Japan)

9.2 National Sientific Collaborations

- Centro de Investigación y Desarrollo de la Armada, CIDA
- Centro de Inv. Energéticas, Medio Ambientales y Tecnológicas, CIEMAT
- Institut Jaume Almera, CSIC, Barcelona.
- Instituto de Ciencia de Materiales de Madrid, ICMM-CSIC
- Centro Nacional de Microelectrónica, Barcelona, CNM-CSIC- ISOM
- Instituto de Microelectrónica de Madrid, IMM-CNM-CSIC
- Instituto Nacional de Técnica Aeroespacial, INTA
- Universidad Autónoma de Madrid
- Universidad Complutense de Madrid
- Universidad de Cádiz
- Universidad Miguel Hernández de Alicante
- Universidad de Oviedo
- Universidad de Valencia
- Universidad de Málaga
- Universidad Rey Juan Carlos

9.3 External Services (ICTS)

The services offered by CT-ISOM relate to technologies available at the Institute:

- **SAMPLE GROWTH**
    - Joule metallization (Au, AuGe, AuZn, Ni, etc)
    - e-beam metallization (Au, Pt, Ti, Al, etc.)
    - Chemical Vapour Deposition (CVD) for insulators (Si-O-N systems)
    - Sputtering for magnetic materials (Fe, Ni, Co, FeNi, etc.)
    - Molecular Beam Epitaxy (MBE) for semiconductors (AlGaInAs and AlGaInN materials systems)
    - Electrodeposition of Au, Ni, CoP, etc.
    - Air-bridge contacts fabrication
- **PROCESSING TECHNIQUES**
    - **Lithography**
        - E-line nanolithography (line resolution > 10 nm)
        - Electron beam lithography (EBL) (resolution > 300 nm)
        - Photolithography (resolution > 1 micron)
        - Optical Mask design
    - **Chemical, Thermal and Mechanical Treatment**
        - Cleaning (Organic, acid chemicals...)
        - Polishing (machine and hand)
        - Precission cutting
        - Reactive Ion Etching (RIE)
        - Wet Etching
        - Rapid Thermal Annealing (RTA)
    - **Soldering and packaging**
        - Soldering, TO-5, TO-8, other packaging
- **SAMPLE CHARACTERIZATION**
    - **Optical Characterization (materials)**
        - Photoluminescence at IR-VIS-UV at temperatures within the range 10-300K
        - Electroluminescence
        - FTIRS (600 nm-20 microns)
        - Ellipsometry
    - **Optoelectronic Characterization (structures and devices)**
        - Spectral responsivity of detectors (from 12 microns to 200 nm)
        - Spectral laser emission (from 600 to 1700 nm)
        - Spectral luminescence emission (from 200 nm to 2.5 micros)
        - L-I curves in UV-VIS-IR lasers
    - **Electrical and Magnetical Characterization**
        - Resistivity measurements, room temperature
        - Hall measurements, variable with temperature (100-300K)
        - C-V and I-V measurements (temperature and frequency dependence)
        - Hysteresis cycles for thin films
    - **Microscopic, Morphological and Structural Characterization**
        - Thin film thickness measurements (*Dek-Tak* profiler)
        - Nomarski contrast microscope
        - EDX characterization and morphological measurements by SEM
        - AFM and MFM Characterization
        - X-Ray Diffraction

The Institutions that received services from CT-ISOM during the period 2007-2009 are the following:

2007

- **Universidad de Valladolid**

Researchers: D. César Pérez Muñoz
Research line: Experiencias sensoriales con cantilevers

- **Universidad de Valencia. (Instituto de Ciencias e Materiales)**

Researchers: D. José Marqués
Research line: Fabricación de cavidad resonante de heteroestructura y lente fotónica en guía óptica micrométrica.

- **University of Birmingham. (Materials Department)**

Researchers: D. Jon Preece
Research line: E-beam Lithography on Organic Self-Assembled Monolayers

- **Universidad Autónoma de Madrid. (Departamento de Física de Materiales)**

Researchers: D. José Manuel Calleja Pardo
Research line: Fabricación de nanocolumnas de GaN e InN para espectroscopía óptica

- **University of Cambridge. (Dept. of Materials Science and Metallurgy)**

Researchers: D. Mark Blamire
Research line: "E-Line" nanolithographic patterning of nano-pillar arrays for the purpose of realising spin-torque devices.

- **Univ Complutense Madrid. (Dpto Física de Materiales)**

Researchers: Dª. Arantzazu Mascaraque
Research line: Propiedades mecánicas de nanoestructuras metálicas en óxido de titanio

- **Universidad Rey Juan Carlos**

Researchers: D. Ángel Luis Álvarez
Research line: Caracterización estructural (medida de espesores), óptica (microscopía de contraste) y de respuesta eléctrica (I-V, C-V) de diodos orgánicos electroluminiscentes (OLEDs)

- **Universidad de Salamanca .Facultad de Físicas**

Researchers: D. Enrique Diez
Research line: Procesado de pozos cuánticos y superredes de InGaAs/InAlAs y GaAs/AlGaAs y obtención de Grafeno a partir de HPOG

- **Universidad de Oviedo .Grupo de Láminas Delgadas y Nanoestructuras Magnéticas**

Researchers: D. Javier Diaz
Research line: Estudio microscópico de la magnetostricción en aleaciones amorfas de FeCoB.

- **Instituto Energía Solar-UPM**

Researchers: D. Ignacio Rey-Stolle
Research line: Caracterizaciones complementarias de materiales fotovoltaicos basados en Semiconductores II-V

- **Universidad Complutense Madrid. (Departamento de Química Orgánica)**

Researchers: D. Guillermo Orellana
Research line: Corte de precisión de varilla de vidrio poroso

- **Instituto de Ciencia de Materiales de Madrid-CNM-CSIC**

Researchers: Dª. Luisa González Sotos
Research line: Dependencia de la energía e intensidad de emisión de fotoluminiscencia de puntos cuánticos InAs/AlAs, InP/InGaP con ciclos RTA

- **Institut Català de Nanotecnologia.Campus de la UAB.Barcelona**

Researchers: Dª. Eva Pellicer
Research line: Fabricación de dispositivos de espín basados en nanotubos de carbono.

- **Universidad Autónoma de Madrid (Departamento de Física de Materiales)**

Researchers: D. José Manuel Calleja
Research line: Fabricación de estructuras n-i-n con pozos cuánticos de InGaN para el estudio de dispositivos electrostictivos mediante espectroscopía Raman.

- **Universidad de Oviedo**

Researchers: D. Javier Fernández Calleja
Research line: Caracterización magnética y estructural de películas delgadas de Co.

- **Universidad Politécnica de Valencia. Grupo de Comunicaciones Ópticas y Cuánticas. Valencia**

Researchers: D. Pascual Muñoz
Research line: Fabricación de arrayed waveguide gratings con mounting optimizados.

- **Centro Láser-UPM. Madrid**

Researchers: D. Rafael Casquel
Research line: Caracterización de dispositivos fotónicos basados en estructuras resonantes.

- **Universidad Miguel Hernández. Elche**

Researchers: D. José Luis Alonso
Research line: Metalización y caracterización de sistemas híbridos polímero-nanopartículas para aplicaciones en fotodetectores y dispositivos fotovoltáicos.

- **INTA- Dto.de C.C. del Espacio y Programas Espaciales Instituto Nacional de Técnica Aeroespacial – Madrid**

Researchers: Dª. Marina Diaz Michelena
Research line: Colaboración para el desarrollo de un mini/micro imán permanente sobre una estructura de silicio micromecanizada

- **Imperial Collage of London.Material Department.Reino Unido**

Researchers: Dª. Anna Axelsson
Research line: Template-Growth and Nano-Dots patterning of ferroic materials using Nanolithography

- **Facultad de Físicas-Universidad de Salamanca**

Researchers: D. Enrique Diez
Research line: Procesado de pozos cuánticos y superredes de InGaAs/InAlAs y GaAs/AlGaAs y obtención de Grafeno a partir de HPOG (II)

2008

- **Instituto de Acústica-CSIC**

Researchers: D. Francisco Montero Espinosa
Research line: Integración de array cMUT en placa por wirebonding

- **Universidad Autónoma de Madrid. Departamento de Física de Materiales.**

Researchers: D. José Manuel Calleja Pardo
Research line: Fabricación de estructuras n-i-n con pozos cuánticos de InGaN para el estudio de dispositivos electrostictivos medante espectroscopía Raman.

- **Universidad de Valencia. ICMUV. Valencia**

Researchers: D. Paulo F. Gomes
Research line: Espectroscopía de puntos cuánticos aislados tipo II de InP/GaAs

- **Universidad de Valencia. ICMUV. Valencia**

Researchers: D. Mauricio Morais de Lima
Research line: Moduladores y conmutadores ópticos por medio de ondas acústicas de superficie

- **Instituto de Química y Física, ROCASOLANO-CSIC. Madrid**

Researchers: D. Mikel Sanz Monasterio
Research line: Caractarización por rayos X y AFM de muestras de diferentes semiconductores depositadas por ablación láser (PLD) en diferentes sustratos (Si(100), Cuarzo) y medida del espesor de la capa depositada

- **Instituto de Cerámica y Vidrio. CSIC- Madrid**

Researchers: D. José Francisco Fernández
Research line: Estudio de la respuesta funcional de interfases en óxidos

- **Escuela Universitaria de Ingenieria Técnica de Telecomunicación. Departamento de Física Aplicada a las Tecnologías. UPM**

Researchers: Dª. Elvira Paz Pérez de Colosía
Research line: Litografía de nanoestructuras en láminas delgadas de hierro

- **Instituto de Ciencia de Materiales de Madrid-CNM-CSIC**

Researchers: D. Jonathan Rodríguez
Research line: RTA sobre CdTe epitaxial

- **Universidad Complutense de Madrid. Facultad de CC Químicas. Madrid**

Researchers: Dª. Virginia Bouzas
Research line: Propiedades magnéticas de nanopartículas de Fe2

- **Universidad Complutense de Madrid. Facultad de CC Químicas. Madrid**

Researchers: Dª. Laura Miranda
Research line: Caracterización magnética del sistema AT-Co-O2,5+δ (AT = Ba, Sr, Ca; $0 \leq \delta \leq 0.5$)

- **Walter Schottky Institute, Technische Universität München. Germany**

Researchers: D. Markus Dankerl
Research line: Nanostructuring of diamond surfaces for biosensing applications

- **Universidad de Salamanca**

Researchers: D. Enrique Díez
Research line: Procesado de pozos cuánticos y superredes InGaAs/InAlAs y GaAs/AlGaAs y obtención de grafeno a partir de HPOG

- **Universidad de Barcelona**

Researchers: D. Miguel Rubio Roy
Research line: Superficies nanoestructuradas para aplicaciones tribiológicas

- **Instituto de Ciencia de Materiales de Madrid (ICMM-CSIC)**

Researchers: D. Manuel Vázquez
Research line: Fabricación de nanohilos de Permalloy para estudios de interacción magnetostática

- **Centro Láser –UPM. Madrid**

Researchers: D. Miguel Holgado
Research line: Depósito capas de Si, SiO2 y Si3N4 sobre obleas de Si para la realización de estructuras opto-fluídicas mediante técnicas de micro-fabricación láser

- **Universidad de Oviedo**

Researchers: D. Javier Diaz Fernández
Research line: Estudio microscópico de la magnetostricción en aleaciones amorfas de FeCoB

- **Universidad Rey Juan Carlos**

Researchers: Dª. María del Carmen Coya
Research line: Fabricación de máscaras y procesado parcial de diodos orgánicos electroluminiscentes (OLEDs) y transistores orgánicos (OFETs)

- **Instituto de Energía Solar-UPM**

Researchers: D. Aline Cristiane Pan/ D.Carlos del Cañizo
Research line: Caracterización de convertidores fotónicos

- **Universidad de Valencia**

Researchers: D. José Marqués/Juan Martínez Pastor
Research line: Fabricación de cavidad fotónica H1 modificada en GaAs

- **Universidad Complutense de Madrid. Facultad de Farmacia**

Researchers: D. Eduardo Ruiz Hernández/ DªMaría Vallet
Research line: Medida de propiedades magnéticas de biomateriales

- **Universidad de Valencia. ICMUV. Valencia**

Researchers: D. Mauricio Morais de Lima
Research line: Moduladores y conmutadores ópticos por medio de ondas acústicas de superficie-II

- **Universidad Complutense de Madrid. Fac. CC Físicas**

Researchers: D. José María Rico García
Research line: Fabricación de antenas ópticas

- **Universidad de Salamanca**

Researchers: D. Enrique Díez
Research line: Anillos cuánticos y sus aplicaciones a enfriamiento electrónico

- **Escuela Técnica Superior de Ingenieros de Telecomunicación. Dept. Fotónica. UPM**

Researchers: Dª. Beatriz Cerrolaza Martínez/ D. Morten Andreas Geday
Research line: Desarrollo de electrodos de alta resolución para deflector de haz basado en cristal líquido

- **Universidad Alcalá de Henares**

Researchers: D. Fernando Naranjo
Research line: Medida de espesor de capas de Al empleando el perfilómetro

2009

- **Universidad de Salamanca**

Researchers: D. Mario Amado /D. Enrique Díez
Research line: Nanodispositivos en grafeno

- **Instituto de Estructura de la Materia-CSIC. Madrid**

Researchers: Dª. Concepción Domingo
Research line: Fabricación de nanoantenas de oro y caracterización de las mismas mediante SEM y AFM, para su posterior utilización como sustratos en sensores moleculares SERS, SEIRA y SEF

- **Universidad Complutense de Madrid. CAI Técnicas Físicas**

Researchers: Dª. Rosa Cimas Cuevas
Research line: Fabricación de una muestra patrón para estudios de AFM

- **Universidad Complutense de Madrid. Fac. CC Físicas**

Researchers: Dª. Paloma Fernández Sáchez
Research line: Fabricación de contactos para medidas eléctricas en nanohilos de óxidos semicondutores

- **CRHEA-CNRS (Francia)**

Researchers: D. Jean Michel Chaveau
Research line: Nanopattering of ZnO layers

- **Escuela Técnica Superior de Ingenieros Industriales. Laboratorio de Metrología Dimensional-UPM**

Researchers: D. Jesús Vicente y Oliva
Research line: Fabricación de pozos micro y sub-micrométricos para metrología y trazabilidad de volúmenes de líquidos mediante técnicas avanzadas de metrología óptica

- **Instituto de Física Aplicada-CSIC**

Researchers: D. Manuel Muñoz Sánchez
Research line: Defectos variables en etiquetas de permaloy

- **Fac. CC Físicas-UCM**

Researchers: Dª. Elvira González Herrera
Research line: Patterning of Nb films with non superconducting nanometric arrays

- **Universidad Complutense de Madrid. Fac. CC Físicas**

Researchers: D. Carlos Díaz-Guerra Viejo
Research line: Caracterización magnética de nanoestructuras alargadas de óxidos de hierro

- **Universidad de Valladolid**

Researchers: Dª. Mónica Gay Martín/ Dª Mari Luz Rodríquez
Research line: Estudio de la morfología de películas delgadas basadas en bisftalocianinas mediante AFM

- **Universitá de Pavía (Italia)**

Researchers: D. Vittorio Bellani / D. Francesco Rosella
Research line: Proccesing of graphene flakes for the obtention of graphene nano ribbons and electron viliards for transport and optical investigations

- **Instituto de Materiales de Madrid-CNM-CSIC**

Researchers: D. Antonio Rivera de Mena/ Dª Luisa González
Research line: Dispositivos nanoestructurados para Información Cuántica

- **Instituto de Enegía Solar-UPM**

Researchers: D. Ignacio Rey Stolle
Research line: Caracterizaciones complementarias de materiales fotovoltaicos basados en semiconductores III-V (III)

- **Universidad Rey Juan Carlos**

Researchers: Dª. María del Carmen Coya
Research line: Fabricación de máscara óptica y procesado parcial de sustratos para la fabricación de transistores orgánicos (OFETs) para el estudio de las propiedades de transporte de materiales amorfos.

- **Universidad Politécnica de Valencia. Departamento de Química**

Researchers: D. José María Bañuls Polo
Research line: Activación química y biofuncionalización de estructuras fotónicas

9.4 Stays of ISOM members in foreign Institutions

2007

D. Roberto Cuerdo Bragado **"University of California"** Santa Bárbara	**USA**	**12 week/s**
D. Sergio Fernández – Garrido, **"UNIPRESS, Poland"** Varsovia	**Poland**	**12 week/s**
Dª. Raquel Gargallo Caballero **"University of Sheffield"** Sheffield	**United Kingdom**	**12 week/s**
D. Miguel Montes Bajo **"University of Sheffield"** Sheffield	**United Kingdom**	**12 week/s**
D. Álvaro Navarro Tobar **"University of Sheffield"** Sheffield	**United Kingdom**	**12 week/s**
D. Juan Gabriel Madrid **"IMEC (Interuniversity Microelectronic Center)"** Leuven	**Belgium**	**14 week/s**
Dª. Sara Martín Horcajo **"IMEC (Interuniversity Microelectronic Center)"** Leuven	**Belgium**	**14 week/s**
D.José Luis Prieto Martín ***"Cambridge University*** Londres	**United Kingdom**	**4 week/s**
Dª. Rocío Ranchal **"Paul-Drude-Institut für Festkörperelektronik"** Berlín	**Germany**	**48 week/s**
Dª. María del Carmen Sabido **"IMEC (Interuniversity Microelectronic Center)"** Leuven	**Belgium**	**9 week/s**
D. José María Ulloa Herrero **"Technical University Eindhoven"** Eindhoven	**The Netherlands**	**44 week/s**

2008

Dª. Ana Bengoechea Encabo **"Walter Schottky Institute"** Munich	**Germany**	**8 week/s**
D. Roberto Cuerdo Bragado **"University of California"** Santa Bárbara	**USA**	**12 week/s**

Dª. Sara Martín Horcajo
"IMEC (Interuniversity Microelectronic Center)"
Leuven **Belgium** **14 week/s**

D. Juan Gabriel Madrid
"IMEC (Interuniversity Microelectronic Center)"
Leuven **Belgium** **14 week/s**

Dª. Rocío Ranchal
"Paul-Drude-Institut für Festkörperelektronik"
Berlín **Germany** **44 week/s**

Dª. María del Carmen Sabido
"IMEC (Interuniversity Microelectronic Center)"
Leuven **Belgium** **20 week/s**

D. Eugenio Sillero Herrero
"Instituto de física aplicada de estado sólido (IAF), Fraunhofer Gesellschaft"
Friburgo **Germany** **18 week/s**

2009

D. Zarko Gacevic
"CEA-GRENOBLE, CEA/Grenoble, Department of Fundamental Research on Condensed Matter"
Grenoble **France** **12 week/s**

Dª. Raquel Gargallo Caballero
"Paul-Drude Institute für Festkörperelektronik, Microelectronics Department"
Berlin **Germany** **4 week/s**

Dª. Raquel Gargallo Caballero
"Eindhoven University of Technology"
Eindhoven **The Netherlands** **4 week/s**

D. Adrián Hierro Herrero
"Research Institute for Electronics – University of Shizuoka"
Shizuoka **Japan** **4 week/s**

Dª. Rocío Ranchal
"Paul-Drude-Institut für Festkörperelektronik"
Berlín **Germany** **8 week/s**

D. Andrés Redondo Cubero
"Instituto Tecnológico e Nuclear"
Sacavém **Portugal** **6 week/s**

D. Eugenio Sillero Herrero
"Instituto de física aplicada de estado sólido (IAF), Fraunhofer Gesellschaft"
Friburgo **Germany** **13 week/s**

D. José María Ulloa Herrero
"Technical University Eindhoven"
Eindhoven **The Netherlands** **4 week/s**

9.5 Program Committees Membership

2007

Fernando Calle
Member of Steering Committee
16th European Heterostructure Technology Workshop, HETECH'07
Niza (France), 2007

Fernando Calle
Member of Program Committee
Telecom I+D 2007
Valencia (Spain), 2007

Enrique Calleja
Chairman of the Organizing Committee, Session Chairman
14th European Workshop on Molecular Beam Epitaxy
Granada (Spain), 2007

Enrique Calleja
Member of the Conference Committee Board and Advisory Board
3rd Nano and Giga Challenges in Electronics and Photonics (NGC2007)
Phoenix-Arizona (USA), 2007

Enrique Calleja
Member of the Conference Committee Board and Advisory Board
6th Int. Conf. of Light-Matter Coupling in Nanostructures (PLMCN6)
Magdeburg (Germany), 2007

Enrique Calleja
Member of the Conference Committee Board and Advisory Board
7th International Conference on Nitride Semiconductors (ICNS-7)
Las Vegas, (USA), 2007

Adrián Hierro
Member of Local Organizing Committee
14th European Workshop on Molecular Beam Epitaxy
Granada (Spain), 2007

Miguel Ángel Sánchez
Member of Local Organizing Committee
14th European Workshop on Molecular Beam Epitaxy
Granada (Spain), 2007

Maria del Mar Sanz Lluch
Member of Local Organizing Committee
14th European Workshop on Molecular Beam Epitaxy
Granada (Spain), 2007

2008

Fernando Calle
Member of Program Committee
XVIII Telecom I+D 2008
Bilbao (Spain), 2008

Fernando Calle
Member of Local Committee
Conferencia de Dispositivos Electrónicos
Santiago de Compostela (Spain), 2008.

Fernando Calle
Member of Steering Committee
17th European Heterostructure Technology Workshop, HETECH'08
Venecia (Italy), 2008.

Fernando Calle
Member of Local Committee
Congreso IFIP "Open IT-Based Innovation: Moving towards cooperative IT transfer and knowledge diffusion"
Madrid (Spain), 2008

Fernando Calle
Session Chairman
16th Workshop on Compound Semiconductors and Integrated Circuits (WOCSDICE)
Leuven (France), 2008

Enrique Calleja
Member of the Conference Committee Board and Advisory Board
8th Int. Conf. of Light-Matter Coupling in Nanostructures (PLMCN8)
Tokyo (Japan), 2008.

Enrique Calleja
Member of the Conference Committee Board and Advisory Board
15th. Int. Conf. on Molecular Beam Epitaxy (ICMBE-2008)
Vancouver (Canada), 2008

Enrique Calleja
Member of the Conference Committee Board and Advisory Board
35th. Int. Symp. Compound Semiconductors (ISCS-2008)
Freiburg (Germany), 2008

Enrique Calleja
Member of the Conference Committee Board and Advisory Board
5th. Int. Workshop on Nitride Semiconductors, (IWNS-2008)
Montreux (Switzerland), 2008.

Enrique Calleja
Member of the Conference Committee Board and Advisory Board
7th. Int. Symp. on Semicond. Light Emitting Devices (ISSLED-2008)
Phoenix, Arizona (USA,) 2008.

Marco Maicas
Member of Local Committee
INTERMAG 2008
Madrid (Spain), 2008

2009

Fernando Calle
Member of Local Committee
World Wide Web Conference, W3C 2009
Madrid (Spain), 2009

Fernando Calle
Member of Steering Committee
18th European Heterostructure Technology Workshop, HETECH'09
Ulm (Germany), 2009

Fernando Calle
Chairman of the Organizing Committee, Session Chairman
33rd European Heterostructure Technology Workshop, HETECH'09
Málaga (Spain), 2009

Fernando Calle
Chairman of the Organizing Committee, Session Chairman
33rd edition of Wocsdice (Workshop on Compound Semiconductor Devices and Integrated Circuits). WOCSDICE´09
Málaga (Spain), 2009

Enrique Calleja
Session Chairman
33rd edition of Wocsdice (Workshop on Compound Semiconductor Devices and Integrated Circuits). WOCSDICE´09
Málaga (Spain), 2009

Enrique Calleja
Member of the Conference Committee Board and Advisory Board
9th Conf. on Nanotechnology, NANO 2009
Genova (Italy), 2009.

Enrique Calleja
Member of the Conference Committee Board and Advisory Board
11th Int. Conf. on "Optics of Excitons on Confined Systems" (OECS11)
Madrid (Spain), 2009

Enrique Calleja
Chairman of the Organizing Comittee, Session Chairman
1rst. Workshop Spain- Russia on New nanostructured materials and coatings
Madrid (Spain), 2009

Álvaro de Guzmán Fernández González
Member of Local Committee
33rd edition of Wocsdice (Workshop on Compound Semiconductor Devices and Integrated Circuits). WOCSDICE´09
Málaga (Spain), 2009.

Adrián Hierro
Member of Local Committee
33rd edition of Wocsdice (Workshop on Compound Semiconductor Devices and Integrated Circuits). WOCSDICE´09
Málaga (Spain), 2009.

Elías Muñoz
Member of the Conference Committee Board
36th.International Symposium on Compund Semiconductors 2009
Santa Barbara (USA), 2009

Elías Muñoz
Member of the International Advisory Committee
8th. Internacional Conference on Nitrides, Semiconductors, ICNS2009
Jeju (Korea), 2009

Elías Muñoz
Member of the International Advisory Committee
The 33rd edition of Wocsdice (Workshop on Compound Semiconductor Devices and Integrated Circuits). WOCSDICE´09
Málaga (Spain), 2009

José Luis Prieto
Member of Local Organizing Committee
1rst. Workshop Spain- Russia on New nanostructured materials and coatings
Madrid (Spain), 2009

9.6 Invited Seminars held at ISOM

2007

Dr. Angel Velásquez
"MEMS Fluido-Térmicos para aplicaciones aeroespaciales"
Dpto. de Propulsión y Dinámica de Fluidos, Escuela Técnica Superior de Ingenieros Aeronáuticos, UPM, Madrid (Spain)
January 19th, 2007

Prof. Faith Coldren
"Atomic force microscopy investigation of Staphylococcs aureus"
Wake Forest University, North Carolina (USA)
January 26th, 2007

Prof. C. Thomas Foxon
"The growth of high quality GaMnN and GaMnAs samples by MBE for spintronic and NMR applications"
School of Physics and Astronomy, University of Nottingham, University Park, Nottingham (United Kingdom)
January 26th, 2007

Prof. José Antonio Garrido
"Diamond surfaces: a novel platform for biosensors"
Walter Schottky Institut Technische Universität München (Germany)
February 2nd, 2007

Dr. Jennifer Bardwell
"GaN Transistor Research at the National Research Council"
Institute for Microstructural Sciences, National Research Council of Canada (Canada)
February 8th, 2007

D. Juan Carlos Peñas
"Tecnología RF-ID"
Iberwave, Madrid (Spain)
February 9th, 2007

D. Isidoro Padilla
"Nuevo Impulso a la I+D+I en Europa: VII Programa Marco"
Departamento de Ingeniería Electrónica.- ETSI Telecomunicación- Universidad Politécnica de Madrid (Spain)
February 16th, 2007

Prof. Jiro Temmyo
"ZnO-based semiconductor systems for optical devices"
Research Institute of Electronics, Shizuoka University, Hamamatsu (Japan)
February 23rd, 2007

Dra. Esperanza Luna García de la Infanta
"Determination of indium segregation in (Ga,In)(N,As) multi-quantum wells by transmission electron microscopy"
Paul Drude Institute, Berlín (Germany)
March 9th, 2007

Prof. Jon A. Preece
"Precision Chemical Engineering: Creating 3D Nanostructured Surfaces"
School of Chemistry, University of Birmingham (United Kingdom)
March 3rd, 2007

D. Maurício M. de Lima, Jr.
"Modulation of photonic structures by surface acoustic phonons"
Instituto de Ciencia de Materiales, University de Valencia (Spain)
June 1st, 2007

Dr. Marc Ilegems
"III-Nitride microcavity light emitting diodes and lasers"
Institute of Quantum Electronics and Photonics, Ecole Polytechnique Fédérale de Lausanne (Switzerland)
June 8th, 2007

Dr. José María Ulloa
"Capping of InAs quantum dots studied at the atomic scale by cross-sectional scanning tunneling microscopy"
Department of Applied Physics, Eindhoven University of Technology (The Netherlands)
June 15th, 2007

D. Francisco J. Blanco Barro
"Microfluidic-nanophotonic label-free biosensors for lab-on-a-chip applications (Microsistemas microfluídos-biosensores para el desarrollo de un laboratorio en un chip)"
Departamento de Ingeniería Electrónica.- ETSI Telecomunicación, Universidad Politécnica de Madrid (Spain)
July 6th, 2007

Prof. M. Eickhoff
"Group III-Nitrides – from bioelectronics to nanotechnology'"
Walter Schottky Institut, de la Technische Universität de Munich. (Germany)
July 4th, 2007

Prof. Klaus Ploog
"Fundamentals aspects of solid state lighting I"
Paul Drude Institut, Berlín (Germany)
July 3rd, 2007

Prof. Klaus Ploog
Fundamentals aspects of solid state lighting II"
Paul Drude Institut, Berlín (Germany)
July 4th, 2007

Prof. Klaus Ploog
"Fundamentals aspects of solid state lighting III"
Paul Drude Institut, Berlín (Germany)
July 5th, 2007

Prof. Klaus Ploog
"Fundamental aspects of solid state lighting IV"
Paul Drude Institut, Berlín (Germany)
September 6th, 2007

Prof. Klaus Ploog
"Fundamental aspects of solid state lighting V"
Paul Drude Institut, Berlín (Germany)
September 7th, 2007

Prof. Bruno Daudin
"C-plane, a-plane, m-plane GaN quantum dots, quantum wires and quantum well : how to play with the growth mode ?"
CEA/Grenoble, Department of Fundamental Research on Condensed Matter (France)
November 7th, 2007

2008

Prof. Yasushi Nanishi
"Research and Development of AlGaN/GaN High Power and High Frequency Electronic Devices under Support of Japanese Government"
Department of Photonics, School of Science and Engineering, Ritsumeikan University, Kyoto (Japan)
April 4th, 2008

Prof. Yasushi Nanishi
"Growth, doping and characterization of polar / non-polar, InN/InGaN and those nano-structure"
Department of Photonics, School of Science and Engineering, Ritsumeikan University, Kyoto (Japan)
April 15th, 2008

Prof. Manuel Laso
"Sólidos amorfos ideales: sistemas modelo de la materia desordenada"
Departamento de Ingeniería Química, Escuela Técnica Superior de Ingenieros Industriales, Universidad Politécnica de Madrid (Spain)
May 30th, 2008

Prof. Mario J. Martin
"Cálculos de Alto Rendimiento con Tarjetas Gráficas"
Instituto Nacional de Tecnología Aeroespacial Esteban Terradas (INTA) en el departamento de Dinámica de Fluidos con contrato de IMDEA, Madrid (Spain)
June 6th, 2008

Dr. Angelos Kyriazi
"Magnetic resonance imaging of the lungs with the use of hyperpolarised gases"
Instituto de Estudios Biofuncionales, University Complutense de Madrid, Madrid (Spain)
June 13th, 2008

D. Juan José González Menada
"El Hogar Digital"
Telefónica I+D. Madrid (Spain)
June 20th, 2008

Prof. Steven A. Ringel
"Epitaxial Integration of III-V Semiconductors, Devices and Solar Cells with Si via Lattice Engineering"
Ohio State University Institute for Materials Research (USA)
June 30th, 2008

Prof. Steven A. Ringel
"Metamorphic III-V Materials for Infrared and High Speed Devices Based on Sub-Lattice Specific Grading"
Ohio State University Institute for Materials Research (USA)
July 1st, 2008

Prof. Steven A. Ringel
"Deep Level Optical Spectroscopy: Approach to Investigate Defects in GaN-AlGaN Materials and Devices"
Ohio State University Institute for Materials Research (USA)
July 2nd, 2008

Dr. Atsushi Nakamura
"Research activities of Oxide semiconductors at the Research Institute of Electronics"
Research Institute of Electronics (RIE), Shizuoka University, 3-5-1 Johoku, Hamamatsu, Shizuoka (Japan)
July 17th, 2008

2009

D. Alessio Fioravanti
"Controlling Chronic Diseases related to Metabolic Disorders"
Grupo de investigación Life Supporting Technologies, Departamento de Tecnología Fotónica, E.T.S.I. Telecomunicación, Universidad Politécnica de Madrid (Spain)
June 19th, 2009

D. Abelardo León González
"Centro de Investigación Experimental en Aplicaciones y Servicios de Inteligencia Ambiental"
Grupo de investigación Life Supporting Technologies, Departamento de Tecnología Fotónica, E.T.S.I. Telecomunicación, Universidad Politécnica de Madrid (Spain)
June 19th, 2009

Dr. Ian Watson
"3-Dimensional Microstructures in GaN Fabricated Using Sacrificial AlInN Layers"
Institute of Photonics, University of Strathclyde, Glasgow (United Kingdom)
June 26th, 2009

Drª. Jacqueline L. Hall
"Temperature Effects during the Growth of In-rich InGaN Films by Plasma-Assisted Molecular Beam Epitaxy"
School of Physics & Astronomy, Univ. of Nottingham, Nottingham (United Kingdom)
July 8th, 2009

D. Miguel del Pie
"Advanced Measurements-Signal Integrity…and more"
LeCroy, Madrid (Spain)
September 22nd, 2009

9.7 Internal Seminars by ISOM members

2007

D. Álvaro Navarro Tobar
"Noise study in photodiodes based on InGaN/GaN MQW"
March 16th, 2007

D. Javier Grandal Quintana
"Structural characterization of InN-based layers grown on silicon substrates by MBE"
March 23rd, 2007

Dª. Fátima Romero Rojo
"Passivating Layers Influence on the Electrical Characteristics on AlGaN/GaN HEMTs: a Comparative Study"
April 27th, 2007

D. Sergio Fernández Garrido
"Improved growth mode diagram for plasma-assisted MBE growth of (0001) GaN"
May 18th, 2007

D. David López-Romero
"E-beam nano-lithography: present and future at Institute for Optoelectronic Systems and Microtechnology'"
June 22nd, 2007

D. Miguel González-Guerrero
"Giant magneto-impedance effect in electrodeposited CoP layers and CoP-Cu-CoP sandwich structures"
June 29th, 2007

D. Jorge Pedrós
"Dispositivos SAW en estructuras de nitruros del grupo III: propagación y modulación óptica y electrónic"
July 6th, 2007

2008

D. Fernando González Posada-Flores
"A comparative study by ion beam analysis and X-ray diffraction in GaN-based HEMT heterostructures"
May 9th, 2008

Dª. María Utrera López
"Crecimiento ordenado de Nanocolumnas de GaN sobre Si mediante Epitaxia de Haces Moleculares "
May 23rd, 2008

Dª. Rocío San Román Alonso
"Optimización de un sistema de "sputtering"para el depósito de películas delgadas de nitruro de aluminio"
July18th, 2008

2009

Prof. Claudio Aroca Hernández-Ros
"Seminario de Seguridad y uso de la Sala Blanca del ISOM"
February 13rd, 2009

Dr. Gonzalo Fuentes Iriarte
"Fabricación, diseño y caracterización de filtros de ondas acústicas de superficie'"
February 20th, 2009

D. Miguel Montes
"InAs/(Ga,In)(N,As) Quantum Dot LEDs Emitting at 1.3-1.5 μm"
February 27th, 2009

Dr. Carlos Angulo Barrios
"Slot-waveguides for biochemical sensing and other optofluidic applications"
March 6th, 2009

D. Eugenio Sillero Herrero
"Nanodiamond micromechanical resonators"
March 13rd, 2009

D. Zarco Gacevik
"Growth and characterization of lattice-mismatched AlGaN/GaN and lattice-matched InAlN-GaN distributed Bragg reflectors by MBE"
March 27th, 2009

Dª. Fátima Romero Rojo
"Electrical and Microstructural Characteristics of Ohmic Contacts formation on AlGaN/GaN HEMT"
April 3rd, 2009

Dr. José María Ulloa
"1.3 – 1.55 mm InAs/GaAs quantum dots capped with GaAsSb: effect of the Sb content on the structural and optical properties"
April 24th, 2009

D. Juan Gabriel Madrid
"Sputtering System Optimization"
May 29th, 2009

D. Juan Pereiro Viterbo
"Diseño, crecimiento, caracterización y fabricación de detectores de luz ultravioleta y visible basados en pozos cuánticos de nitruros del grupo III"
December 11st, 2009

D. Fernando González-Posada Flores
"Aspectos estructurales, deformación y superficies en relación con la fiabilidad de transistores de alta movilidad electrónicas basados en heteroestructuras de AlGaN/GaN"
December 18th, 2009

9.8 Scientific workshops and meetings organized by ISOM members

2007

"THE 14TH EUROPEAN WORKSHOP ON MBE", SIERRA NEVADA, GRANADA, SPAIN, 5 -7 MARCH 2007

ISOM participated in the active organisation of the **14th European Workshop on Molecular Beam Epitaxy (MBE)**, held in Sierra Nevada (Granada) **during 5-7 March of 2007**. This Workshop, that started 25 years ago in Germany (1st European Workshop on MBE, Stuttgart, Apr. 1981), is celebrated with a biannual periodicity and it stands as one of the most renown and prestigious scientific meetings on MBE. Traditionally, it has covered the whole spectrum of activities related to the MBE growth technique, as well as its applications, such as: growth issues on a wide variety of semiconductors, metals, superconductors, magnetic and organic films, as well as the characterization techniques applied to them. Device applications represent a key aspect of this Workshop, so that, participants from Industries represent a substantial added value. The 14th European MBE Workshop lasted three days, and it included plenary oral presentations, as well as regular oral and poster contributions, with an approximate number of attendees around 150, coming from 13 different European countries.

A very relevant aspect of this Workshop was to promote the participation of PhD students and young researchers, so that, special efforts were committed to maintain a low fees rate for them.

http://www.isom.upm.es/mbe

The 14th edition of the EURO-MBE Workshop took place in Sierra Nevada, a well known skiing resort in Granada, Spain, which is also around 50 miles away from the mediterranean coast.

2008

"UPM-TAIWANESE DELEGATION WORKSHOP" MADRID, SPAIN, 28TH OF NOVEMBER 2008

The 28th of November 2008, our Institute hosted a delegation of prestigious scientists from Taiwan, lead by Prof. Chih-Chung Yang from the Institute of Photonics and Optoelectronics of the National Taiwan University in Taipei. The members of the delegation had broad experience in optoelectonics, with specialties ranging from Nitride and oxide semiconductor deposited by MOCVD and MBE to Bio-fluids, including solar cells, plasmonics, lasers, biophotonics, flexible electronics, etc. All these fields, clearly within the expertise and the objectives of the ISOM, made the visit very fruitful and several potential collaborations were established during the visit.

Yang, Chih-Chung (C. C.)
Office Address:
Institute of Photonics and Optoelectronics,
National Taiwan University,
No. 1, Roosevelt Road, Section 4, Taipei, Taiwan, ROC
phone: 886-2-23657624
fax: 886-2-23652637
e-mail: ccy@cc.ee.ntu.edu.tw
websites: http://cc.ee.ntu.edu.tw/~ccy/
http://homepage.ntu.edu.tw/~square/index.html

Visitors/ Name	Title/Affiliation	Education	Research Interests
Yang, Chih-Chung (C. C.)	**Professor**, Institute of Photonics and Optoelectronics, National Taiwan University	**Ph. D.,** Department of Electrical Engineering, University of Illinois at Urbana-Champaign, USA	Nitride and oxide semiconductor MOCVD and MBE growths, solid-state lighting, solar cell, surface plasmonics, nano-photonics and optoelectronics, bio-photonics
Wuu, Dong-Sing	**Professor**, Department of Materials Science and Engineering, National Chung Hsing University	**Ph. D.**, Department of Electrical Engineering, National Sun Yat-Sen University, Taiwan	Nitride and oxide semiconductor MOCVD growths, solid-state lighting, solar cells, flexible electronics, optoelectronics
Wang, An-Bang	**Professor**, Institute of Applied Mechanics, National Taiwan University	**Ph. D.**, Erlangen-Nuernberg University, Germany	Bio-fluid and Micro-Flow Systems, Thermal Management in Optomechatronic Systems, Flow Separation and Control, Drop & Bubble Dynamics, Coating in Display technology, Advanced Measurement Techniques of Fluid mechanics, Micro Air Vehicle
Ho, Jeng-Rong	**Professor**, Graduate Institute of Opto-Mechtronics, National Chung Cheng University	**Ph. D.**, Department of Mechanical Engineering, University of California at Berkeley, USA	Laser material processing and fabrication, fabrication of polymeric optoelectronics, modeling & simulation of transport of energy induced by an ultra-short laser pulse
Cheng, I-Chun	**Assistant Professor**, Institute of Photonics and Optoelectronics, National Taiwan University	**Ph. D.**, Department of Electrical Engineering, Princeton University, USA	flexible electronics and optoelectronics, amorphous silicon thin film devices, nanocrystalline silicon thin film devices, thin film mechanics
Lin, Hoang Yan	**Associate Professor**, Institute of Photonics and Optoelectronics, National Taiwan University	**Ph. D.,** Department of Electrical Engineering, National Taiwan University, Taiwan	Micro-optics and nano-optics, display technology, solid-state lighting, solar cell
Tarng, Yeong-Shin	**Professor**, Department of Mechanical Engineering, National Taiwan University of Science and Technology	**Ph.D.,** Department of Mechanical Engineering, University of Florida, USA	Mechatronics, Image Processing, Inspection Automation, Process Optimization, Artificial Intelligence, Deign of Automated Machines

2009

"THE 33RD EDITION OF WOCSDICE (WORKSHOP ON COMPOUND SEMICONDUCTOR DEVICES AND INTEGRATED CIRCUITS)", MÁLAGA, SPAIN, 17-29 MAY 2009

The 33rd WOCSDICE took place in Malaga**, from the 17th to the 20th of May, 2009**. The Symposium was organized by ISOM-UPM, in Spain, with the aim of bringing together scientists and engineers working in the area of III-V Compound Semiconductor devices and integrated circuits for microwave, mm-wave, and optoelectronic applications. Additionally, diamond, organic semiconductors and several nanotechnology fields were also included.

The local organizing team was composed by Fernando Calle, Adrián Hierro, Miguel Ángel Sánchez, Alvaro de Guzmán Fernández, Gonzalo Fuentes and José María Ulloa.

More than 100 participants attended Wocsdice 2009, from 57 institutions of 14 countries (mainly Europe and USA), as shown in the graph.

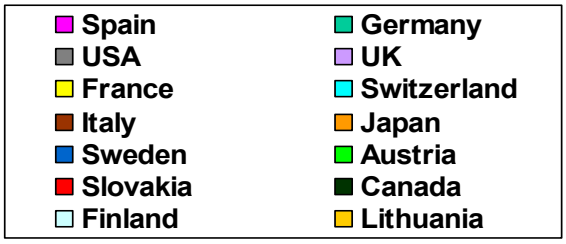

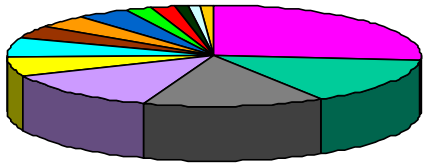

There were 17 one-hour technical sessions on the following topics:

1 Nitrides: Material aspects
2 Nitrides for Optoelectronics
3 Oxides
4 Diamond
5 Power electronics
6 Narrow bandgap Electronics
7 Narrow bandgap Optoelectronics
8 Nitride HEMTs: Material aspects
9 Nitride HEMTs: Processing
10 Solar Cells
11 Organic Devices
12 Novel Devices; Concepts
13 Novel Devices; Structures
14 Integrated Circuits
15 Nitride HEMTs: Devices
16 Nitride HEMTs: High temperature
17 Nitride HEMTs: Reliability

13 invited talks were given by leader speakers in their respective areas:

- Prof. Yasushi Nanishi (Ritsumeikan Univ., Japan), Recent Progress and challenges of InN for device applications
- Prof. Jiro Temmyo (Shizuoka Univ., Japan), Material and device aspects of MOCVD ZnO
- Prof. Volker Cimalla (IA Friburgo, Germany), MEMS for harsh environments
- Prof. José Millán (IMB-CNM-CSIC, Spain), Power electronics for a rational use of energy
- Prof. Rudolf Hey, (Paul Drude Institute, Germany), THz lasers and amplifiers
- Prof. Eric Tournie (Univ. Montpellier, France), Sb-based QDot emitters and detectors
- Prof. Tomás Palacios (Massachussets Inst of Technology, USA), GaN transistors: Redefining the limits of electronics
- Prof. Aris Christou (Univ. Maryland, USA), Integrated Power Sources with TF-MOSFETs for Flexible Electronics
- Prof. Steve Ringel (Ohio State Institute, USA), Solar cells using metamorphic substrates
- Prof. Antonio Gnudi (Univ. Bologna, Italy), Graphene-based high-performance nanoelectronic devices
- Prof. Chris Ford (Univ. Cambridge, U.K.), Novel designs for quantum computers and quantum communication systems
- Prof. Philippe Dueme (Thales Group, France), Integrated Circuits in GaN Technology: an European perspective
- Prof. Dimitris Pavlidis (Univ. Darmstadt, Germany), Energy harvesting using semiconductors

The sessions included 67 additional oral presentations, of a general outstanding quality. The proceedings, published in an electronic format, were provided to all participants.

In summary, the objectives of this workshop were fully satisfied from both the scientific and interchange perspectives.

More info may be found at http://www.wocsdice2009.org/

From left to right: Fernando Calle, Steve Ringel, Adrián Hierro and Tomás Palacios.

2009

"WORKSHOP HISPANO-RUSO", MADRID, SPAIN, 28-29 OCTOBER 2009

The 28 and October 29, 2009, **Workshop on Nanotechnology Russian Hispano** in the Board Room of Building A of the ETSIT-UPM.
The event was organized by the Institute of Optoelectronics and Microtechnology Systems (ISOM) and School of Telecommunications Engineering of the Polytechnic University of Madrid in coordination with the Russian Embassy in Spain.
Attendees at this conference were Russian scientists in nanotechnology and also Spanish scientists in different fields of nanotechnology, mostly from Madrid region. The program brought together over 20 papers that led round-table discussions.
The workshop lasted two days. In the first day, the workshop was opened by the attaché to the Russian ambassador, the research vice-rector of the UPM, the director of the ETSIT and the director of the ISOM, chairman of the workshop. The first days hosted all the presentations fom both Russians and Spanish attendees
The second day was organized with rounded tables around the different topics and the meeting ended with a reception at the Russian embassy.
One objective is to establish collaborations between scientists of both countries.

The organizers and hosts welcome to the Workshop "New nanostructured materials and Coatings" ISOM-ETSIT-UPM. Salón de Grados de Escuela Técnica Superior de Ingenieros de Telecomunicación.

9.9 Awards and Other Activities

2007

- David Ciudad Río-Pérez, "Premio al Investigador Novel en Física Experimental", Real Sociedad Española de Física.
- Javier Miguel Sánchez, "Premio a la Mejor Tesis Doctoral en Fundamentos y Tecnologías Básicas de la Información y las Comunicaciones y sus Aplicaciones", COIT/AEIT
- José María Ulloa, "Premio Extraordinario de Doctorado", University Politécnica de Madrid.
- Miguel Montes Bajo, "Graduate Student Award", Fall European Materials Research Society Conference (E-MRS), Estrasburgo (France).
- Raquel Gargallo, "Premio a la Mejor Presentación Oral", 6ª Conferencia de Dispositivos Electrónicos (CDE07), El Escorial (Madrid).
- Dr. Gonzalo Fuentes Iriarte, promotor de Ebomer "Tercer Premio a los mejores Planes de Negocio, IV Competición de Creación de empresas, Actúa-UPM", Universidad Politécnica de Madrid.

2008

- Carlos Rivera de Lucas, "Premio a la Proyección Investigadora", Premios Anuales de Investigación UPM.
- Carlos Rivera de Lucas, "Premio ISDEFE a la Mejor Tesis Doctoral en Seguridad y Defensa", Colegio Oficial de Ingenieros de Telecomunicación.

2009

- Dr. Carlos Angulo Barrios, "Premio UPM de Proyección Investigadora, Premios Anuales de Investigación de la UPM", Universidad Politécnica de Madrid.
- Dr. Carlos Angulo Barrios, "Primer Premio del Certamen de Divulgación Científica y Tecnológica UPM, Artículo titulado: Microanillos de luz para detectar virus ", Universidad Politécnica de Madrid.
- Dr. Carlos Angulo Barrios, miembro del equipo promotor de BIOD (Bio-optical detection), "Segundo Premio a los mejores Planes de Negocio, VI Competición de Creación de empresas, Actúa-UPM", Universidad Politécnica de Madrid.
- Dr. Carlos Rivera de Lucas, "Premio Extraordinario de Doctorado (curso 2006-2007)", Universidad Politécnica de Madrid.
- Dr. José Luis Prieto Martín, "Primer Premio de Fotciencia, en la categoría micro, que presenta unos diminutos champiñones generados electrolíticamente", Certamen Fotociencia 2009.
- Miguel Montes Bajo, "Graduate Student Award", Spring European Materials Research Society Conference (E-MRS), Estrasburgo, Francia.

10 FUNDING INSTITUTIONS

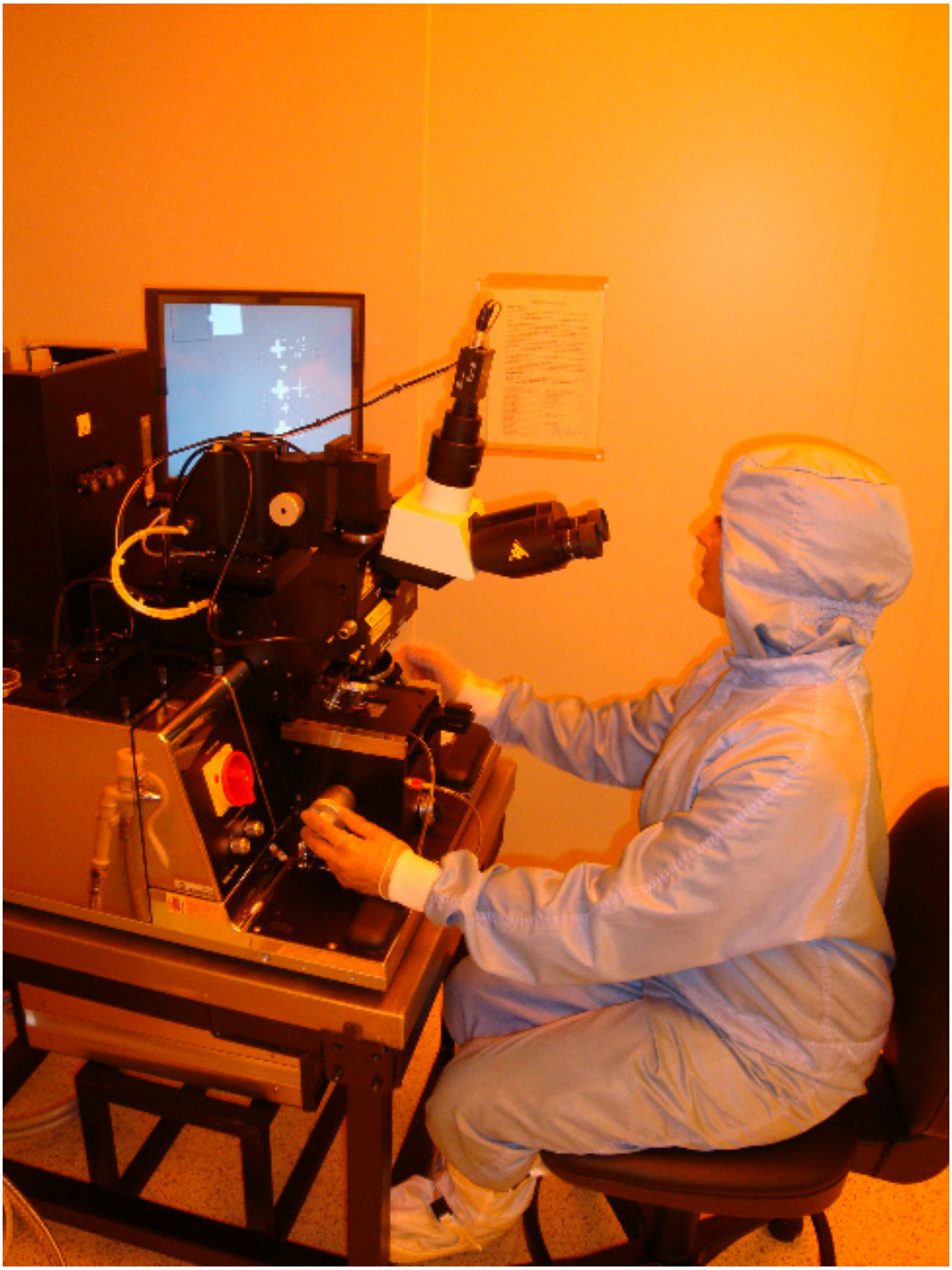

Our Institute has two optical mask aligners, a KarlSuss MJB3 and the recently purchased MJB4 with a resolution of 500 nm.

This picture shows the MJB4 with a screen for the alignment and a chuck that allows wafers up to 4". The different processes require the use of a wide variety of photoresists (ie, 4214, SU8, PMMA).

10.1 International Companies and Public Institutions

- Sixth and Seven Framework Programme for Research and Technological Development (EU)
- Marie Curie Actions (EU)
- European Regional Development Fund (FEDER)
- European Space Agency -ESA
- European Defense Agency –EDA
- Western European Union (WEU) - WEAO Research Cell.
- European Office of Aerospace Research and Development.

10.2 National Companies and Public Institutions

- Comunidad Autónoma de Madrid
- Ministerio de Educación y Ciencia, Ministerio de Ciencia e Innovación (MICINN)
- Ministerio de Industria, Turismo y Comercio
- Ministerio de Defensa-CIDA
- Universidad Politécnica de Madrid
- Real Casa de la Moneda, Fábrica Nacional de Moneda y Timbre de España
- INDRA SISTEMAS, S.A.
- METRO MADRID S.A
- ACCIONA ENERGIA SOLAR

11 MEMBERS

NAME AND SURNAME		MAIL	PHONE	ROOM
SENIOR RESEARCHERS				
Angulo Barrios, Carlos		cbarrios@die.upm.es	915495700 Ext 4414	C-200
Aroca Hernández, Claudio	*(Technical Coordinator)*	caroca@fis.upm.es	915495700 Ext 2001	A-032
Calle Gómez, Fernando	*(Subdirector)*	calle@die.upm.es	913367316	C-225
Calleja Pardo, Enrique	*(Director)*	calleja@die.upm.es	913367315	C-221
Fernández González, Álvaro de Guzmán		guzman@die.upm.es	915495700 Ext 4203	B-107
Fuentes Iriarte, Gonzalo		gonzalo.fuentes@upm.es	915495700 Ext 4417	C-200
Hierro Cano, Adrián		ahierro@die.upm.es	915495700 Ext 4231	C-225
Laso Carbajo, Manuel		mlaso@etsii.upm.es	913363015	ETSII
Maicas Ramos, Marco César		maicas@fis.upm.es	915495700 Ext 2009	A-033
Muñoz Merino, Elías		elias@die.upm.es	913367321	C-223
Prieto Martín, José Luis	*(Secretary)*	joseluis.prieto@upm.es	915495700 Ext 2004	A-032
Sánchez García, Miguel Ángel		sanchez@die.upm.es	915495700 Ext 4203	B-107
Sánchez Sánchez, Pedro		psanchez@fis.upm.es	913367241	A-032
Sanz Lluch, Mª del Mar	*(Person in charge ICTS)*	mmsanz@die.upm.es	915495700 Ext 4221	B-010
DOCTORS				
Barbagini, Francesca		fbarbagini@die.upm.es	915495700 Ext 4416	C-200
Jimeno Aguilar, Nieves		njimeno@etsii.upm.es	913363015	ETSII
Karayiannis, Nikolaos		nkarayiannis@etsii.upm.es	913363015	ETSII
Lefebvre, Pierre		pierrelefebvre@die.upm.es	915495700 Ext 4416	C-200
Pérez García, Lucas		lucas.perez@fis.ucm.es	913944747	UCM
Ranchal Sánchez, Rocío		rociran@fis.ucm.es	913944496	UCM
Ristic, Jelena		jelena.ristic@die.upm.es	915495700 Ext 4415	C-200
Tadjer, Marko Jak		marko.tadjer@upm.es	915495700 Ext 4417	C-200
Yamamoto, Kenji		kyamamoto@die.upm.es	915495700 Ext 4415	C-200
Ulloa Herrero, José María		jmulloa@die.upm.es	915495700 Ext 4415	C-200
PH.D. STUDENTS				
Akerman, Johanna		jakerman@fis.upm.es	915495700 Ext 2007	A-032
Bengoechea Encabo, Ana María		abengo@die.upm.es	915495700 Ext 4219	B-039.1
Cuerdo Bragado, Roberto		rcuerdo@die.upm.es	915495700 Ext 4226	C-206
Gacevic, Zarko		gacevic@die.upm.es	915495700 Ext 4226	C-206
Gargallo Caballero, Raquel		rgargallo@die.upm.es	915495700 Ext 4219	B-039.1
López Ponce, Manuel		mlopez@die.upm.es	915495700 Ext 4226	C-206
Martín Horcajo, Sara		smartin@die.upm.es	915495700 Ext 4226	C-206
Milla Rodrigo, María José		mjmilla@die.upm.es	915495700 Ext 4219	B-039.1
Montes Bajo, Miguel		mmontes@die.upm.es	915495700 Ext 4226	C-206
Redondo Cubero, Andrés		andres.redondo@uam.es	914973628	UAM
Rodriguez Madrid, Juan Gabriel		jgrodriguez@die.upm.es	915495700 Ext 4226	C-206
Romera Rabasa, Miguel		mromera@fis.upm.es	ESC. 2007	A-032
Romero Rojo, Fátima		fromero@die.upm.es	915495700 Ext 4226	C-206
San Román Alonso, Rocío		rocio.sanroman@die.upm.es	ESC.4235	B-039
Sillero Herrero, Eugenio		esillero@die.upm.es	915495700 Ext 4226	C-206
Tabares Jimenéz, Gema		gtabares@die.upm.es	915495700 Ext 4226	C-206
BSc.D. STUDENTS				
Cascales Fernández, José		jcascales@die.upm.es	915495700 Ext: 2009	A-033
Kurtz de Griñó, Alejandro		alejandrokurtz@gmail.com	915495700 Ext: 4231	B-039
ADMINISTRATION AND TECHNICIANS				
Contreras González, Fernando		fcontreras@die.upm.es	915495700 Ext 4408	ISOM
García González, Oscar		oscar@die.upm.es	915495700 Ext 4408	ISOM
Juárez Migueláñez, Montserrat		montse.isom@die.upm.es	913366832	C-231
López-Romero Moraleda, David		dromero@die.upm.es	915495700 Ext 4418	ISOM
Romero Estepa, Juan Antonio		ja.romero.estepa@upm.es	915495700 Ext 4418	ISOM
Sabido Siller, María del Carmen		mcsabido@die.upm.es	915495700 Ext 4418	B-010
Sánchez Sánchez, Juan Ramón		jrsanchez@die.upm.es	Esc. 4222	ISOM
EXTERNAL COLLABORATORS				
Albert, Steven		salbert@die.upm.es	915495700 Ext 4219	B-039.1
Brazzini, Tommaso		tbrazzini@die.upm.es	915495700 Ext 4219	B-039.1
Llavona Serrano, Angela		angelallavona@fis.ucm.es	915495700 Ext 4219	UCM
Muñoz Sánchez, Manuel		manuel.munoz@fsp.csic.es	915495700 Ext 2007	A-032